Die Expeditionen ANTARKTIS XVI / 3 - 4 des Forschungsschiffes „POLARSTERN“ 1999

The Expeditions ANTARKTIS XVI / 3 - 4 of the Research Vessel „POLARSTERN“ in 1999

Hrausgegeben von / Edited by
Ulrich Bathmann, Victor Smetacek, Manfred Reinke
unter Mitarbeit der Fahrtteilnehmer /
with contributions or the participants

Ber. Polarforsch. 364 (2000)
ISSN 0176 - 5027

ANTARKTIS XVI/3 – 4

18 MÄRZ 1999 – 08 JUNI 1999

KOORDINATOR/COORDINATOR

Heinrich Miller

ANT XVI/3: Cape Town – Cape Town

FAHRTLEITER/CHIEF SCIENTIST

Victor Smetacek

ANT XVI/4: Cape Town – Bremerhaven

FAHRTLEITER/CHIEF SCIENTIST

Manfred Reinke

ANT XVI/3

1. Introduction/Einleitung 6

2. Weather 12

3. Physical Control of Primary Production and of biogeochemical fluxes at the antarctic polar front 16
3.1 Underway Measuremets of Hydrographic and Biological Variables with the Towed Undulating Vehicle 'Scanfish' 19
3.2 CTD Stations and Water Bottle Sampling 23
3.3 Underway Measurements of Currents with the Vessel-Mounted Acoustic Doppler Current Profiler 31
3.4 Measurements with Moored Instruments 34
3.5 Measurements of Acoustic Backscatter by Vessel-Mounted and Moored ADCPs as Proxies of Zooplankton Abundance 36

4. Distribution of nutrients (AWI) 38

5. determination of the stable C and N isotopes in the particulate organic matter (AWI 43

6. Field Distribution of Iron in a Section of the Antarctic Polar Frontal Zone 44

7. Phytoplankton 51

8. Surface chlorophyll measurements 53

9. Biophysical measurements 58

10. Study of the mechanisms controlling phytoplankton growth in late summer-early autumn in the Southern Ocean with special attention to iron and silicate physiology 60

11. Fluorescence of Marine Phytoplankton 64

12. Phytoplankton dynamics in austral autumn in the Southern Ocean 68

13. Responses to iron limitation of natural phytoplankton assemblages collected around the Polar Front and single species cultures of Antarctic diatoms. 75

14. Light adaptation by natural phytoplankton populations, and its control by iron limitation. 77

15. Krill Biology and Krill Physiology 84
15.1 General outline 84
15.2. Examining overwintering strategies of Antarctic krill (Euphausia superba) 87

16. Zooplankton at the Antarctic Polar Front 89

17. Biomass Production, Substrate Dynamics and Community Structure of the Heterotrophic Picoplankton at the Polar Front and the Weddell Sea in Fall 91

18. Census of Marine Birds and Mammals 101

19. Source regions and transport paths of iron in the Antarctic Circumpolar Current 110
19.1 Objectives 110
19.2 Sampling strategy, sample processing and first on board analyses 111

20. Export production measured through the 234Th/238U disequilibrium in surface water. 114

21. Real-Time Satellite Information 119
21.1 SeaWiFS for Mapping Chlorophyll_a 119
21.2 DMSP Special Sensor Microwave/Imager 120
21.3 NOAA Weather Satellites 121
21.4 Sea Ice Information 122

22. Participants / Fahrtteilnehmer ANT XVI/3 128

23. Participanting Institutes / Beteiligte Institute 129

24. Ship's Crew / Schiffsbesatzung ANT XVI/3 130

ANT XVI/4

A. Fahrtroute ANT XVI/4	131
B. Itinerary ANT XVI/4	132
C. PODEV Nachfolge	133
D. The Scientific Computimg Network on RV "Polarstern"	134
E. Nahrungsökologie und Energetik des antarktischen Krill	134
F. Trophodynamics and energetics of the Antarctic krill	135
G. Source regions and transport paths of iron in the Antarctic Circumpolar Current	135
H. Bio-optik und Bio-chemie von Eisalgen und Phytoplankton	137
I. Bio-optics and bio-chemistry of ice algae and phytoplankton	138
K. Participants / Fahrtteilnehmer ANT XVI/4	138
L. Participanting Institutes / Beteiligte Institute	138
M. Ship's Crew / Schiffsbesatzung ANT XVI	139

FAHRTABSCHNITT ANT XVI/3 KAPSTADT – KAPSTADT (18.3.99 – 10.5.99)

1. INTRODUCTION/EINLEITUNG

U. Bathmann und V. Smetacek (AWI)

Wissenschaftlicher Bericht der Polarstern-Expedition ANT XVI/3:
Frontendynamik und Biologie II

Polarstern verließ planmäßig am 18.3. Abends Kapstadt in Richtung Süden. Die erste wissenschaftliche Arbeit der Expedition ANT XI/3 war das Ausbringen einer ozeanographischen Verankerung, die gemeinsam vom Institut für Meereskunde Kiel und dem Hydrographischen Institut der Univ. Kapstadt vorbereitet wurde und hydroakustische Meßverfahren zur Strömungsermittlung verfolgt. Nach Erreichen des Meßgebeites an der Polarfont wurden deren hydrographische Charakteristika mittels eines Schleppsystems (s. Kapitel 3.) aufgenommen. Eine Raute von 5 Verankerungsystemen wurde nördlich, in und südlich der Polarfrontzone ausgebracht (s. Kapitel 3.4) um die Strömungsdynamik und die Partikelsedimentation hochfrequent in mehreren Tiefenintervallen bis nahe zum Meeresboden über 6 Wochen zu vermessen.

Die Expedition verfolgte zwei wissenschaftliche Zielsetzungen, die jeweils in IGBP Kernprojekte eingebunden sind:

A. Erfassung der mesoskaligen Hydrographie in Beziehung zur Biologie und Geochemie an der Polar Front (Southern Ocean Joint Global Ocean Flux Study, SO JGOFS)

B. Ernährungsstrategien vom antarktischen Krill *Euphausia superba* im Herbst (Southern Ocean Global Ocean Ecosystem Dynamics, SO GLOBEC),

Die Untersuchungen zum Thema A werden von einem interdisziplinären Team, zusammengesetzt aus Mitgliedern von 3 AWI-Fachbereichen sowie Institutionen in den Niederlanden (12 Wissenschaftler) und UK (3) durchgeführt. Letztere sind Partner in den EU-Projekten MERLIM und CARUSO. Die meisten niederländischen Teilnehmer stammen aus dem NIOZ und sind im Rahmen des Niederländisch-Bremischen Abkommens (NEBROC) an der Fahrt beteiligt. Ziel der miteinander verzahnten Projekte ist die Ermittlung der Faktoren: mesoskalige Frontendynamik, Eisen- und Siliziumverfügbarkeit sowie Wegfraß bei dem Aufbau und Absinken von Diatomeenblüten an der Polar Front.
Diese Fahrt ist die Dritte einer Reihe, die die Rolle des Südpolarmeeres als Quelle oder Senke vom atmosphärischen CO2 untersucht. Bei der ersten Fahrt (ANT X/6) stellten sich die überragenden Rollen der Eisenverfügbarkeit sowie der mesoskaligen Hydrographie an Fronten bei der Erzeugung von Diatomeenblüten und der gekoppelten Aufnahme von CO2. Bei der zweiten Fahrt (ANT XIII/2) wurde ein Grid an der Polar Front sehr genau vermessen und die Beziehungen zwischen der Frontendynamik, der Eisenverfügbarkeit und den relevanten biologischen Prozessen während des Sommers ermittelt. Der Aufbau dickschaliger Diatomeenpopulationen konnte auf den Wegfraß der weniger geschützten Arten zurückgeführt werden. Die Schalen solcher dickschaligen Arten akkumulieren im Sediment, weshalb die Region unterhalb des Zirkumpolarstroms mit Abstand die größte Siliziumsenke im Weltmeer darstellt. Die jetzige Fahrt nimmt die Situation an der Polarfront im Herbst auf.

Zu Beginn der Reise wurde ScanFish - ein zwischen Oberfläche und 250m Tiefe undulierendes Instrument, das Temperatur, Salzgehalt, Chlorophyllfluoreszenz und Druck mißt - zwischen 46° und 52°S entlang des 20° E Meridians geschleppt, um

die Lage der Frontensysteme zu erkunden. Danach wurden 5 Verankerungen mit Strommessern (davon 3 mit Sedimentfallen) im Kreuz über die Polarfront ausgebracht und ein Grid von ca. 140 x 140 km mit 15km Intervallen mit dem ScanFish vermessen. Anschließend wurde ein Transekt mit 7 Stationen durch das Meßgebiet gelegt. Die Ergebnisse zeigen, daß wir einen südlichen Meander der Polarfront angeschnitten hatten: Warmes, silikat- und planktonarmes Oberflächenwasser war dabei, die Wassermasse südlich der Front zu überschichten. Im südlichen Wasser waren die Planktongehalte für die Jahreszeit überraschend hoch und dominiert durch eine Population der Diatomee *Fragilariopsis kerguelensis,* deren Schalen den Hauptanteil des am Boden akkumulierenden Diatomeenschlamms ausmacht. Detaillierte Untersuchungen des Zustands dieser Art quer zur Front zeigen, daß verschiedene Stadien des Lebenszyklus sich vom Norden nach Süden abwechselten. Das Maximum der Population befand sich zwischen 60 und 100m Tiefe, weil die südliche Oberflächenschicht, in der die Blüte herangewachsen war, zum Zeitpunkt der Messungen subduziert wurde. Laborexperimente werden zur Klärung der Autökologie dieser enigmatischen Art beitragen. Die Eisengehalte im Meßgebiet waren sehr fleckenhaft und deuteten auf einen Eintrag durch Niederschläge hin.

Das Untersuchungsgebiet für die zweite Zielsetzung (B) dieser Fahrt wurde aus gegebenem Anlaß von der Lazarew See (20° E) in das Schelfgebiet vor Neumayer (8° W) verlegt.

Die Biologie des Antarktischen Krills zur Zeit der sich ausbreitenden Meereisdecke ist kaum bekannt. Integrierte Untersuchungen werden im Rahmen von SO-GLOBEC im internationalen Verbund durchgeführt, um die Mechanismen und Prozesse zu untersuchen, die dem Krill erlauben, seine grossen Bestände über das Jahr aufrechtzuerhalten. Folgende Überwinterungsstrategien des Krill werden diskutiert: Fraß von Eisalgen und/oder Zooplanktern vor allem Copepoden, Hungern unter Reduktion des Grundumsatzes oder Verzehrung der eigenen Körpersubstanz sowie Lipidreserven. Studien, die alle Aspekte gleichzeitig berücksichtigen, fehlen bisher. Diese Fragestellung wird auf zwei Forschungsfahrten mit FS Polarstern bearbeitet, wobei die jetzige Expedition die Situation im östlichen Weddellmeer verfolgt. Die zweite Fahrt wird Mai 2001 zusammen mit anderen Forschungseisbrechern durchgeführt; beide Fahrten sind Bestandteil eines BMBF-Verbundprojekts.

Auf dem Weg ins Untersuchungsgebiet wurde im eisfreien Ozean bei Maud Rise kein Krill angetroffen, stattdessen dominierten Salpen (gelatinöse Zooplankter) die planktonarme Wasserkörper bevorzugen. Dagegen wurden Krillschwärme sehr unterschiedlicher Ausdehnung und Individueendichte im Gebiet des sich ausdehnenden Meereises am Kontinentalhang vor Neumayer nachts in 50 bis 150 m Wassertiefe angetroffen und beprobt. Die Profile des schiffsgebundenen Acoustic- Doppler -Current-Profilers (ADCP) lassen vermuten, daß sich diese Krillschwärme am Tage in über 500 m Wassertiefe zurückziehen. Unmittelbar unter den flachen Eisschollen wurde kein Krill gefunden.

Die physiologischen Leistungen der mit Vertikalhols schonend gefangenen Individuen (Adulte und Furcilien) werden zur Zeit in Experimenten bestimmt (Freßverhalten, Respiration, Exkretion), das Nahrungsspektrum der Tiere im Herbst ermittelt (Mikroskopie, delta15N und delta13C Isotope, Lipidklassen und Fettsäurezusammensetzung, freie Aminosäuren, Darmfluoreszenz, Karotinoide und Chlorophylle) und Überwinterungsmechanismen (Wachstum, Hungerfähigkeit, C/N-Gehalt, Trockengewicht, Gesamtlipide, Verdauungsenzyme, Chitinasen sowie Proteine) untersucht. Die Freßversuche von Krill an Bord ergaben, dass die Nahrungsaufnahme der Tiere deutlich gegenüber der im Sommer gemessenen Raten reduziert ist. Auch die Respiration und Exkretion dieser Tiere ist fast eine Größenordnung geringer als im Sommer, selbst wenn den Tieren ausreichend

frisches Futter unterschiedlicher Qualität angeboten wird. Sollten sich diese Ergebnisse durch die weiteren Analysen bestätigen, bedeutet dies, daß Krill bereits im Herbst seine physiologischen Aktivitäten reduziert. Ob bei einer Verbesserung der Nahrungsressourcen nach Heranwachsen der Algen in der Untereisschicht der Metabolismus der Tiere entsprechend angepasst wird, bleibt noch zu klären.

Nach Rückkehr zur Polarfront konnte aus Zeitmangel das Grid nur sehr grob wiederholt werden. Alle Verankerungen wurden anschließend geborgen und wir sind jetzt dabein den Stationstransekt bei 20°E zu wiederholen. Die Ergebnisse zeigen deutliche Veränderungen gegenüber der ersten Vermessung. Es bleibt noch zu klären, ob unsere Befunde regionalen Charakter haben, oder für den gesamten Lauf des ACC gültig sind. Die vom Satelliten SeaWifs erzeugten Chlorophylliverteilungen sind für den ACC wegen der dichten Bewölkung sowie der relativ geringen Oberflächenkonzentrationen antarktischer Blüten schwer zu interpretieren. Unsere Daten erlauben nun eine Kalibrierung der fleckenhaften Information von SeaWifs, um Nettoflüsse der biogenen Elemente Kohlenstoff und Silizium zu rekonstruieren und modellieren.

Diese Fahrt wurde auf den Internetseiten der Süddeutschen Zeitung mit aktuellen Beiträgen und Bildern begleitet.

Polarstern lief planmäßig am 10.5. in Kapstadt ein.

Cruise leg ANT XVI/3 Cape Town – Cape Town
Report of the RV Polarstern cruise leg ANT XVI/3:
Frontal dynamics and Biology II

Introduction
U. Bathmann and V. Smetacek

RV Polarstern left Cape Town as planned on the evening of 18th March with 48 scientific personnel and 43 crew members on board. After deploying an oceanographic mooring carrying hydroacoustic instruments for estimating currents which is part of a joint project of the Institut für Meereskunde, Kiel with the University of Cape Town, Polarstern steamed south to the first of the study sites. The cruise had two scientific aims both of which were part of IGBP core projects:

A Elucidating the relationship between mesoscale hydrography and biology and biogeochemistry of the Polar Front (Southern Ocean Joint Global Ocean Flux Study, SO JGOFS)
B Nutrition strategies of Antarctic Krill (*Euphausia superba*) in autumn (Southern Ocean Global Ocean Ecosystem Dynamics, SO GLOBEC)

The JGOFS related work was carried out by an interdisciplinary team from the physical, geological and biological divisions of the AWI together with scientists from the Netherlands (12 scientists) and the UK (3 scientists). Most non-German scientists participated in the framework of the Netherlands Bremen cooperation programme (NEBROC) as well as 2 EU projects MERLIM and CARUSO. This cruise is the third of a series studying the role of the Southern Ocean as source or sink of atmospheric CO2. The first cruise (ANT X/6) showed the overarching effect of iron availability in relation to mesoscale physics on the build-up of diatom blooms along the Polar Front and the resultant draw-down of CO_2 from the surface layer. The relationship between physics, trace metal availability and phytoplankton was studied in more detail during ANT XIII/2 by mapping a 3-dimensional grid with a towed, undulating instrument package. The data indicated that the accumulation of thick-shelled diatoms in the study region during the cruise was a result of heavy grazing pressure on the remaining phytoplankton. The shells of the heavily silicified species sink out of the surface layer and accumulate in the sediments which is probably the reason why the region underlying the southern Antarctic Circumpolar Current (ACC) is the major silica burial site in the ocean. The Polar Front is a prominent feature of the ACC and divides it into 2 branches most easily distinguished by their silicate content: Silica is never depleted south of the Polar Front and phytoplankton blooms were upto now observed only north of it. The previous cruises were carried out in spring and summer respectively; ANT XVI/3 addressed the autumn situation.

The 20°E meridian was selected as the study site primarily because bottom topography was smoother than further to the West. The location of the fronts and their hydrographical features were recorded by towing an undulating instrument package (SeaScan, see Chapter 4) along a transect between 46° S and 52°S following which the study site was fixed. Three moorings with current meters and sediment traps were deployed along the 20°E transect and two moorings without traps equidistant from the others along 49°20 S, the approximate position of the Polar Frontal jet. A grid of 140 x 140 km and with 15 km transect space in the centre of the diamond configuration of the traps was mapped with SeaScan. The 3-dimensional continuous mapping was accompanied by measurements of various chemical and biological properties of the surface water. The results indicated that the grid was located on a southward protruding meander of the Polar Front. Warmer water with lower silica and phytoplankton concentrations was subducting colder denser southern ACC water. A band of fairly high phytoplankton biomass was located at about 80m depth.

The situation encountered contrasted with earlier cruises where higher phytoplankton biomass was found north of the frontal jet and subducted silica-rich but phytoplankton-poor water to the south. Following mapping of the grid, a transect with 7 stations was carried out through its centre for sampling the water column. These results indicated that phytoplankton biomass was dominated by the thick-shelled pennate species *Fragilariopsis kerguelensis* that contributes the bulk of the silica ooze underlying the southern ACC. Detailed examination of the population across the front showed distinct differences in cell size and chain length that probably represented different life cycle stages. The subducted population at depth seemed to be in good condition. Laboratory experiments were carried out to assess the autecology of this enigmatic species. The iron concentrations in surface water of the grid were very patchy and interpreted as representing recent rainfall events.

Due to an emergency that arose at the station, the study site for the second research aim of the cruise was shifted from the continental shelf at 20° E to the shelf adjacent to the Neumayer station (8° W).

The biology of Krill in autumn, when the sea-ice cover starts expanding, is poorly known. Integrated studies have been initiated by SO GLOBEC in order to ascertain the mechanisms and processes that enable krill to maintain its population of long-lived individuals over the whole year. The following overwintering strategies are being debated: Krill either feed on ice algae and/or copepods, or starve and use body reserves including lipid. They are known to shrink on starvation and have survived many months in the laboratory without food. During ANT XVI/3 research necessary to find out the life history strategy of this pivotal organism was carried out along the eastern Weddell shelf. A subsequent cruise will study the situation along the western Antarctic Peninsula in 2001 together with ice-breaking vessels of other nations.

No krill was encountered in the ice-free waters around the Maud Rise on the way to the study area. Instead, salps dominated the plankton-impoverished water masses. Krill swarms of varying size and density were encountered and sampled during the nights between 50 and 150 m depth along the shelf break at the edge of the expanding ice cover. The profiles of the ship´s ADCP suggest that the krill swarms retreated during the day to depths exceeding 500 m. No krill was found immediately under the sea-ice cover.

The physiological properties of individuals (adults and furcilia) gently caught by vertical nets is being studied in experiments (feeding behaviour, respiration, excretion), the food spectrum of the autumn-caught individuals estimated (microscopy, delta 13C and delta 15N isotopes, lipid classes and fatty acid composition, free amino acids, gut fluorescence, carotinoids and chlorophylls) and overwintering mechanisms (growth and shrinking rates, starvation ability, C/N ratio, dry weight, total lipids, digestive enzymes, chitinases and proteases) studied. The feeding experiments carried out on board showed that the ingestion rates were greatly reduced compared to summer rates. Respiration and excretion rates were also lower by an order of magnitude than in summer, even when the animals were offered sufficient amounts of food of varying composition. Should these results be confirmed by subsequent analyses, they will indicate that krill reduces its metabolism by autumn independent of food availability. It is unclear how long such a seasonal adjustment takes place and whether the krill start feeding at normal rates when the ice algae start proliferating, remains to be ascertained.

After returning to the Polar Front, time constraints forced repetition of grid mapping at a coarser scale. All the moorings were successfully recovered after that and the transect along 20°E was repeated at the end. The results showed distinct changes in comparison to the earlier study. It remains to be seen whether our results are of regional relevance or applicable to the entire ACC. Because of cloud coverage over the ACC, remotely sensed information (by SeaWifs) on chlorophyll distribution is patchy and incomplete and phytoplankton blooms diffiult to assess because of their low concentrations (compensated by the depth to which they extend). Our data now enable calibration of the patchy information from SeaWifs in order to reconstruct and model net fluxes of carbon and silica.

The cruise was accompanied by regaular reports and photographs in the web site of the Süddeutsche Zeitung.

RV Polarstern reached Cape Town as planned on the 10th May 1999.

2. WEATHER

K. Flechsenhar (DWD)

Cruise, courses, weather and ice

RV Polarstern left the port of Cape Town on Thursday, March 18th at 20.00 hrs and steamed under fair weather conditions southward. The 40th latitude south, was crossed on the 20th and the ship came under the influence of several low pressure systems, which move generally eastward between 50° and 65° S, giving this part of the ocean the historical names "Roaring Forties" and "Howling Fifties". So westerly winds between 6 and 8 Bft occured on 20th and 21st, with the seas about 3 m. Nevertheless moorings belonging to the Kiel Institut für Meereskunde, could be set out regularly.

The wind decreased on the 22nd, but on the 23rd, the first snowfall was observed at 48°S, Wind SW 8 to 9 Bft , sea 3.5 m , temperature about 2°C. The ship dwelt until April 6th in the area around 50°S 20°E, operating intensive station work, tracking profiles with the ScanFish and putting 5 moorings in a square of about 30 Nm side length. The weather was partly fair, partly stormy with Bft 8 to 9, gusts up to Bft 11 from NW to SW. As the ScanFish could be operated under bad weather conditions - only bringing the ScanFish in and out needs a rather calm ship - and other station work had been done under good weather conditions, almost no time had been lost and the program continued as planned.

On April 6th RV Polarstern headed to Neumayer Station on a SW course. The next morning the course was changed to S, as the ship's meteorological station warned of an approaching storm and advised this deviation. Upon doing this, the ship found itself on April 9th in the rather calm center of a depression at 60°S 18.5°E, where intensive station work could be carried out.
Until April 12th we proceeded now W to SW. This located the ship south of the depressions moving east between the latitudes 60° and 65° S, and the dominating strong easterly wind could be used in our favour and the ship made good speed.

The first iceberg was sighted on April 6th at 50.4°S, temperature of air and water 3°C. In the evening of April 12th the edge of the sea-ice was reached at 69°S, 6°W, temperature of air -12°C, of water -1.7°C. The weather was calm and clear when Polarstern broke through the new ice, which became thicker and thicker. In the morning of April 13th we went alongside of the shelf ice edge, about 18 km north of the Neumayer Station.

Here the weather was cold and clear at first, and the planned journeys to Neumayer and back could be done without a risk. As on this cruise Polarstern had no helicopter on board, the trips had to be done over land (ice) by Pistenbully. So about 4 hours had to be calculated for one trip there and back. At the day´s end a light snow drift set in, which increased until the late evening to a heavy snow storm, so that "Polarstern" had to cast off the shelf ice edge.
The easterly storm increased to Bft 8 to 9 on 14th and reached Bft 11during the 15th, before it decreased in the evening. During this storm situation the ship lay calm and was protected in the ice. An intended walk and sampling on the sea ice had to be given up, because of the bad weather.

Until the evening of April 20th the ship maneuvered under good weather conditions - except some snow fall on the 16th - in the sea ice, operated stations, taking samples and doing measurements on the ice. On April 21st the ship was back in open water at 68°S 1.5°W. The sea was calm and we headed now to the position 54°S 20°E, which was reached on April 25th. During this long northeasterly transect, Polarstern was placed between a ridge of high pressure in

the west and a depression in the east, which moved synchronous with the ship eastward and created a strong but favourable southwest wind.

During the night of the 24th and early morning of the 25th, northwest wind Bft 8 was reported, but decreased during the day, so that the intended station work could be done. After that the ship steered north on the meridian 20° E towing the ScanFish. The last iceberg was sighted on the 26th near 52° S . In the morning of April 27th we arrived at 49.8° S 19.8° E under the influence of a high-pressure system, and the first of the five moorings could be recovered, after a fog patch had moved away. However the plan, to pick up a second mooring in the afternoon, had to be cancelled because of poor visibility and the end of daylight.

As the visibility did not improve and the sea became rough, profile tracks with the ScanFish were carried out until the morning of April 29th, before the second mooring was taken on board in the afternoon. This was soon followed by the recovery of moorings three and four on April 30th, these operations beeing carried out under rough, but sufficient weather conditions.

Finally mooring five was recovered in the morning of May 1st under the influence of a calm high pressure system. After the end of a further station the ship steamed southward to 52°S 20°E, where on May 2nd, more intensive station work was done. Here again a northerly to northwesterly storm, which occurred during the night from May 1st to May 2nd, had a favourable effect. The station work itself however could be done under better weather conditions during the day. From now, the ship sailed northward exactly on the meridian 20° east, operating station works about every 30 Nm. Doing this, Polarstern came into the cold side of a storm center, which developed in this area and caused windforce Bft 10 with severe snow squalls from SW during the noon of May 3rd. Therefore one station, planned at 50.5°S, had to be skipped.

On May 4th and 5th the sea was rough and frequent snow showers occured, nevertheless the operations continued as planned. On May 6th the sea calmed down and the temperature reached up to 9° C. Finally the last station work was done in the evening of May 7th under calm weather conditions, caused by a large and stable high, which accompanied Polarstern on her way to Cape Town , which was reached in the morning of May 10th.

Fig. 2.1: Distribution of wind directions in area between 48°S/20°E and 52°S/20°E for period 23.03.-07.04.99

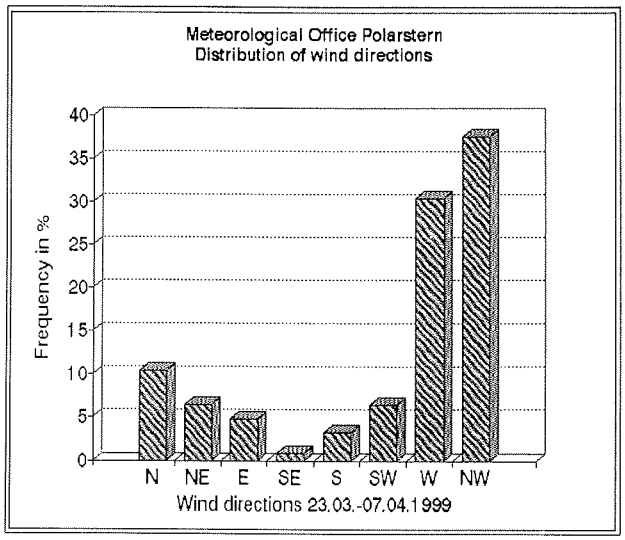

Fig. 2.2: Distribution of wind forces/Bft. in area between 48°S/20°E and 52°S/20°E for period 23.03.- 07.04.99

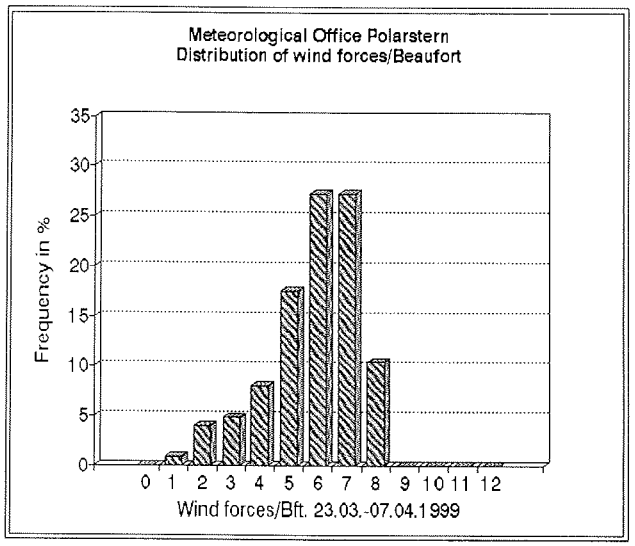

Fig. 2.3: Distribution of wind directions in area 48°S/20°E and 52°S/20°E for period 26.04.-05.05.99

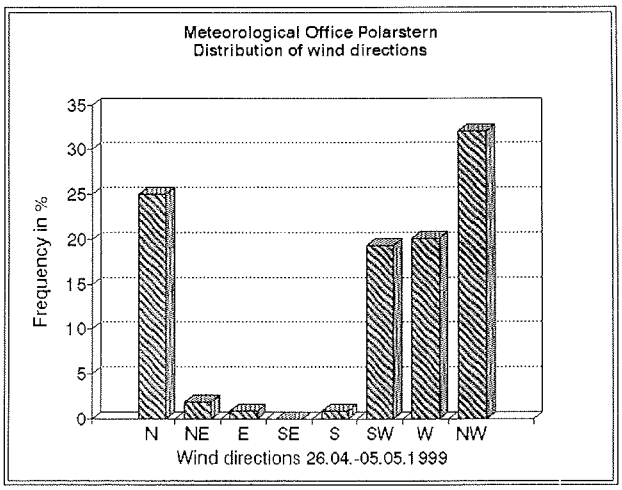

Fig. 2.4: Distribution of wind forces/Bft. in area 48°S/20°E and 52°S/20°E for period 26.04.-05.05.99

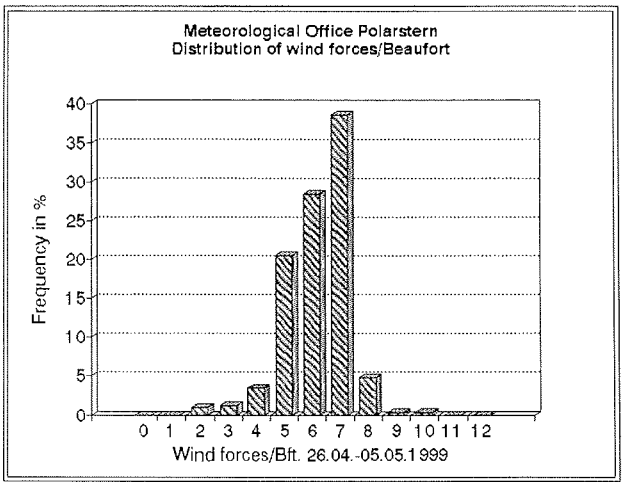

3. PHYSICAL CONTROL OF PRIMARY PRODUCTION AND OF BIOGEOCHEMICAL FLUXES AT THE ANTARCTIC POLAR FRONT

V. Strass (AWI), H.Leach (LIV)

Physical processes relevant to marine primary production play a central role in the climate system as a feedback mechanism between possible climate changes, which may result from alterations of the CO_2 concentration in the atmosphere, and the drawdown of carbon to the deep ocean and sediment by way of the biological pump. Within the global ocean, the Southern Ocean has an exceptionally high potential of influencing global climate by virtue of the biological pump, due to the excess of macro nutrients which are recently not consumed by primary production. Whereas most parts of the open Southern Ocean are rather low in phytoplankton biomass despite the high concentration of major nutrients, typifying the Southern Ocean as a HNLC (High Nutrient Low Chlorophyll) region, enhanced phytoplankton abundances are frequently reported from the circumpolar fronts. Which physical processes, however, make the fronts distinct in terms of primary production is not yet fully understood.

The physics of fronts can influence primary production by horizontal advection, or by the frontal dynamics which force vertical motion and the associated variation of stratification during frontal formation and decay. Vertical motion can resupply the photic zone with nutrients (macro and micro nutrients, e.g. iron) in the one place and carry phytoplankton down to aphotic depths and force sedimentation in the other place. The cross-front circulation associated with the vertical motions is able to modify the depth of the mixed layer within which the densest blooms favourably occur. The relevant horizontal scales, however, may be quite small (few tens of kilometres) and the time scales rather short (some days), posing considerable demands on the measuring system being used.

A previous survey, ANT-XIII/2, performed using an appropriate measuring technique in austral summer 1995/1996, revealed a close correlation of primary production, phytoplankton biomass and zooplankton abundance with frontal features such as meanders and eddies at the Antarctic Polar Front. Mesoscale cross-front circulation related to baroclinic instability was identified as a process of potential influence on mixed layer depth and thus on availability of light for photosynthesis within the mixed layer. However, the effect of cross-front circulation on shallowing of the mixed layer depth was masked by the seasonal stratification in high austral summer. Moreover, no substantial vertical export of biogenic material to greater depth was observed during ANT-XIII/2. An immediate outcome of ANT-XIII/2 hence was the need to assess the influence of mesoscale dynamics on primary production and sedimentation at other times of the year, particularly during the cooling season of austral autumn.

The primary physical measurements during this autumn cruise, ANT-XVI/3, were made by use of an instrument package combining a towed undulating vehicle (Scanfish) and a vessel-mounted acoustic Doppler current profiler (VM-ADCP) which allowed the mesoscale density and velocity structures of a front being mapped simultaneously with other physical and biological variables down to 250 m depth at high horizontal resolution in quasi-synoptic manner. To complement the quasi-synoptic maps, temporal variations of the current field in the survey area were recorded with an array of five moorings (Fig.3.0) equipped with acoustic and rotor current meters; three of the moorings also carried sediment traps. The hydrographic structure at greater depth was meassured with a CTD (Conductivity Temperature Depth) sonde lowered at a number of stations; the bottle sampler connected to the CTD allowed the collection of water from depth for analysis of dissolved constituents and suspended matter.

The different measurements are described in more detail in separate sections below. The Scanfish measurements are presented in section 3.1. Section 3.2 deals with CTD station work and water bottle sampling. The measurements of currents made underway by use of the VM-ADCP are presented in section 3.3, while section 3.4 contains a description of the moorings. Finally, section 3.5 deals with the measurements of acoustic backscatter by the vessel-mounted and moored ADCPs, respectively, as proxies of zooplankton abundance.

FS POLARSTERN

ANTXVI/3

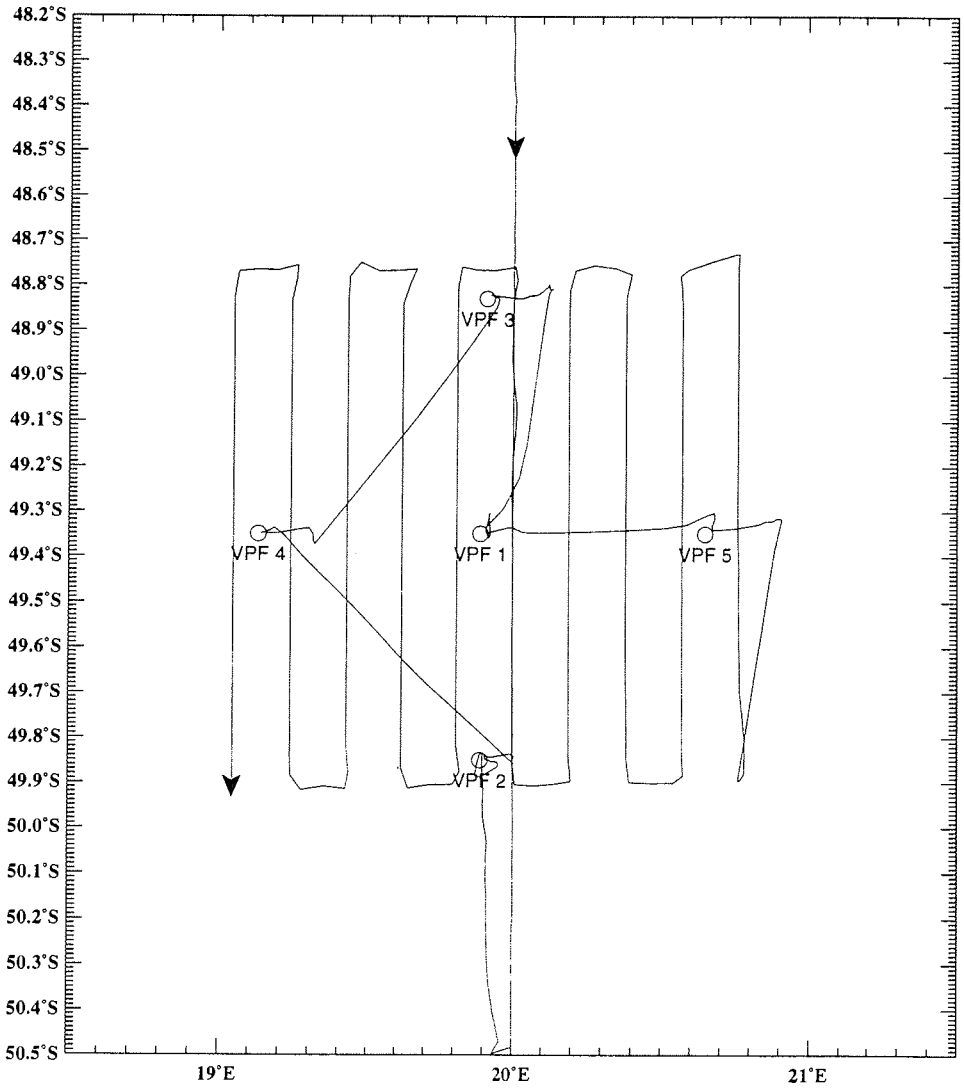

Fig.3.0: Cruise track from March 22 to April 2, 1999, during deployment of the five moorings, VPF1 - VPF5, and the subsequent Scanfish/VM-ADCP frontal survey.

3.1 Underway Measuremets of Hydrographic and Biological Variables with the Towed Undulating Vehicle 'Scanfish'

V. Strass, H. Leach, S. Gonzales, P. Roth, C. Dieterich, A. Macrander and M. Velthuis

The Scanfish (GMI Scanfish MK II) is a streamlined, wing-shaped body towed behind the steaming ship. By electrically tumable flaps at its rear end the Scanfish can be made to undulate vertically throught the upper water column according to the parameter settings entered at the control unit on deck. The depth range was enhanced by use of an active winch (Type Cormac 1500 assembled by Svendborg Skibshydraulik A/S) holding 2500 metres of 8.3 mm thick unfaired COAX towing cable, cable which was paid out during dive of the Scanfish and retrieved during climb. A depth range from 5 to 250 m was achieved at optimal towing speeds, between 5.5 and 7.5 knots. Those towing speeds, combined with a dive/climb rate of 0.4 m/s of the fish, resulted in a nominal horizontal resolution (half wavelength) of 2.6 to 3.6 km along-track. Scanfish attitude while being towed, as well as the scientific data, were monitored and recorded in real-time on deck.

The scientific payload of the Scanfish consisted of a CTD (Sea-Bird Electronics SBE 911*plus*) and a fluorometer (Chelsea Instruments). From the CTD measurements the hydrographic variables of state, pressure (depth), temperature, salinity and density were determined, while the fluorometer readings were used to derive chlorophyll concentration as an indicator of phytoplankton biomass. The CTD temperature measurements are assumed accurate to 0.001 °C according to the manufacturers specifications. Salinity was calibrated by relating the data from the upper Scanfish tuming points to concurrent readings from the hull-mounted thermosalinograph (POLDAT-TSK), which themselves were calibrated against salinity samples analysed using a salinometer (Guildline Autosal 8400A) in reference to I.A.P.S.O. Standard Seawater. The accuracy of the calibrated Scanfish salinities was estimated by the rms (root mean sqared) deviation as 0.005 (salinity units according to the Practical Salinity Scale PSS-78). The Scanfish fluorometer readings (Fl) were converted into concentrations of chlorophyll *a* (Chl) using a model in which the yield (Y = Fl/Chl) changes with ambient light. This enables to remove the quenching effect. The light dependency with depth was determined from underwater light profiles measured by Bernd Kroon. Horizontal changes of yield were taken into account by comparison with Chl determined by an accurately calibrated Tumer Designs flow-through fluorometer linked to the ship's sea water supply.

Measurements with the Scanfish were made during two meridional sections along 20° E (Runs 01 and 11) and during two mesoscale surveys (Runs 04 and 12), as indicated in Table 3.1. The mesoscale surveys encompass an area of 126 km * 122 km in the latitudinal and longitudinal directions, respectively, with the longitudinal direction resolved by 10 parallel meridional legs during the first survey and by 5 legs during the second survey. Altogether, Scanfish was towed with success for a total distance of 2786 km.

Tab. 3.1: Scanfish Runs

	Start				End			
Run	Date	Time	Lat. S	Lon. E	Date	Time	Lat. °S	Lon. °E
01	22-03-99	06:42	46°00.61'	20°00.79'	24-03-99	21:11	51°59.58'	19°59.30'
04	29-03-99	08:10	49°52.20'	20°47.04'	02-04-99	08:38	49°54.46'	19°02.83'
11	26-04-99	00:39	53°06.00'	19°59.94'	27-04-99	06:03	49°52.70'	19°48.56'
12	27-04-99	14:58	49°22.00'	20°34.00'	29-04-99	05:22	49°39.40'	19°25.68'

Fig.3.1a,b: Vertical distributions of potential temperature (a) and chlorophyll (b) concentration between 48° 46' S and 49° 54' S along 20° E, the central section of the first Scanfish front survey, Run04. The temperature section reveals a temperature minimum layer (Tmin layer, characteristic of a water mass termed Winter Water) that is centered at the depth range 180 to 200 m. The northern terminus of the Tmin layer, coinciding with the descent of the 2 °C isotherm, per definition marks the Antarctic Polar Front (APF). The sharp thermocline on top of the Tmin layer identifies the seasonal pycnocline. The seasonal pycnocline, obviously, is not identical with the depth of the mixed layer. The mixed layer is much shallower, shallower than 50 m, resulting from a surface layer of slightly warmer water and apparently of more northerly origin. The chlorophyll section shows a deep Chl maximum centered between 60 and 70 m which extends from the southern end to roughly the position of the APF. The highest concentrations within the deep Chl maximum occur above the lowest temperatures within the Tmin layer. Apparently, the deep Chl maximum is formed by subduction, caused by overlayering of warm, and yet chlorophyll-poor, water at the surface which crossed the APF from the north.

Fig. 3.1c,d: Horizontal distributions of temperature at 180 m, roughly the depth of the Tmin layer (top panel) and chlorophyll concentration at 70 m, roughly the depth of the deep Chl maximum, during the first mesoscale Scanfish survey, Run 04. The 2 °C isotherm shown in the temperature map approximately marks the course of the Antarctic Polar Front (compare with the horizontal current field shown in Fig. 3.3.2); a slight meander of the APF, a southward displacement around the central longitude, is evident. As revealed by comparison with the Chl map, the APF is associated with a horizontal gradient of the chlorophyll concentration; the highest chlorophyll concentrations, exceeding 0.6 mg m^{-3}, are found at the southwestern and southeastern corners of the survey area, correlated with the lowest temperatures.

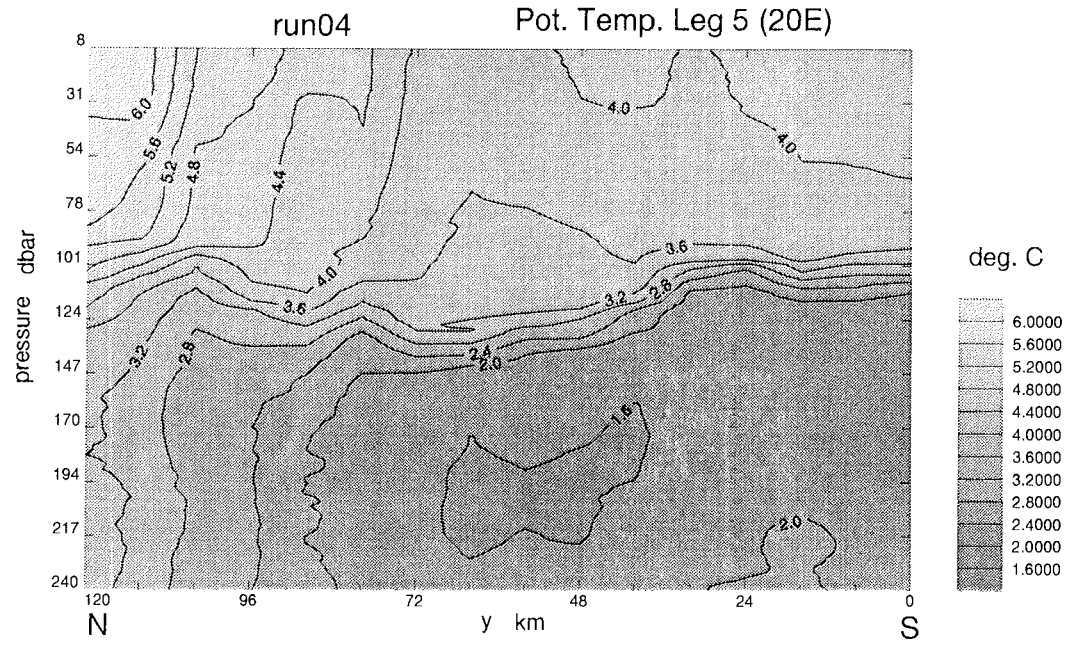
run04
Pot. Temp. Leg 5 (20E)
pressure dbar
8
31
54
78
101
124
147
170
194
217
240
120
96
72
48
24
0
N
y km
S
deg. C
6.0000
5.6000
5.2000
4.8000
4.4000
4.0000
3.6000
3.2000
2.8000
2.4000
2.0000
1.6000

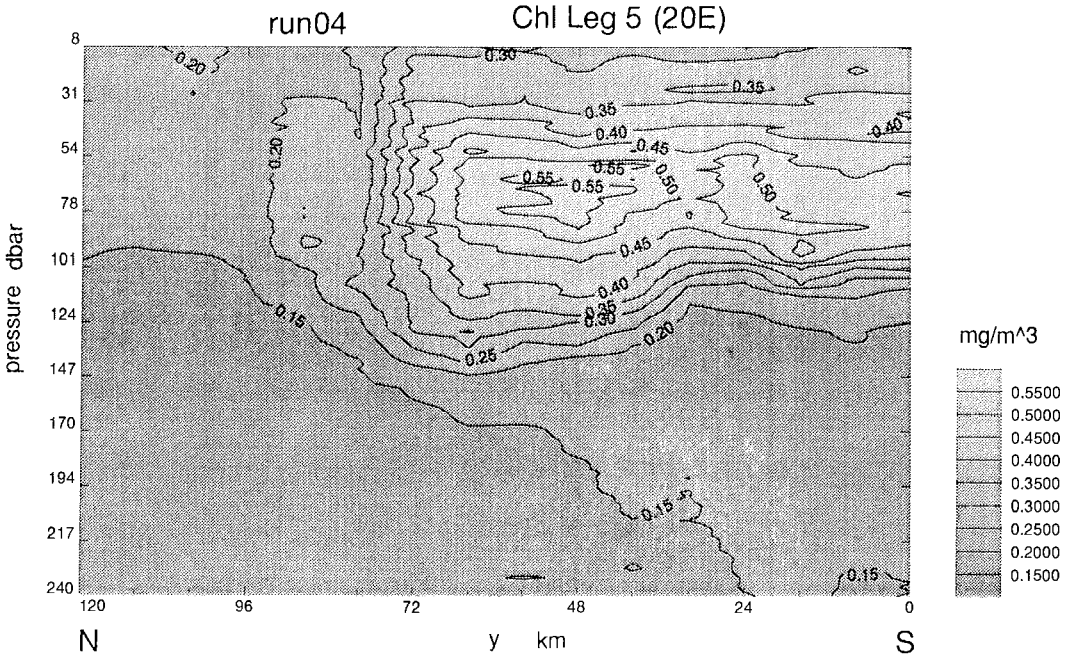
run04
Chl Leg 5 (20E)
pressure dbar
8
31
54
78
101
124
147
170
194
217
240
120
96
72
48
24
0
N
y km
S
mg/m^3
0.5500
0.5000
0.4500
0.4000
0.3500
0.3000
0.2500
0.2000
0.1500

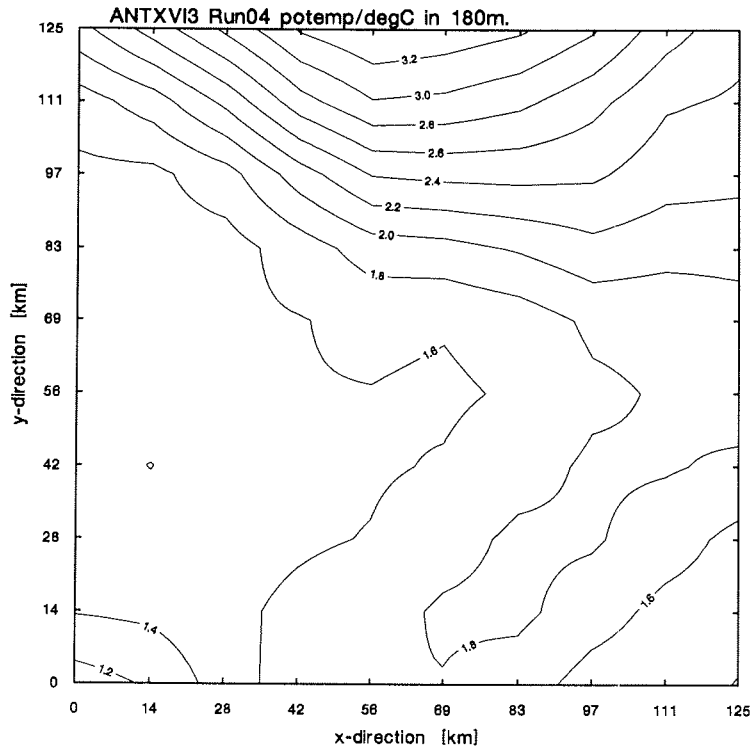
ANTXVI3 Run04 potemp/degC in 180m.
y-direction [km]
x-direction [km]
0
14
28
42
56
69
83
97
111
125
3.2
3.0
2.8
2.6
2.4
2.2
2.0
1.8
1.6
1.4
1.2

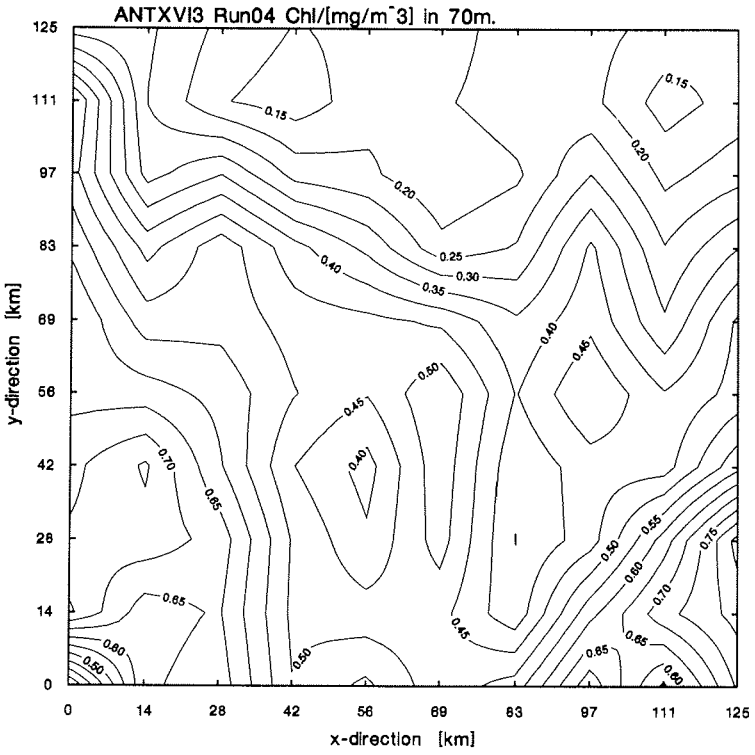
ANTXVI3 Run04 Chl/[mg/m^3] in 70m.
y-direction [km]
x-direction [km]
0
14
28
42
56
69
83
97
111
125
0.15
0.20
0.25
0.30
0.35
0.40
0.45
0.50
0.55
0.60
0.65
0.70
0.75
0.80
0.85

3.2 CTD Stations and Water Bottle Sampling

V. Strass, A. Macrander, C. Dieterich, P. Roth, S. Gonzales and H. Leach

The CTD used for conventional deployments at hydrographic stations was also type Sea-Bird Electronics SBE 911*plus*. The CTD was supplemented by a transmissometer (Wet Labs, 660 nm wavelength) and a chlorophyll-sensitive fluorometer (Dr. Haardt BackScat). The CTD and peripheral instruments were attached to a multi-bottle water sampler type Sea-Bird SBE 32 Carousel holding 24 12-liter bottles. The performance of the CTD was controlled by use of SIS reversing thermometers and pressure gauges attached to 8 of the water bottles. Salinity derived from the CTD measurements was calibrated to a final accuracy of better than 0.003 by comparison to salinity samples, taken from the water bottles, which were analysed by use of the Guildline-Autosal-8400A salinometer.

The main purpose of the CTD station deployments (Fig.3.2.1) was to reveal the hydrographic structures also at depths (Fig. 3.2) below the Scanfish range. Many of the overall 78 CTD casts (see Table 3.2), however, were performed to supply the water sample volume needed by other groups for chemical and biological research.

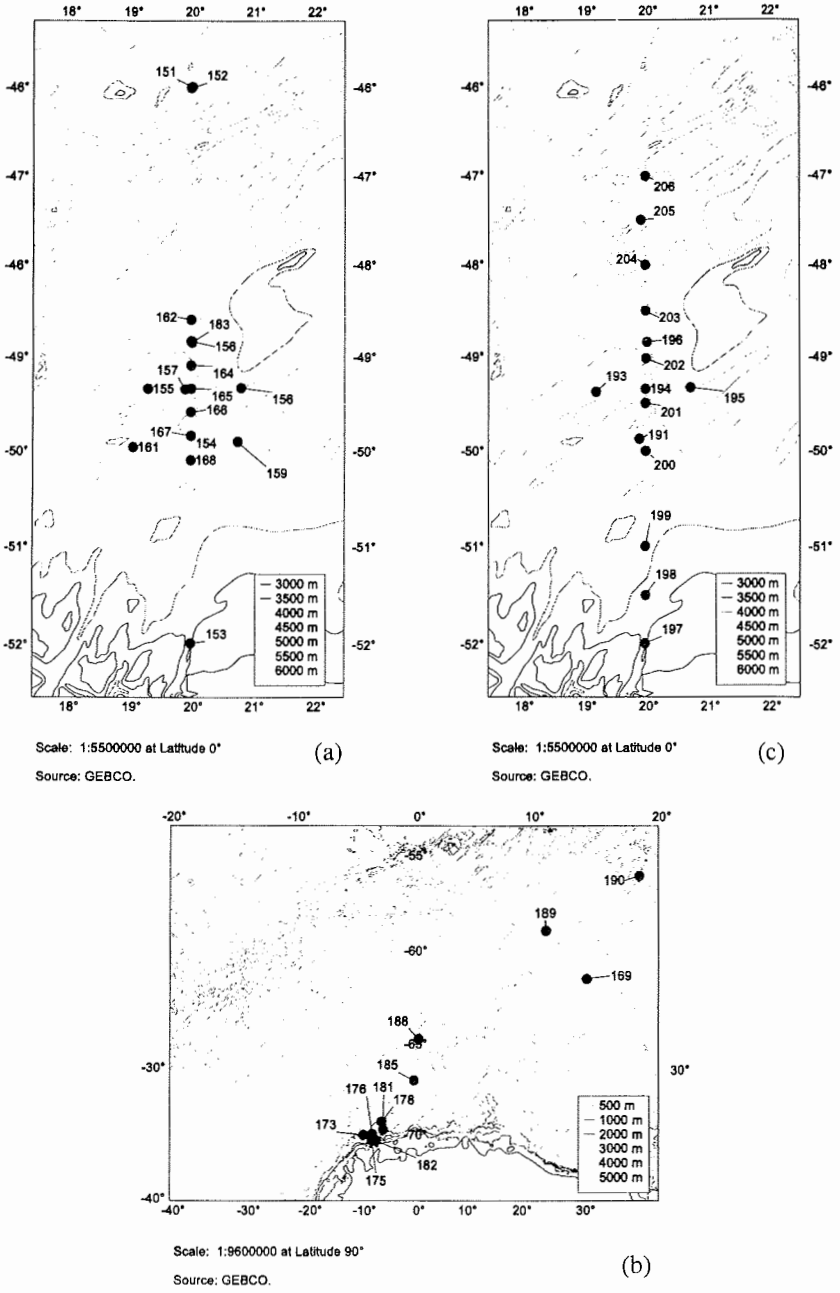

Fig.3.2.1: Maps of CTD station positions; stations performed before April 7 (a), stations done between April 7 and 26 (b), and stations performed after April 26, 1999 (c). The position of the northernmost station of the cruise, Station 207 (Tab. 3.2) is not shown.

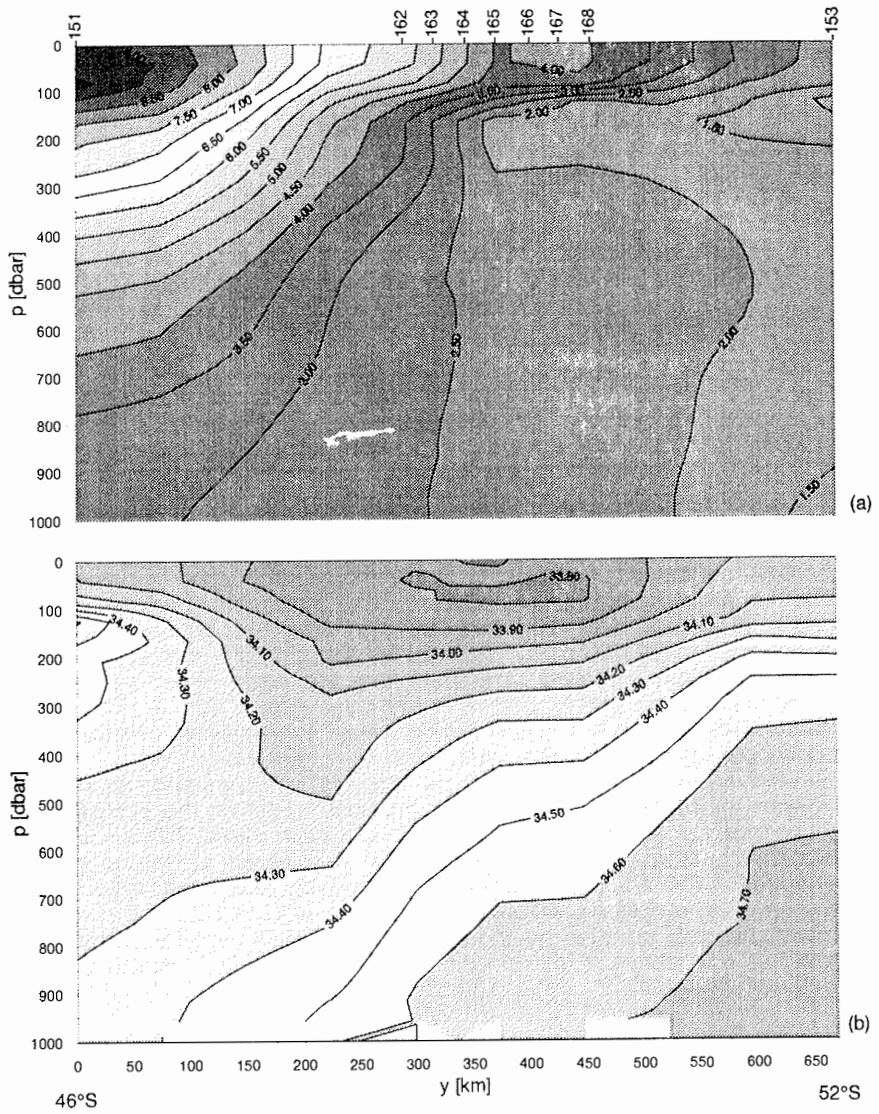

Fig. 3.2.2: Vertical distributions of potential temperature (a) and salinity (b) along 20° E, based on CTD stations; CTD station numbers are indicated on top.

(continuation on next page)

Fig. 3.2.2, continued

Fig. 3.2.2: Vertical distributions of potential temperature (a), salinity (b), uncalibrated fluorescence (c) and light transmission (d) along 20 °E, based on CTD stations; CTD station numbers are indicated on top. The temperature section (a) reveals the northern terminus of the temperature minimum layer. the position of the APF, between stations 164 and 165, i.e. between 49° 06' and 49° 20' S (Tab. 3.2). The northward subduction of the low-salinity surface water between stations 151 and 162 (b) is characteristic of the Subantarctic Front (SAF); the salinity increase southward of station 168 is related to a front termed Southerly Polar Front. The fluorescence section (c) shows a deep maximum, between 50 and 100 m depth, at stations 165, 166 and 167 (49° 20' - 49° 50 ' S), coinciding with the deep chlorophyll maximum revealed by the Scanfish survey done before; this deep maximum appears separated from the even higher values further south which are approximately uniform in the layer above 100 m. The section of light transmission (d) shows a less distinct deep transmission minimum, but a more continuous decrease to the south. The light transmission section also reveals a band of decreased values (increased turbidity) which extends to 1000 m or even deeper around the centre latitude of the section, below the subducted deep Chl (fluorescence) maximum between 50 and 100 m depth. Fluorescence itself is not significantly increased where transmission is lowered at depths greater 150 m, suggesting that chlorophyll pigments are already degraded in the material causing the lowering of light transmission at depth. A high sedimentation rate of biogenic material is also indicated by the sediment trap (see contribution by U. Bathmann) attached to mooring VPF2 (position of CTD station 167, where low transmission extends deepest).

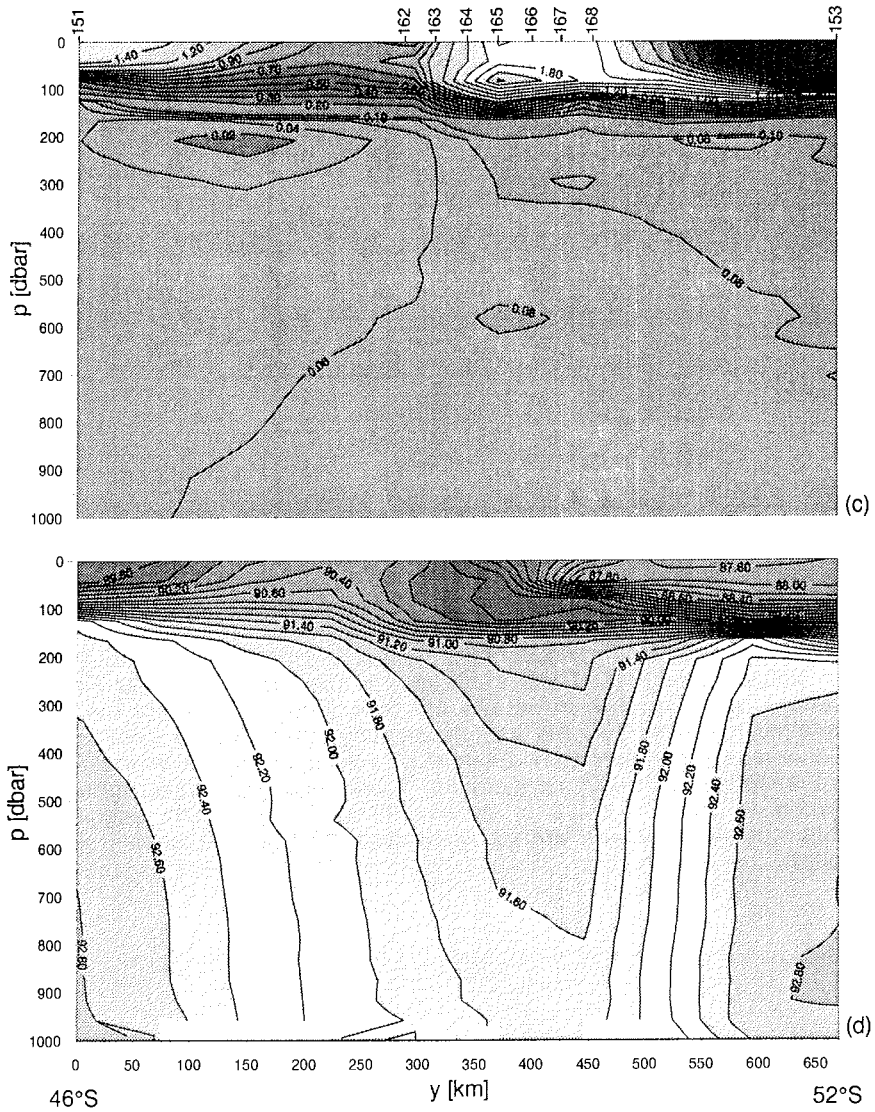
151
162
163
164
165
166
167
168
153
p [dbar]
(c)
(d)
46°S
y [km]
52°S

Fig. 3.2.3: Vertical profiles of potential temperature (left column), fluorescence (middle column) and light transmission (right column) at CTD stations 197/01 (top row), 198/01 (middle row) and 199/01 (bottom row); station positions as indicated in Fig. 3.2.1. The profiles are drawn at full vertical resolution. The small-scale noise and the spikes, sharp maxima or minima in the profiles of fluorescence and transmission, respectively, reflect the particulate nature of the fluorescent or attenuating substance. The most numerous and most pronounced spikes are found at station 198/01. That station, located in the Southerly Polar Front, exhibits a distinct two-layer structure above the core depth (200 m) of the Tmin water: a relatively shallow (50 m) and moderately warm mixed layer with maximum fluorescence and minimum transmission values; below, between 80 and 180 m, an intermediate layer with temperature, fluorescence and transmission values very similar to surface values at station 197/01 to the south, suggesting that the intermediate layer was formed by subduction of surface water of more southerly origin.

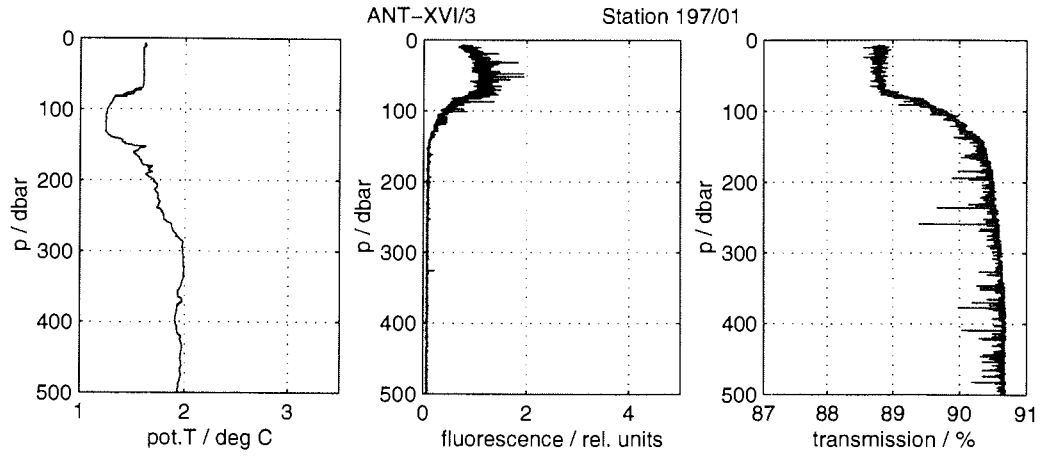
ANT-XVI/3
Station 197/01
p / dbar
pot.T / deg C
fluorescence / rel. units
transmission / %

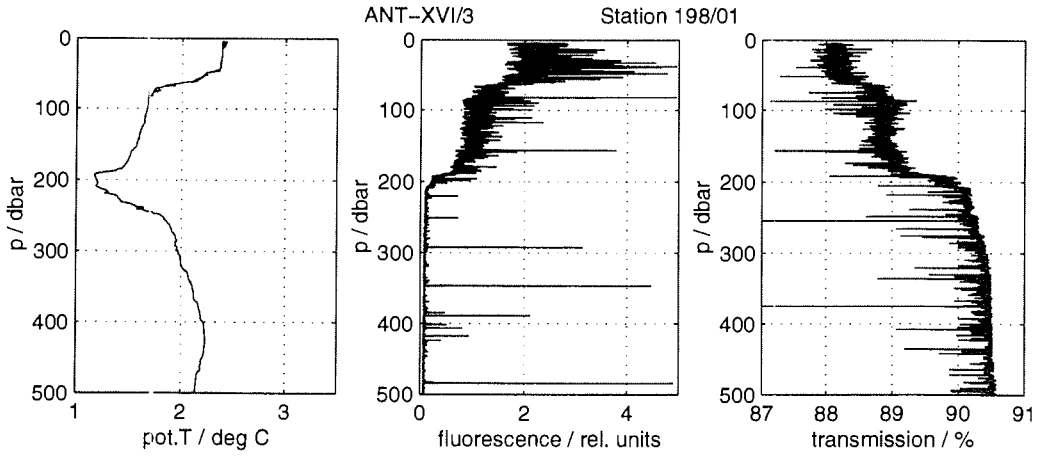
ANT-XVI/3
Station 198/01
p / dbar
pot.T / deg C
fluorescence / rel. units
transmission / %

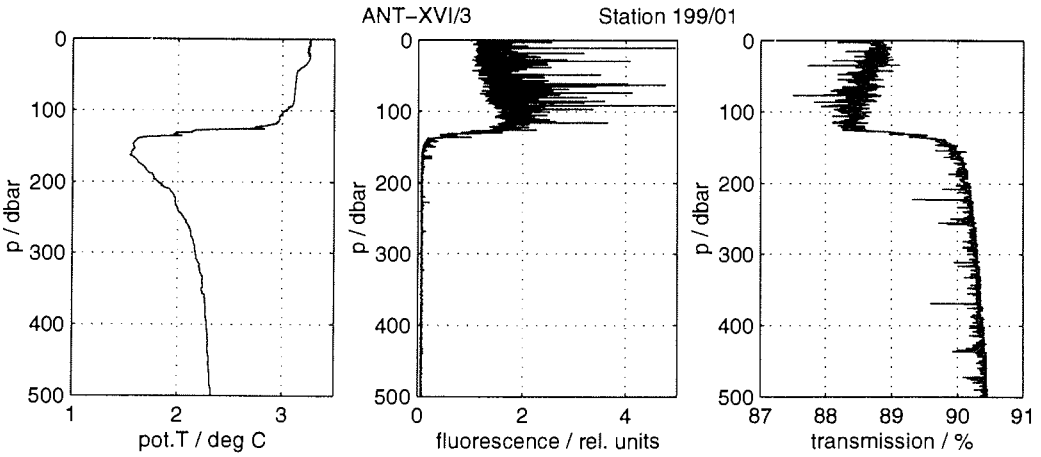
ANT-XVI/3
Station 199/01
p / dbar
pot.T / deg C
fluorescence / rel. units
transmission / %

Tab. 3.2: List of CTD Stations

Station/ Cast	Date	Time	Latitude Start	Longitude Start	Latitude End	Longitude End	Water Depth	CTD Depth	Gear Deployed
151/01	21.03.1999	15:41	45°59.48'S	20°01.18'E	45°59.52'S	20°02.22'E	4780	1040	
152/01	22.03.1999	6:05	46°00.07'S	20°00.16'E	46°00.06'S	20°00.04'E	4909	325	MN, start SF 1, start IF
153/01	24.03.1999	23:45	51°59.00'S	20°00.00'E	52°00.69'S	20°00.17'E	3451	3451	stop SF 1, stop IF, no data, to bottom
153/02	25.03.1999	3:46	52°00.94'S	19°59.95'E	52°01.38'S	19°59.91'E	3414	1001	
154/01	26.03.1999	9:11	49°50.03'S	19°59.84'E	49°51.23'S	20°00.04'E	4668	4668	VPF 2, to bottom
154/02	26.03.1999	13:52	49°51.39'S	20°00.16'E	49°51.45'S	20°00.34'E	4357	500	Bongo, MER, start IF
155/01	26.03.1999	22:56	49°20.15'S	19°17.98'E	49°21.57'S	19°18.85'E	4669	4669	VPF 4, MN, Bongo, stop IF, to bottom
156/01	27.03.1999	10:43	48°49.65'S	20°00.26'E	48°49.64'S	20°02.34'E	4831	4831	VPF 3, MN, to bottom
156/02	27.03.1999	15:33	48°49.35'S	20°03.44'E	48°49.33'S	20°03.84'E	4791	101	MER, ISP
156/03	27.03.1999	22:08	48°48.70'S	20°07.59'E	48°48.50'S	20°07.50'E	4748	1800	
157/01	28.03.1999	3:14	49°20.49'S	19°54.09'E	49°21.68'S	19°55.29'E	4613	4613	VPF 1, to bottom
157/02	28.03.1999	9:47	49°19.94'S	19°59.93'E	49°20.36'S	20°00.51'E	4611	505	MN, MER
157/03	28.03.1999	12:27	49°20.73'S	20°02.20'E	49°20.74'S	20°02.31'E	4620	22	
158/01	28.03.1999	20:02	49°19.77'S	20°49.35'E	49°19.28'S	20°52.25'E	4537	4537	VPF 5, MN, Bongo, to bottom
159/01	29.03.1999	5:56	49°53.85'S	20°45.87'E	49°53.53'S	20°46.22'E	4137	505	MN, start SF 4, start IF
161/01	03.04.1999	9:43	49°57.49'S	19°03.84'E	49°57.86'S	19°03.77'E	4684	500	GoFlo, Bongo, MER, ISP, stop SF 4, stop IF
162/01	04.04.1999	9:54	48°35.67'S	20°00.02'E	48°36.76'S	20°00.95'E	4098	995	MN, MER, 20°E section
162/02	04.04.1999	13:23	48°37.46'S	20°02.51'E	48°37.62'S	20°03.31'E	4180	300	FRRF
163/01	04.04.1999	16:13	48°50.36'S	20°00.68'E	48°50.62'S	20°02.35'E	4706	1000	GoFlo, MN, 20°E section
163/02	04.04.1999	20:15	48°51.44'S	20°05.74'E	48°51.70'S	20°06.61'E	4649	299	FRRF, no data
163/03	04.04.1999	22:08	48°52.35'S	20°07.22'E	48°52.68'S	20°07.18'E	4660	98	Bongo
164/01	05.04.1999	0:20	49°05.08'S	20°00.20'E	49°05.34'S	20°00.97'E	4579	200	MN
164/02	05.04.1999	2:33	49°05.46'S	20°02.11'E	49°05.91'S	20°03.68'E	4542	1001	20°E section
165/01	05.04.1999	5:37	49°20.04'S	19°59.97'E	49°20.35'S	20°00.39'E	4572	1010	GoFlo, MN, 20°E section
165/02	05.04.1999	10:02	49°21.68'S	20°00.56'E	49°22.41'S	20°00.42'E	4463	201	no data
166/01	05.04.1999	12:13	49°34.90'S	19°59.96'E	49°35.17'S	19°59.80'E	4675	301	FRRF
166/02	05.04.1999	14:58	49°35.67'S	19°59.28'E	49°35.83'S	19°59.42'E	4830	150	MN
166/03	05.04.1999	16:17	49°36.29'S	20°01.49'E	49°36.64'S	20°01.75'E	4663	1000	20°E section
167/01	05.04.1999	18:56	49°50.09'S	19°59.99'E	49°50.21'S	20°00.16'E	4610	1005	GoFlo, 20°E section
167/02	05.04.1999	21:27	49°50.40'S	20°00.13'E	49°50.51'S	19°59.99'E	4606	200	FRRF
167/03	05.04.1999	23:50	49°51.10'S	19°58.60'E	49°51.20'S	19°58.10'E	4079	31	MN, Bongo
168/01	06.04.1999	4:05	50°05.32'S	19°59.94'E	50°05.59'S	19°59.92'E	4701	1000	20°E section
168/03	06.04.1999	6:16	50°06.22'S	19°59.97'E	50°06.22'S	19°59.97'E	4653	120	MN

168/04	06.04.1999	7:44	50°07.14'S	20°00.32'E	50°07.88'S	20°00.31'E	4590	200	
169/02	08.04.1999	23:41	60°00.13'S	18°31.50'E	59°59.83'S	18°32.08'E	4744	4849	GoFlo, MN, ISP, to bottom
173/01	15.04.1999	23:08	69°49.17'S	08°04.59'W	69°48.83'S	08°05.83'W	1985	151	Bongo
175/01	16.04.1999	13:17	70°10.89'S	06°51.17'W	70°10.22'S	06°52.54'W	1773	1730	GoFlo, to bottom
176/01	16.04.1999	18:49	69°50.22'S	06°40.73'W	69°50.41'S	06°41.01'W	2368	191	MN, Bongo
178/01	18.04.1999	1:18	69°11.90'S	05°00.97'W	69°11.64'S	05°01.20'W	2527	51	RMT, Krill water
178/02	18.04.1999	2:05	69°11.07'S	05°02.45'W	69°10.96'S	05°02.92'W	2507	50	Bongo, Krill water
181/01	19.04.1999	2:19	69°39.06'S	04°50.41'W	69°38.77'S	04°50.63'W	2356	302	Bongo
182/01	19.04.1999	9:21	70°13.80'S	06°07.77'W	70°13.23'S	06°11.48'W	1231	1188	GoFlo, MN, ISP, to bottom
182/02	19.04.1999	15:07	70°11.94'S	06°18.80'W	70°11.18'S	06°23.09'W	1821	451	FRRF
182/03	19.04.1999	23:03	70°07.88'S	06°38.84'W	70°07.69'S	06°39.47'W	1974	21	IceIron, Krill water, no data
182/04	19.04.1999	23:58	70°07.19'S	06°40.85'W	70°07.06'S	06°41.16'W	1911	20	Krill water
185/01	21.04.1999	7:39	66°59.85'S	00°00.49'E	66°59.07'S	00°02.30'E	4644	4760	GoFlo, MN, to bottom
186/01	22.04.1999	8:15	64°43.21'S	00°36.41'E	64°43.15'S	00°36.62'E	3321	19	Bongo, Krill water
186/02	22.04.1999	9:15	64°42.82'S	00°36.51'E	64°42.78'S	00°36.42'E	3274	21	Krill water, no downcast data
189/01	24.04.1999	8:58	58°08.45'S	13°14.54'E	58°08.79'S	13°14.24'E	5413	149	Bongo
189/03	24.04.1999	9:59	58°09.02'S	13°14.33'E	58°09.14'S	13°14.37'E	5466	19	Krill water
190/01	25.04.1999	10:22	54°00.89'S	19°58.43'E	54°01.54'S	19°58.14'E	3450	1849	GoFlo
190/02	25.04.1999	13:04	54°02.09'S	19°58.07'E	54°02.15'S	19°58.01'E	3517	103	Bongo, ISP, start SF 10, start IF, no data
191/02	27.04.1999	9:56	49°52.44'S	19°54.22'E	49°52.88'S	19°54.06'E	3953	601	VPF 2, stop SF 10, start SF 12
193/01	29.04.1999	14:51	49°22.29'S	19°12.04'E	49°22.99'S	19°13.21'E	4742	4722	VPF 4, stop SF 12, stop IF, to bottom
194/03	29.04.1999	21:41	49°20.63'S	20°00.20'E	49°22.92'S	20°03.04'E	4478	4560	VPF 1, GoFlo, Bongo, to bottom
195/01	30.04.1999	14:36	49°19.76'S	20°44.03'E	49°19.48'S	20°44.91'E	4497	4514	VPF 5, Bongo, to bottom
196/03	30.04.1999	0:18	48°50.43'S	20°01.63'E	48°52.01'S	20°02.92'E	4660	4739	VPF 3, MN, Bongo, to bottom
196/04	01.05.1999	4:54	48°52.47'S	20°04.33'E	48°52.55'S	20°05.03'E	4637	601	
197/01	02.05.1999	9:56	51°59.19'S	19°59.52'E	51°59.57'S	19°58.86'E	3448	1004	20°E section
197/04	02.05.1999	15:04	52°00.40'S	20°00.26'E	52°00.45'S	20°00.39'E	3450	304	MN, GoFlo, ISP
198/01	02.05.1999	23:51	51°29.80'S	20°00.24'E	51°29.59'S	20°00.87'E	3069	1005	20°E section
198/03	03.05.1999	2:37	51°29.29'S	20°01.50'E	51°29.12'S	20°01.92'E	3054	603	GoFlo, MN
199/01	03.05.1999	6:51	50°59.76'S	19°59.96'E	50°59.66'S	20°00.35'E	4322	1001	Bongo, 20°E section
199/03	03.05.1999	9:24	50°59.54'S	20°00.74'E	50°59.46'S	20°01.79'E	4271	1005	20°E section
200/01	03.05.1999	17:59	50°00.02'S	19°59.99'E	50°00.05'S	20°00.41'E	4379	1008	20°E section
200/04	03.05.1999	22:25	50°01.15'S	20°01.87'E	50°02.02'S	20°02.60'E	4674	300	GoFlo, MN, Bongo
201/01	04.05.1999	4:01	49°29.70'S	20°00.19'E	49°29.72'S	20°01.06'E	4040	1001	20°E section
201/04	04.05.1999	6:53	49°29.73'S	20°02.22'E	49°29.79'S	20°02.95'E	4426	600	MN, Bongo
202/01	04.05.1999	10:45	49°01.07'S	20°00.57'E	49°02.19'S	20°02.73'E	4508	999	20°E section
202/05	04.05.1999	16:27	49°02.92'S	20°07.77'E	49°02.85'S	20°08.66'E	4364	300	GoFlo, MN, Bongo
203/01	04.05.1999	20:33	48°30.34'S	20°00.56'E	48°30.71'S	20°01.78'E	4370	1004	20°E section

203/05	05.05.1999	0:30	48°32.15'S	20°02.93'E	48°32.28'S	20°03.43'E	4293	300	MN, Bongo
204/01	05.05.1999	4:31	47°59.98'S	20°00.09'E	48°00.45'S	20°00.66'E	4626	1002	GoFlo, MN, Bongo, 20°E section
204/04	05.05.1999	10:53	48°00.80'S	20°02.33'E	48°00.79'S	20°02.50'E	4718	300	
205/01	05.05.1999	14:43	47°29.89'S	19°55.77'E	47°30.28'S	19°59.87'E	4109	1001	, 20°E section
206/01	05.05.1999	19:03	47°00.26'S	20°00.04'E	47°00.29'S	20°00.67'E	5056	1001	GoFlo, MN, ISP, 20°E section
207/01	06.05.1999	23:06	44°00.99'S	19°33.49'E	44°02.42'S	19°35.76'E	4576	4626	GoFlo, MN, ISP, to bottom
207/05	07.05.1999	12:19	44°06.78'S	19°50.25'E	44°07.12'S	19°51.62'E	4603	300	

3.3 Underway Measurements of Currents with the Vessel-Mounted Acoustic Doppler Current Profiler

V. Strass and J. Langreder

Vertical profiles of ocean currents down to roughly 300 m depth were continuously measured with a Vessel Mounted Acoustic Doppler Current Profiler (VM-ADCP; manufacture of RDI, 150 kHz nominal frequency), installed at the ship's hull behind an acoustically transparent plastic window for ice protection. The ADCP has four transducer heads, arranged in a square formation, which point diagonally outwards at an angle of 30° relative to the vertical. The transducer heads simultaneously emit a sound pulse approximately every second, and record echoes retumed from particles in suspension in the water. The echoes are range-gated into a series of vertical bins and analysed for their Doppler frequency shift which is related to the water velocity. Determination of the velocity components in geographical coordinates, however, requires that the attitude of the ADCP transducer head, its tilt, heading and motion is also known. Attitude variables of the VM-ADCP were taken from the ship's navigation system.

The instrument settings were chosen to give a vertical resolution of current measurements of 4 m in 80 depth bins, and a temporal resolution of 2 min after ensemble averaging. Calibration data for the ADCP velocity measurements were obtained during the cruise, but have yet not completely been evaluated; therefore, the VM-ADCP current measurements shown in Figs. 3.3.1 and 3.3.2 have to be considered as preliminary. Processing of the VM-ADCP data was done using the CODAS software package (developed by E. Firing and colleagues, SOEST, Hawaii).

Fig. 3.3.1: Horizontal currents in the depth range 152 - 186 m measured with the VM-ADCP along 20 °E between latitudes 45 °S and 52 °S. The band of strong eastward currents in the latitude range 46 °S to 47 °S is related to the Subantarctic Front, the band of enhanced eastward currents centered at 49 °S marks the Antarctic Polar Front, and the strong currents around 51.5 °S are associated with a front termed the Southerly Polar Front.

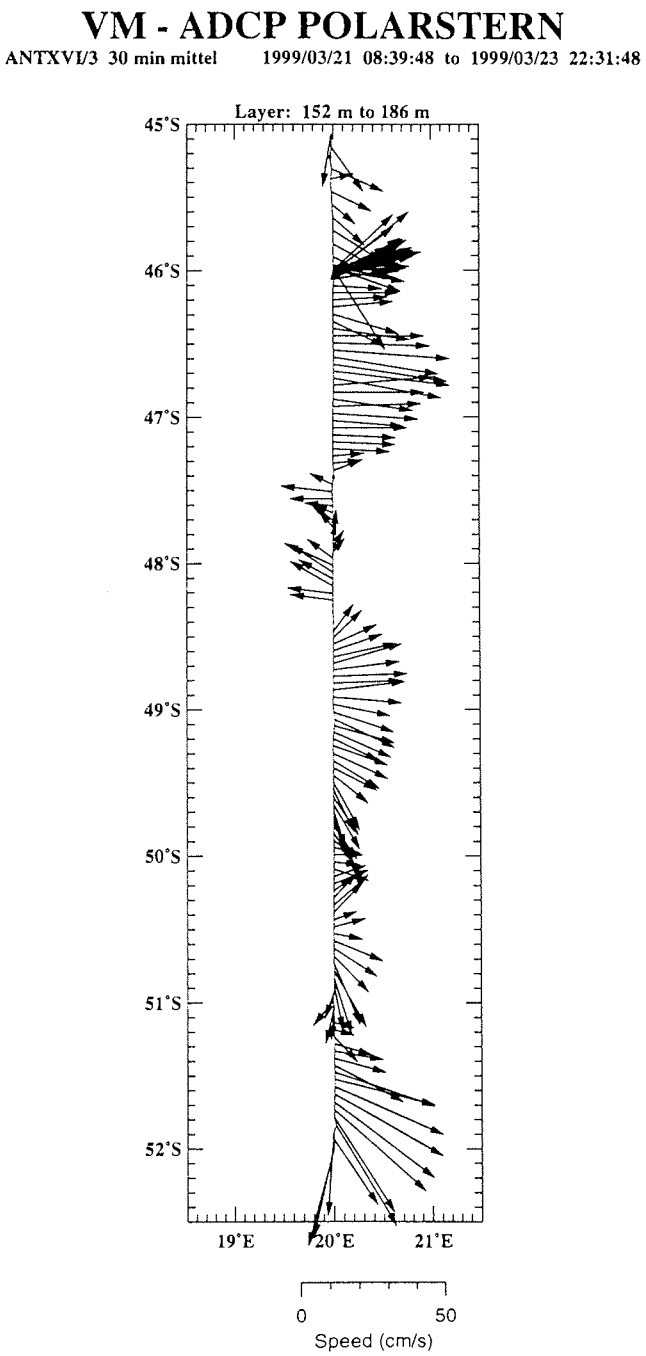

Fig. 3.3.2

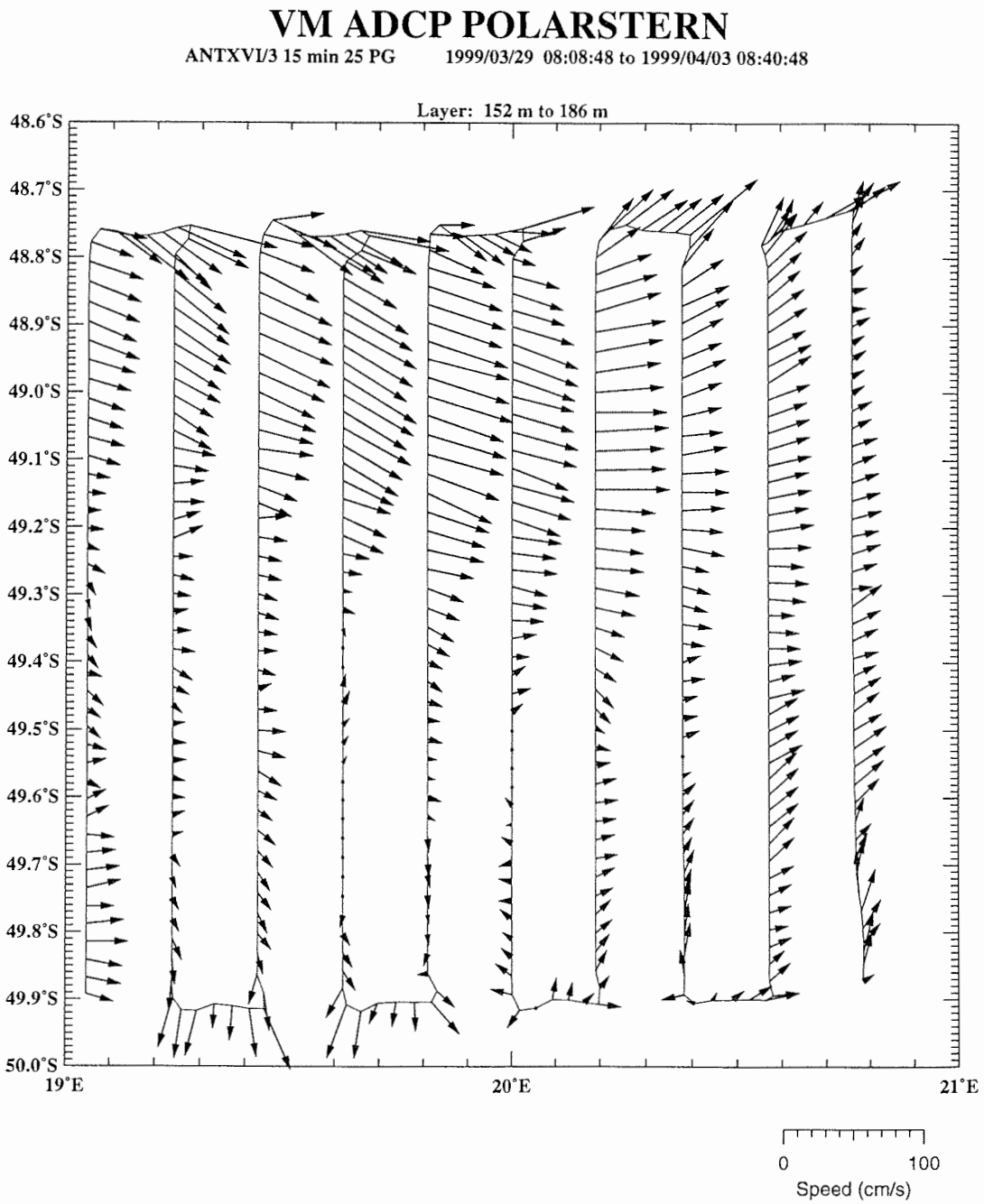
VM ADCP POLARSTERN
ANTXVI/3 15 min 25 PG 1999/03/29 08:08:48 to 1999/04/03 08:40:48
Layer: 152 m to 186 m
48.6°S
48.7°S
48.8°S
48.9°S
49.0°S
49.1°S
49.2°S
49.3°S
49.4°S
49.5°S
49.6°S
49.7°S
49.8°S
49.9°S
50.0°S
19°E
20°E
21°E
0
100
Speed (cm/s)

3.4 Measurements with Moored Instruments

V. Strass, M. Monsees, J. Langreder and U. Bathmann

Temporal variations of currents, hydrographic properties, and sedimentation in the frontal survey area were monitored by five moorings arranged in a diamond-shaped array (Fig.3.0). The moorings were deployed at the begin of the cruise and recovered at its end, for a duration of almost 5 weeks. To each of the five moorings were attached five Aanderaa rotor current meters, in part equipped with pressure, temperature and conductivity sensors. While the rotor current meters were distributed over the deeper part between the sea floor and a few hundreds of meters depth, upward looking self-contained (SC-) ADCPs were placed at the top of each mooring; one of the SC-ADCPs (all manufactured by RDI) was type 150 kHz Narrow-Band, two were type 150 kHz Broad-Band, and two were type 75 kHz Workhorse Long-Ranger. All SC-ADCPs and all rotor current meters, except of a failure in heading measurements by one of the Aanderaa's and a rotor loss by another one, worked properly throughout the deployment period during which data were taken at intervals of half an hour or less. Three of the moorings, those distributed along the meridional line (Fig.3.0) also included sediment traps (manufactured by Howaldt Deutsche Werft), of which two worked properly and revealed a striking difference in sedimentation between the southern and northern side of the Polar Front. In addition, the most southern mooring held a CO_2 recorder (from the Plymouth Marine Laboratory, R. Bellerby) on its top position. The set-up of that latter mooring is shown in Fig.3.4 as an example.

Fig. 3.4: Schematic drawing of mooring VPF-2, layed for the duration March 26 to April 27, 1999, at a position just south of the Antarctic Polar Front. From top to bottom, the mooring carried one CO_2 recorder (from the Plymouth Marine Laboratory, R. Bellerby), one RDI 150 kHz Broad-Band ADCP, one Aanderaa RCM8 rotor current meter, one sediment trap (HDW-SF), and four further RCM8 current meters. Connection between mooring line and anchor weight was through a pair of releases (one Mors and one EG&G; other moorings also included Benthos releases).

Fig. 3.4.

Mooring ID : VPF 2 Position : 49 50.40 S 19 54.29 E
Project : ANT XVI/3 Deployed : 08:13 , 26.03.1999
Waterdepth : 3950 m Released : 07:20 , 27.04.1999
Anker zuletzt!

-Depth-Dist.	Segments	Instruments		Time-in	Time-out
	1 Float				
- 47-3903		CO2-Recorder		06:25	08:05
	200 m (4.3mm)				
- 248-3702		ADCP SN 1626		06:36	08:05
	50 m				
	2 Floats	SMM500 SN 117			
- 304-3646		RQM8 VTC P1000	SN 9201	06:42	08:22
		XT 6000	SN 58116		
	50 m				
- 361-3589		HDW-Sedimentfalle		06:49	08:25
	40 m				
	100 m				
	500 m				
	4 Floats				
-1007-2943		RQM8 VTC P3000	SN 9211	07:03	08:44
	500 m				
	500 m				
	4 Floats				
-2013-1937		RQM8 VTP5000 o.Rotor	SN 12325	07:18	09:03
	500 m				
	500 m				
	2 Floats				
-3019- 931		RQM8 VT P5000	SN 12330	07:25	09:22
	2 • 200 m				
	2 • 200 m				
	50 m				
	6 Floats				
-3875- 75		RQM8 VT	SN 10497	08:03	09:42
	20 m				
		AR 661	SN 451	08:08	09.44
	1m Kette	EG&G	SN 14106		
	50 m				
	2m Kette				
	Anker 1000kg				

3.5 Measurements of Acoustic Backscatter by Vessel-Mounted and Moored ADCPs as Proxies of Zooplankton Abundance

V. Strass and J. Langreder

All acoustic Doppler current profilers, the ship's VM-ADCP as well as the moored SC-ADCPs have, routinely, also taken measurements of the backscattered echo amplitude. The amplitude of the received echo depends on the amount of scatterers, and their target strength, contained within the ensonified volume of water. It also depends, due to spreading of the sound beams and the absorption of sound energy by seawater, on the slant range between the transducer and the water volume.

The most effective scatterers are expected to have sizes in the order of the acoustic wavelengths, i.e. 1 or 2 cm, as implied by the ADCP frequencies of either 150 or 75 kHz, respectively. This is approximately the size of larger zooplankton. During the cruise advantage was taken of this relationship by using the backscatter signal of the VM-ADCP to decide on the deployment of nets for catching krill. Patterns of diurnal migration observed quite regularly in the VM-ADCP measurements (e.g. Fig.3.5) also indicate the influence of zooplankton on the backscatter signal.

Calibration of backscatter amplitude, yet to be done, has to take place in two distinct steps. First, calibration to give absolute Mean Volume Backscatter Strength (MVBS) in dB consists of correction for sound attenuation due to beam spreading and energy absorption, and of correction for differences of transfer efficiencies of the individual transducers and background noise levels. The background noise level effecting the VM-ADCP was determined at sea during the cruise. When the physical calibration has been performed an attempt shall be made to correlate MVBS with zooplankton abundance derived from net catches. That correlation, however, will be influenced by the presence of different zooplankton species with different compositions of soft tissue, hard shells and gaseous inclusions, for instance.

Fig.3.5: Vertical section of uncalibrated backscatter amplitude (agc) recorded with the VM-ADCP during one day (day 90 of year 1999, time of day referenced to UTC) while performing the front survey; the geographic position is indicated in the two lowest panels. The vertical dimension (y-axis) of the top two panels is scaled by bin number; bin zero is centered at 15 m depth, and the bin width is 4 m. While the top panel is based on raw profiles of agc, in the second top panel the agc decrease along the vertical due to sound attenuation is removed by presenting agc deviation from its daily mean within depth bins. The shown pattern is composed of a mixture of regional and temporal changes; however, similarities with other days of surveying in and adjacent to the front region suggest that at least the overall decrease during daylight hours (local noon is around day 90.45) results from vertical migration of zooplankton. Several scattering layers, with different diurnal vertical movements, can be distinguished.

Fig. 3.5.

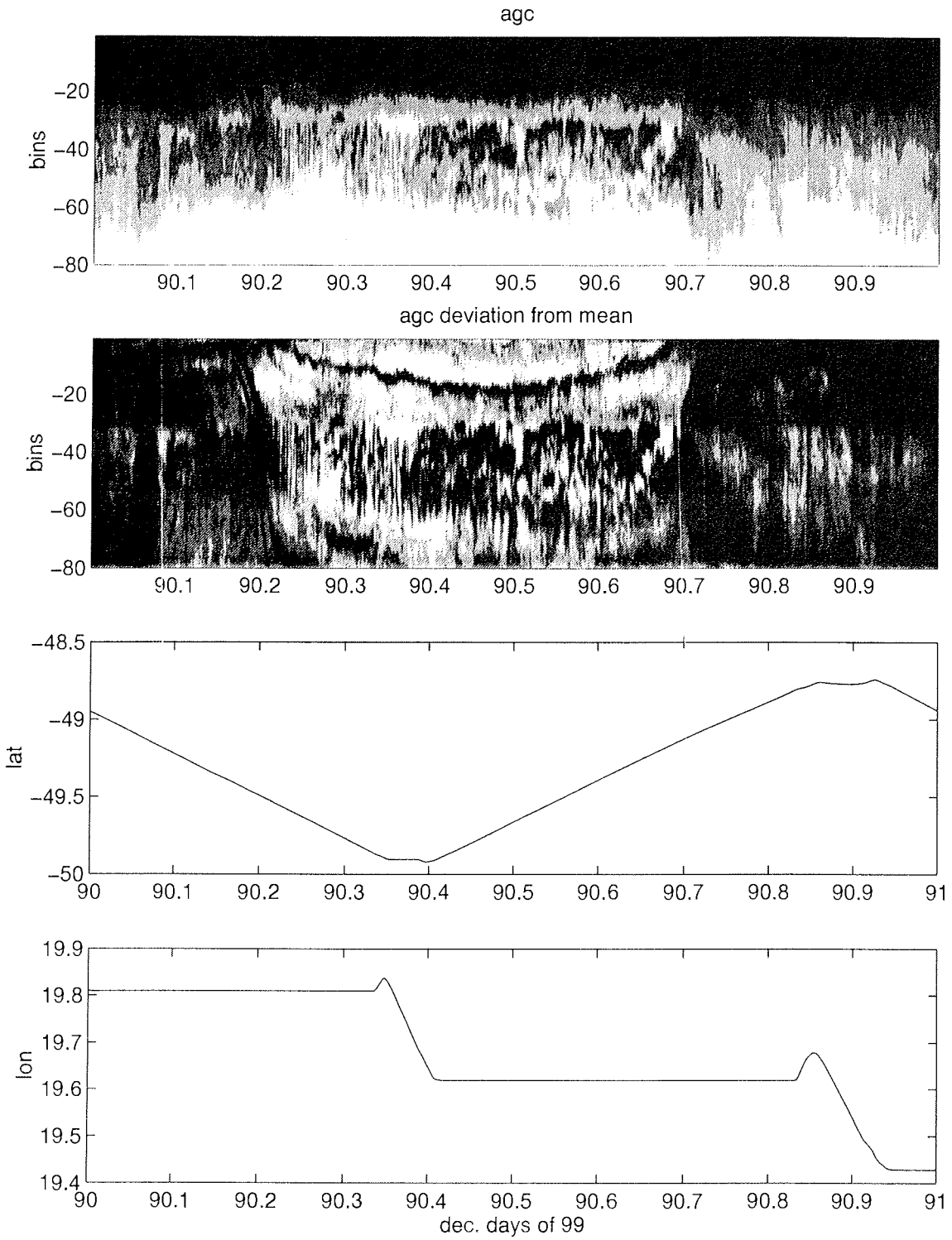
agc
bins
-20
-40
-60
-80
90.1
90.2
90.3
90.4
90.5
90.6
90.7
90.8
90.9
agc deviation from mean
bins
-20
-40
-60
-80
90.1
90.2
90.3
90.4
90.5
90.6
90.7
90.8
90.9
lat
-48.5
-49
-49.5
-50
90
90.1
90.2
90.3
90.4
90.5
90.6
90.7
90.8
90.9
91
lon
19.9
19.8
19.7
19.6
19.5
19.4
90
90.1
90.2
90.3
90.4
90.5
90.6
90.7
90.8
90.9
91
dec. days of 99

4. DISTRIBUTION OF NUTRIENTS

C. Hartmann, G. Kattner, A. Ratje (AWI)

The distribution and dynamics of nutrients in the Southern Ocean were investigated especially in the Polar Front during the two Scanfish grids by underway sampling with high spatial resolution and during CTD transects. Furthermore on the way to the German Neumayer base and back to the Polar Front until about 43°N underway surface sampling was conducted. The investigation of the interactions between nutrients and phytoplanktion are one of the major topic as well as the relation of nutrients to the hydrography. The data will be compared with those from the ANT XIII/2 expedition in 1996/97 to get information about seasonal changes by comparing the autumnal situation now with that from summer of the former cruise.

Sampling and methods

Nutrients were determined from underway samples, CTD bottles and Goflo bottles. Underway samples were taken from about 8 m depth by means of the membrane pump installed on board Polarstern. The sampling intervals were 10 min during the Scanfish grids and 20 min on the way south to the Neumayer base and back north to the Polar Front. The determination of silicate, phosphate, nitrate, nitrite and ammonium essentially followed the routinely used methods for seawater analysis and was performed with a Technicon Autoanalyser II system.

Preliminary data and results

Nutrients are closely related to the frontal systems. Their concentrations are generally high and are not limiting phytoplankton growth. Only north of the Polar Front silicate is low probably limiting the growth of diatoms. In contrast, nitrate and phosphate concentrations were always high in this area. In the Polar Front region surface silicate values were sightly increasing whereas towards the south the concentrations drastically rose reaching values of up to 70 µM. Nitrate concentrations already increased at the Subtropical Convergence to more than 10 µM and further increased towards the Polar Front to about 20 µM reaching highest surface value of 29 µM in the south. Surface phosphate concentrations (data not shown in the Figures) ranged between 1.3 and 1.6 µM in the Scanfish grid area and were highest with 2.2 µM in the south around 68°S in accordance with enhanced silicate and nitrate values.

The nutrient concentrations during the first Scanfish survey clearly showed the Polar Front. Silicate increased from about 3 µM north of the Front to about 6 µM in the south. Whereas in the middle area of the grid concentrations showed only slightly increasing gradients, they increased up to 16 µM and 14 µM in the western and eastern bounderies, respectively. This distribution revealed a meander-like structure in the survey area.

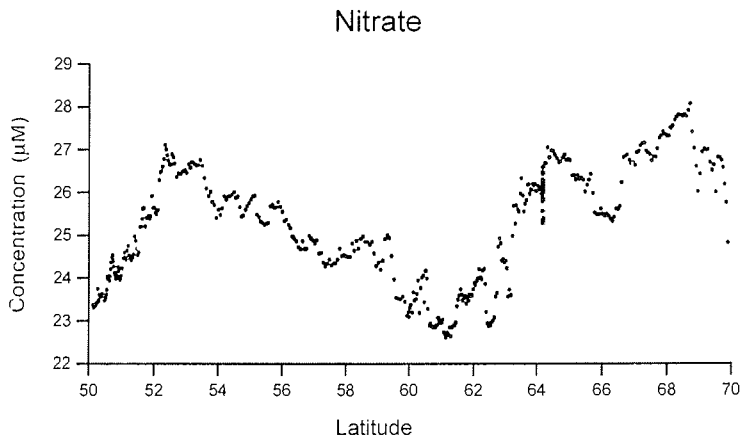
Nitrate
Concentration (µM)
29
28
27
26
25
24
23
22
50
52
54
56
58
60
62
64
66
68
70
Latitude

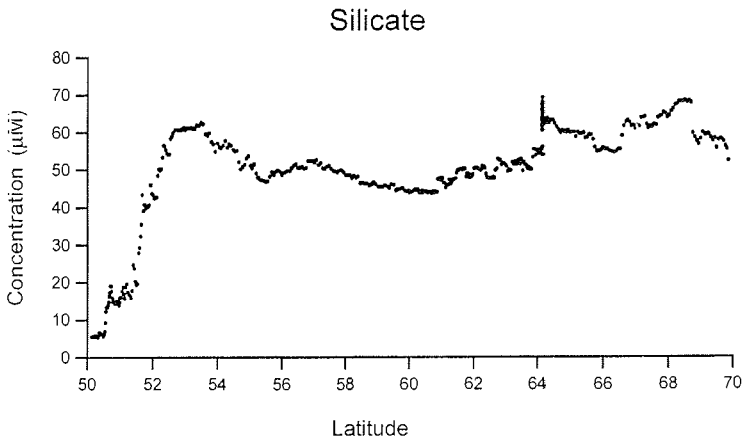
Silicate
Concentration (µM)
80
70
60
50
40
30
20
10
0
50
52
54
56
58
60
62
64
66
68
70
Latitude

Fig. 4.2a
2. Scanfish grid. silicate

Fig. 4.2b
2. Scanfish grid. nitrate

Silicate

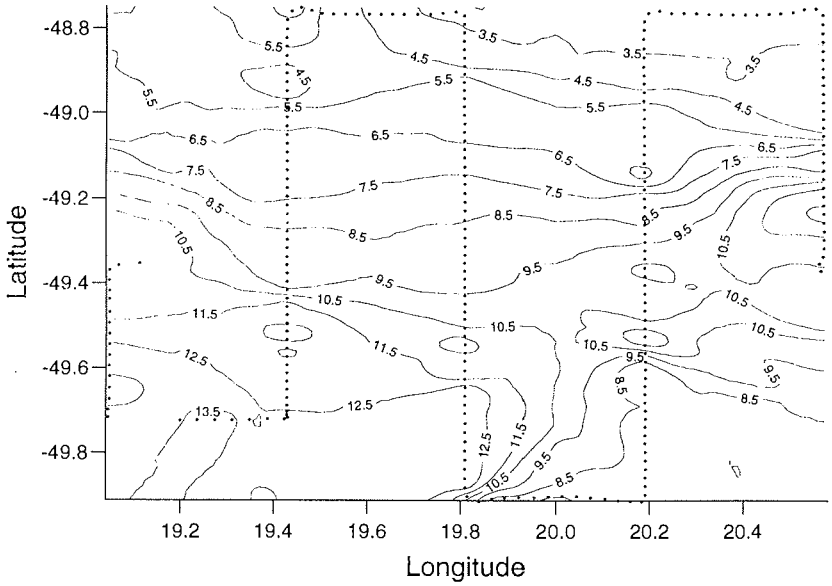

Nitrate

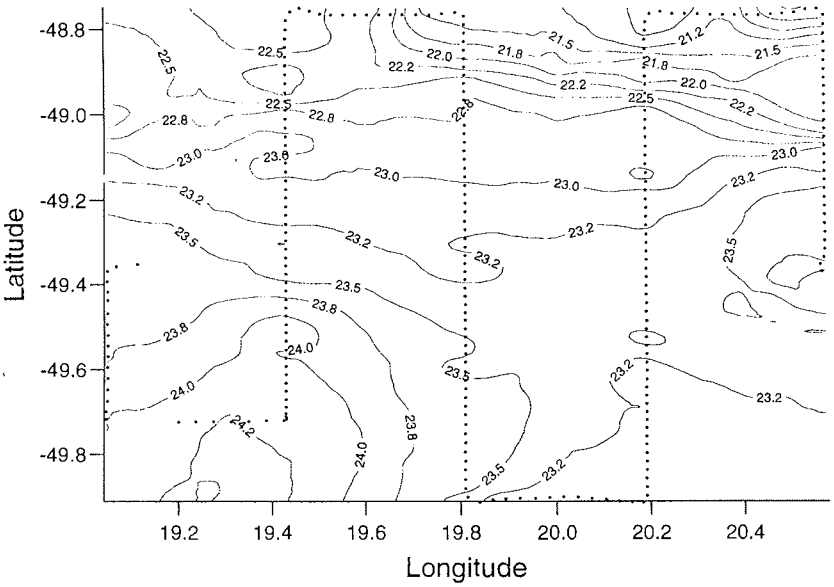

Fig. 4 3a
silicate data from the 2. CTD transect still under processing

Fig. 4 3b
nitrate data from the 2. CTD transect still under processing

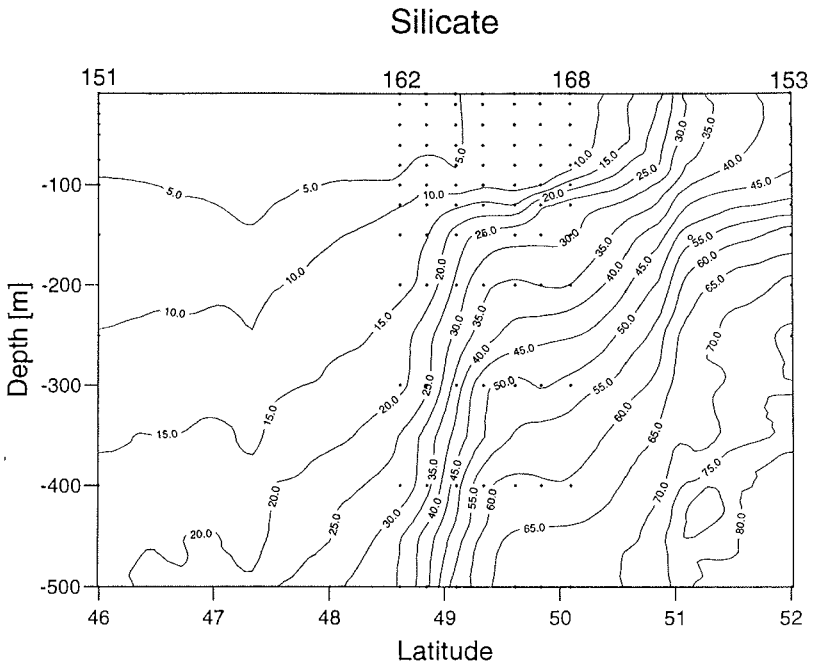

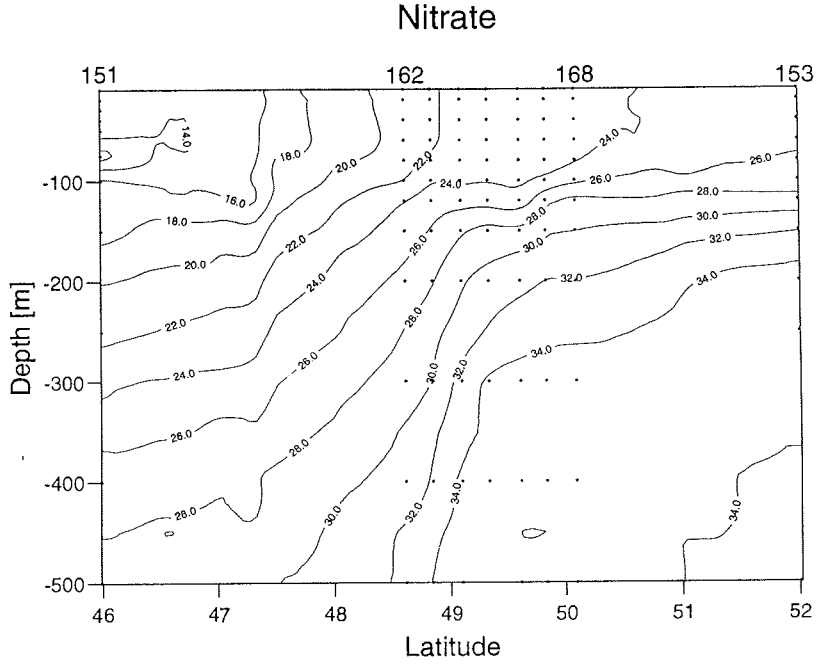

Nitrate concentrations north of the Polar Front were about 20 µM. In the Front they increased to 22.5 µM. In comparison to the silicate distribution nitrate only increased slightly to 24 µM in the eastern part of the grid. Due to the generally high concentrations nitrate reflected less clearly the meandering structure than silicate.

The surface silicate concentrations measured from north of the Scanfish grid towards the Neumayer base strongly increased south of the Polar Front reaching values of more than 60 µM, slightly decreasing further to the south. Until 64°S values were around 50 µM with small variations. Further south silicate peaks with up to 70 µM, staying contantly higher with some variations and then dropped very sharply in the Antarctic coastal current to about 60 µM.

The surface nitrate concentrations slightly increased in the Polar Frontal region to values of about 23 µM in the southerly Polar Front and in paralell with silicate to values of about 27 µM further south which than dereased to values of again 23 µM around 60°S. Highest values of up to 29 µM were found further south which also decreased again close to the Antarctic continent.

5. DETERMINATION OF THE STABLE C AND N ISOTOPES IN THE PARTICULATE ORGANIC MATTER

A. Dauelsberg, K.-U. Richter (AWI)

Work on board

In total 67 positions were sampled for the measurement of the distribution of the stable C- and N Isotopes in the total POM-Pool. This sampling consisted in 5 to 9 l filtrations out of the seawater supply from the ships membranepump on GF/F and MK360 quarzfiberfilters and should allow a characterisation of the isotopic distribution pattern in the suspended particles at the surface during the cruise.

To investigate the distribution in the different sizefractions of the total POM pool at 20 CTD-stations 80 l seawater from the mixed layer were further processed to split up the sample into the following POM-sizefractions: >100 µm, 100-20 µm, 20-8 µm, 8-3 µm, 3-1 µm and 1-0.4 µm. To get enough material for the isotopic measurements in each sizefraction, the particles out of these large volume samples were enriched by a cascade of sreen and membrane filters in special magnetic stirred filter housings.

This filtation procedure results in an enrichment of the marine particles in a volume of 1 L for the >100 µm and the 100-20 µm sizefraction. For the membrane fitration steps the final volume was reduced to 200 ml . Out of these enriched subsamples 20 ml for microscopic investigation of the composition of the organic matter were sampled and fixed. The residual volume was filtered over quarzfiberfilters and stored for isotopic measurement by isotope-ratio-mass-spectrometry.

Additional to the sizefractionated isotopic POM-samples, subsamples for the measurement of DOC, DIC and nutrients were taken. To compare the samples enriched from a large volume with the original plankton composition a subsample of 250 ml volume was taken directly from the niskin bottle of each sampled CTD cast.

The sampling for the investigation of the isotopic composition of the different sizefractions focused on the phytoplankton composition at the Polar Frontal Zone as well as the bloomconditions found at 52° S and should allow a comparison with the summer conditions during the previous JGOFS cruise ANT XIII/2.

To characterise the isotopic POM-composition in the second investigation area in the ice covered coastal current region a few CTD casts were sampled additionally.

6. FIELD DISTRIBUTION OF IRON IN A SECTION OF THE ANTARCTIC POLAR FRONTAL ZONE

P.L. Croot, J.T.M. de Jong (NIOZ)

Introduction

It is now well established that iron can play a role as a (co)limiting nutrient for phytoplankton in High Nutrient Low Chlorophyll (HNLC) regions of the ocean (e.g. de Baar, 1994 and de Baar et al., 1995), such as the waters of the Southern Ocean. However many questions remain about the biogeochemistry of iron in these regions. In particular, little is known about the sources of iron to the Southern Ocean, and the chemical nature of these inputs. This present work seeks to examine the contributions of the possible iron sources to the study region. These sources include the following: precipitation (dry/wet), advection of coastal water-masses from South America, iceberg melt-water, upwelling of iron rich deep water and hydrothermal sources.

The concentration of iron in deep waters is of particular interest, as little data is available for the Southern Ocean at present, and there is currently much debate (Johnson et al., 1997; Boyle, 1997; Luther and Wu, 1997) about the residence time and distribution of iron in the deep throughout the world's oceans. Typically in the old deep waters of the North Pacific, dissolved iron concentrations are approximately 0.6 nM, Johnson et al. (1997) proposed that this deep water value was found throughout the global ocean. Their hypothesis was however based on few points from younger deep waters, and would require that there was no fractionation between the Pacific and the Atlantic for iron. This result is somewhat in opposition to what is seen for other elements which show a biologically recycled profile and chemistry similar to iron (e.g. Zn, Th), as they are found at higher concentrations in the older Pacific deep waters than in the younger Atlantic deep waters. Thus in the present work we seek to investigate the deep water distribution of iron in Circumpolar Deep Water (CDW), Antarctic Bottom Water (ABW), North Atlantic Deep Water (NADW) and Antarctic Intermediate Water (AAIW). This work will also enable us to better model the cycling of iron in deep waters and place more realistic constraints on our estimates of iron supplied by upwelling waters.

To further assess the exact role of iron in phytoplankton bloom development, and the sources and sinks of iron in the Southern Ocean, it is important that accurate chemical analyses of iron are performed in combination with *in situ* measurements of several other sensitive physical, chemical and biological parameters. This multidisciplinary approach to studying the Antarctic Paradox has already been previously carried out successfully during previous cruises, onboard the Polarstern. This work has included EPOS 1988/89 in the Weddell and Scotia Seas, ANT X/6 in the Polar Frontal Zone at 6° W (1992), ANT XII/4 (1995) in the Antarctic sector of the South-East Pacific and ANT XIII/2 in the Polar Frontal Zone at 10° E.

Methods

During cruise ANT XVI/3 the structure of a sector of the Polar Front Zone was studied. The work was characterized by high density sampling and profiling of a small area of the frontal system, mainly focused on the ScanFish transect grids.

Spatial distribution of iron:

A total of 16 vertical profiles were measured, (see table 1), with 4 deep (> 1000 m) stations being occupied. The majority of these stations were situated in the PFR. A number of stations were also occupied between the primary research area and the German base "Georg von Neeumayer" to gather data on iron

concentrations in the Antarctic Circumpolar Current (ACC), the Weddell Sea and the Antarctic Coastal Current.

During the ScanFish transects, surface water was sampled. Most of the grid was sampled at one hour intervals, however during the 2nd major survey this was increased to half hour frequency. Samples were taken using a peristaltic pump connected to a polyurethane coated 'ironfish' (towed fish, torpedo style – 1m length and weighing 50kg in air), by acid cleaned polyethylene tubing. The 'ironfish' was towed alongside the ship at a distance of several meters from the hull at a maximum speed of 10 knots (ScanFish absent), when the ScanFish was towed simultaneously; speed was reduced to 6 knots. A water sample was delivered to and filtered inline (0.2 μm Sartorious filter) in the clean container every hour. The samples collected from the underway system were analyzed for dissolved iron onboard ship, analysis of the same samples for Al and other metals will be performed back in the home laboratory.

While in the sea-ice, the opportunity was taken to obtain some 'clean' snow and ice samples from the surrounding ice floes. The iron content of these samples will provide us with an indicator of the contribution of melting or freezing sea ice to the iron content of the coastal current and the seasonal ice zone.

Specimens of salps were collected and frozen, where possible, to examine the iron content of these 'vacuum cleaners' of the sea. Salps can filter several tens of litres of seawater per day (Dubischar and Bathmann, 1997), making them an effective remover of particulate material in the Southern Ocean. High grazing pressure by salps, may have a strong influence on the ratio between particulate and dissolved phases of iron.

Measurement of iron

To prevent sample contamination, trace metal clean techniques were applied. Samples were taken at predetermined depths using trace metal clean, Teflon™-coated General Oceanics GoFlo samplers with a volume of 10.8 l. These bottles were attached to a Kevlar hydrowire and tripped using Teflon messengers. On retrieval, the bottles were mounted on a specially designed bottle rack inside the anteroom of the NIOZ Class-100 clean air container. The GoFlo's were pressurized to 0.2 bar with clean dry N_2 gas, and connected inline to a Sartorious filter cartridge (0.2 μm) to obtain clean filtered samples. Samples were first taken for macronutrients, then dissolved metals (including samples for speciation work), finally unfiltered samples were taken. All samples for total metal analysis were acidified to pH < 2 with ultraclean quartz distilled concentrated nitric acid.
Total dissolvable (unfiltered) and total dissolved iron (0.2 μm) were measured on-board using a flow injection technique with in-line pre-concentration on a chelating resin followed by chemiluminescence detection (FIA-CL) (de Jong et al., 1998; Obata et al., 1993; Landing et al., 1986). Iron from an acidified sample is buffered on line and preconcentrated onto a column of immobilizied 8-hydroxyquinoline. After a loading time of 4 minutes, the column is washed with deionised water and the iron is eluted with dilute hydrochloric acid. The iron mixes with luminol, hydrogen peroxide and ammonium hydroxide to produce chemiluminescence in the flow cell of a photomultiplier tube connected to a photon counter. The chemiluminescence occurs as a result of the iron catalyzed oxidation of luminol (3-aminophtalhydrazide) by hydrogen peroxide, producing blue light (424 nm). The accuracy of the method was checked and confirmed using NASS-4 reference sea water. Throughout the cruise, the blank and detection limit (3x standard deviation of blank) remained constant at 0.032 and 0.01 nM respectively. Reproducibility was typically 2% at the 0.3 nM concentration and better than 10% at the 0.06 nM level.

The other trace metals (Mn, Al, Cd, Ni, Cu, Se, Zn and Co) will be analyzed in the home laboratory using a variety of well established techniques (includes FIA-CL, and both anodic and cathodic stripping voltammetry).

Preliminary results and discussion

Surface dissolved iron concentrations in the Polar Frontal Zone were found to vary considerable during both surveys. However for the second survey, iron concentrations were significantly lower (0.04 – 0.6 nM, average 0.16 nM) than during the initial survey of the ScanFish box (0.12 – 3 nM, average 0.56 nM). For the first survey (see figure 1), there was a trend towards higher iron levels in the southern part of the grid , and also a possible correlation with rain events during the survey work. It is hoped to later make back trajectory calculations of the air masses involved, to perhaps determine if these clouds could have contained significant continental aerosol dust.

Vertical profiles of dissolved iron from the Polar Frontal Region typically showed surface enrichment with a minimum at approximately the chlorophyll maximum. Often these profiles also exhibited higher iron concentrations just on or below the pycnocline, which may be evidence for regeneration of dissolved iron by zooplankton grazing. Samples from the coastal current (Station 182) showed high levels of both dissolved and total iron in the deep surface mixed layer (figure 2), much of this iron may have been supplied from iceberg melt in the summer or from coastal runoff from under the continental ice shelf. These high iron levels may help explain why this region is so productive during the spring and summer.

Data from the deep stations showed fairly uniform profiles for dissolved iron, all exhibiting a nutrient (regeneration) profile (see figure 3). Deep concentrations were typically around 0.3 – 0.4 nM, significantly below the Johnson et al. (1997) 0.6 nM. Later analysis will concentrate on looking at the iron concentrations of the individual water masses to try and understand the distribution of iron in the deep ocean.

In conclusion, iron concentrations in the Southern Ocean were found to be very low throughout much of the area surveyed, but higher concentrations were again found in the Polar Front as has been shown before on previous cruises (ANT X/6 and ANT XIII/2). However for this cruise the correlation between chlorophyll and iron was not so strong, as it has been for previous cruises carried out during the summer, and this may reflect the lower light levels (light limitation) found during the autumnal period. Additional measurements and data analysis are needed however to clarify the observed distribution and behaviour of iron in the Southern Ocean water samples at this time.

References

de Baar, H. J. W. (1994). von Liebeg's Law of the Minimum and Plankton Ecology (1899-1991). *Progress in Oceanography*, 33, 347-386.

de Baar, H.J.W., J.T.M. de Jong, D.C.E. Bakker, B.M. Löscher, C. Veth, U. Bathmann and V. Smetacek. (1995). Importance of iron for plankton blooms and carbon dioxide drawdown in the Southern Ocean. *Nature*, 373, 412-415.

Boyle, E. (1997). What controls dissolved iron concentrations in the world ocean? - a comment. *Marine Chemistry*, 57, 163-167.

Dubischar, C.D. and U.V. Bathmann. (1997) Grazing impact of copepods and salps on phytoplankton in the Atlantic sector of the Southern Ocean. *Deep-Sea Research II* , 44, 415-433.

de Jong, J.T.M., J. den Das, U. Bathmann, M.H.C. Stoll, G. Kattner, R.F. Nolting and H.J.W. de Baar. (1998) Dissolved iron at subnanomolar levels in the Southern Ocean as determined by ship-board analysis. *Analytica Chimica Acta*, 377, 113-124.

Johnson, K. S., R. M. Gordon and K.H. Coale. (1997). What controls dissolved iron concentrations in the world ocean? *Marine Chemistry*, 57, 137-161.
Landing, W.M., Haraldsson, C. and Paxeus, N. (1986). Vinyl polymer agglomerate based transition metal cation chelating ion-exchange resin containing the 8-hydroxyquinoline functional group. *Analytical Chemistry*, 58, 3031-3035.
Luther III, G. W. and J. Wu (1997). What controls dissolved iron concentrations in the world ocean? - a comment. *Marine Chemistry*, 57, 173-179.
Obata, H., Karatani, H. and Nakayama, E. (1993). Automated determination of iron in seawater by chelating resin concentration and chemiluminescence detection. *Analytical Chemistry*, 65, 1524-1528.

Table 6.1: Stations occupied during ANTXVI/3, sample depths and samples taken.

Station #	Sample Depths	Samples Taken
161	20, 40, 60, 80, 100, 150, 200, 400, 600, 1000m	Filtered and Unfiltered
163	20, 40, 60, 80, 100, 150, 250, 500, 750, 1000m	Filtered only
165	20, 40, 60, 80, 100, 150, 250, 500, 750, 1000m	Filtered only
167	20, 40, 80, 100, 150, 250, 500, 750, 1000m	Filtered only
169	20, 40, 60, 80, 100, 150, 300, 400, 700, 1000, 2000, 2500, 3000, 3500, 4000, 4500m	Filtered and Unfiltered
174	50 m	Filtered and Unfiltered
182	20, 40, 60, 100, 150, 200, 300, 800, 1100m	Filtered and Unfiltered
185	25, 50, 100, 250, 500, 1000, 1500, 2500, 3500, 4500m	Filtered and Unfiltered
190	20, 40, 60, 80, 100, 130, 250, 400, 700, 1000m	Filtered and Unfiltered
194	25, 50, 100, 150, 250, 500, 1000, 2000, 3000, 4000m	Filtered and Unfiltered
197	20, 40, 60, 80, 120, 200, 300, 400, 700, 1000m	Filtered and Unfiltered
200	20, 40, 60, 80, 200, 300, 400, 700, 1000m	Filtered and Unfiltered
202	20, 40, 60, 80, 120, 200, 400, 600, 800, 1000m	Filtered and Unfiltered
204	20, 40, 60, 80, 120, 200, 400, 600, 800, 1000m	Filtered and Unfiltered
206	20, 40, 60, 80, 130, 200, 300, 500, 700, 1000m	Filtered and Unfiltered
207	25, 50, 120, 410, 500, 1000, 1500, 2000, 2750, 3500m	Filtered and Unfiltered

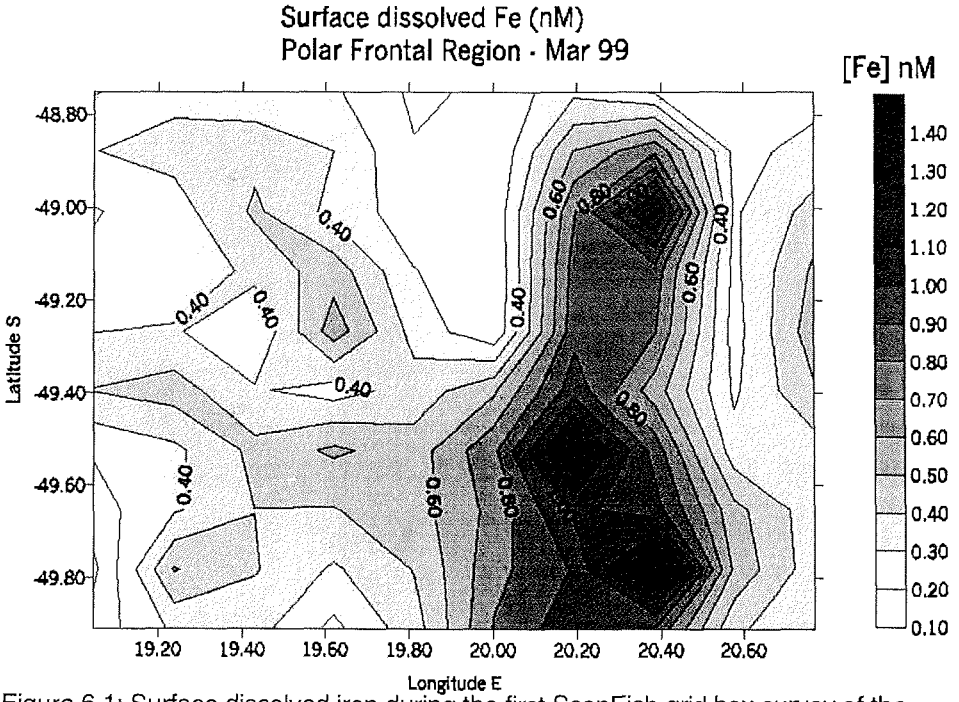

Figure 6.1: Surface dissolved iron during the first ScanFish grid box survey of the Polar Frontal Region.

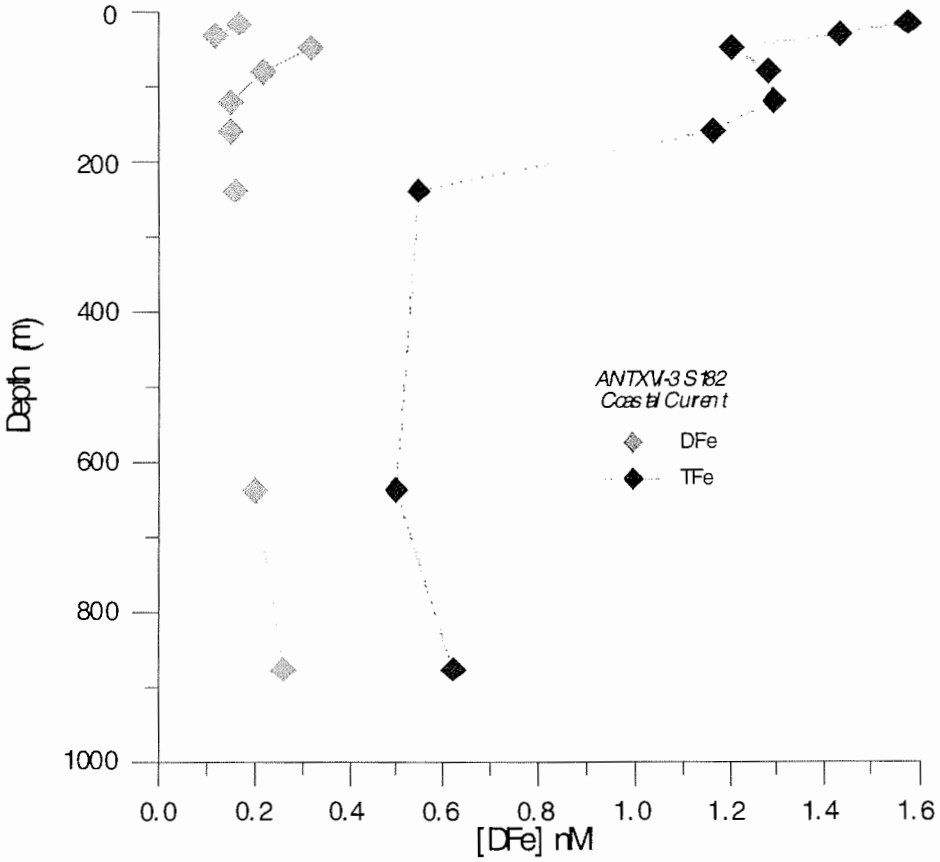

Fig. 6.2: Dissolved (0.2 µm) and total iron in the coastal current around Antarctica, at Station 182 (70° 13.8' S, 6° 7.77 W).

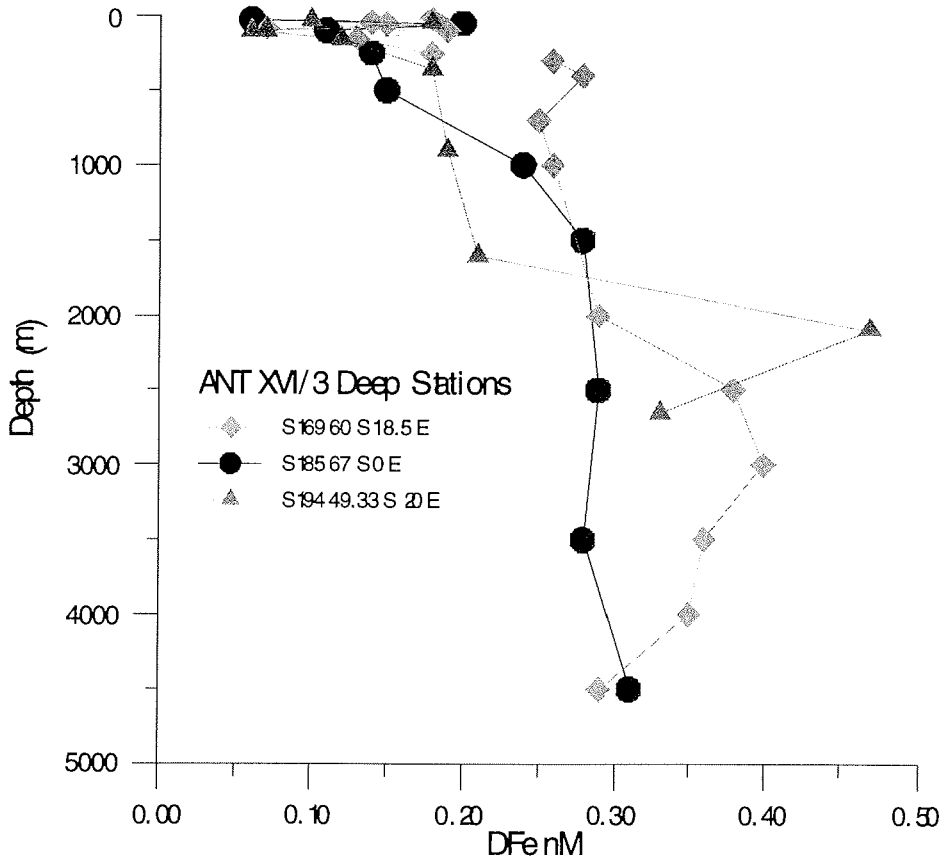

Fig. 6.3: Dissolved iron in the water column from some of the deep stations occupied during the course of ANTXVI/3.

7. PHYTOPLANKTON

The *Fragilariopsis kerguelensis* project
U. Freier, P. Assmy, V. Smetacek (AWI)

Diatoms play a key-role in nutrient, silica and CO2 flux in southern Antarctic ocean. While high macronutrient levels do not limit algal growth, only low phytoplankton biomasses are reported in southern oceans. Along the polar front algal communities are dominated by key-species such as *Fragilariopsis kerguelensis*, *Thalassiosira lentiginosa* and *Thalassiothrix spp.* which form in particular thick silicified frustules. Selective grazing pressure and /or reduced mortality can lead to community selection and former accumulation. High sinking rates of these species, uptake, transportation and accumulation into sea-floor sediments have important influence of worlds nitrogen, silica and carbon-cycle.

Objectives

- Isolation of single strains of *Fragilariopsis kerguelensis* for unialgal cultivation
- Isolation of total DNA of unialgal *F. kerguelensis* strains for later molecular analysis
- Sampling of phenotypic information about population-polymorphism's
- Quantification and qualification of biomass-dominance and phytoplankton composition along the polar front
- Determination of growth-patterns in different euphotic depths in relation to macronutrient distribution

Work at Sea

Phytoplankton was sampled at all stations along the polar front with a hand-net (20µm mesh) from 20m depth to the surface. Samples were also taken from the inner-ship sea-water pipe by continuos 20µm mesh net-concentration. Along two transects at the polar front, intensive CTD- sampling from 20m, 40m, (60), 80m and 120m water-depths was done by using the same experimental approach.

Microscopic work at sea contains:
Photographic documentation of polar front phytoplankton with a *Zeiss Axiovert 135* microscope. Counting of *F. kerguelensis* cells and evaluation of cell state in correlation to :

- cell autofluorescens
- cell size
- chain length
- grazing pressure
- lipid content
- cell-dividing activity

Phytoplankton species composition of polar frontal samples were taken for Utermöhl-counting.

Microscopic isolation of unialgal strains of *F. kerguelensis* by microprepa-ration: In total 106 unialgal strains of *Fragilariopsis kerguelensis* could be isolated from geographic distinct seawater-samples. Three weeks later 46 of them show sufficient cell-accumulation in unialgal cultures. Total DNA of so far 4 strains could be isolated on board by varied CTAB procedure.

Preliminary results, Microscopic observations
Direct observation of fresh plankton CTD-samples from station 162 to station 168 show distinct growth-patterns between cell size and chain length :

Fig. 12.1: Relation of average chain-length (No. of cells) and cell-size (µm) (total counts:11.802 cells)

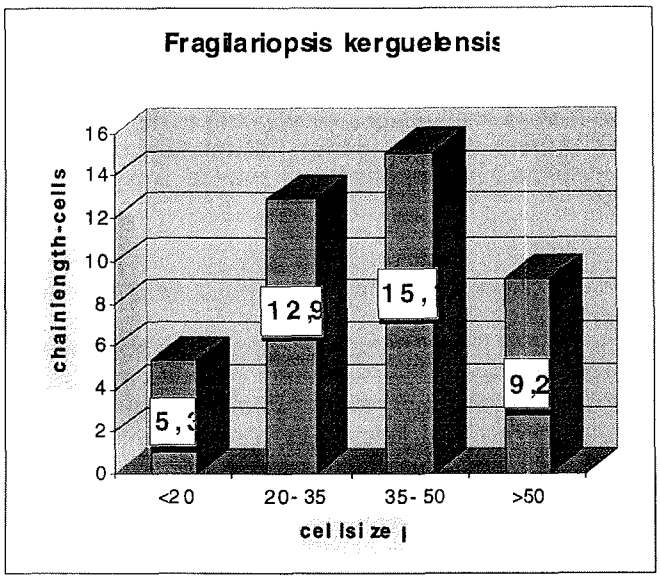

Four distinct chain forming groups of *F. kerguelensis* can be characterised in the first polar frontal transect by cell-size observation. Small cells up to 20 µm cell-size and largest cells with larger than 50µm form shorter chains with an average of 5.3 cells, respective 9.2 cells/chain. Cells between 20µm to 50µm show longer chain-formation with an average of 12.9 to 15.1 cells/chain. In this range single chains occur with a cell content up to 80-120 cells/chain, whereas longer chains >18 cells/chain were never found for the former small-size groups. Precautional interpretation indicates that *F. kerguelensis* form phenotypic divergence in growth-patterns. Mainly cells between 20µm-50µm seem to cause dominant biomass building.

Analysis of these data with correlation to sampling-depths, cell-dividing activity, lipid-content, mortality-rate and other ANT XVI-3 data like macro-nutrient-levels, fluoreszens etc. will bring a clearer view of population-dynamics and growth-pattern.

Total DNA preparation and analysis from further unialgal cultures by various molecular methods will show how phenotypic divergence is based in genetic differences. Isolation and sequencing of genes which are involved in intra-cellular silica-processes shall bring new insights in cell-silica-cycle. Analysis of operon structure, promotor regulation and gene expression will lead to the molecular regulation of thick or thin silicified frustules in respect to ecological behaviour and importance in worlds cilica-cycle.

8. SURFACE CHLOROPHYLL MEASUREMENTS

B. Kroon

Introduction

As a measure for the relative presence of phytoplankton, chlorophyll-a (Chl-a) measurements were carried out during the duration of the cruise. Chl-a has two different functions in phytoplankton. A minor portion of cellular Chl-a is located at the very core of the two photosystems, and carry out the actual photochemical reaction in which solar energy, already trapped inside the large pigment-antennae systems, is converted into stable chemical energy. In the order of a million of these reaction center are available for a typical phytoplankton cell; variations in the abundance of these Chl-a molecules exist within and between species, however, they do not significantly change the ratio between Chl-a and biomass concentration defined as cellular carbon. The major portion of Chl-a is located in the core and peripheral antennae systems, at a stoichiometric ratio of 80 to 1200 per reaction center, depending on speciation or environmental conditions. Due to the potentially large variations in accessory Chl-a relative to biomass concentrations, the observed Chl-a levels should be considered as a very proxy measure for phytoplankton biomass levels.

Chl-a was measured by fluorescence using a flow-through system on excitation with blue light. The absorbed light energy can dissipate through only five pathways, the major three being: photochemistry, heat, or fluorescence. Since these pathways are occurring in parallel, and hence directly competing, any change in one of the pathways will influence the fluxes through the other pathways. During a single day, rates of photosynthesis will vary greatly from sunset to sunrise. As a consequence, redox states and electrochemical gradients vary strongly within the photosynthetic machinery, which in its turn leads to changes in the observed fluorescence levels. In order to estimate Chl-a from fluorescence, one needs to carefully correct for these so called 'light quenching' effects. Even during night time, but then as a consequence of interference between metabolic processes in the cytoplasm and the redox state of chloroplastic components, quenching can be observed as well.

During this cruise, Chl-a was measured over a large spatial and temporal domain. Sudden changes in observed Chl-a levels definitely indicate a change in the total phytoplankton community in response to triggers imposed by chemical or physical driving forces. However, Chl-a levels exclusively do not allow to interpret whether the changes took place as a result of changes in biomass levels, relative species abundance, or both. Future correlation with parameters describing cell abundance and size classes might well be used to confine the interpretation of Chl-a levels to biogeochemically more relevant biomass concentrations.

Sampling and Methods

Fluorescence was measured on water samples continuously taken from 8 meter depth by means of a Turner Design fluorometer at 10 seconds interval averaged and stored at 5 minutes intervals on the ships data logging system. Every 3 to 4 hours duplicated of 1 liter of seawater were filtered onto Whatman

GF/F filters and stored at –80 °C fur subsequent extraction in 90% acetone and analysis as described in the JGOFS core measurement protocol.

The 'light quenching' effect reacts to instantaneously exposed irradiance levels, as well as to the integral total exposure during up the last several hours before actually measuring the fluorescence level. Restoration of the quenching effect to non-quenched values follows a first order kinetic response.
As a result, the 'light-quenching' effect should in itself behave as a sinusoidal function of the time of day. We therefore fitted the calibrated values for the ratio of fluorescence to Chl-a as a sinusoidal function of the time of day, and such data analysis was carried out in 24 hour portions of the entire data set. An example of such a sinusoidal interpolation is shown in Fig. 8.1. In several instances, two or three sinusoidal functions were needed to acquire a satisfactory fit.

Results

The Chl-a levels in the grid enclosing the frontal features of the Antactic Polar front reveal slight variations in absolute numbers, between 0.1 to 0.5 µg/l. However, the northerly of the Polar Front located around 49.2 Latitude, Chl-a levels are on average lower than south of the Polar Front (Fig. 8.2A). The Chl-a distribution followed the temperature profiles measured in the same period well (Fig. 8.2B). The surface temperature contours clearly show the meandering structure of this frontal system.

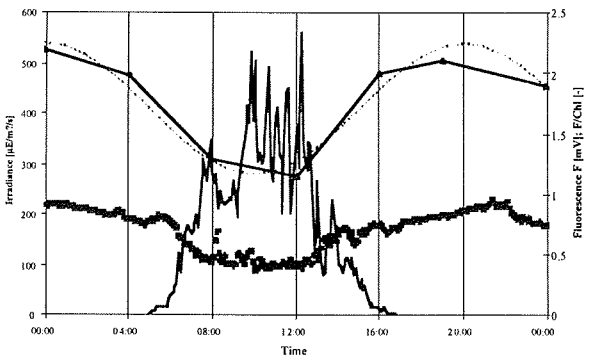

Figure 8.1: Incident solar irradiance (left Y-axis, solid line), measured in situ surface fluorescence levels (right Y-axis, solid dots), measured ratio of fluorescence per Chl-a (triangles, right Y-axis) and interpolated values of fluorescence - Chl-a ratio (dotted line, right Y-axis) as a function of local time. In this example, measured on 26.03.99, the observed diurnal trend in *in situ* fluorescence is largely caused by the 'light quenching' effect, as can be seen from the similar time dependence in the measured ratio of fluorescence yield per Chl-a.

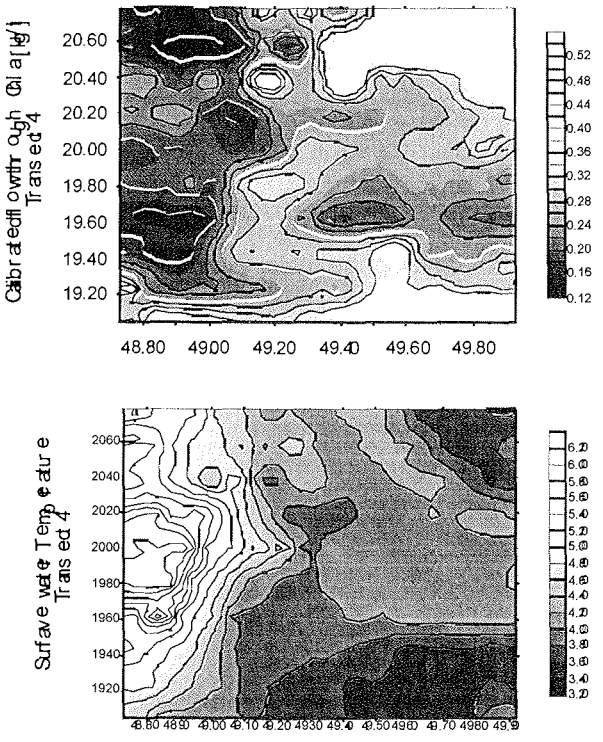

Figure 8.2: Chl-a (8.2A, Top panel) and surface temperature (8.2B, bottom panel) contour plots around the Polar Front. Note that the left side of the X-axis corresponds to the North, and the origin of the Y-axis to the East.

We did not have the opportunity to accurately document the temporal dynamics of the Chl-a distribution in the Polar front. However, the Chl-a distribution that we observed during the South - North travel between April 22 and May 6 (Figs. 8.3A and B) does indicate that the composite picture shown in Fig. 8.2 is subject to short-term changes. Between 22.04.99 and 29.04.99 (Fig. 8.3A) we clearly detected a Chl-a maximum around 51°S / 20°E, which was even higher than the Chl-a maximum that was associated with the Polar Front at 49° S / 20° E. As we shortly cruised southward on 29.04.99 from 49° S to 52° S (Fig. 8.3B), we again passed both regions were we observed the Chl-a maxima just a few days before. This time however, the Chl-a bloom associated with the Polar Front was higher than the Chl-a maximum at 52° S at the same longitude. In addition, both maxima were slightly shifted southward.

Between 26.03.99 and 05.05.99 34 CTD casts were samples and analyzed for Chl-a, silicate, POC and carbonate (data not shown). Except for Chl-a, all samples await further analysis at the home institute. The Chl-a depth profiles showed that the mixing layer mostly extended to about 100 meters, while mixing depths were limited to about 50 meters on some locations.

On 6 positions, we characterized the underwater light climate in 13 different spectral bands ranging from 360 nm to 720 nm (data under analysis). Due to the low Chl-a levels, the 1% light depths occurred at 100 to 120 meters. In combination with biophysical measurements (see section Biophysical Measurements) the data indicate that even at the 1% light level, sufficient was available to support positive growth rates.

Acknowledgements: Angus Atkinson, Dorothea, Katrien, Philipp, Thomas, Ullie Freier, Klaus-Uwe, Anke, Ruth, Bettina for carrying collecting & filtering the samples. Philipp for analyzing the major portion of the samples.

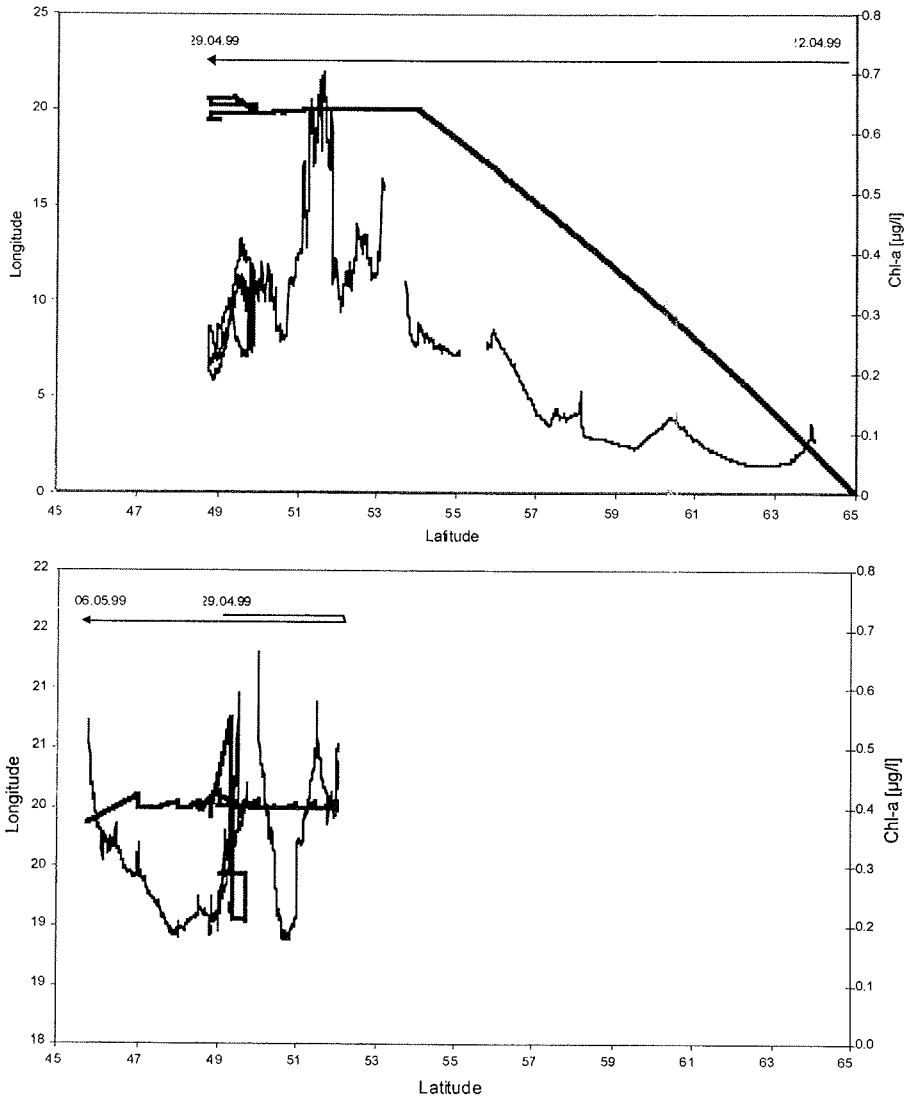

Figure 8.3: Transects of Chl-a concentrations measured between 22.04.99 to 20.04.99 (8.3A, top panel) and between 29.04.99 to 06.05.99 (8.3B, bottom panel).Fat lines indicate the longitudinal positions, thin lines Chl-a concentrations. Note that the Y-axes differ in both figures.

9. BIOPHYSICAL MEASUREMENTS

B. Kroon, T. Mock (AWI)

Introduction

Primary production of phytoplankton results from the physical and chemical environment in which the phytoplankton lives, and from the cellular structures that carry out the photochemical processes. If we assume that the physical environment can influence primary production, we might then argue that biophysical / biochemical structures will reflect the different physical characteristics in which the phytoplankton lives. In other words, the environment offers resources that can be used for photochemical processes, but those organisms having a cellular make up that best use the resources do have a competitive advantage over other organisms. In order to evaluate the strength of phytoplankton species to use the environmental resources we developed a novel theoretical framework, based on the fact that a phototrophic organism requires a particular number of electrons to reduce elements (C, H, O and N) and incorporate elements into new biomass. The number of electrons required to synthesize one C-mole of any phytoplankton species is called γ_x, the general degree of reduction of biomass, which can be calculated from knowledge on the elemental composition of biomass. The rate at which electrons are generated, R_e, depends on the rate constants for the photochemical reactions and the dynamics of light energy available to fuel the photochemical reactions. The ratio of R_e and γ_x defines the growth rate of phytoplankton.

Our primary goal of ANTXVI/3 was to collect the dominant phytoplankton species and transfer them to our home laboratory in order to cultivate axenic cultures. These cultures can then be used to measure all parameters required to determine γ_x, and all necessary rate constants to calculate R_e as a function of the physical conditions that we encountered in the various water masses during the cruise.

Results

Batch and continuous cultures of phytoplankton (ice algae as well as 'open water' species) were maintained during ANTXVI/3 and /4. The samples were successfully transferred to the home laboratory. At the moment of this writing, isolation procedures are successfully carried out to yield axenic cultures of: *Fragilariopsis cylindrus, F. kurta, F. kerguelensis, Thallasiosira antarctica, Chaetoceros sp., Pseudonitschia seriate, Corytrhon cryoplyllum,* and *Rhozisolenia sp.* Due to unstable power supply on board of the Polar Stern, we were only able to carry out a few biophysical measurements during the cruise. An example of such a measurement and its analysis is shown in Figs. 9.1 and 9.2. Ongoing work at the laboratory is carried out on all available cultures.

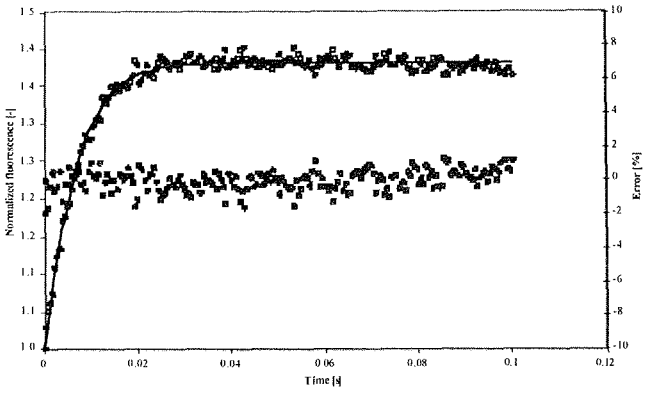

Figure 9.1: Example of a fluorescence induction analysis on a sample from 90 meters depth at Station 168. The sample was dark adapted for 4 hours prior to the measurement The raw data (open symbols, Fo normalized data, average of 5 measurements) were fitted with a model on energy flows in Photosystem II (solid line). The error between model and data (closed symbols) lies well within +/- 2% (r_{-} = 0.989, n=5). The model output yields biophysical rate constants that characterize the following processes: energy trapping in the reaction center, energy losses in closed reactions centres, heat and fluorescence losses in the antenna pigments, energy transfer between different photosystem II complexes. The quantum yield for photochemistry is calculated from the rate constants. These rate constants are needed as input parameters to a larger model to predict rates of photochemistry, R_e.

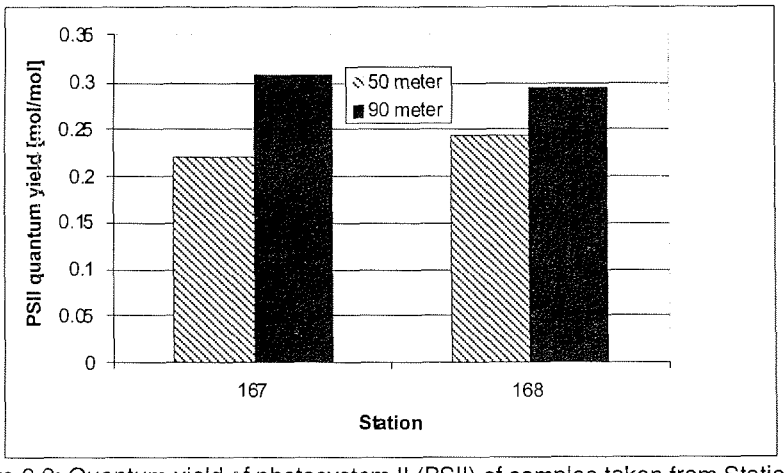

Figure 9.2: Quantum yield of photosystem II (PSII) of samples taken from Station 167 and 168 (South of the Polar Front), analyzed as described in the legend of Fig. 9.1. The samples taken from 90 m both had higher quantum efficiencies, which was primarily caused by a higher rate constant for energy trapping in PSII. Since the samples were dark adapted for at least 4 hours, we ascribe the observed differences to real structural differences, and not as a consequence of previously (*in situ*) experienced light levels.

10. STUDY OF THE MECHANISMS CONTROLLING PHYTOPLANKTON GROWTH IN LATE SUMMER-EARLY AUTUMN IN THE SOUTHERN OCEAN WITH SPECIAL ATTENTION TO IRON AND SILICATE PHYSIOLOGY

V. Schoemann (ULB)

Introduction

Recent literature reveals the complex interplay of silicate and iron limitation in regulating diatom blooms and related biogeochemical cycles in the Southern Ocean (de Baar et al. 1998, Takeda, 1998, Hutchins and Bruland 1998). In particular, it has been shown that iron limitation sustains highly silicified diatoms characterized by a higher sinking rate compared to diatoms growing under replete Fe (Takeda, 1998, Hutchins and Bruland 1998). The effect of iron limitation on the carbon metabolism and the diatom silification level was addressed by running shipboard experiments and using radiotracer techniques under different iron concentrations.

Objectives

The general aim of this project was to determine the kinetics of the biological processes controlling the organic carbon production of late summer-early fall Antarctic phytoplankton. In particular, we studied:
- the phytoplankton photosynthesis, growth and respiration parameters;
- the diatoms silica metabolism;
- the total and intracellular uptake of iron by phytoplankton.

Work at Sea

All the material used for sampling and during the experiments was treated according to the recommended ultraclean methods to avoid trace metal contamination.

Sampling

Natural phytoplankton assemblages were collected at 5 stations in the Southern Atlantic Sector between 49°S and 70°S. Sampling was carried out, using either Go-Flo bottles mounted on the Teflon coated rosette frame from NIOZ or with Go-Flo's attached to a kevlar cable. The Go-Flo's were emptied and the samples further treated in a trace metal clean cooled container (NIOZ) or in class 100 laminar flow bench. Sub-samples were taken for running the radiotracer incubation experiments as well as for measuring the following associated parameters (some of the analyses being supported by other cruise's participants):
- dissolved iron by flow injection analyses (J. de Jong, NIOZ)
- silicate, phosphate, nitrate and ammonium (G. Kattner, C. Hartmann, A. Ratje)
- Biogenic silica
- POC/PON (M. van Leeuwe)
- phytoplankton (<2µm) countings and cells vitality by flow cytometry (M. Veldhuis, F. Brocken)
- species composition, cell density and biovolumes of large phytoplankton in lugol samples under an inverted microscope
- Chlorophyll *a*
- Pigment composition by HPLC (M. van Leeuwe)

• fluorescence by fast repetion rate fluorimetry (M. Davey)
• ^{15}N-Nitrate and ammonium uptakes (K. Timmermans)

Photosynthesis
In order to determine the photosynthetic parameters -the photosynthetic efficiency, α; the index of photoinhibition, β; the maximal specific rate of photosynthesis, Kmax and the light adaptation parameter, Ik- P/E curves were established using the ^{14}C methodology. Short-term incubations (2-3 h) of 1 ml-seawater samples spiked with 5 µCi of $H^{14}CO_3$ were run at *in situ* temperature and under different light intensities (0-600 µmol.m^{-2}.s^{-1}). After incubation, the excess inorganic ^{14}C was degassed for 24 h after addition of 6N HCl. Radioactivity was determined by liquid scintillation (scintillation cocktail Ecolume) with a Packard (tri-carb 160 CA) analyzer.

Phytoplankton growth, respiration and the Fe and Si metabolism
A serie of process-level experiments were conducted to improve the knowledge of light and nutrient (Fe and Si) control of phytoplankton growth in the Southern Ocean. In particular:
• the effect of iron limitation on silicon and carbon assimilation;
• the carbon, iron and silicate phytoplankton stoichiometry and its regulation by ambient Fe;
• the quantitative determination of key phytoplankton parameters: maximal specific rate of photosynthesis, maximal specific rate of protein synthesis, half saturation constant for Fe total and intracellular uptake, VmaxSi, VmaxFe.
The experimental procedure was as follows:

Parallel long-term ^{14}C, ^{55}Fe (e.g. Fig. 10.1) and ^{32}Si incubations were conducted at 100 µmol m^{-2} s^{-1} at *in situ* temperature and mimicking the light-dark cycle. These experiments were performed with natural phytoplankton assemblage; Fe-enriched (addition of 0.25, 0.5, 1.0 and 2.5 nM of $FeCl_3$ during 2 days); and Fe-enriched culture of *Chaetoceros dichaeta*.

At each inculation time, 250-450 ml were filtered using Whatman GF/F or Nuclepore membranes according to the radiotracer. ^{14}C-Whatman GF/F were acidified (HCl 0.1N) to eliminate excess inorganic carbon and then frozen at -20°C. The ^{14}C filters will be later speciated as described in Lancelot and Mathot (1985) in order to distinguish between carbon assimilated into 4 pools of cellular constituents: small metabolites, lipids, polysaccharides and proteins. Phytoplankton growth and respiration will be estimated by mathematical fitting of the data relative to kinetics assimilation of ^{14}C into proteins and storage products according to the equations described in Lancelot et al. (1991).

^{32}Si-Nuclepore membranes were soaked with 1 ml HF (2.9N) to hydrolyse the particulate silica and scintillation cocktail (UltimaGold-XR) was added before radioactivity was measured by liquid scintillation.

Two ^{55} Fe-filtrations were processed at each incubation time to distinguish between total Fe uptake (adsorption + intracellular) and intracellular Fe uptake (e.g. Fig. 10.2). The latter was isolated by applying, during the filtration, the leaching method of Hudson and Morel (1989) based on the use of Ti

complexed with citrate and EDTA. The radioactivity on the filters was determined by liquid scintillation after the addition of scintillation cocktail (Ready Safe).

All the results obtained on phytoplankton physiology will be synthesized for their incorporation in the SWAMCO model of Lancelot et al. (1997), further developed for its application at the scale of the Southern Ocean and over seasonal cycles in the scope of the Belgium BELCANTO and the EC CARUSO projects.

References

Baar, de, H.J.W., de Jong, J.T.M., Nolting, R.F., van Leeuwe, M.A., Timmermans, K.R., Bathmann, U., Rutgers van der Loeff, M. & J Sildam. 1998. Low dissolved Fe and the absence of diatom blooms in remote Pacific waters of the Southern Ocean. *Mar. Chem.* Submitted.

Hutchins, D.A., & K.W. Bruland. 1998. Iron-limited diatom growth and Si:N uptake ratios in a coastal upwelling regime. *Nature*, **393**, 561-564.

Lancelot, C. & S. Mathot. 1985. Biochemical fractionation of primary production by phytoplankton in Belgian coastal waters during short- and long-term incubations with ^{14}C-bicarbonate. II. *Phaeocystis pouchetii* colonial population. *Marine Biology*, **86**, 227-232.

Lancelot, C., Becquevort, S., Menon, P. & J.-M. Dandois. 1997. Ecological modelling of the planktonic microbial food-web. In : Belgian Scientific Research Programme on the Antarctic. Scientiific results of Phase III (1992-1996), S. Caschetto, ed., Federal office for scientific, technical and cultural affairs, Brussels. 1-78.

Mathot, S., Lancelot, C. & J.-M. Dandois. 1992. Gross and net primary production in the Scotia Weddel sector of the Southern Ocean during spring 1988. *Polar Biol.*, **12**, 321-332.

Takeda, S. 1998. Influence of iron availability on nutrient consumption ratio of diatoms in oceanic waters. *Nature*, **393**, 774-777.

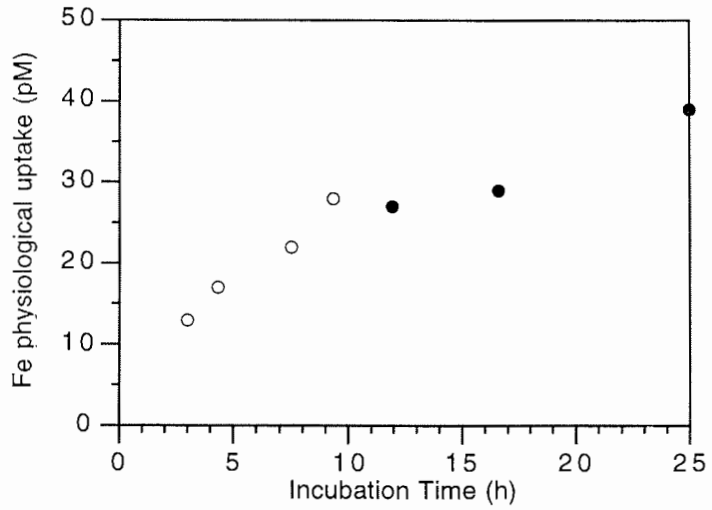

Fig. 10. 1 : Preliminary results of the physiological Fe uptake of a natural phytoplankton assemblage in relationship to the incubation time.

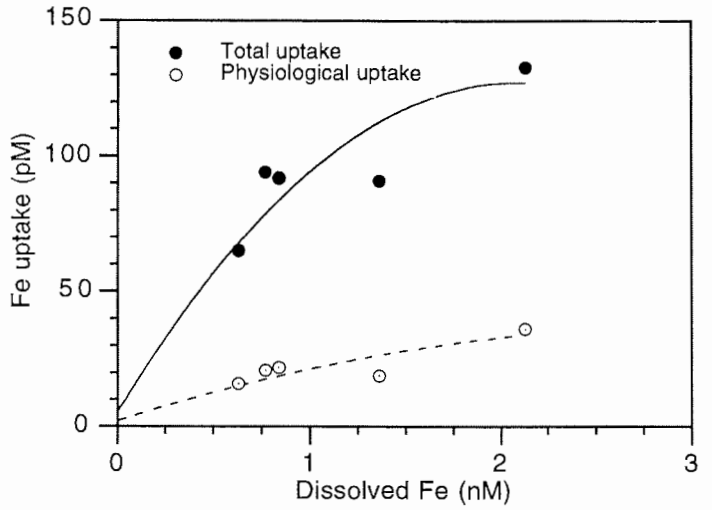

Fig. 10.2 : Preliminary results of the total (•) and physiological Fe uptake (o) after the incubation of a natural phytoplankton assemblage at different dissolved Fe concentrations.

11. FLUORESCENCE OF MARINE PHYTOPLANKTON

M. Davey (MBA)

Objectives

Characterisation of photosynthetic activity of phytoplankton in the surface layer and nutritional status of the population with respect to iron availability.

Work included two main components:

1. Measurement of horizontal variation in the abundance and potential photosynthetic activity of phytoplankton in the surface water during transects using Fast Repetition Rate Fluorometry, (FRRF).
2. Assessment of the photosynthetic parameters of discrete samples from nutrient manipulated on board experiments using field samples and laboratory cultures

The FRRF, like other fluorometers, measures the fluorescence signal emitted from chlorophyll within a body of water. Fluorescence emission can be regarded, in a simplified way, as a means by which the photosynthetic apparatus can dissipate excess energy captured by the light harvesting apparatus in algal cells. Under physiological conditions, fluorescence is emitted from chlorophyll in only one part of the photosynthetic apparatus referred to as photosystem II, (PSII). It is, therefore, the light saturation kinetics of the reaction centre and the efficiency of the light harvesting apparatus of PSII, which is examined by FRRF. The fluorometer delivers a flash sequence comprising two parts, the "saturation" sequence, a series of short sub-saturating actinic flashes, (typically 100 flashes of 1μs duration at 1μs intervals), followed by the "relaxation" sequence, (typically 20 flashes of 1μs with 20μs intervals). These flash sequences are generated, (and the emission signal measured), in two similar chambers. One chamber is open and measures fluorescence under ambient light; the other is shielded from light and measures fluorescence emitted by cells immediately after transfer to darkness. The measurements from the two chambers can be used independently, or in combination, to provide values of biophysical parameters, which are derived from the fluorescence emission, (saturation profile) associated with the light stimulus of the flash sequence. The flashes gradually saturate the photosystems of the algal cells in the water body. As the photosystems become saturated the excess energy is increasingly dissipated as fluorescence and it is the changing fluorescence emission throughout the flash sequences which provides information about the light harvesting efficiency and initial reaction kinetics of PSII. The theory of fast repetition rate fluorescence is outlined in Kolber *et al* 1998.

The measurements of interest during the flow through measurements, made during this cruise, were the values of minimum fluorescence, (F_o) and the maximum fluorescence (F_m). Fo is fluorescence emitted at the beginning of the flash sequences, F_m is the fluorescence emitted once all the reaction centres are closed or saturated by the light of the flash sequence. The difference between these two values is termed the variable fluorescence (F_v). F_m is an index of the total chlorophyll concentration and F_v provides an index of the concentration of functional reaction centres. The ratio of the variable to maximal fluorescence is an indication of the efficiency of PS II. The theoretical maximum value for this ratio is 0.65, values of F_v/F_m between 0.6 – 0.65 are indicative of efficient, nutrient-replete cells, values of less than 0.3 in surface waters suggest cells are subject to considerable nutritional limitation.

Methods

During this cruise the fluorometer was used in a "flow-through" mode. During transects, horizontal profiles were resolved by semi-continuous measurements made on surface water. Fluorescence parameters measured by passing water from the ship "in-flow" water supply through the detection chambers of the FRRF. The fluorometer was positioned inside the ship so data was collected from the dark chamber only. The collection of reliable data from the light chamber would have required continual adjustment of the irradiance levels so that the light entering the light chamber matched *in situ* irradiance levels. The FRRF was immersed in a container, into which seawater flowed continuously, fulfilling two roles; firstly the flow rate through the dark chamber could be effectively decreased reducing turbulence and formation of air bubbles. Secondly the water also acted as a means to cool the instrument which heats up rapidly in continuous use and reduced the accuracy of fluorescence parameters. The flow rate through the container was approximately 3-4 L per minute and the residence time approximately 1-2 min. The fluorometer was programmed under the boot protocol for data acquisition. The protocol dictates the number, duration and interval between flashes in the flash sequence. In addition it controls the number of flash sequences averaged internally by the instrument over a single acquisition. The number of flash sequences per acquisition was adjusted to 16 to reduce the "noise" previously observed under similar measurement strategies. This protocol resulted in approx. 3 acquisitions per minute. The sensitivity of the photomultiplier tubes in the detection chamber was adjusted automatically by setting the instrument to "autogain". This allows data to be acquired over a large range of chlorophyll concentrations without losing the data from regions of very low or very high chlorophyll. Every 24 –36h the instrument was switched off and the files transferred to the computer to be analysed. In addition the optical windows of the instrument were cleaned and blank measurements on 0.2mm filtered seawater.

A number of vertical profiles were carried out as part of shallow CTD casts. During this work data was collected using both chambers was used to measure fluorescence quenching and provide estimates for primary productivity throughout the water column (data not processed). To improve the reliability of measurements the CTD was paused at fixed depths for 5 to 10mins in order to collect a sufficient number of observations to allow meaningful averages to be determined.

Whilst making all discrete measurements, (including blanks), the fluorometer was placed in the cold-room, where the ambient temperature was between 0 and 4°C. The protocol was modified, changing the number of flash sequences per acquisition to 10 and the number of acquisitions per sample to between 30 and 50. Samples, (60 to 100ml) were left in the dark for a minimum of 2 h then sealed in the dark chamber and shielded from external light. Each was measured at least twice and the values of F_o, F_m and F_v/F_m averaged. The results for the work are reported in this volume in the section written by Klaas Timmermans.

Results

Transect measurements: Despite 8 to 10 fold changes in chlorophyll concentration in the surface water in some regions the Fv/Fm ratio often showed only small changes, over the same time period. This suggested that although the abundance of chlorophyll and cells may have varied, the physiological state of cells in many regions of transects were similarly poor with F_v/F_m values between 0.2 to 0.35. Although the ratio alone is not an indication of specific nutrient limitation in itself, it suggests that the PSII reaction centres in the phytoplankton present were functioning at levels below maximum efficiency.

In the first "Scanfish" box, a general trend in F_v/F_m ratio was apparent. Slightly higher values for Fv/Fm (and for Fm), were observed in the northern parts of the box, from 0.3 - 0.4, (+/- 10%), in contrast to the values in the southern area of the box, values in the region of 0.2.

The most striking changes in F_v/F_m throughout a single transect occurred as the ship approached the Neumayer station during Run 8. Although cells numbers and chlorophyll concentrations were some of the lowest recorded throughout the cruise, as the ship proceeded south into the ice and over the continental shelf significant increases in F_v/F_m were observed. Except for three peaks on the Fm value, which corresponded with increases in cell numbers, (flow cytometry results of Marcel Veldhuis), chlorophyll concentration remained consistently low, see Figure1.a & b.

Concluding remarks

The preliminary results of this work indicated than on the whole the surface waters of the cruise appeared to contain algae, which were under moderate nutritional stress. Using the index of F_v/F_m as an indication of photosynthetic activity or potential the algae encountered in the ice fields appeared to be the most robust. The traditional use of chlorophyll concentrations to indicate phytoplankton productivity can be used only.

Measuring field populations naturally involves looking at mixed populations of prokaryotic and eukaryotic algae. Whilst the field conditions maybe favourable for some algal species it maybe not be the case other parts of the algal population. The fluorescence signals measured by the FRRF are from the whole population, and represent at best an average value. If the population is dominated by a particular species which is undergoing physiological changes in response to environmental changes then the measurements may be biased. During a bloom situation a high F_v/F_m may accurately describe the condition of the photosynthetic physiology of the dominant population. However values between 0.2 and 0.4 could indicate generally nutrient depleted algae or may describe a mixture of sub-populations, some of which are nutrient limited others which under the same condition are nutritionally replete.

Additional problems in measuring any fluorescence parameters include the influence of light on fluorescence activity, diel variations in fluorescence caused by exposure of cells to light and light or photochemical quenching of fluorescence. During the hours of darkness there was a marked decrease in the signal "noise" which was probably due to more accurate measurements of F_o. The measurement of F_o requires all the reaction centres to be open. When algae were exposed to daylight it appeared to take minutes to hours for the reaction centres to become fully re-opened. For this reason increasing the
Residence time of algae in the dark chamber of the instrument would possibly have resulted in greater precision of F_o and therefore F_v/F_m measurement.

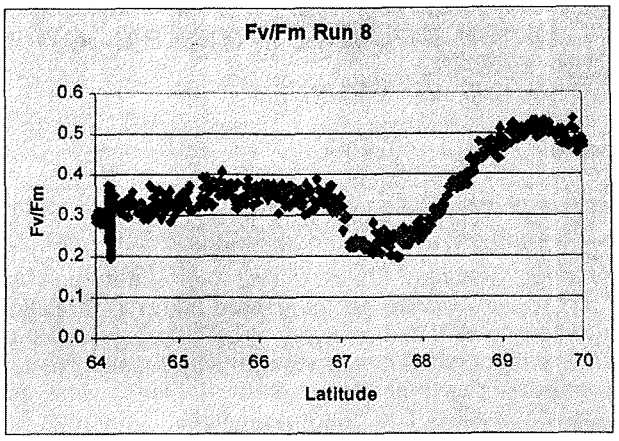

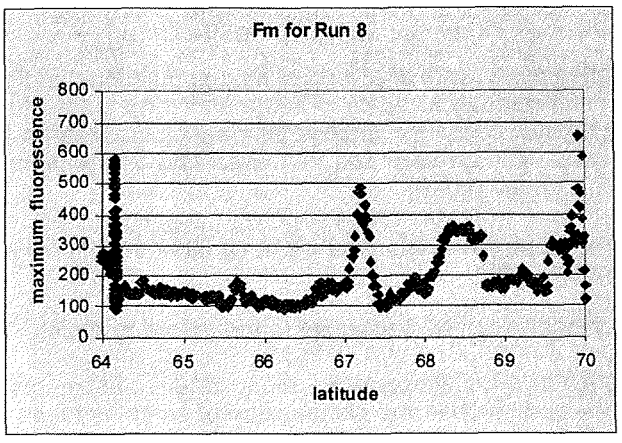

Figures 11 a & b. Variation of fluorescence parameters throughout the transect from 64° to 70°S.
11a : Variation of variable fluorescence throughout run 8.
11b : Variation of Fm, throughout run 8.

Reference:

Kolber, Z. S., Prasil, O., Falkowski, P. G. (1998). Measurement of variable chlorophyll fluorescence using fast repetition rate techniques: defining methodology and experimental protocols. *Biochim. et Biophys. Acta* 1367: 88-106.

12. PHYTOPLANKTON DYNAMICS IN AUSTRAL AUTUMN IN THE SOUTHERN OCEAN

M.J.W. Veldhuis, F. Broken (NIOZ)

General objective

The main objective of this cruise was to investigate the phytoplankton abundance, distribution and physiology in detail in the Polar Front (48-50°S) and down to the Antarctic continent (70°S) during austral autumn (March to May 1999). For this purpose discrete samples were taken and analysed applying flow-cytometry allowing detailed analysis of cellular bio-optical properties (size, scatter and chlorophyll fluorescence) of single cells. Next, different biochemical properties like total DNA content and lipids were assessed applying fluorescent probes. The general physiological status (viability) of the phytoplankton cells was derived from the status of the plasma membrane using a green fluorescent DNA-specific dye which is non-permeable in healthy cells.

In addition, subsamples were analysed of field populations and cultures of phytoplankton subjected to a variety of treatments targeted to study the role of iron in the algal physiology. For detailed information we refer to Timmermans and Van der Wagt, Van Leeuwe and Van Oijen and Schoemann (also presented in this cruise report).

Finally, a first attempt was made to analyse on-line bacteria using a green fluorescent nuclear-stain.

The general objective can be separated in the following topics:

1) Determination of the phytoplankton abundance, cell size, chlorophyll fluorescence and biochemical composition of samples taken in a grid across the Polar Front (48S - 52S). Investigate the relationship with general physical and chemical structure of the water-masses encountered.
2) Effect of (deep) vertical mixing properties on the general physiological status (photopigment adaptation and viability) of different phytoplankton communities.
3) Effect of nutrient limitation (silicate and iron) on phytoplankton composition and growth.

Ad 1) Spatial abundance was mainly based on surface sampling, using the on-line plankton pump. Transects sampled were from Cape Town towards the grid of the Polar Front and from the grid towards the Antarctic continent (station Neumayer). Each transect was sampled twice. Samples were taken at a 1 h interval which equals a 3 to 12 nm distance between the sampling points depending on ships speed. These data provided a general impression of numerical abundance and size class distribution of area between 40°S and 70°S (ranging from 20°E at the north to 8°W at the continent).

In the Polar Front additional samples were taken of the upper 200 m of the water-column. For this purpose subsamples were taken from the CTD-rosette, equipped with Niskin bottles. Since sampling was focussed on a grid (48.7 °S

– 49.9 °S and 19 °E- 21° E) a 3D (latitudinal, longitudinal and depth) distribution can be given of phytoplankton properties (numerical abundance, size and chlorophyll fluorescence). Data will be compared with physical parameters (temperature, salinity, density, fluorescence) of the CTD as well as those obtained with the towed undulating platform (Scanfish).

Samples were taken for cellular DNA analysis of phytoplankton and bacteria. In case of phytoplankton cellular DNA content can be used in combination with HPLC-analysis of plant-pigments for species determination (e.g. *Phaeocystis* sp.) Same data can also be used to calculate total phytoplankton biomass based on the following empirical relationship:

$$C = 10^{((LOG10(1.106*DNAnorm*\mathrm{Pr}o_{DNA})+1.4701)/1.0992)}$$

C = carbon content per cell [pg C/cell]
DNA_{norm} = DNA content of phytoplankton relative to signal of internal standard (Prochlorococcus sp)
Pro_{DNA} = DNA relative DNA content of *Prochlorococcus* sp. (0.0155 rel. units)

After Veldhuis, Cucci and Sieracki (1997)

Additional samples were taken for analysis for other biomarkers (neutral lipids a storage product particularly present in diatoms using the dye Nile Red). These samples will be analysed at NIOZ. The relative amount of neutral lipids can be determined on the level of individual groups.

Ad2) The physiological status (viability) of the separate algal groups/species was examined by testing the integrity of the plasma membrane. This method has recently been proven to be a rapid and reliable method to test first signs of autolysis of the plankton cells. In general healthy, growing cells will not stain upon addition of a DNA membrane-impermeable dye whereas cells in stressed conditions show partly or totally comprised plasma membrane. The dye will easily pass the plasma membrane and as a result, the genome of these cells will be stained showing a bright green/yellow fluorescent signal. The great advantage of this method is that it detects an early stage of autolysis, when phytoplankton cells still possess their pigments and full DNA content. During the cruise samples of the upper part of the water column were examined for their viability. Different groups will be compared with depth and along a gradient over the Polar Front and adjacent water masses. In addition subsamples were kept in the dark for several days to test the ability of polar phytoplankton to deal with prolonged dark conditions. These conditions may occur when phytoplankton cells are exported out of the euphotic zone due to deep mixing or sinking.

Ad3) Effects of different environmental stress factors (silicate, iron and light) were tested by various colleagues in a variety of short or long-term incubation experiments. Our contribution was restricted to the analysis of above-mentioned aspects of the phytoplankton community.

Material and Methods

The basic instrument applied in the single cell analysis of the phytoplankton community was a bench top flow cytometer (Coulter XL-MCL). This instrument is equipped with a 15mW laser (488 nm excitation) and emission bands in the green/yellow (FL1: 525 ± 20 nm); orange (FL2: 575 ± 20 nm) and red (FL3: >630 nm). In addition forward light scatter is collected as a fourth parameter. Phytoplankton is distinguished from other particles based on their chlorophyll fluorescence signal collected in the red detector (FL3). In its basic configuration the size range on the instrument ranged from 2 to ca. 30 µm. Larger phytoplankton, big diatoms, chains or *Phaeocystis* colonies can be and were occasionally detected but since numbers of these particles per ml are low (ca. 1 ml or less) proper quantification of these cells is not possible (statistically non significant results).

Practical considerations

Due to the low numerical abundance relatively large volumes needed to be analysed to meet proper statistics. On the other hand the ambient temperature ranged from –1.8 to ca. 5° C thus prohibiting long exposure of the freshly collected live samples to room temperature. As a result 0.5 to 1 ml of fresh samples was analyses causing no significant loss due to heating.

Samples were analysed based on the presence of clearly distinguishable phytoplankton groups up to a maximum of 4 size classes or species. The presence of chain forming diatoms occasionally limited a clear cut-off of the different cluster. The presence of multiple cellular algae could be derived from the DNA-signals showing multiple peaks associated within a single cluster. Fresh samples were analysed as soon as possible after collecting (<1 h) and were stored prior to analysis in the dark on melting ice.

Viability test

To test the integrity of the plasma membrane or viability of the cells, to 1 ml of sample 10-20 µl of SYTOX Green solution was added (1:100 fold diluted). Samples were incubated for at least 1 hour in the dark on melting ice prior to analysis. The increase in green fluorescence (FL1) was recorded and compared with the unstained cells and the DNA signal in paraformaldehyde fixed cells. Low values indicate high degree of viability whereas FL1 signals closely matching that of full DNA signal are indicative of non–viable cells.

DNA

The genome size of phytoplankton was estimated using preserved samples. The green fluorescence (FL1) of samples treated with the dsDNA pecific stain PicoGreen (1:5 diluted stock solution). Samples were incubated for 1 hour in the dark prior to analysis.

In a separate run, numerical abundance of bacteria was estimated after diluting samples with TX100 buffer (1: 2, final concentration 0.2%). PicoGreen was used as nucleic acid stain (1:9 diluted, 10 µl per 450 µl of sample). For this purpose the flow cytometer was slightly modified to enhance the sensitivity of the scatter signal. In all field and incubation samples at least two but at

some stations and in older cultures often three bacterial population could be distinguished based on their DNA content.

Results

In total over 5000 samples were analysed and most of the data has been processed on board. Therefore the number of post-cruise samples to be analysed remains limited to several hundreds of lipid tests of field samples.

In general phytoplankton numbers were low (<2500 cells/ml), in some cases close to the Antarctic shelf extremely low (<100 cells/ml) in the surface waters. For comparison in the temperate zone (44°S) numbers were still in the order of 40,000 cells per ml. For comparison autumn values are 2 to 5 fold lower than previous measurements made applying flow cytometry in the spring condition across the Polar front down to the ice shelf (Jochem et al,1997). As in most oceanic waters examined flow-cytometric data showed a covariance of size and fluorescent properties of the phytoplankton (Fig1).
Yet, due to presence of chain forming diatoms larger algal groups could not always clearly be separated and are certainly not exactly quantified.

Picophytoplankton was present only north of 48°S with numbers ranging from 1,000 to 5,000 per ml. Phycoerythrin containing *Synechococcus* were only found north of 45°S.

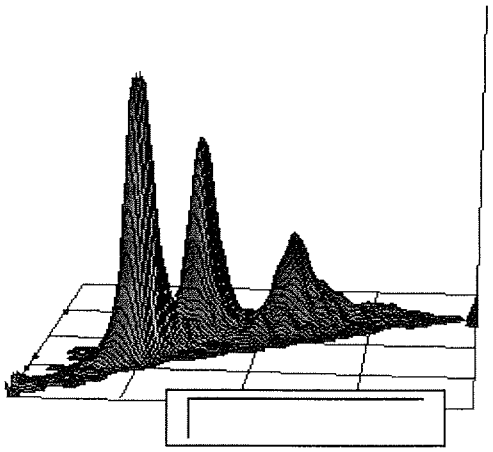

Figure 12.1 isometric projection of size versus chlorophyll fluorescence signals.

Typical example showing covariance of size and chlorophyll signals and decrease in numerical abundance with increasing cell size

The vertical profiles of phytoplankton distribution showed a uniform pattern of a nearly equal numerical distribution over the (wind) mixed layer of the water column. Due to this constant mixing process relative size and chlorophyll

fluorescence of the cells remained also fairly constant. A moderate increase in chlorophyll fluorescence was measured only below the mixing layer. Nevertheless, the increase in chlorophyll fluorescence, hence pigmentation, was only minor and never exceeded a factor 3.

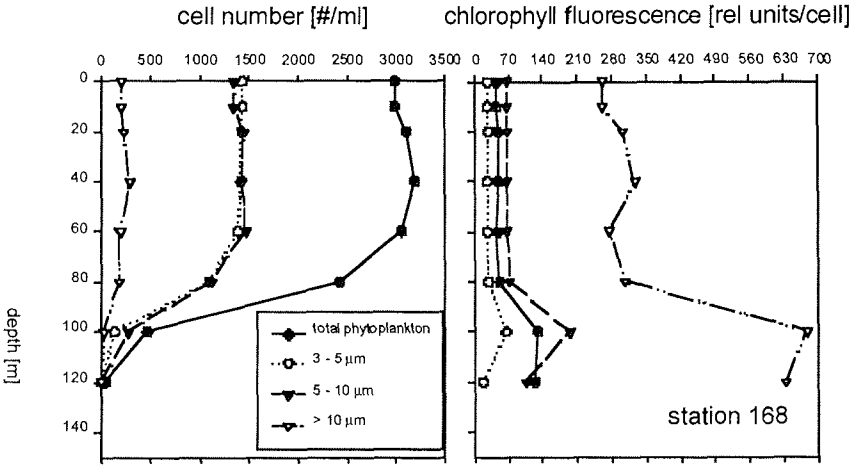

Figure 12.2 Typical example of vertical distribution of major algal size classes (left); relative chlorophyll fluorescence per cell of each algal group (right).

A completely different vertical distribution profile existed at the Antarctic shelf edge. At this area a sharp peak in cell numbers was found at a depth of 250 m. Since all size classes showed a peak at the depth it is unlikely that this elevated phytoplankton biomass is caused by rapid sinking of the larger material from the upper water column. This is confirmed by the fact that chlorophyll signals also showed little changes even below the 1% light depth zone (ca. 120 m).

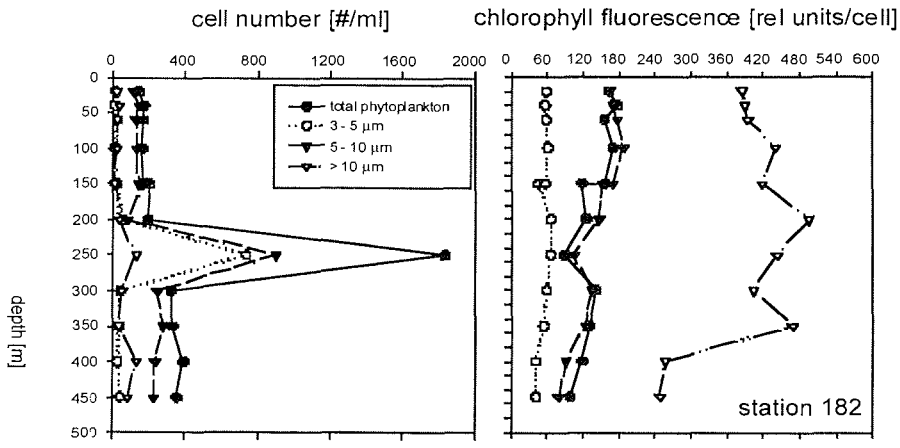

Fig. 12.3 Vertical profile of cell numbers and chlorophyll distribution of station 182, close to the Antarctic shelf edge.

Viability

The viability tests showed considerable changes with respect to the dominant species both in time and space. In general viability of larger phytoplankton, most likely diatoms (5 ->10 µm), in the silicate-deprived waters of the northern part of the Polar Front was low, i.e. green fluorescence signals of these cells closely matched that of DNA signal in preserved samples (Fig. 12.4 left cluster). In other species a more gradual signal was observed indication considerable interspecific variation. Further data processing is needed to match this type of measurement with nutrient concentrations and prevailing light and physical conditions (mixing regime) of the water column. Since cruise covered a time span over 7 weeks and several regions were visited more frequently an indication can be given of the general phytoplankton physiology during the austral autumn of the Polar Front.

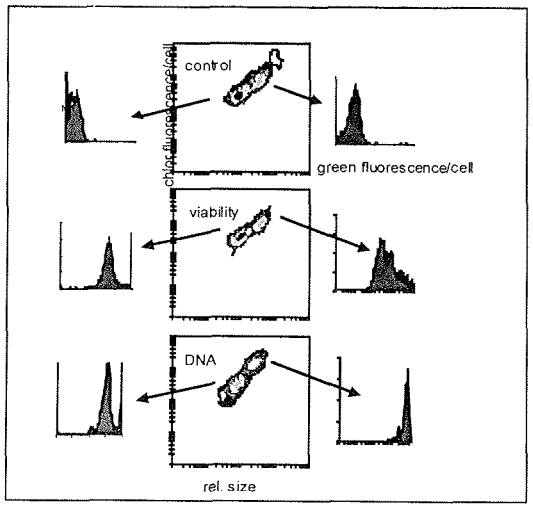

Figure 12.4 Bivariate plots of relative size and chlorophyll distribution show two clusters of phytoplankton. Frequency distribution of green fluorescence signal of these population at three conditions: control, live stained with SYTOX Green and preserved cells (showing maximum staining of the DNA).

DNA

DNA measurements of field samples often showed multiple peaks within a single phytoplankton population. Detailed analysis of the DNA signal of this group using the peak versus integrated mode revealed multiple DNA peak associated with a single particle. In like manner chlorophyll fluorescence of these clusters showed also a much larger variation than normal found for a single population. Microscopic observations confirmed the presence of small chain forming diatoms (1 to 4 cells).

In two cases the growth rate of a single population was measured using the DNA-cell-cycle method which is based on the frequency of cells synthesising DNA. This was done for a field population during the survey of the grid and on a sample containing ice-algae.

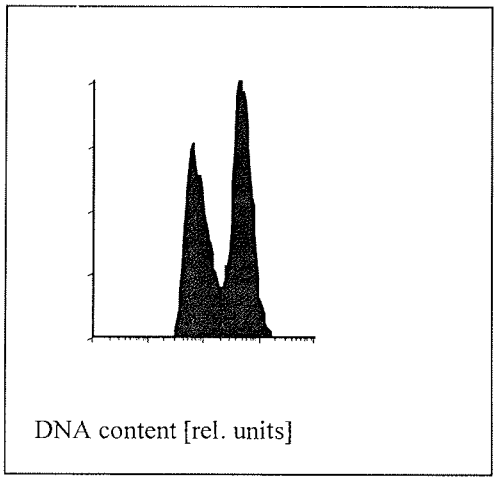

Figure 12.5 Frequency distribution histogram of relative DNA content of bacterial population

The number of bacteria counted using PicoGreen as a green fluorescent dye ranged from 3 – 6 *10^6 per ml rapidly in the surface waters. The general trend was towards lower numbers south of the Polar Front. Bacterial numbers also declining down the euphotic zone in general co-varying the phytoplankton biomass. Bacterial DNA measurements showed clearly the presence of two groups of bacteria distinctly differing in DNA content (ca. 4-6 fold, Fig. 12.5). Although this separation in two DNA-groups is commonly observed in most oceanic systems it is only in the Southern Ocean that they are so distinctly separated.

13. RESPONSES TO IRON LIMITATION OF NATURAL PHYTOPLANKTON ASSEMBLAGES COLLECTED AROUND THE POLAR FRONT AND SINGLE SPECIES CULTURES OF ANTARCTIC DIATOMS.

K. R. Timmermans, B. van der Wagt, M. J.W. Veldhuis(NIOZ), M.Davey (PML)

During the ANT XVI/3 with R.V. Polarstern, the responses to iron limitation of natural phytoplankton assemblages collected around the Polar Front, as well as the responses to iron limitation of single species cultures of Antarctic diatoms were investigated in the Southern Ocean. Both approaches were used to shed light on the effect of iron limitation on phytoplankton physiology, and more generally, to investigate the role of iron in biological forcing of the oceanic carbon cycle.

The natural phytoplankton assemblages were incubated for a short time (1- 6 days) in order to prevent major changes in species composition. The experiments with the Antarctic diatoms brought from the home laboratory lasted longer up to several weeks. Main tools to investigate the effects were the flowcytometer (FCM) and the Fast Rate Repetition Fluorometer (FRRF). The FCM was used to determine the cell numbers (and thereby the growth rate), as well as the size distribution and chlorophyll a fluorescence of the phytoplankton. Parameters available for assessing photosystem II (PSII) are maximum fluorescence yield (Fm) and the variable fluorescence yield (Fv). Whilst Fm provides an index of chlorophyll concentrations, Fv can be used to indicate the abundance of functional PSII reaction centres. The ratio of variable to maximum fluorescence is indicative of PSII efficiency, which itself is dependent upon the nutritional status of the phytoplankton cells. In the experiments, the FRRF was used to determine Fv/Fm, and hence the iron status of the phytoplankton.

The results from the field experiments tend to suggest iron stress in the natural phytoplankton assemblage. In some cases, phytoplankton incubated with iron showed, within 24 – 48 hours, slightly elevated values of Fv/Fm compared with the controls (Fig. 13.1). When desferal (a natural iron complexing agent) was added to the natural phytoplankton, a stronger response was sometimes obtained. So, it seems to be that the natural phytoplankton was occasionally iron stressed, but certainly not severely iron limited.

The experiments with the single species cultures of diatoms confirmed the results from the field studies. *C. brevis*, a species with typically low iron requirements, could not be grown into iron limitation without addition of desferal, a natuaral iron binding compound. In a gradient of increasing desferal concentrations, growth rates were increasingly limited. After transfer of a iron limited (desferal) culture of *C. brevis* to low light conditions, the cells were not capable to synthesize extra chlorophyll.

C. dichaeta, a chain forming diatom with higher iron requirements than *C. brevis*, could be grown into Fe limitation readily. A good dose-response relationship between iron and growth rates was established. Not only the growth rates but also the chain length (cells per chain) proved to be a good indicator of the iron status of the cells (Fig. 13. 2). Light also was an important factor determining growth rate: irrespective of the iron concentrations offered, *C. dichaeta* did not grow under a 12:12 hours light:dark regime, growth was only possible under a typical long day light regime.

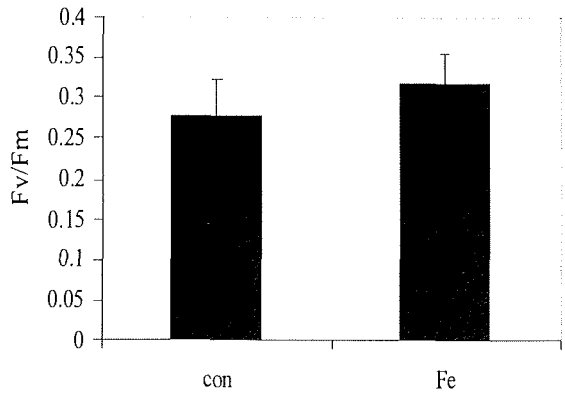

Figure 13.1. Fv/Fm in control (con) and Fe enriched (Fe) natural phytoplankton (experiment 7), 24 hours after addition of the iron spike.

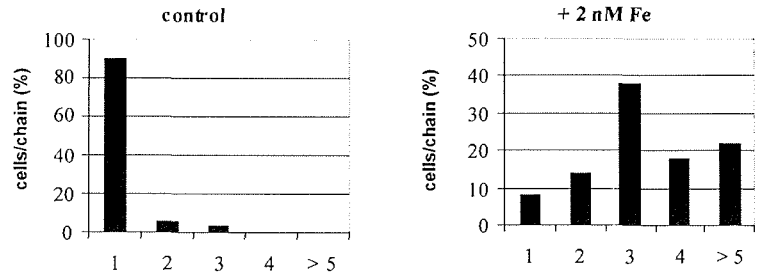

Fig. 13.2. Percentage of chains of C. dichaeta with 1, 2, 3, 4, or 5 or more cells per chain in control and 2 nM iron addition incubations (note the differences in scales).

Finally, during the cruise first attempts were made to study intracellular markers of iron limitation in *C. brevis*. Using the FCM, diurnal dynamics in DNA and fatty acids were monitored in relation to iron concentrations in the seawater. Upon addition of iron to a iron limited culture of *C. brevis* it was found that enhanced DNA synthesis took place, whereas no changes in fatty acid composition were observed.

In conclusion, during ANTXVI/3 some signs of iron stress in phytoplankton were found in the Southern Ocean. However, it is highly unlikely that the true oceanic phytoplankton species, with low iron requirements are iron limited under these conditions. Species with higher iron requirements might be iron stressed under the conditions encountered in the field. The FCM and especially the FRRF turned out to be powerful tools to make an assessment of the immediate effects of iron on phytoplankton.

14. LIGHT ADAPTATION BY NATURAL PHYTOPLANKTON POPULATIONS, AND ITS CONTROL BY IRON LIMITATION.

M.A. van Leeuwe, T. van Oijen (RUG)

Introduction

The Southern Ocean is a turbulent area, with deep wind mixed layers. The open ocean area is furthermore characterized by low concentrations of trace metals. The low biomass of phytoplankton, generally encountered in these regions, is hypothesized to be under control of the variable light climate and low iron concentrations (Chisholm et al. 1991). Iron is essential in photosynthesis, as it forms a structural component of the photosystems. An interaction of iron and light limitation can be envisioned, if iron-deplete cells are unable to use the available light. Previous experiments have shown that photosysthesis is indeed limited by iron limitation (van Leeuwe et al.1998). It was also found, however, that the pigment composition was not affected by iron limitation. This was confirmed in lab experiments, where it was found that the light utilization efficiency was target of iron limitation, whereas the absorption capacity of the cells was not affected (van Leeuwe & de Baar subm.). This led to the hypothesis that whereas on the long term photoadaptation by phytoplankton is not limited by iron limitation, short term adaptation may well be inhibited. Two aspects of photoadaptation were studied on this cruise.

Photoadaptation on a short time scale requires flexibility of the photosynthetic membranes (Kroon et al. 1994), and involves changes in cell metabolism. The integrity of the membranes is affected by iron limitation. Therefore, a quick response by the algae to changes in light conditions may be inhibited. To study the response in photosynthesis, fluorescence was measured. In addition, chlorophyll was analyzed. During periods of reduced photosynthetic activity, cells may use a storage pool of polysaccharides, to support a basic metabolism. Iron limitation results in a reduction in this pool, and thus affects the vitality of the cell under light stress. Various cell metabolites, including carbohydrates, are studied to gain insight in the way cell metabolism is affected by iron limitation.

Material & Methods

1. Deck incubations

Deck incubations were performed to study the photosynthetic response of algae under natural conditions. At dawn, surface water was sampled using buckets, at several sites in the Polar Frontal region (Table 1). The plankton was incubated in 20L polycarbonate bottles (Nalgene) in a deck incubator, at 4 different light intensities (100, 60, 40, 20% of incedent irradiance). After 5 hrs of daylight samples were taken for fluorescence measurements and pigment composition. In addition, cellular fluorescence and cell size were recorded using flow cytometry. At sunset, and after 5 hours of darkness, samples were taken for carbohydrates, POC/PON, chlorophyll and flow cytometry.

2. Iron-enrichment experiments.

a. Short term incubations

Sea water was enriched with iron, to study physiological responses of the phytoplankton community. Samples were taken with clean Go-Flo's attached to a teflon coated rosette frame (Table 1). Upon retrieval on deck, the Go-Flo's were mounted to the wall of a clean cooled container. The Go-Flo's were sampled through teflon tubing, which was led through the container wall. The clean sea water was incubated in acid-cleaned 20L polycarbonate bottles (Nalgene), at 80-100 µmol photons m^{-2} s^{-1} at a 12:12h light dark regime, at 2°C. Samples were taken in the late evening, early morning. After 24 and 36 hours, samples were taken for POC, chl*a*, cell metabolites, and samples were taken for subexperiments.

Subexp.1.

The samples were spiked with ^{14}C, and placed at 20 µmol and 100 µmol photons m^{-2} s^{-1}. At regular time intervals, samples were filtered. fractionation analysis at home will be performed to record the development of the storage pool of polysaccharides over the day. In addition, at t=24h and t=36 hours, samples were taken for POC/PON, chl.*a* and carbohydrates.

Subexp.2.

Samples were placed at 20 and 100 µmol photons m^{-2} s^{-1}. After 5 hours, fluorescence was recorded with a dual amplitude modulated fluorometer (PSI). After 36 hours samples were taken for chl.*a*. In addition, at t=24h and t=36 hours, samples were taken for POC/PON, chl.*a* and pigment composition.

b. Long term incubations.

A remaining questions is, whether or not iron limitation affects the C-N ratio of the cells. Light conditions may hereby play a crucial role (Stefels & van Leeuwe 1998). Sea water was sampled with the Go-Flo's either mounted on the rosette frame, or attached to a kevlar wire, and by sampling from the iron fish (see de Jong et al). The plankton was incubated in the clean cool container, in 2.5L polycarbonate bottles (Nalgene), at three different The plankton was incubated in the clean cool container, in 2.5L polycarbonate bottles (Nalgene), at three different light intensities (ca. 100, 50 and 25 µmol photons m^{-2} s^{-1}). Growth and nutrient consumption was followed over several days (6-8). The time was given to allow any possible changes in cell metabolism, related to iron limitation, to become expressed in carbon and nitrogen content. At the end of the experiment, samples were taken for POC, PON and chl.*a*.

Preliminary results.

1. Deck incubations.

The most prominent feature in the deck incubations, is the increase in cell size with increasing light intensities (Fig. 14.1). The changes in cellular fluorescence are less pronounced. A slight decrease in fluorescence with decreasing light intensities seems apparent on sunny days, on cloudy days cellular fluorescence seems to increase. The flow cytometer data have to be treated with care, especially since the delay between sampling time and measurement varied between samples, which did influence the considered parameters. It can be concluded however, that cells do respond to changes in irradiance by varying their absorption capacity, on a relative short time scale. Changes in chlorophyll content have yet to be analyzed.

2. Iron-enrichment experiments.

Data on the short term experiments are too preliminar to make any statements about. Considering the development of cell numbers on a short time scale, growth rates of the phytoplankton population were too low to distinguish any effect of iron limitation (Fig. 14.2). Over a longer time span, it is clear that growth is most optimal at the 50% light intensity, meaning ca. 40-50 µmol photons m^{-2} s^{-1}. Notably, the non-enriched cells showed a faster increase in cell number than the iron-enriched cells (Fig. 14.2). The fluorescence patterns were similar for both the non-enriched and the iron-enriched cells (Fig. 14.3). Cellular fluoresence increases with decreasing light intensity. The cell size appeared smaller for iron-deplete than for iron-replete cells. Nutrient consumption shows a different pattern (Fig. 14.4). Especially the phosphate data indicate that growth in the iron-enriched bottles picks up only after 4 days. At day 6, the iron-enriched cells clearly consumed more nutrients than the non-enriched cells.

It can be hypothesised that, when provided iron, the cells need some days to adjust to the new conditions, and to consume the iron. In the meantime growth appears arrested. Only when saturated with iron, growth starts again. Additional data on carbon and iron uptake might shed more led light on the processes controlling growth of the phytoplankton population at the Polar Front.

This work was supported by
J. de Jong (analyses of iron concentrations)
V. Schoemann (isotope experiments)
G. Kattner, C. Hartmann, A. Ratje (nutrient analyses)
M. Veldhuis & F. Brocken (flow cytometry)
K. Timmermans & B. vd. Wagt (general assistance).

Table 1. Overview of the experiments performed during ANT XVI/3

experiment	*date*	*location*	*station*	*comments*	*sample*
1. Deck incubations					
1	26 March	49°50.519 S - 20°0.463 E	154	Polar front	bucket
2	27 March	49°20.202 S - 19°21.729 E	155	Polar front	bucket
4	31 March	49°32.84 S - 20°11.43 E	-	Polar front	bucket
5	1 April	49°29.649 S - 19°48.566 E	-	Polar front	bucket
2. short term iron enrichments					
6	3 April	49°59.805 S - 19°3.81 E	161	Polar Front	Go-Flo
7	6 April	49°50.119S - 20°0.054 E	167	Polar Front	Go-Flo
9	9 April	59°59.841 S - 18°32.096 E	169		Go-Flo
11	19 April	70°10.998 S - 6°27.836 W	181		Go-Flo de Jong
13	21 April	66°58.637 S - 0°3.159 E	185		Go-Flo
15	25 April	54°2.712 S - 20°0.716 E	190		Go-Flo
17	27 April	49°22.245 S - 20°33.960 E	191	Polar Front	Go-Flo
18	29 April	49°22.268 S - 20°1.989 E	194	Polar Front	Go-Flo
19	4 May	50°0.374 S - 20°1.306 E	200	Polar Front	Go-Flo
3. long term iron enrichments					
3	29 March	49°30 S - 20°5 E	-	Polar Front	iron fish
8	7 April	49°50.119 S - 20°0.054 E	167		Go-Flo exp.7
10	16 April	70°10.05 S - 6°53.120 E	175		Go-Flo de Jong
16	27 April	52°00 S - 20°00 E	-		iron fish

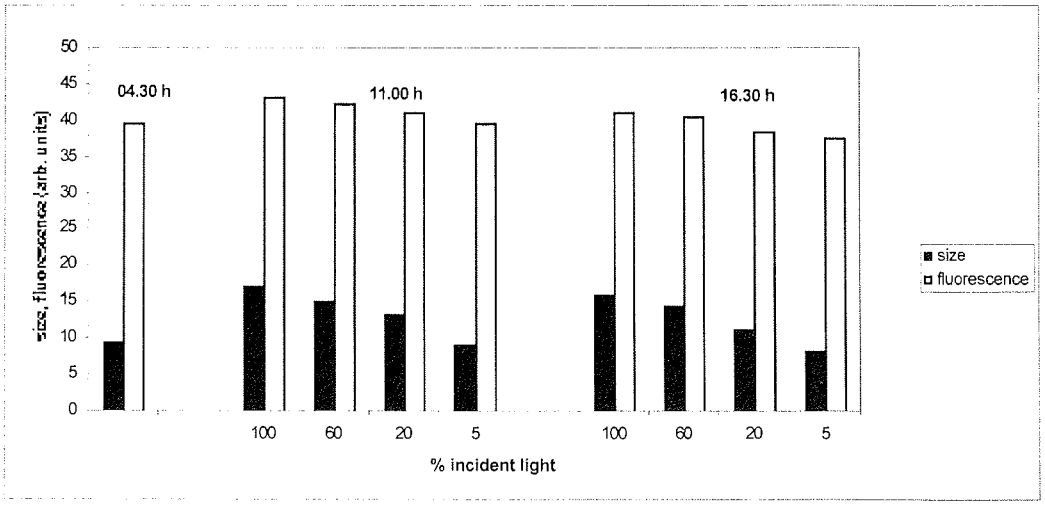

Fig. 14.1. Cell size and cellular fluorescence as determined by flow cytometry for experiment 4. Samples were measured at t=0, t=6.5 and t=12 hours. Large cells are excluded by the flow cytometer.

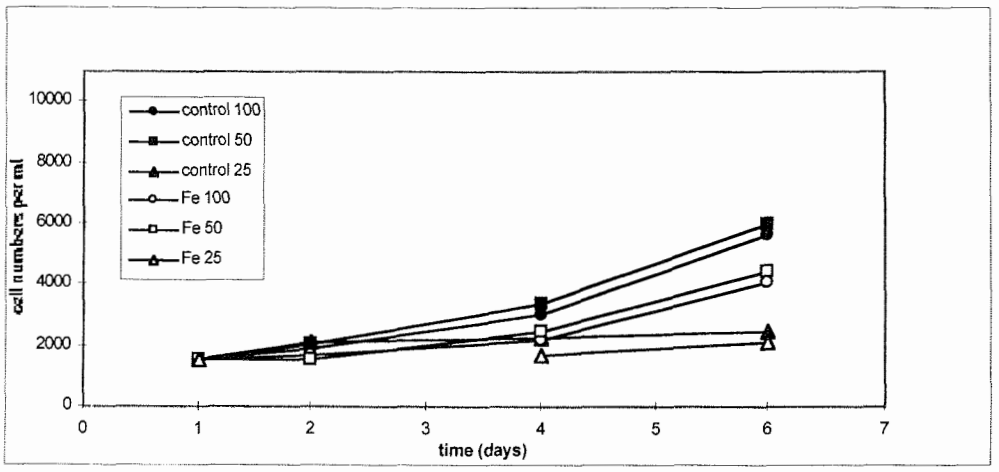

Fig. 14.2. Cell growth of natural phytoplankton populations over the course of six days, for iron enriched (open symbols) and non enriched bottles (filled symbols) of experiment 3. Plankton populations were incubated at three different light intensities.

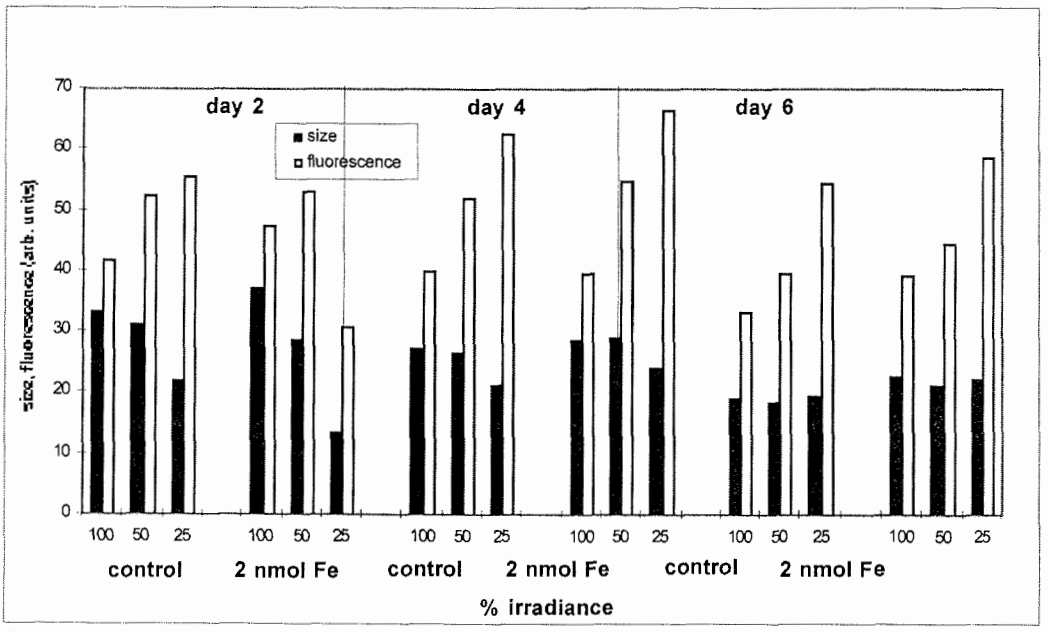

Fig. 14.3. Cell size and cellular fluorescence as determined by flow cytometry for experiment 3. Samples were measured at t=2, 4 and 6 days. Plankton populations were incubated at three different light intensities.

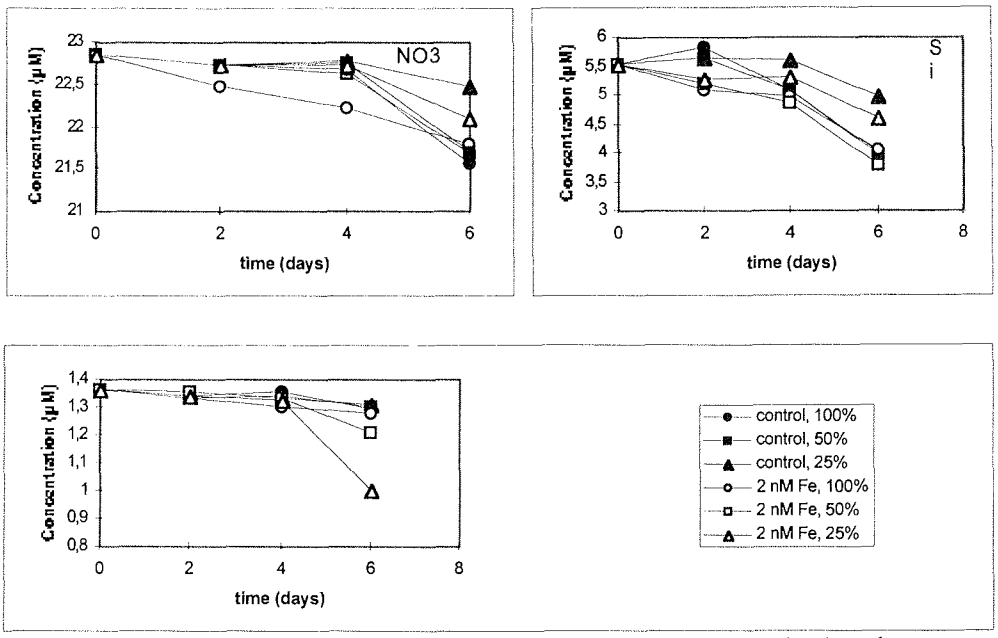

Fig. 14.4. Concentrations of nitrate, phosphate and silicate in the incubation bottles of experiment 3, for iron-enriched (open symbols) and non-enriched bottles (filled symbols).

Table 2: Samples for pigment distribution and for particulate carbohydrate were taken at the following stations:

pigment distribution	particulate carbohydrate
151 (10, 30, 50, 75m depth)	153 (20, 60m)
153 (20, 60m)	154 (20, 60m)
154 (20, 60m)	156 (10, 20, 40, 60, 80, 100m)
156 (10, 20, 40, 60, 80, 100m)	162 (as 156)
157 (as 156)	163 (as 156)
161 (as 156)	164 (as 156)
162 (as 156)	165 (as 156)
163 (as 156)	166 (as 156)
164 (as 156)	167 (20,40,60,80,100m)
165 (as 156)	168 (as 156)
166 (as 156)	181 (20, 40 60, 300m)
167 (as 156)	190 (as 156)
168 (as 156)	197 (as 156)
181 (20, 40 60, 300m)	198 (as 156)
190 (as 156)	199 (as 156)
197 (as 156)	200 (as 156)
198 (as 156)	202 (as 156)
199 (as 156)	203 (as 156)
200 (as 156)	204 (as 156)
202 (as 156)	205 (as 156)
203 (as 156)	
204 (as 156)	
205 (as 156)	
207 (as 156)	

In addition, several surface waters samples for pigment distribution were taken from the ship's sea water supply, covering the box (04.1-04.10), and on transect towards the continent. After filtration over GF/F Whatmann filters, samples were quick-frozen using liquid nitrogen, and thereupon stored at -80°C. At the home laboratory, the samples will be analyzed using HPLC, according to Gieskes & Kraay (1992).

For particulate carbohydrate, several surface waters samples were taken from the ship's sea water supply, covering the box (04.1-04.10).
Samples were filtered over GF/F filters Whatmann and stored at -20 °C. At the home laboratory, the samples will be analyzed using GC.

References

Chisholm, S.W. & Morel, F.M.M. (1991) *Limnol. & Oceanogr.* 36: 1851-1864
Kraay et al. 1992 *J. Phycol.28*:708-712
Kroon, B.M.A. (1994) *J. Phycol.* 30: 841-852
Stefels, J. & van Leeuwe, M.A. (1998) *J. Phycol.* 34: 486-495
van Leeuwe, M.A. Timmermans, Witte, H.J., Kraay, G.W., Veldhuis, M.J.W. & H.J.W. de Baar 1998 MEPS 166:43-52
van Leeuwe, M.A. & H.J.W. de Baar subm. Eur. J. Phycol.

15. KRILL BIOLOGY AND KRILL PHYSIOLOGY

A. Atkinson (BAS), U. Bathmann (AWI), B. Meyer-Harms (AWI), K. Schmidt (IOW), D Stübing (Uni. B)

15.1 General outline

The biology of Antarctic krill *Euphausia superba* during sea-ice formation is rarely known. Integrated research on international level is organised by the IGBP programme Southern Ocean GLOBEC (Global Ocean Ecosystem Dynamics) to study mechanisms and processes which allow the sustainability of the standing stocks of the Antarctic krill throughout an annual cycle. A crucial time period is autumn and winter as food during this time period of about 6 to 8 months in the pelagic environment gets very sparse. The following overwintering strategies are discussed in the scientific literature: utilisation of ice algae and/or zooplankton (mainly copepods), starvation in concert with reduced metabolisms or with utilisation of body proteins, lipid reserves. Investigations of all these aspects simultaneously are missing so far and, thus, were conducted here. The investigations will be carried out during two expeditions with RV POLARSTERN, the first being ANT XVI/3, and field studies at ROTHERA Antarctis Station, all sponsered by a BMBF project.

The main objectives of the current project were to establish:

6. if, when and what feed larvae and adult krill during the overwintering period, and
7. to determine available food sources for krill, and
8. to quantify specific ingestion and assimilation rates for single developmental stages of E. superba.

These objectives are essential for better understanding of the reproduction success and therefor for krill stock assessments.

Field observation and sampling

In the open ocean in the vicinity of Maud Rise, no krill swarms were found. Instead salps, jelly pelagic tunicates dominated the mesozooplankton of the otherwise plankton poor water column. In contrast, krill swarms were recorded on intensive search cruise tracks in the ice covered area of the Antarctic Coastal Current and the shelf slope (Fig. 15.1).

The swarms appeared to be patchily distributed and apparently concentrated in the front between the Coastal Current and Weddell Gyre. Vertical profiles of the ship mounted Acoustic-Doppler-Current-Profilers (ADCP) indicate that during night time swarms migrated up the water column to 50 to 150 m while during day they decend well below 400 m water depth (Fig. 15.2).

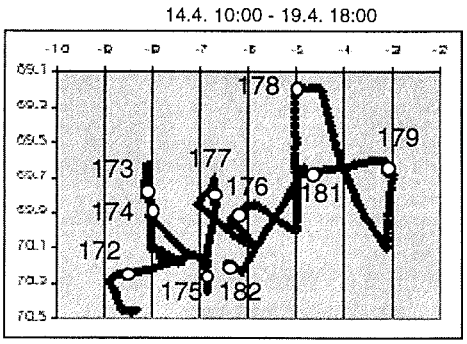

Fig 15.1: Krill search cruise tracks during ANT XVI/3. Staring point is located in the southern west corner of Neumayer Station on 14 April 1999. Numbers indicate stations where vertical net toes were conducted to catch krill. Stations of high krill abundances were # 173, 174, 177, 176.

As current speeds along fronts are much higher than in the adjoining waters it appeared that the swarms were migrating in the fast frontal lane which would sweep them into the southern Weddell Sea, where they have been observed in abundance in the winter pack ice. The highest densities were found in winter within broken floes piled together along pressure ridges and it has been suggested that the food and refuge from predators offered by the winter pack ice is a key factor enabling maintenance of the large krill population. On our cruise, the ice cover which extended well north of the Coastal Current, was still a thin layer of broken floes, and the krill had not yet entered this potential winter habitat.

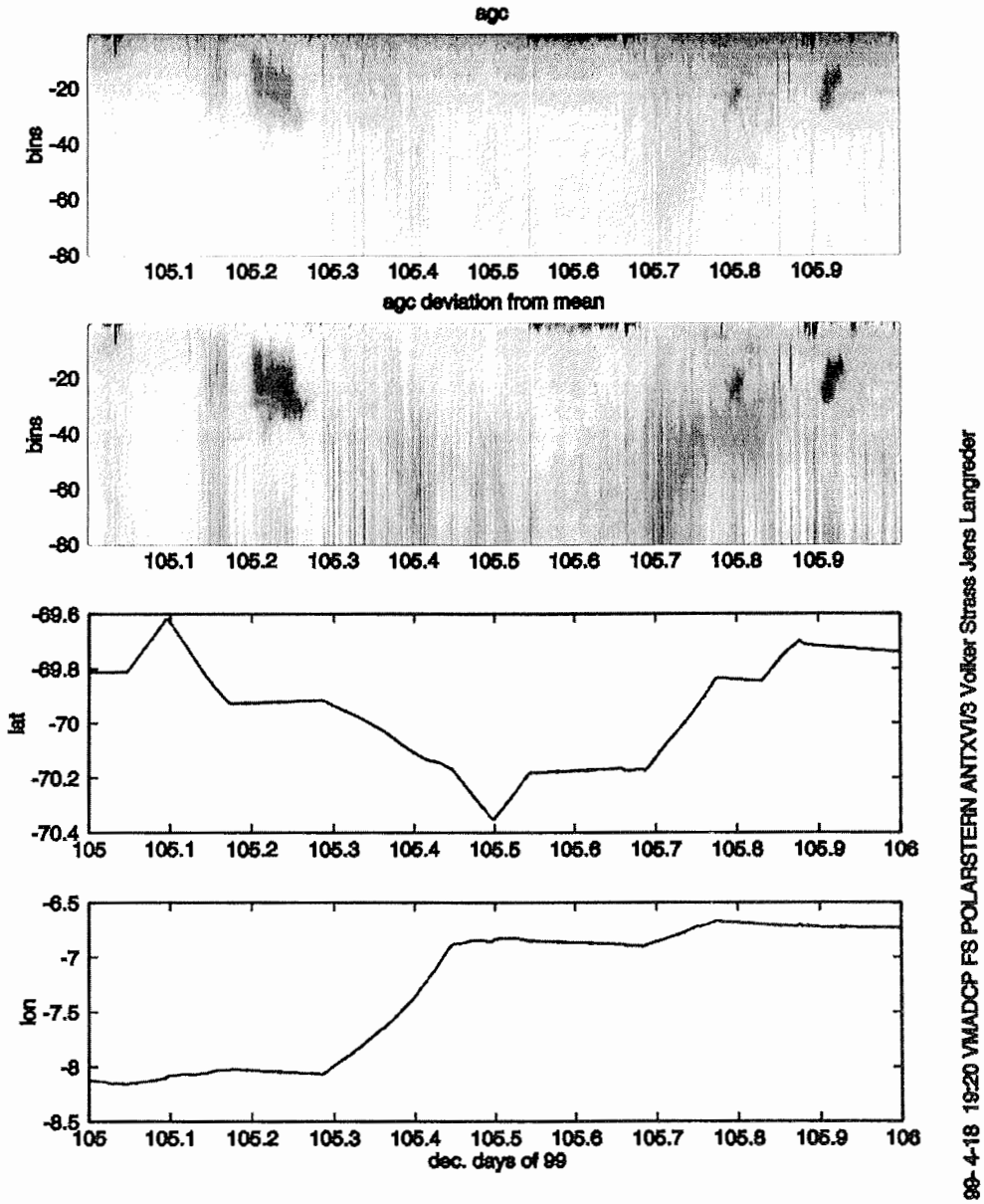

Fig. 15.2: Back scatter (AGC) and corrected back scattering signals (b) by migrating zooplankton and krill detected from the downward looking, ship mounted ADCP during the 24 hrs of 18 April 1999 of the upper 250 m water column. Latitude (c) and longitude (d) of ships position is also given versus time on day 105 of the year 1999. Courtesy by Jens Langredder.

15.2. Examining overwintering strategies of Antarctic krill (Euphausia superba)

During summer krill are considered to be mainly herbivorous, feeding on phytoplankton, but the scarcity of algae during autumn and winter has raised questions on how krill survive this long dark season of ice cover. Suggested overwintering strategies include: 1) reduction in metabolic rate, 2) utilisation of lipid stores, 3) body shrinkage, 4) feeding on ice algae and 5) switching to carnivorous feeding. Our aim was to examine these strategies simultaneously at the onset of winter, comparing the responses of adult krill, juveniles and furcilia larvae.

The first component of the project was to catch various maturity stages of krill and freeze them immediately, for later laboratory analysis. This will include determination of elemental composition, nitrogen isotope ratios, lipid store and analysis of stomach content to determine both whether they were feeding and the major dietary items. Approximately 200 adults and juvenile krill and numerous furcilia were frozen from 2 main locations at the shelf break (locations see above). Examination of juveniles and adult krill showed that they were indeed feeding at the time of capture, but probably at low rates as very little food was seen in their guts. Alongside the netting for krill, potential food sources were characterised by vertical (0 to 200 m depth) tows with a Bongo net for zooplankton food sources and water bottle profiles for microplankton food sources. There were substantial numbers of copepods (chiefly *Metridia gerlachei* and *Calanus propinquus* in the vicinity of the krill swarms we fished, although water column fluorescence was at the lower detection units of our fluorometer. We did not observe krill in the immediate vicinity of the ice, and the aggregations we sucessfully caught krill from were seen on the ADCP at mainly in > 50 m depth. However, ice algae were a potential food source, as evident by localised brown discoloration of the ice. Ice algae were collected, analysed and used as food for krill, although a high degree of patchiness precluded its biomass quantification on an areal basis.

The second part of the study was to complete a series of laboratory experiments to determine feeding, respiration and excretion rates of furcilia, juvenile and adult krill. Values for freshly caught individuals were compared with those acclimated to a variety of feeding regimes; namely filtered seawater (i.e. starvation), natural sawater, natural sawater plus ice community and, for juveniles and adults, natural seawater plus ice community and copepods. Because of patchiness it is not possible to determine precisely the concentrations of that foraging krill may encounter, so we gave them this varierty of food types and concentrations to estimate their physiological response to both type and quantity of food. The method was to maintain batches of krill for 10 day periods, during which they were allowed to feed on one of the above food regimes for 24 hours to monitor diet and feeding rate. Then they were switched to filtered seawater for 24 hours to measure their respiration and ammonium excretion rate, after which the cycle was repeated, returning the krill to their given food regime. Container sizes were as large as possible to allow free swimming of the krill while rates were measured. For adults and juveniles 50 - 60 L containers were used for feeding and 12 L for respiration and excretion while for the 7 to 8 mm long furcilia, 2.5 L containers were used.

Table 15.1: Preliminary results of juvenile and adultkrill feeding rates on *Metridia gerlachei* and *Calanus propinquus*.

Date	Provisional clearance rate on *Metridia gerlachei* and *Calanus propinquus* (ml mg DM h^{-1})	
	juvenile krill ca. 40 mg DM)	adult krill (ca. 190 mg DM)
20.4.99	1.4	1.1
22.4.99	2.4	0.9
24.4.99	2.4	1.3
26.4.99	2.1	1.3

Table 15.2: Ammonium excretion, respiration rates and oxygen (O) and nitrogen (N) ratios of freshly caught animals (FCA), starving adults and furcilia (SK) and animals feeding on natural seawater (NSW), natural seawater plus ice community (NSW + IC) and on natural seawater plus ice community plus copepods (NSW+IC+C) prior to incubation.

adult krill (ca. 211 mg DM) n = 5				
excretion rates (µg NH_4 mg DM h^{-1})				
FCA	SK	NSW	NSW+IC	NSW + IC + C
0.015	0.012	0.010	0.017	0.018
respiration rates (µg O_2 mg DM h^{-1})				
-	0.515	0.886	0.885	0.834
O/N ratio				
-	37	77	46	41
furcilia larvae (ca. 0.5 mg DM) n = 6				
excretion rates (µg NH_4 mg DM h^{-1})				
0.077	0.057	0.093	0.078	-
respiration rates (µg O_2 mg DM h^{-1})				
1.138	0.629	1.238	1.534	-
O/N ratio				
13	10	12	17	-

Feeding rates of krill obtained in the laboratory are partly dependent on the method used (e.g container volume, etc.) but our initial impression is that, while krill were indeed feeding both in the laboratory and in the wild, within the 10 day timescale of our experiments, they did not fully utilise the high food concentrations offered. For instance, using a similar experimental settup at South Georgia during summer, clearance and ingestion rates on copepods were about 5 to 10 times higher than found on this cruise. Preliminary results of juveniles and adult feeding rates on *Metridia gerlachei* and *Calanus propinquus* are are shown in Table 15.1.

Excretion and respiration rates show a more varied picture (Table 15.2). For adults and juveniles ammonium excretion rates were 30% of representative summer values, although respiration rates were within the wide range of summer values. Mass specific respiration and exretion rates for furcilia were 5 to 9 times greater than for adult krill, probably reflectingtheir ca. 1000 x smaller size than adults.

16. Zooplankton at the Antarctic Polar Front

R. Alheit, A. Atkinson, U .Bathmann, B. Meyer-Harms

In previous cruises to the Polar Front at the Atlantic Sector of the Southern Ocean during spring and summer, zooplankton of the upper 200m water column was dominated by small calanoid and cyclopoid copepods. In 1992, south of the Front, salps dominated the otherwise poor plankton communities of the southern ACC. Grazing rates of medium to large sized copepods north of the front were calculated to be less than 3 percent of daily primary production, and, thus, negligible for top down control of primary producers. In contrast, the grazing rates of the small sized zooplankton below 1 mm body length might be high enough to reasonably control phytoplankton biomass.

Our aim of the study was to test...

i) if the high standing stocks of small sized copepods prolong during austral autumn in the vicinity of the Polar front and
ii) if the grazing of this community might be sufficient to control phytoplankton standing stocks, we performed our sampling programme and laboratory experiments during the study of physics and biology at the Polar Front in autumn 1999.

Sampling Programme

The sampling of the zooplankton of the upper 1000 m water column was performed by means of an multinet equipped with 5 (small version) and 9 (large version) nets of 55 or 100 µm mesh size. Vertical hols were located between ths standard depths of 1000, 500, 200, 100, 50 an 0 m, respectively. Samples were prepared for further analysis of species and developmental stages in buffered formalin, or for genetic analysis and determination of lipid content by freezing individuals.

Feeding experiments with Oithona

On some stations Apstein nets were pulled by hand in the upper 30 m water column to retrieve living Oithona species. 200 of adult femals were sorted under the dissection microscope directly after capture and transfered into filtered sea water of ambient temperature.

Six feeding experiments were done on *Oithona* spp. (< 90% *O. similis*) in the vicinity of the Polar Front, four during the first visit (27, 28, 30 March and 5, 9 April) and one during the second visit (5 May). Individuals were collected gently with a 55 micron hand net and incubated in mixed layer seawater enriched with large diatoms. Both the rates and selectivity of feeding on natural particulate material will be determined by a combination of microscopic and HPLC analysis.

Preliminary analysis on the 3 rd and 5 th experiments showed that the large diatom taxa (e.g. *Corethron penatum*, *Rhizosolenia* spp, *Thalassiothrix* spp. were cleared at high rates (about 1000 ml per mg dry mass per day), while clearance rates on the characteristic Polar Front diatom *Fragilariopsis kerguelensis* were negligible.

Likewise the smaller diatoms, *Pseudonitzschia* spp. and *Chaetoceros* spp. were avoided. Methodological problems precluded offering the copepods ambient (i.e. 'average') food concentrations, but at enriched concentrations, estimated carbon rations exceeded 50% of body carbon per day.

These provisional results suggest that *Oithona similis* can eat the large, bloom forming diatoms which are of similar lengths to themselves. The abundances of *Oithona* spp. obtained with the multinet will be combined with their clearance rates to estimate their potential impact on the standing stocks of specific microplankton taxa.

17. BIOMASS PRODUCTION, SUBSTRATE DYNAMICS AND COMMUNITY STRUCTURE OF THE HETEROTROPHIC PICOPLANKTON AT THE POLAR FRONT AND THE WEDDELL SEA IN FALL

M.Simon (Uni O), B. Rosenstock, W. Zwisler LIUK)

Introduction

The Polar Front of the Southern Ocean is one of the major global regions for the export of organic carbon out of the oceanic surface layer and thus of key importance for the global carbon cycle (Falkowski et al. 1998). The rate of export and sinking through the mesopelagic zone is controlled by various factors such as nutrient depletion, senescence of diatoms, and zooplankton grazing but also to a great extent by the consumption of organic matter and its oxidation to CO_2 by the heterotrophic picoplankton (HPP). Yet, still little work has been done to study and understand the seasonal variation of the plankton dynamics and the role of the HPP at the Polar Front. Even less is known about the structural composition of the HPP and its dominant components in the Southern Ocean (Massana et al. 1998, Murray et al. 1998, Simon et al. 1999). During the cruise ANT XVI/3 with RV *Polarstern* from 18 March to 10 May 1999 we carried out studies in this context and asked the following questions:

What are the rates of biomass production and turnover of labile and refractory dissolved organic matter (DOM_{lab}, DOM_{ref}) by HPP during the austral fall?

In which respect does UV-B irradiation affect the turnover and availability of DOM_{lab} and DOM_{ref} and the biomass production of HPP?

How is the community of the HPP composed at the Polar Front and the Weddell Gyre and how does it relate to dynamics of DOM_{lab} and DOM_{ref}?

We performed three consecutive studies on a transect at the 20 °E meridian from 48.30 to 54 °S between 25 March and 4 May 1999 at a total of 15 stations (Nr. 153, 154, 156, 157, 163, 165, 166, 167, 190, 197, 198, 200, 201, 202, 203) and compared them to the Weddell Gyre (stations 169, 185) and the Antarctic coastal current under the pack ice (stations 174, 182).

Methods

Numbers of HPP were counted by standard epifluorescence microscopy after DAPI staining. Their biomass production was measured by the leucine method using ^{14}C-leucine at a final concentration of 10 nM (saturating concentration) and assuming a 2-fold intracellular isotope dilution (Simon & Azam 1989). Turnover rates of ^{3}H-amino acids, ^{3}H-glucose and ^{14}C-protein were determined by adding 0.1 nM and 5 nM (protein) of the label to water samples and measuring the fraction of label taken up per hour. We also took samples for the analysis of dissolved free and combined amino acids and carbohydrates and dissolved organic carbon (DOC) which were kept at –25 °C and will be analyzed later in the home lab. So we will be able to determine uptake rate of free amino acids and carbohydrates and relate them to the carbon demand of the HPP.

The consumption of various fractions of DOM by HPP was determined in dilution cultures growing at ambient temperatures on isolated humic and non-humic DOM of low and high molecular weight (LMW, HMW) separated by ultrafiltration of 3000 Da (filtrate and retentate). The humic fractions were separated on XAD-2 raisins and re-added to the dilution cultures at approximate in situ concentrations.

The effects of UV-irradiation on DOM and the growth and substrate utilization by HPP were investigated by on deck-incubations at in situ temperature for 3 to 5 days of 0.8 µm (HPP) and 0.2 µm filtered (DOM) samples in quartz bottles and relative to a dark control. UV-B and UV-A were excluded with MylarD and polyethylene foil, respectively. To examine photochemical effects on DOM and its availability to consumption by HPP concentrates of HPP (from the particle-free water) were kept in the dark at in situ temperature and added again to the DOC after incubation for one day. Responses to the various treatments by HPP and DOM were measured by HPP abundance, production and uptake of ^{3}H-amino acids and ^{3}H-glucose, the consumption of the humic and non-humic fractions of DOC, dissolved amino acids and carbohydrates.

The community structure of the HPP is being assessed by fluorescent in situ hybridization with rRNA-targeted oligonucleotide probes (FISH, Amann et al. 1995) and by the analysis of PCR-amplified fragments of the 16S rDNA by denaturing gradient gel electrophoresis (DGGE; Muyzer et al. 1993). On various profiles and during the course of the experiments on the consumption of LMW- and HMW-DOM and UV-effects samples for DGGE and FISH were filtered onto 0.2 µm Nuclepore filters and the latter fixed with paraformaldehyde (4% in PBS buffer, pH 7.2). They will be further processed in the lab at home. Previous work showed that the FISH method is well suitable for such studies (Simon et al. 1999).

Results and discussion

At the Polar Front, numbers of HPP between 20 and 200 m ranged from 1.5 to 5.8×10^8 l^{-1} with highest numbers in the upper 100 m which covered the depth of the mixed surface layer. Typical pattems of the vertical distribution are given in Fig. 17.1. The highest numbers, but not biomass production, of a single profile occurred at the end of the survey north of the Polar Front at station 203. Biomass production rates of HPP in the upper 200 m ranged between <2 and 29 ng C l^{-1} h^{-1} and most values in the upper 100 m between 10 and 25 ng C l^{-1} h^{-1}(Fig. 1). Numbers and biomass production often did not covary but showed inverse relationships, i.e. at peaks of production relatively low numbers occurred. Turnover times of dissolved free amino acids and protein in the upper 100 m varied between ca. 5 and 30 days and increased with depth. Usually they were shorter than that of glucose but the latter often was relatively shorter in the upper mesopelagic zone (Fig. 17.1).

Integrated values of the biomass production of HPP in the upper 200 m ranged between 30 and 78 mg C m^{-2} d^{-1} with the highest value at 52 °S at the beginning of the study (Fig. 17.2). Values in the region of the Polar Front, i.e. between 49 and 50 °S, and at two bloom situations at 52 and 54 °S in late March and early May were enhanced as compared to other stations. Even though some variations occurred at the Polar Front it was surprising how close integrated values remained at single locations but measured one to six weeks apart. Production rates integrated for the water column below the mixed layer, from 125 to 1000 m, ranged from 20 to 66 mg C m^{-2} d^{-1} with a pronounced and persistent maximum at the Polar Front (Fig. 17.3). The organic matter available to consumption by HPP below the euphotic zone and the mixed layer predominantly is provided by sinking particulate organic matter or carbon (POM, POC) originating from the phytoplankton in the mixed layer and being decomposed and partly dissolved by particle-associated microbes (Smith et al. 1992). Thus, the consumption of organic matter by HPP below the mixed layer provides a minimum estimate of the POM export flux from the mixed layer (Cho & Azam 1988). Assuming a gross growth efficiency of the HPP as 30%, a typical value found in many aquatic environments (Søndergaard & Middelboe 1995), total consumption of organic carbon by HPP below the mixed layer amounts to 60 to 200 mg C m^{-2} d^{-1} and mean values of 105 to 130 mg C m^{-2} d^{-1} at the Polar Front. These numbers should be equivalent to the minimum export flux of POC.

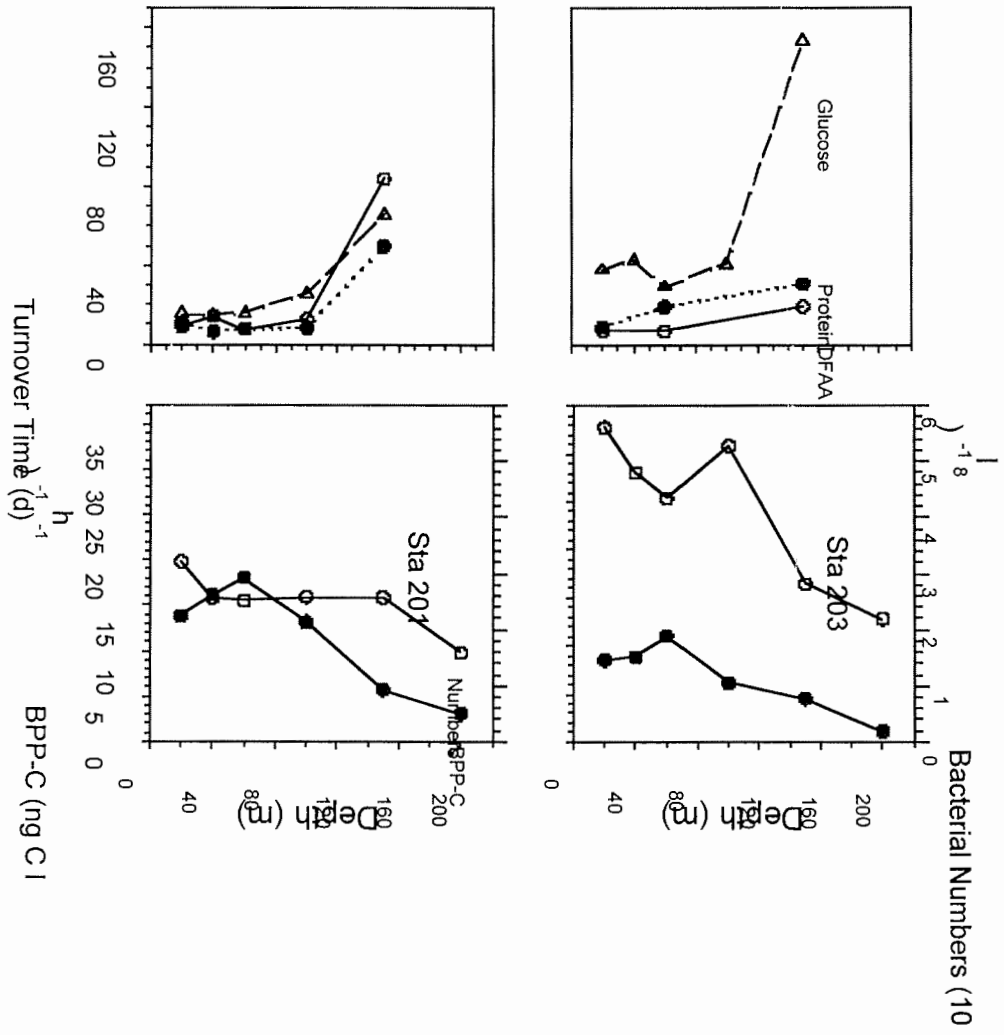

Fig. 17.1: Depth distribution of numbers and production (BPP-C, left panel) and of turnover times of free amino acids (DFAA), protein and glucose of heterotrophic picoplankton (right panel) at stations 201 (49° 30.0' S, 20 °E) and 203 (48° 30.0' S, 20 °E) on 3 May 1999 at the Polar Front .

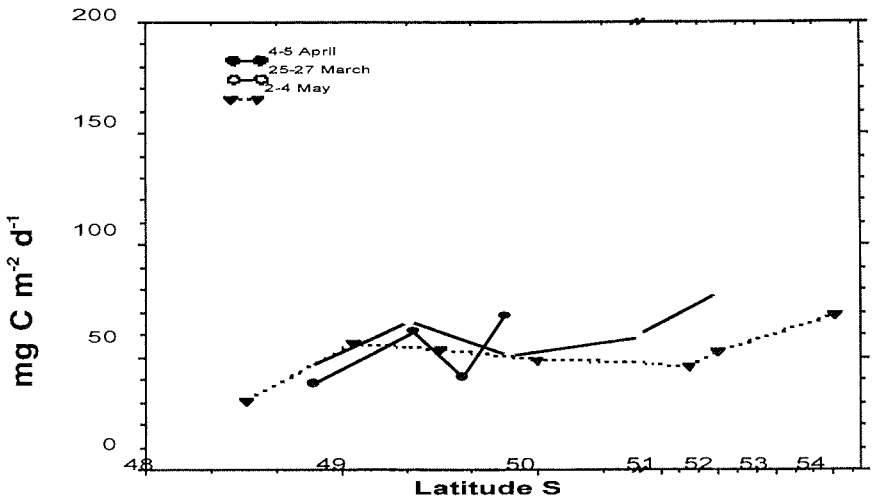

Fig. 17.2: Production rates of the heterotrophic picoplankton integrated from 0 to 200 m along 3 transects at 20 °E across the Polar Front in the austral fall 1999.

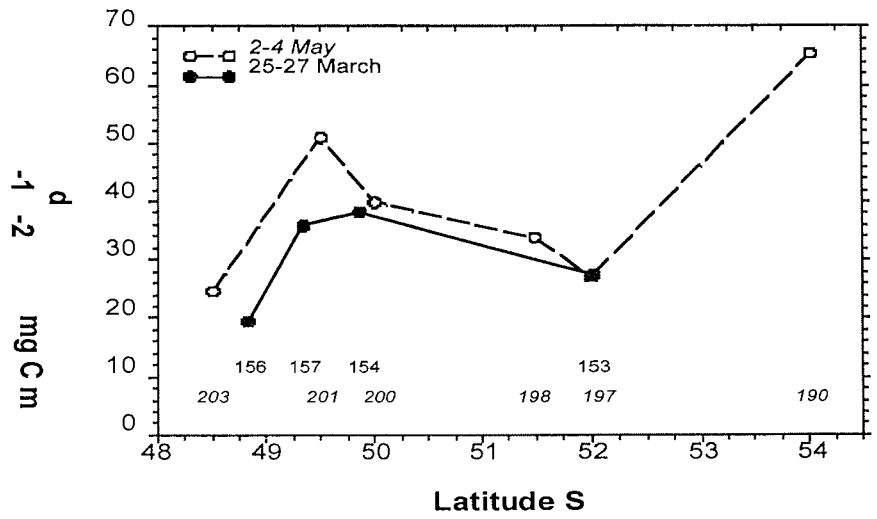

Fig. 17. 3: Production rates of the heterotrophic picoplankton integrated from 125 to 1000 m along 2 transects at 20 °E across the Polar Front in the Austral fall 1999.

Numbers and rates of biomass production of the HPP in the Weddell Gyre and below the newly formed pack ice were not significantly different from those measured at the Polar Front (Fig. 4). In fact, in one profile at Station 182 (70°13' S, 6° 11' W) measured below the pack ice, we found the highest integrated production rates between 125 and 1000 m, 102.9 mg C m^{-2} d^{-1} due to a mixed layer and high amounts of phytoplankton extending to 450 m.

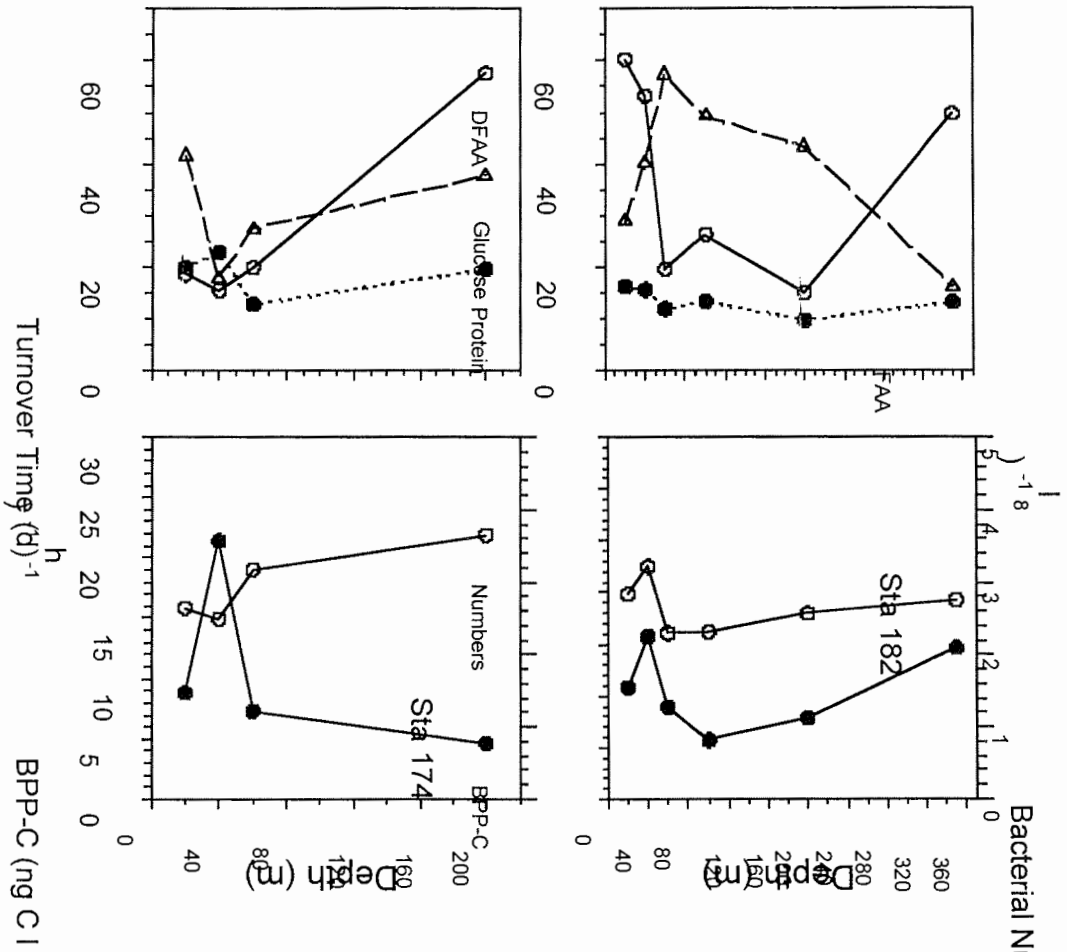

Fig. 17. 4:
Depth distribution of numbers and production (BPP-C, left panel) and of turnover times of free amino acids (DFAA), protein and glucose of heterotrophic picoplankton (right panel) at stations 174 (49° 30.0' S, 20 °E) and 182 (70°13' S, 6° 11' W) under the pack ice in late April 1999 in the Antarctic coastal current.

We expect to find differences in the community structure of the HPP with depth at the Polar Front and also as compared to the colder Weddell Gyre and Antarctic coastal current in our analysis by FISH and DGGE. According to the results of Simon et al. (1999) in the latter psychrophilic HPP communities composed of bacteria of the *Cytophaga/Flavobacteria* cluster dominate as compared to mesophilic communities with much fewer bacteria of this cluster at the Polar Front.

Rates of HPP biomass production integrated for the upper 200 m are at the lower end of values measured by Lochte et al. (1997) in a region of the Polar Front at 6 °W during October and November and also 50% lower than values measured by Simon et al. (1997) in a region at 10 °E in December and January. Hence, the data we measured indicate that the activity of HPP and supply of organic matter by phytoplankton is only 25 to 50% of that earlier in the season and at bloom conditions in the austral spring and summer.

HPP utilization of LMW- and HMW-DOM

Bacterial utilization of different fractions of the DOC-pool was investigated twice at the Polar Front and once in the northern fringe of the Antarctic circumpolar current (ACC, station 190, 54°S, 20°E) and under the pack ice (Station 182, 70°13' S, 6° 11' W). Results are shown as maximum rates of HPP biomass production reached in each assay (Fig. 5). So far, production rates in the HMW- and LMW-DOM assays can not be compared because concentrations of dissolved organic carbon (DOC) will be analyzed only after return in the home lab. At the Polar Front in the LMW fraction, HPP uptake of non-humic LMW-DOC was much higher than in the humic fraction.

Presumably free amino acids and carbohydrates, but also small oligomeres served as the main substrates but further details can be shown only after the analysis of the different substrates. At the stations in the ACC and under the ice the humic DOM-fractions were relatively more important for the growth of HPP even though absolute rates were substantially lower. The same is true for HMW-DOM. Humic DOM in the HMW-fraction also seems to play a more important role for HPP at the Polar Front. At station 157 this fraction was an even more important substrate for the HPP as compared to the non-humic DOM.

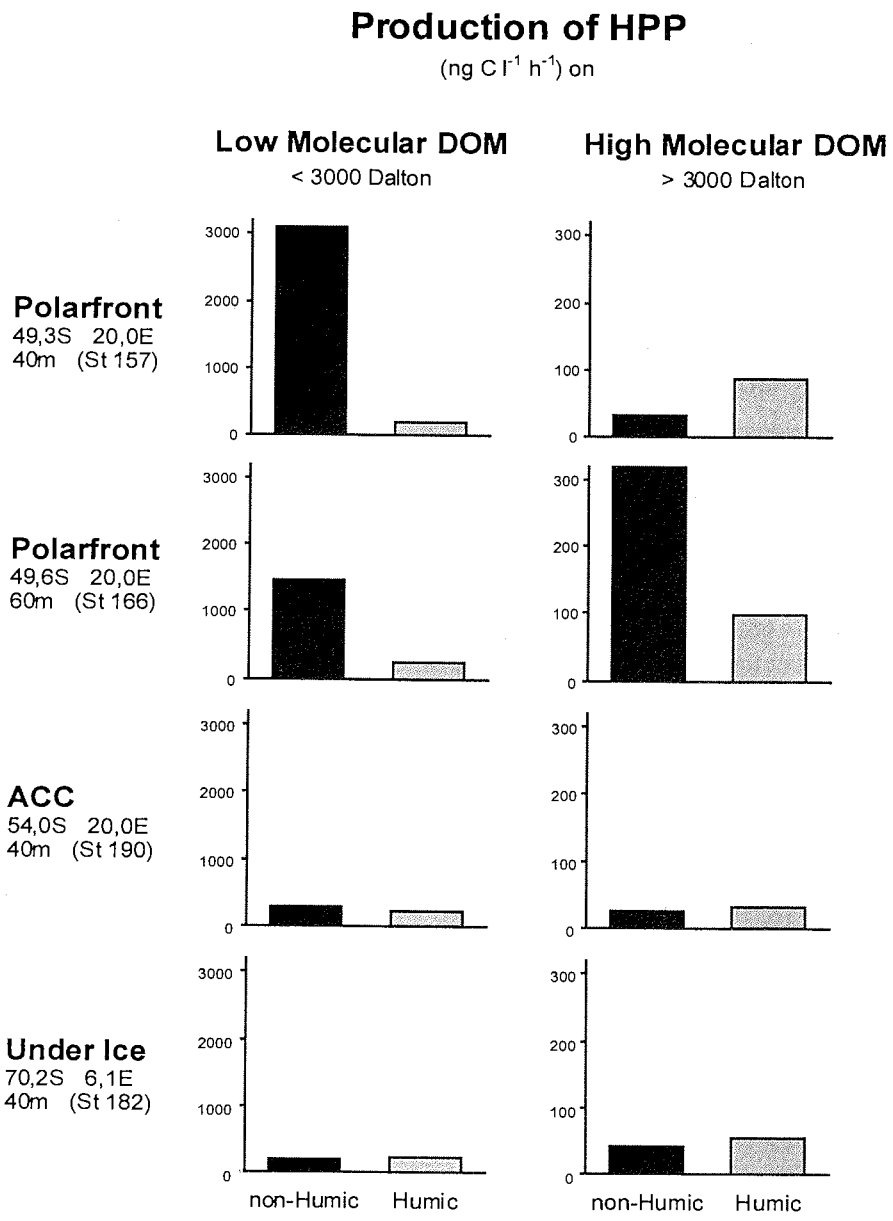

Fig. 17. 5: Utilization of humic and non-humic DOM of low- and high- molecular weight by HPP at four locations in the Southern Ocean.

UV-effects

The effect of UV-irradiation on HPP and DOM was investigated at three different locations in the Southern Ocean. The activity of HPP decreased with the wavelength from the dark control over PAR to UV-A and UV-B, indicating a detrimental effect on the HPP of short-wave irradiation. On the other hand, HPP activity and growth rates increased when they utilized the sunlight-exposed DOM relative to a control with non-exposed DOM. Hence, the lability of the DOM was enhanced after exposure to sunlight. When the HPP of various depths was exposed to full light conditions (PAR, UV-A, UV-B) the responses differed substantially (Fig. 6). With increasing depth there was a remarkable increase in the growth and substrate uptake relative to the dark control, indicating that the HPP at greater depths was less susceptible to short-wave irradiation and that in the upper water layers HPP seem to be more sensitive to UV-radiation.

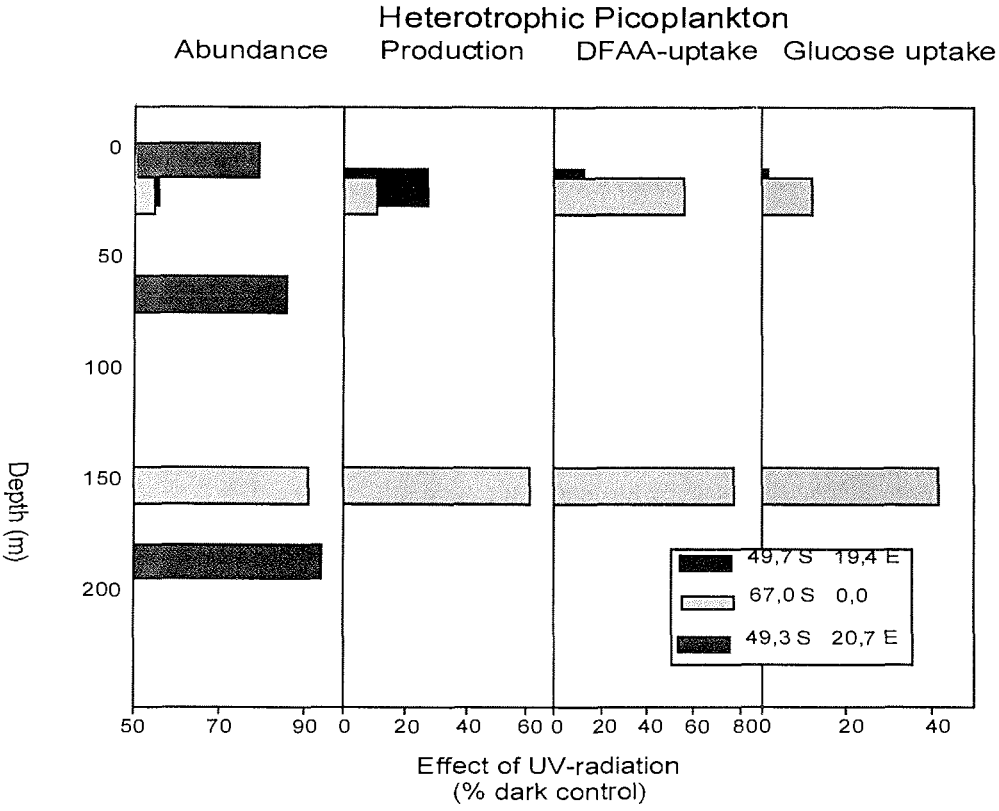

Fig. 17.6: Effects of full-light (PAR, UV-A, UV-B) on the abundance, production, and uptake of amino acids and glucose of HPP of various depths from three stations relative to a dark control.

REFERENCES

Amann, R. I., Ludwig, W., Schleifer, K.H. 1995. Phylogenetic identification and in situ detection of individual microbial cells without cultivation. Microbiol. Rev. 59: 143-169.
Cho, B.C., Azam, F. 1988. Major role of bacteria in biogeochemical fluxes in the ocean's interior. Nature 332: 441-443.
Lochte, K., Bjørnsen, P.K., Giesenhagen, H., Weber, A. 1997. Bacterial standing stock and production and their relation to phytoplankton in the Southern Ocean. Deep Sea Res. 44: 321-340.
Massana, R., Taylor, L.T., Murray, A.E., Wu, K.Y., Jeffrey, W.H., DeLong, E.F. 1998. Vertical distribution and temporal variation of marine plankton archaea in the Gerlache Strait, Antarctica, during early spring. Limnol. Oceanogr. 43: 607-616.
Murray, A.E., Preston, C.M., Massana, R., Taylor, L.T., Blakis, A., Wu, K.Y., DeLong, E.F. 1998. Seasonal and spatial variability of bacterial and archaeal assemblages in the coastal waters near Anvers Island, Antarctica. Appl. Environ. Microbiol. 64: 2585-2595.
Muyzer, G., De Waal, E.C., Uitterlinden, A.G. 1993. Profiling of complex microbial populations by denaturing gradient gel electrophoretic analysis of polymerase chain reaction-amplified genes coding for 16S rRNA. Appl. Environ. Microbiol. 59: 695-700.
Simon, M., Azam, F. 1989. Protein content and protein synthesis rates of planktonic marine bacteria. Mar. Ecol. Prog. Ser. 51: 201-213.
Simon, M., Rosenstock, B., Hennes, K. 1997. Bacteria, viruses and marine snow. Fahrtbericht der Expedition ANT XIII/2. Berichte z. Polarforschung 221: 107-112.
Simon, M., Glöckner, F.O., Amann, R. 1999. Different community structure and temperature optima of heterotrophic picoplankton in various regions of the Southern Ocean. Aquat. Microb. Ecol., in press.
Smith, D.C., Simon, M., Alldredge, A.L., Azam, F. 1992. Intense hydrolytic enzyme activity on marine aggregates and implications for rapid particle dissolution. Nature 359:139-142.
Søndergaard, M., Middelboe, M. 1995. A cross-system analysis of labile dissolved organic carbon. Mar. Ecol. Prog. Ser. 118: 283-294.

Acknowledgments

We are most grateful to the excellent support by the crew of the RV Polarstern under the leadership of captain U. Pahl. This work was supported by a grant from the Deutsche Forschungsgemeinschaft awarded to MS (Si 360/11-1).

18. CENSUSES OF MARINE BIRDS AND MAMMALS

J.A. van Franeker (IBN-DLO)

INTRODUCTION

The interdisciplinary approach in Polarstern's JGOFS and GLOBEC studies in the Southern Ocean offers an excellent framework for gaining knowledge of the pelagic ecology of marine top predators, as their numbers and distribution can be viewed in the ligth of physico-chemical and biological conditions in their environment. The obtained information can assist in the compilation of population estimates for Antarctic species and in the identification of particular environments or geographical areas on which they depend (van Franeker 1996, van Franeker et al. 1999). Such information is needed in issues of management of the Antarctic environment, for example in the framework of the Convention on the Conservation of Antarctic Marine Living Resources (CCAMLR). The links between top predator populations and their main prey such as krill are a major objective in SO-GLOBEC studies.

Although previous study showed that Antarctic top predators play a minor role in terms of direct carbon consumption (van Franeker et al. 1997) , they may be a forcing power in the ecosystem structure. Moreover, their species composition, abundance and distributional pattems may assist in revealing trophic structure and abundance of lower ecosystem levels not easily studied directly (van Franeker et al. subm.). Top predators thus can contribute significantly to the understanding and quantification of carbon fluxes in marine systems.

METHODS

Observations of seabirds, seals and whales were made from an outdoor observation post installed on top of the bridge of Polarstern. The unobstructed clear view to all sides is required for quantitative observations. Only from this position it is reasonably possible to identify which birds are associated with the ship and have to be omitted from quantitative density counts. Bird observations are based on the snapshot method (Tasker et al. 1984) which has an advantage over the BIOMASS (1984) method in that it accounts for bias by bird movement. Quantitative differences between snapshot and BIOMASS methods have been evaluated in van Franeker (1994). As far as possible, additional bird data during ANTXVI-3 were collected to continue the calibration between methods, not only to BIOMASS, but also the vector method of Spear et al. (1992) which offers an alternative way to avoid bias from movement.

Birds as well as seals are counted in a band transect in time blocks of ten minutes from the moving ship. Ship speed and transect width can be used to convert observed numbers of animals to densities per unit of surface area for each ten-minute period. The width of the transect band for seals and birds usually was 300m, taken as 150m to each side of the ship. Depending on viewing conditions such as seastate, light level and glare, the transect width was adapted to allow optimal quantitative observations. For seals and whales, line transect methods (Hiby and Hammond 1989) were used simultaneous with the band transect methods. Although band-transect methods were the standard method for seal censuses (Laws 1980), the Antarctic Pack Ice Seal Program (APIS) now recommends line-transect methods where possible (SCAR Group of Specialists on Seals 1994; Anonymous 1995). Dedicated whale surveys use line-transect methods as a standard (Hiby and Hammond 1989), but these are not always possible in studies like this one due to the low number of animals observed.

In this report 'effective transect widths' for different whale groups were estimated to make calculations. Preliminary results in this paper are thus all based on the band-transect system. Methods to convert top predator densities to their daily food- or carbon requirements are based on published literature of field metabolic rates and were described in detail in Van Franeker (1992) and Van Franeker et al (1997). Data for seals were adjusted for diumal changes (Erickson et al. 1989) using personal data on haul-out behaviour of the Crabeater Seal.

In addition to the quantitative counts, qualitative information was collected on the occurrence of species outside transect bands or during oceanographical stations.

Ten-minute records of ice conditions were made in association with the top predator study. These provide small-scale details that add to the ice observations according to the SO-JGOFS protocol (Garrity, this issue). The 10-minute bird and ice observations are included in the 'ANTXVI-3 surface-database' which combines the whole range of continuous measurements from the surface layer. For information on ice observations in association with top predator counts, see Van den Brink & van Franeker (1997).

RESULTS AND DISCUSSION

From Cape Town ANTXVI-3 cruised southwards to the Antarctic Polar Front (APF) near the 20°East meridian to conduct a detailed grid in the frontal area. Bird observations were started well north of the APF. From there we made a long transect southwest to Neumayer for krill and ice studies in the seasonal ice zone. Long transect and APF grid were repeated during the northward voyage. For details on transects see elsewhere in this issue.

In total 1096 ten-minute top predator observations were conducted during the ANTXVI-3 cruise during transects south of 40°S. Most of these, 1034 counts were systematic density counts, the remainder being initial trials or non-systematic counts during very poor weather conditions. A large number of counts was conducted in the APF area between 49° and 50° South (337 counts), but the remainder was fairly evenly distributed among all latitudes south into the seasonal ice zone and the shelf edge near Neumayer.
A full list of all species of marine birds and mammals observed during transects south of 40°S is given in Appendix 1 with three indicators of abundance. 'Nr seen' refers to the total number recorded, including ship associated birds. By comparing this figure to 'avg dens' the average density (n/km^2) during the whole cruise, it is possible to obtain an impression of the level of ship-attraction in the different species. Finally, the 'max dens' column provides information on the maximum density recorded in any of the 10 minute counts. Relative species composition, distribution and abundance differed from those observed during the earlier studies in this area (van Franeker et al. 1997; van Franeker & van den Brink 1997) showing seasonal influences and changes in phytoplankton bloom areas and sea ice distribution.

Quantitative data on toppredators and associated ice observations (cover, floesize, floedevelopment and bergs), have been included in the SO-JGOFS Surface Registration Database which is available to participants. Top predator data inserted into this database are, for each available 10 min period, density (individuals/km^2), biomass (kg/km^2), and carbon consumption rates (mgC/m^2/day) of the combined top predator community, viz. birds, seals and whales.

A summary of data in the surface database is given in Fig. 18.1 and 2 as the averages of density, biomass and carbon consumption per degree of latitude.

Comparison of the graphs illustrates that, at least in ecosystem studies over larger areas, data on abundance (density) and biomass of top predators (Fig.1) are poor descriptors of their role in the system. The highly variable proportions of tubenosed seabirds, penguins, seals and whales in the community are the reason for this, and emphasize that only a common denominator like food consumption (expressed as carbon consumption rates in Fig. 18.2) is a correct approach in system studies. Although this seems obvious, density or biomass comparisons within or between biological compartments are regularly made. Fig. 18.2. also supplies fluorescence in the surface layer as a very preliminary indicator of phytoplankton abundance and/or productivity (but suffers similar and other restrictions as discussed for animal density and biomass above).

The large scale pattern of top predator distribution is similar to that observed in the earlier JGOFS cruises in the area. In and near the sea-ice zone, biomass and food-consumption rates of top predators exceed those elsewhere by order(s) of magnitude because of the relative abundance of large birds (penguins), seals and whales. Data for the ice zone are shown 'off-scale' in Fig. 18.1 and 2 to be able to illustrate patterns in open waters further north. Clear patterns in density, biomass and carbonconsumption are visible in a wide area around the APF. Mismatches between various peaks in the graphs are again caused by variable proportions of differently sized bird groups (e.g. prions versus penguins) and/or the presence of mammals (e.g. fur seals) in particular zones. Data suggest rapid responses by top predators to prey types associated with developmental stages and/or depth distribution of phytoplankton-blooms. Further analyses will attempt to focus on this issue. The detailed data in the APF grid may assist in this.

Top predator observations in the initial grid transect over the APF could only cover part of the area, mainly the south, due to relatively long periods of darkness. Nevertheless, patterns in toppredator species composition and abundance were evident. These strongly differed from those in a similar study in the APF in summer1995/1997 (van Franeker et al. subm). Small zooplankton surface feeding birds, abundant over midsummer phytoplankton blooms had been replaced in the early winter situation by a community of larger birds and deep diving species (penguins, fur seals). Fig. 18.3 illustrates that carbon consumption by this community was highest at the lower end of the grid area, south of the oceanographical APF. Other studies on board suggest gradual subduction of northward flowing water with an older phytoplankton bloom towards the APF. Top predator distributions suggest that this water is associated with higher trophic levels suitable as prey for (diving) predators. Gradual deepening of the water towards the APF could then mean that efficient exploitation of prey was still possible in the south, but that subduction became to deep when coming closer to the APF.

In conclusion, top predator studies during ANT XVI-3 on the one hand confirmed major phenomena seen in earlier studies, but on the other hand supplied strong information on seasonal change and small scale variations important in the overall understanding of ecosystem processes in the Southern Ocean.

References

Anonymous 1995. Report of the 1995 APIS Program planning meeting. APIS Report No.1. National Marine Mammal Laboratory, Seattle. 26pp.

BIOMASS Working Party on Bird Ecology. 1984. Recording observations of birds at sea (revised edition). BIOMASS Handb. 18: 1-20.

Erickson, A.W., Bledsoe L.J., and Hanson M.B. 1989. Bootstrap correction for diurnal activity cycle in census data for Antarctic seals. Mar. Mammal Sci. 5: 29-56.

Hiby A.R. and Hammond P.S. 1989. Survey techniques for estimating cetaceans. In: Donovan G.P.(ed). The comprehensive assessment of whale stocks: the early years. Rep.Int.Whal.Comn (Special Issue II). Cambridge. pp 47-80.

Laws, R.M. (ed) 1980. Estimation of population sizes of seals. BIOMASS Handbook No. 2: 21 pp. SCAR, Cambridge.
SCAR Group of Specialists on Seals 1994. Antarctic Pack Ice Seals: indicators of environmental change and contributors to carbon flux. APIS Program, draft implementation plan, Aug. 1994. SCAR Group of Specialists on Seals, Seattle.7 pp.
Spear, L., Nur, N., Ainley, D.G. 1992. Estimating absolute densities of flying seabirds using analysis of relative movement. Auk 109: 385-389.
Tasker M.L., Hope Jones P, Dixon T, and Blake B.F. 1984. Counting seabirds at sea from ships: a review of methods employed and a suggestion fro a standardized approach. Auk 101:567-577.
Van den Brink, N.W., & van Franeker, J.A. 1997. Sea ice observations and icebergs. pp 12-17 in: U.Bathmann, M.Lucas & V.Smetacek (eds). The Expeditions ANTARKTIS XIII/1-2 of the Research Vessel "POLARSTERN" in 1995/96. Berichte zur Polarforschung Nr.221
van Franeker, J.A. 1992. Top predators as indicators for ecosystem events in the confluence zone and marginal ice zone of the Weddell and Scotia seas, Antarctica, November 1988 to January 1989 (EPOS Leg 2). Polar Biol. 12:93-102.
Van Franeker, J.A. 1994. A comparison of methods for counting seabirds at sea in the Southern Ocean. J. Field Ornithol. 65(1): 96-108
Van Franeker, J.A. 1996. Pelagic distribution and numbers of the Antarctic Petrel *Thalassoica antarctica* in the Weddell Sea during spring. Polar Biology 16: 565-572.
Van Franeker, J.A., Bathmann, U.V., & Mathot, S. 1997. Carbon fluxes to Antarctic top predators. Deep Sea Research II 44(1/2): 435-455.
van Franeker, J.A., & van den Brink, N.W. 1997. Censuses of marine birds and mammals. pp 116-121 in: U.Bathmann, M.Lucas & V.Smetacek (eds). The Expeditions ANTARKTIS XIII/1-2 of the Research Vessel "POLARSTERN" in 1995/96. Berichte zur Polarforschung Nr.221.
Van Franeker, J.A., Gavrilo, M., Mehlum, F., Veit, R.R., & Woehler, E.J. 1999. Distribution and abundance of the Antarctic Petrel. Colonial Waterbirds 22(1): ..... (in press)
Van Franeker, J.A., Van den Brink, N.W., Bathmann, U.V., Pollard, R.T., & de Baar, H.J.W. (subm). Responses of seabirds, in particular prions (*Pachyptila* sp.), to small scale processes in the Antarctic Polar Front. Deep Sea Research submitted

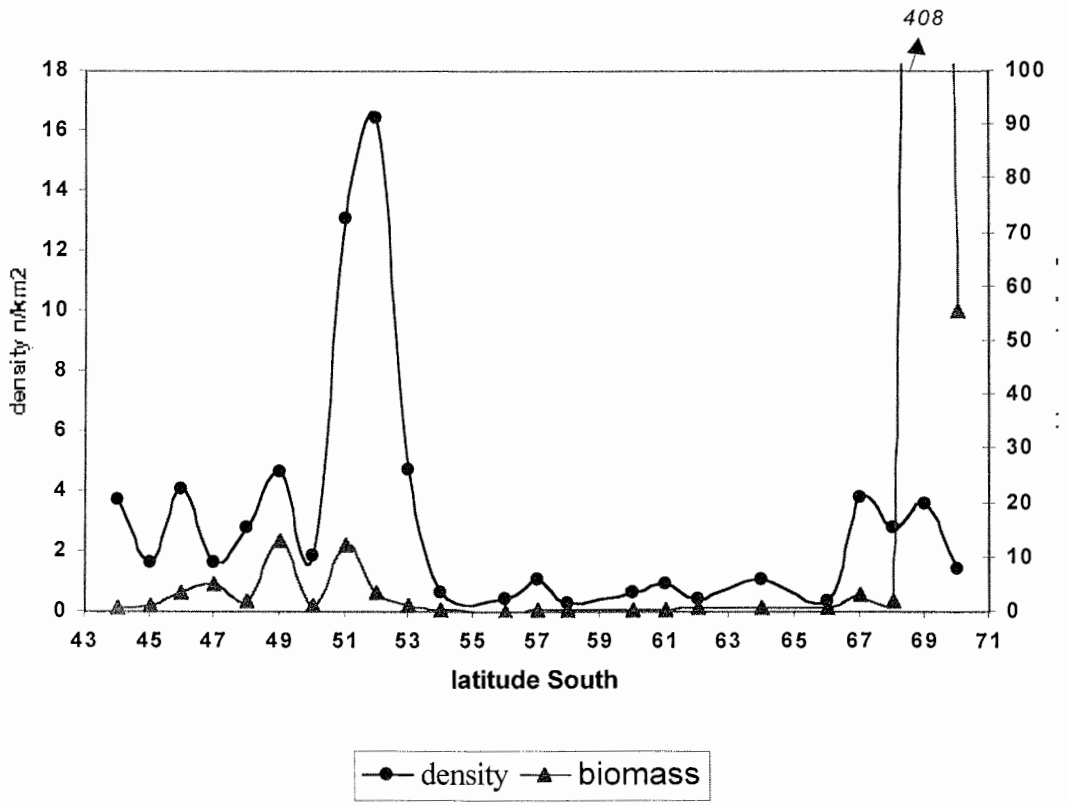

Fig. 18.1:Density and biomass of top predators (birds, seals and whales) during ANT/XVI-3. Averages per degree of latitude, all transects combined (n = 1034 ten minute counts).

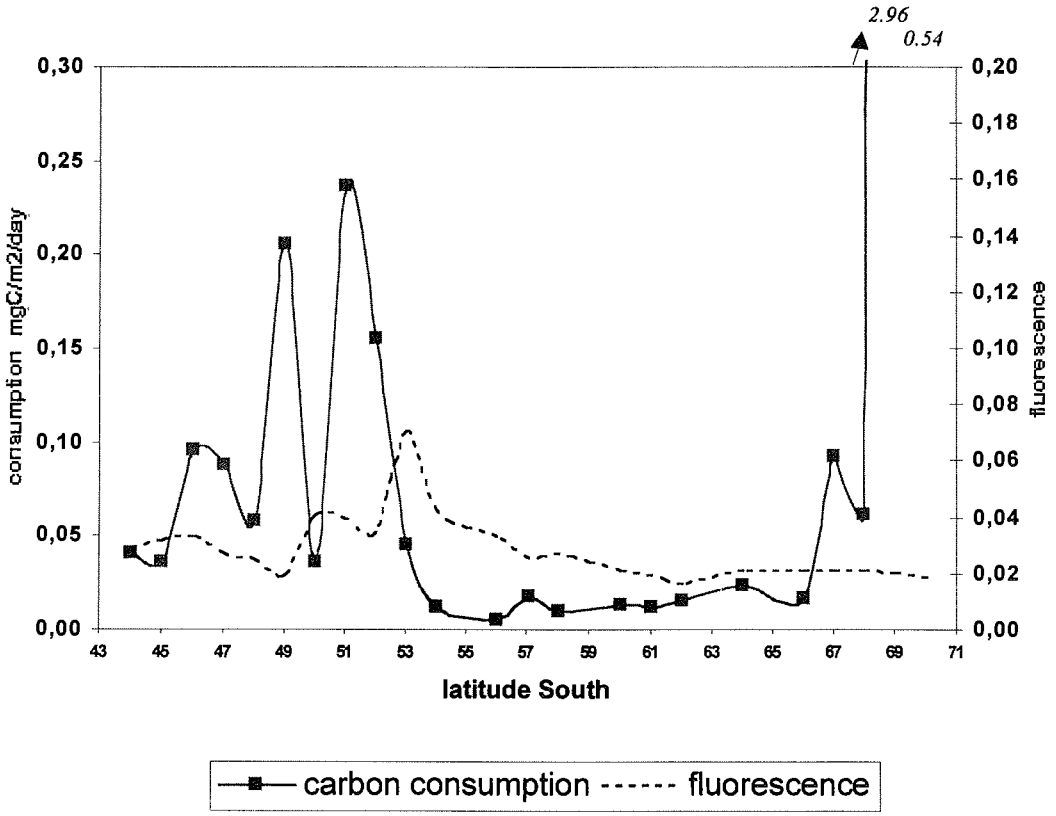

Fig. 18.2: Daily carbon consumption of top predators (birds, seals and whales) during ANT/XVI-3. Averages per degree of latitude, all transects combined (n = 1034 ten minute counts).

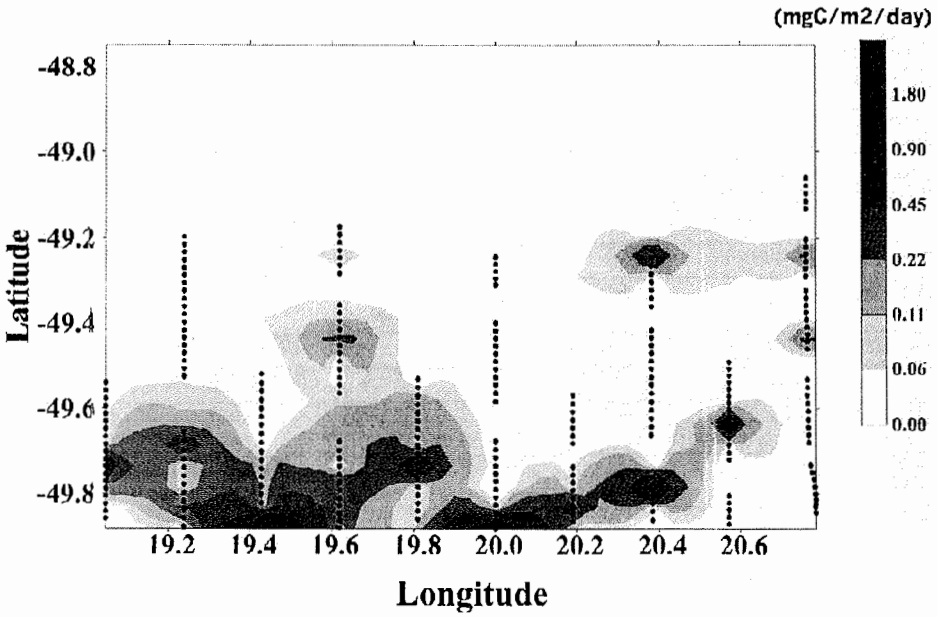

Fig. 18.3: Contour plot of daily carbon consumption rates by top predators in the Antarctic Polar Front Grid Transect. Dots indicate positions of 10 min counts.

APPENDIX 18

Marine birds and mammals observed during ANT/XVI-3

Listed are all species or groups seen south of 40°S, Mar-May'99.'Nr.seen' is total number of individuals recorded, including ship associated animals or those out of transect. 'Avg dens' is average density as number of individuals per km^2 over all observations (1034 counts over a total transect area of 849.5 km^2). 'Max dens' is maximum density observed in any of these counts.

Missing density figures indicate that the species was only seen out of the transect area or during non-systematic observations (as opposed to density ' 0.00' meaning that average density was below 0.005 individuals per km2). Individuals not identified to species level are grouped in the nearest taxon. Most unidentified Prions believed to be *P.vittata*.

PENGUINS	nr seen	avg dens	max dens	
King Penguin	30	0.02	8	*Aptenodytes patagonica*
Emperor Penguin	63	0.03	5	*Aptenodytes forsteri*
unidentified penguin	11	0.01	3	*penguin sp.*
Unidentified Pygoscelis	9	0.01	1	*Pygoscelis sp.*
Adelie Penguin	139	0.13	22	*Pygoscelis adeliae*
Chinstrap Penguin	107	0.02	7	*Pygoscelis antarctica*
Unidentified Eudyptes	62	0.07	30	*Eudyptes sp.*
Rockhopper Penguin	4	0.01	6	*Eudyptes crestatus*
Macaroni Penguin	15	0.00	5	*Eudyptes chrysolophus*

ALBATROSSES	nr seen	avg dens	max dens	
Wandering Albatross	377	0.01	2	*Diomedea exulans*
Mollymauk sp.	5	0.00	3	*Diomedea 'mollymauk'*
Black-browed Albatross	49	0.01	2	*Diomedea melanophris*
White-capped Albatross	9	0.00	2	*Diomedea cauta*
Yellow-nosed Albatross	1			*Diomedea chlororhynchos*
Grey-headed Albatross	120	0.01	2	*Diomedea chrysostoma*
Sooty Albatross	54	0.00	3	*Phoebetria fusca*
Light-mantled Sooty Albatross	227	0.02	2	*Phoebetria palpebrata*

OTHER TUBENOSES	nr seen	avg dens	max dens	
Southern Fulmar	456	0.05	5	*Fulmarus glacialoides*
Antarctic Petrel	5019	0.17	18	*Thalassoica antarctica*
Cape Petrel ('Pintado Petrel')	376	0.02	4	*Daption capense*
Snow Petrel	571	0.08	4	*Pagodroma nivea*
Giant Petrel sp.	17	0.00	2	*Macronectes sp.*
Northern Giant Petrel	19	0.01	2	*Macronectes halli*
Southern Giant Petrel	66	0.01	2	*Macronectes giganteus*
Unidentified Prion	2394	1.03	126	*Pachyptila sp*
Prion or Blue P.?	105	0.01	5	*Pachyptila/Halobaena sp*
Broadbilled Prion	3	0.00	3	*Pachyptila vittata*
Fairy Prion	44	0.02	6	*Pachyptila turtur*
Great-winged Petrel	231	0.04	3	*Pterodroma macroptera*
White-headed Petrel	97	0.03	3	*Pterodroma lessonii*
Kerguelen Petrel	375	0.06	5	*Pterodroma brevirostris*
Soft-plumaged Petrel	470	0.10	5	*Pterodroma mollis*
Grey Petrel	159	0.03	3	*Procellaria cinerea*
White-chinned Petrel	1700	0.10	37	*Procellaria aequinoctialis*
Great Shearwater	23	0.01	2	*Puffinus gravis*

Sooty Shearwater	200	0.09	37	*Puffinus griseus*
Little Shearwater	52	0.04	5	*Puffinus assimilis*
Blue Petrel	509	0.08	2	*Halobaena caerulea*
Wilsons Storm-petrel	1			*Oceanites oceanicus*
Black-bellied Storm-petrel	323	0.17	11	*Fregetta tropica*
Diving Petrel sp.	34	0.03	3	*Pelecanoides sp.*

OTHER BIRDS	**nr seen**	**avg dens**	**max dens**	
Art/Ant/Ker Tern	27	0.03	5	*Sterna sp medium*
unidentified small tern	3	0.00	1	*Sterna sp small*

MAMMALS	**nr seen**	**avg dens**	**max dens**	
Seal (Phocid) sp	12	0.01	2	*Phocidae sp*
Crabeater Seal	151	0.15	32	*Lobodon carcinophagus*
Leopard Seal	1	0.00	1	*Hydrurga leptonyx*
Weddell Seal	3			*Leptonychotes weddellii*
Ross Seal	1	0.00	1	*Ommatophoca rossii*
Antarctic Fur Seal	14	0.01	3	*Arctocephalus gazella*
Ant. Fur Seal male	5	0.01	3	*Arctocephalus gazella*
unidentified medium whale	2	0.00	0	*Cetacean medium*
unidentified small whale	2			*Cetacean small*
Sei/Fin? Whale	1	0.00	0	*Baleanoptera sp*
Minke Whale	8	0.00	1	*Balaenoptera acutorostrata*
Southern Right Whale	1			*Eubalaena australis*

other observations	**nr seen**	**avg dens**	**max dens**
Seaweed	27	0.03	5
Brown Spot (unknown origin)	8	0.01	2
Driftwood(timber)	1	0.00	2
Plastic-foam	3	0.00	3
Plastic: user objects	1		
Metal oildrum 44 gallon	3	0.00	1

19. SOURCE REGIONS AND TRANSPORT PATHS OF IRON IN THE ANTARCTIC CIRCUMPOLAR CURRENT

C. Hanfland, M. Rutgers van der Loeff, H.-J. Walter, U. Westernstroeer (AWI)

19.1 Objectives

Whereas the distribution and growth controlling effects of iron are studied in other programs (chapters 13, 14), our aim is to identify the sources and transport mechanisms of the iron into the Atlantic Sector of the Southern Ocean. This study is part of the EU-project CARUSO, and of a parallel DFG project. Principle iron sources are: aeolian inputs from southern South America and the Antarctic Peninsula, advective inputs from their respective continental shelves, and upwelling of deep water.

Release of iron from the continental shelves can be traced by ^{228}Ra. It is a daughter product of ^{232}Th, which is common in terrigenous sediment but nearly absent in seawater due to its particle reactive behaviour. In contrast, radium is soluble in water and can accumulate to high activities over fine-grained sediment (Rutgers van der Loeff 1994). According to its half-life of 5,8 years, the activity of ^{228}Ra will decrease with distance from the source and is extremely low in the open ocean. In the fast eastward moving Antarctic Circumpolar Current, however, the half-life of ^{228}Ra should be long enough for a high ^{228}Ra signal to be traced from the Patagonian or Antarctic shelves to the eastern South Atlantic. First indications for the significance of this pathway come from the enhanced activity of ^{228}Th, the daughter product of ^{228}Ra measured in surface waters at 53°S on the transect Cape Town-Neumayer (Geibert et al. 1998).

Aeolian input of iron into SE-Atlantic surface waters can be identified with ^{232}Th and Al from the various continental source regions. Both elements have residence times in surface waters of less than 1 year, thus excluding large scale horizontal advection. A strong signal of ^{232}Th and Al in surface waters therefore reflects a high input of dust particles into this region (e.g. Helmers & Rutgers van der Loeff 1993). The neodymium (Nd) isotope signal of suspended matter enables us to elucidate the source(s) of the dusts. Juvenile terrigenous material derived from the subduction related magmatism of southern S-America, the Antarctic Peninsula and oceanic islands (e.g. the South Sandwich Islands) carries a high $^{143}Nd/^{144}Nd$ isotope ratio, compared to terrigenous material from old continental crust (East Antarctica, S-Africa) which has a very low $^{143}Nd/^{144}Nd$ ratio.

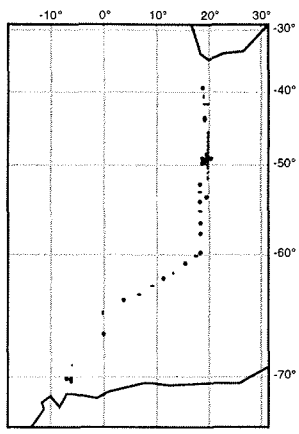

Fig. 1: Sample locations of surface water samples for the analysis of dissolved radium. Open circles represent stationary sampling; closed circles stand for sampling during steaming of the ship and represent integrated values.

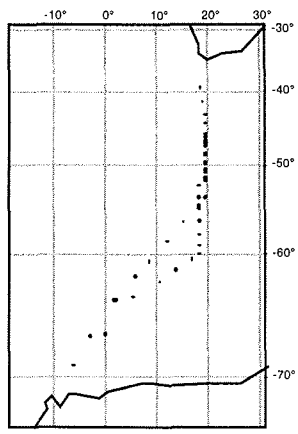

Fig. 2: Sample locations of surface water samples for suspended particulate matter for the analysis of Nd isotopes and other trace metals. All samples have been taken during steaming of the ship and represent integrated values.

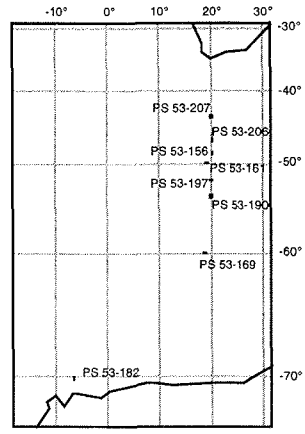

Fig. 3: Sample locations of deep water stations for the analysis of dissolved radium and particulate Nd isotopes. Every station also has a surface water sample.

19.2 Sampling strategy, sample processing and first on board analyses

The sampling for the regional distribution of dissolved Al in surface waters was done in conjunction with the sampling of Fe by the NIOZ Group. The sampling for dissolved ^{228}Ra and for the $^{143}Nd/^{144}Nd$ isotope signature of suspended particulate matter was run parallel in most places, albeit at a much lower regional resolution than for Al and Fe (Fig. 19.1, 2). This is because filtration of large volumes of seawater (usually several thousand litres) is required for analysis. In order to obtain a two-dimensional distribution of dissolved ^{228}Ra and of particulate $^{143}Nd/^{144}Nd$, eight deep casts, each going down to depths between 1000 m and 1800 m, were deployed in coordination with the sampling for Fe and Al by the NIOZ group on a N-S transect through the ACC into the Eastern Weddell Sea (Fig. 19.3). These large volume samples have been collected by time-programmed in situ-pumps, filtering water for about 2 hours at specific depths.

It was the first time that gamma spectroscopy has been used on board POLARSTERN, providing the possibility of screening a lot of samples for various radionuclides. Furthermore, ^{234}Th (half-life of 24 days) could be meausured directly with a satisfying precision to be used as a yield tracer, thereby (in combination with on board beta counting) giving the possibility of processing the samples for dissolved radium by the ^{228}Th-ingrowth method without adding any spike.

Samples measured by gamma spectroscopy during ANT XVI/3 included material from sediment traps, suspended particles from surface waters taken by a continuous flow centrifuge and ashed cartridges for dissolved radionuclides (see sections below).

19.2.1 Dissolved radium

Large volumes of water (between 1000 and 9000 litres) from the ship's seawater supply were passed through two MnO_2-coated polypropylene cartridges put in series. An uncoated cartridge served as a prefilter to separate the particulate and dissolved (< 1μ) fractions. If taken during steaming time the samples represent a mixed value over a sampling distance of up to 70 nautical miles. The cartridges with the particulate fraction were sealed in plastic bags and frozen for further analyses, e.g. Th and Pa isotopes. The coated filters were rinsed to remove all salt, dried at 50°C and ashed in a muffle furnace at 400°C. Further processing comprised the dissolution of the ash and removal of all initial ^{228}Th (the daughter product of ^{228}Ra) by ion exchange chromatography to obtain a pure radium-fraction. After about a year of storage, this fraction will be analyzed for the ingrown ^{228}Th to calculate back on the original ^{228}Ra values. Ultimately, this so-called ^{228}Th-ingrowth method will yield the activity ratio $^{228}Ra/^{226}Ra$. Preliminary gamma counting results of the cartridge ash yield measurable ^{228}Th off South Africa, on the Antarctic continental shelf and in the Polar Front region around 50°S. The ^{228}Th-ingrowth method will show if these peaks can be related to increased ^{228}Ra values.

For the quantitative determination of ^{226}Ra, discrete samples of 20 litres of seawater were taken parallel to the large volume sampling. Under continuous stirring, a solution of BaCl was added drop by drop to precipitate radium as $BaSO_4$. The precipitate was then concentrated by centrifugation and stored in plastic tubes to be measured at home. The ^{228}Ra-content of each of the samples can then be calculated from the $^{228}Ra/^{226}Ra$ values from the cartridge sample and the absolute ^{226}Ra-concentration from the subsample.

Five in situ-pumps, each loaded with two MnO_2-coated cartridges, have been deployed on the deep stations (fig. 3) and will be processed in our laboratory at the AWI as described for the surface samples.

19.2.2 Collection of suspended particles for Nd isotope analysis and other trace elements

Suspended particulate matter in surface waters was collected by underway sampling with a continuous flow centrifuge (flow rate 700-1000 litres of sea-water/hour). Sample volumes ranged from 2000 to 7000 litres. Concentrations of particulate matter were highest in the Antarctic Zone of the ACC, decreasing to the north and south, with extremely low concentrations in the Eastern Weddell Sea. After collection the material was freeze-dried and homogenized. Further treatment consists of gamma counting for ^{234}Th and ^{7}Be, the latter being a cosmogenic radionuclide with a relatively short half-life of 53 days and representing an indicator for recent wet and dry deposition. First results of on board gamma counting from samples collected in the first grid survey point to higher concentrations of ^{7}Be in surface waters south of the Polar Front than north of it, similar to the concetrations of iron measured in the grid across front gradients (NIOZ group, chapter 6). ^{7}Be was also observed in the first sample collected during the grid survey by the sediment trap at the southern mooring (VPF2), whereas it was below detection limit in subsequent collection periods and in the northern trap. The apparent relationship between ^{7}Be and Fe is probably an indication for an enhanced atmospheric deposition of iron and supports similar indications from the relationship between Fe and rainfall as measured on the ship (chapter 6). The analysis of Al (NIOZ group) will show whether there are indeed indications for enhanced fluxes of aeolian material south of the Polar Front which have led to the development of the plankton bloom there.

The Nd isotope measurements will be carried out on selected samples with high Fe, Al and ^{7}Be concentrations at the University of Toulouse by TIMS. Deep suspended particles were collected with three in-situ pumps deployed in the upper 1000m (fig. 3). Filtering was performed through a 0.65 micron 293mm-filter. Filtered volumes ranged from 500 to 1200 litres of seawater. Filters were dried and stored at -18° C. Further treatment will follow in the laboratory in Toulouse.

References

Geibert, W., Walter, H.J., Hanfland, C. & Rutgers van der Loeff, M.M. (1998): Surface concentrations of ^{228}Th, ^{230}Th and ^{231}Pa in the Atlantic Sector of the Southern Ocean - the effects on palaeoenvironmental applications. - V.M. Goldschmidt Conference, Toulouse 1998, Mineralogical Magazine 62A, 511-512.

Helmers, E. & Rutgers van der Loeff, M.M. (1993): Lead and aluminium in Atlantic surface waters (50°N to 50°S) reflecting anthropogenic and natural sources in the eolian transport. - J. Geophys. Res., 98, 20261-20273.

Rutgers van der Loeff, M.M. (1994): ^{226}Ra and ^{228}Th in the Weddell Sea. - In: Johannessen, O.M., Muench, R.D. & Overland, J.E. (eds): The polar oceans and their role in shaping the global environment: the Nansen centennial volume, Geophysical Monograph 85, 177-186.

20. EXPORT PRODUCTION MEASURED THROUGH THE 234TH/238U DISEQUILIBRIUM IN SURFACE WATER.

M.M. Rutgers van der Loeff & U. Westernstroer

Introduction

The radioisotope Th-234 is produced at a well-known rate from decay of uranium in seawater. As thorium is a highly particle-reactive element, the downward flux of particles through the water column causes a depletion of Th-234 in surface waters relative to its parent U-238. This depletion can be used to quantify the export flux on a timescale of the half-life of Th-234 (24 days).

We have measured Th-234 in surface waters on N-S transects as a means to map the latitudinal distribution of export production. Moreover we have detemined the activity in profiles sampled with the Rosette in order to quantify the cumulative depletion and estimate the export flux. Comparison of this flux with the flux intercepted by the sediment traps deployed at 350m depth yielded an estimate of the collection efficiency of the traps.

Method

The method used for Th-234 followed Rutgers van der Loeff and Moore (1999). This method requires a sample volume of approximately 20 L. During the expedition an alternative procedure was developed allowing the quantification of total Th-234 on 5-L samples with appreciably less manipulation.

Procedure: To 5 L of seawater are added 125 µl of a $KMnO_4$ solution (6 g/L) and 2 drops of ammonia. After mixing, 200 µL of $MnCl_2$ solution are added (40 g $MnCl_2.4\ H_2O$/L). The sample is mixed and allowed to stand for at least one hour. The sample is then passed by pressure filtration (50 kPa) over a 25-mm graded glass fibre filter (1 µm pore size). The volume of the filtrate is determined by weighing. The filter is rinsed with demineralized water, dried and beta counted. Deep water samples (>500m depth; >500m above seafloor) are used for calibration, assuming equilibrium with U-238. Counting efficiency is 60% and the precision is estimated at 2-3%.

Results

1- Geographical distribution of Th-234 depletion:

The latitudinal distribution of particulate and total Th-234, expressed as activity ratio to the parent U-238, shows distinct export signals which appear to be linked to the position of the ACC fronts, and large areas with little export (Fig. 1a). Highest depletion was observed around 42°S near the subtropical front, around 46°S near the subantarctic front, just south of the Polar Front around 50°S, and in a wider zone around 55°S which may correspond to the ACC/Weddel Gyre boundary. The Polar Front Zone (PFZ) had a relatively low depletion, showing that this Zone had not given rise to appreciable export production in the preceeding few (1-2) months. The bloom that was observed from the chlorophyll distribution on the way south (transect 7) at 52°S was reflected in elevated levels of particulate Th (Fig.1a), but the low depletion of total Th shows that in early April this bloom was very fresh and had not yet caused significant export. The Weddell Gyre was characterized by extremely low particle contents, reflected in low particulate Th-234 activities. Nevertheless a depletion of about 15 % in total Th-234 was observed throughout the Gyre. Only close to the Antarctic continent, in the ice-covered coastal current, Th-234 activities reached equilibrium with U-238.

2- Vertical distribution of Th-234: signals of export and regeneration

Calculation of the export flux of Th-234 requires depth profiles down to the depth where Th-234 is in equilibrium with U-238.We have studied the depletion of Th-234 in surface waters around the Antarctic Polar Front on two previous expeditions to the area. In spring (ANT X/6, Bathmann et al., 1994), we had observed the transition from a near-equilibrium distribution to a strong depletion (up to 38%) indicating an export event (Rutgers van der Loeff et al, 1997), whereas in summer (ANT XIII/2, Bathmann et al., 1997), we had observed a consistent depletion of 17% in the surface water and extending to a depth of 150-200m. In both situations, Th-234 was in equilibrium with U-238 below 200m.

In the present expedition the situation was far less homogeneous in the study area around the Polar Front (cf Fig. 20.1a). In the southern part, the cumulative depletion in the upper 100-150m was 2 to 3 times higher than in the north (Fig. 20.1b). Some stations were visited 3 times over a period of 5 weeks. At the southern station (VPF2, 49°50'S), the depth distribution changed somewhat towards a lower depletion at the surface and a higher depletion at 100m depth, but the integrated depletion remained the same. This can be explained by the deepening of the mixed layer (see section 3 on Physical Oceanography, Strass).

Given the time development of the vertical distribution of Th-234 , the export flux could be calculated according to the non steady state model of Buesseler et al. (1992). However, as the cumulative depletion at the mooring positions VPF2 and VPF3 remained constant in time we may assume here steady state. The corresponding estimate of export fluxes at all stations (Fig. 20.1b) shows a strong gradient across the polar front to high fluxes just south of it, negligible fluxes in the Weddell Gyre, and again an appreciable flux in the coastal current.

A remarkable result of many profiles is a significant Th-234 excess below the pycnocline, which has been reported only in very few occasions (Coale and Bruland, 1987). In the Weddell Gyre, the depletion of approx. 15% in the surface water is limited to a shallow layer of just about 100m. The integrated excess in the depth zone 100-250m is similar (Fig. 20.2), indicating very little export to deeper layers (Fig. 20.1b). Although it is conceivable that this distribution is a remnant of an earlier bloom (i.e. a few months before), it is more likely that it is caused by a steady transport of fine material through the pynocline and mineralization below. We do not know what process is responsible for this transport at the extremely low suspended particle loads, and can only speculate on the possible role of vertically migrating zooplankton.

In the ice-covered coastal current one station (182, Fig. 20.2) showed a small depletion over the entire depth range until 400m. At this station, ice formation had caused a very deep overturn of the water column, mixing chlorophyll to great depths. This explains the very low depletion in the surface water although the depth-integrated depletion implies a significant export to the shelf sediment.

3- Th-234 export and comparison with the flux as measured with the sediment traps

The Th-234 flux intercepted at 350m depth by the sediment traps at moorings VPF2 and VPF3 was quantified with gamma spectroscopy. At VPF2, the flux decreased from 340 dpm m^{-2} d^{-1} at the start of the deployment to 200 dpm m^{-2} d^{-1} three weeks later. This flux is a factor of 6 lower than the flux estimated from the Th-234 profiles (Fig. 1b). At mooring VPF3 the Th-234 was not measurable (<100 dpm m^{-2} d^{-1}) which is again far below the predicted flux. The strong currents (up to 60 cm/s at VPF3, 10-15 cm/s at VPF2, see section on Physical Oceanography, Strass, page xx) must be responsible for this significant undertrapping.

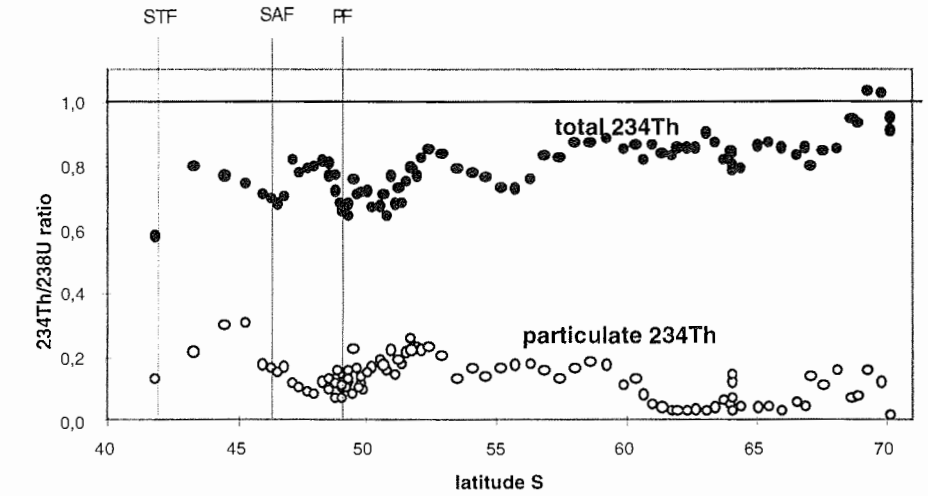

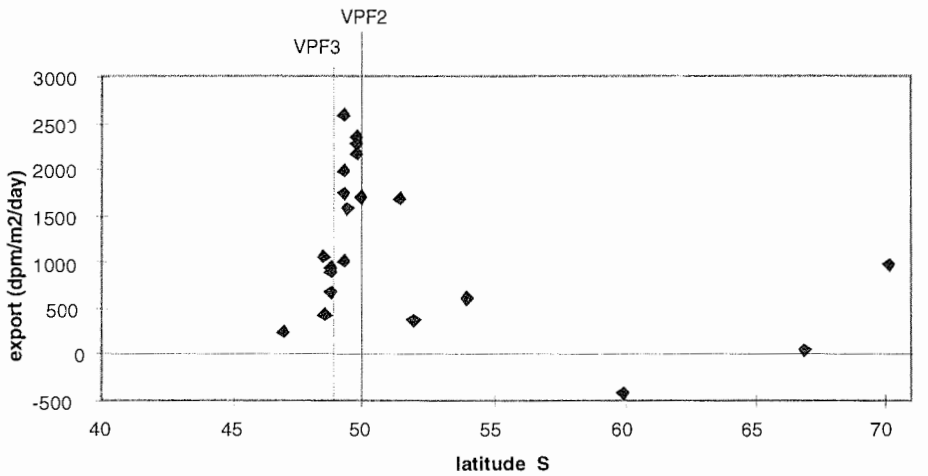

Fig. 1a Particulate (open symbols) and total (particulate + dissolved, closed symbols) Th-234, expressed as ratio to its parent U-238, as function of latitude on the North to South transects, showing strongest depletion near the Subtropical (STF), Subantarcttic (SAF) and south of the Polar Front (PF), and very low particulate levels in the Weddell Gyre.

Fig. 1b Steady-state export flux of Th-234 from the upper 300m, based on depth-integrated depletion relative to U-238, versus latitude, showing the strong gradient across the Polar Front towards the highest fluxes just south of it. The two mooring sites VPF2 and VPF3 clearly represent the high- and low-flux regimes.

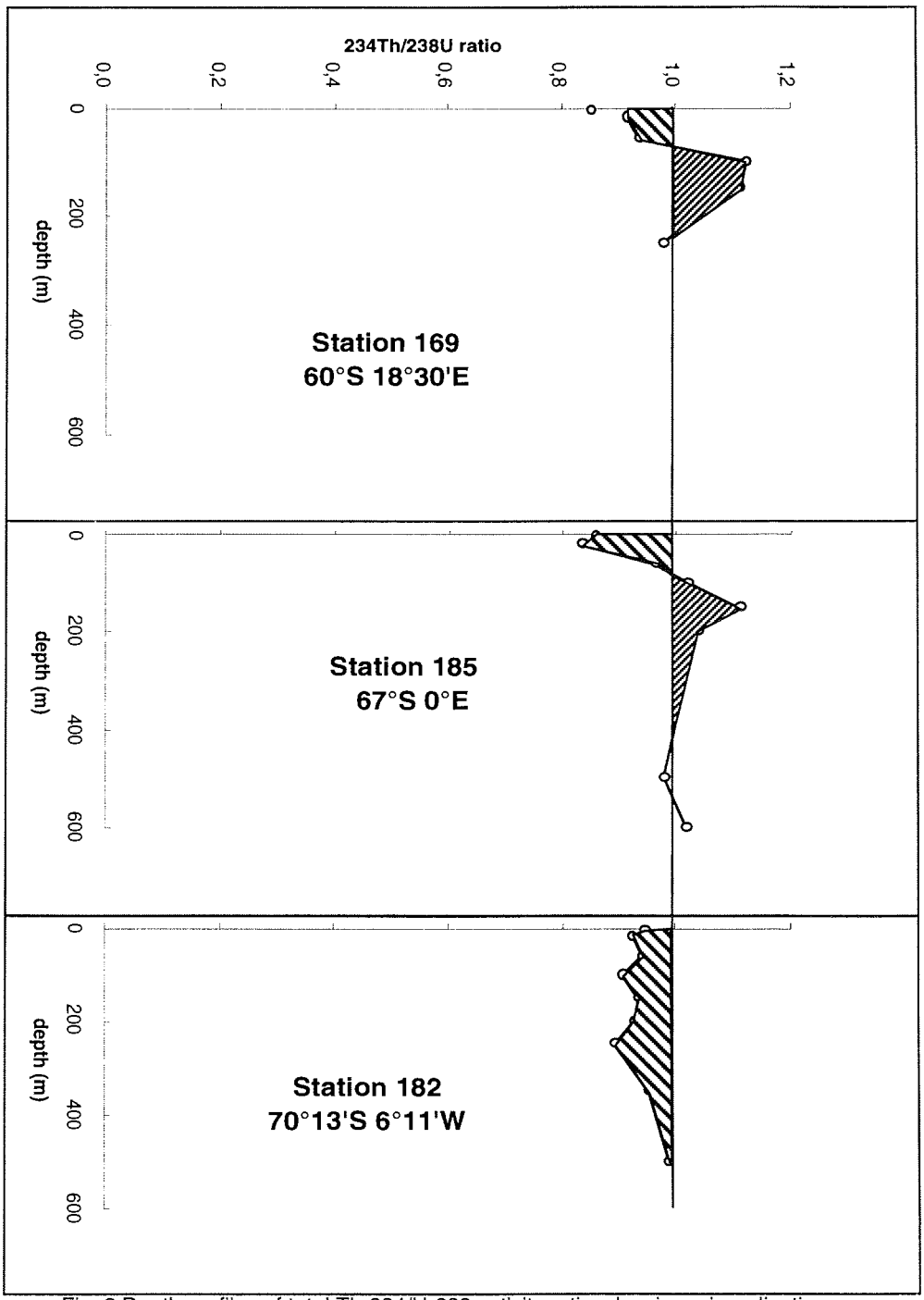

Fig. 2 Depth profiles of total Th-234/U-238 activity ratio, showing mineralization maxima below the pycnocline in the central Weddell Sea (stations 169 and 185), and deep depletion in the coastal current (station 182).

21. REAL-TIME SATELLITE INFORMATION

Caren Garrity

21.1 SeaWiFS for Mapping Chlorophyll_a

In November 1998, the satellite receiving station on the RV „Polarstern" was programmed to receive the Orbview-2 SeaWiFS satellite data in real-time by SeaSpace Corporation installed by Microwave Group-Ottawa River, Inc.. An additional ship-borne TeraScan system for processing was set-up in Cape Town, prior to the departure to the Antarctic. The reception of real-time data can occur if the proper key_code is known, bi-weekly. The RV „Polarstern" real-time receiving station (HAWI) is due to the requirements based on a Principal Investigator (PI) proposal being accepted by NASA and Orbimage from the AWI. The PI at the AWI is Dr. Gerhard Dieckmann. The aim for my work, as a visiting scientist at the AWI, was to establish the capability: a) for receiving SeaWiFS in real-time as well as two other polar orbiting satellites, the NOAA and DMSP (F-series), and b) the opportunity to provide chlorophyll_a maps from satellite orbital data in support of strategic scientific station planning. It was previously known that cloud cover and lack of daylight hours for the SeaWiFS coverage would hinder the acquisition of data in the areas of interest such as the Polar Front near 50°S and 20°E.

The best orbits occurred between 0900-1300 UTC, totaling on average three per day, with about five during the darkness. From March 18 to May 6, a total of 108 SeaWiFS images where archived on tape for further processing. About 60% of these were during the optimal time period. Processing of the SeaWiFS data to a chlorophyll_a product used the most recent calibration table provided by SeaSpace, Orbimage and NASA as well as the mean climatology data. It was not feasible to send the large meteorological and ozone files to the ship on a daily basis due to the large data volume. The cloud free areas could not be predicted, thus a request for these files would not be in real-time. Therefore, the chlorophyll_a products should be reprocessed using the daily meteorological and ozone input for a more accurate product.

One of the goals of the scientists was to locate chlorophyll_a blooms in the vicinity of the Polar Front. The Polar Front did show areas of elevated chlorophyll_a, as compared to the low background values of 0.01 mg/m^3. Using SeaWiFS data in combination with the mean climatology data, instead of the recommended meteorological and ozone data, values as high as 0.3-0.8 mg/m^3 were reached during the second visit to the Polar Front (late April – Early May), with lower values ranging from 0.06-0.2 mg/m^3 during the first survey (latter March). The lowest values, beyond the background, was near the ice edge (0.1 mg/m^3). The pattern of a bloom could not be determined from the daily orbits due to patchy cloud cover. The weekly averaged chlorophyll_a picture obtained from NASA showed as well large data gaps in the area of our interest. We received considerable direct support during the cruise with the SeaWiFS chlorophyll_a products from NASA (Dr. Gene Feldmann and Brian Schieb) which is here thankfully acknowledged. It soon became clear, that there was too much cloud cover to map chlorophyll_a in real time to make a serious impact on the planning of station work.

As mentioned before the scientists desired the real-time chlorophyll_a concentrations for planning purposes, thus the weekly average maps where not useful. The data gaps in real-time images, due to cloud cover, provided a non-operational product, however, the cloud-free areas covered degrees of latitude in some cases, providing data for a calibration/validation project. The Scan Fish was able to map the vertical profiles of chlorophyll_a, with no data gaps, thus became the favourite instrument for scientific planning at the Polar Front.

There are SeaWiFS images of chlorophyll_a that correspond to the in-situ measurements made my Bernd Kroon (personal communication). Using the in-situ data, as well as archived profiles from the past, a calibration/validation (Cal/Val) project for SeaWiFS at the Polar Front could be promising. Addition of the Scan Fish chlorophyll_a mapping to the Cal/Val project will provide a better chance for overlaying SeaWiFS data with this in-situ data. The Scan Fish continuous profiles mapped fluorescence that was calibrated to a chlorophyll_a concentration. Gernerally data from the Scan Fish was from depths of 250 m, for a distance of 4 km on the surface. The daily meteorological and ozone information should be used in the processing of SeaWiFS chlorophyll_a values, instead of an average climatology file for a Cal/Val experiment. The influence of wind-speed on the calculated chlorophyll_a values is not know at the present, and could be part of the Cal/Val effort, and of interest to the SeaWiFS program office at NASA.

21.2 DMSP Special Sensor Microwave/Imager

The Special Sensor Microwave/Imager (SSM/I), located on the Defense Meteorological Satellite Program (DMSP) platforms provides geophysical parameters regardless of cloud cover and darkness. For non-U.S. Military platforms, it provides the following products, South of 60S: (1) sea ice concentration, (2) sea ice type according to WMO (World Meteorological Organization) when the snow cover is dry, (3) wind-speed at the ocean surface, (4) total liquid water and (5) vapour in the atmosphere as (6) rain rate (mm/hr).

The wind-speed maps are of interest to the SeaWiFS Cal/Val, as well as the onboard meteorological office. The iron research group has requested rain rate maps, in order to examine a possible iron input from rain. The bird and mammal scientist requested the sea ice edge position. Sea ice concentration was of importance for navigation in order to aid planning of time between station stops within the sea ice cover extent. The program dictated the ship stay in an area of new and young ice, thus difficult working conditions for on ice work.

In addition to the SSM/I sensors there is the DMSP Optical Linescan System (OLS) that provides 0.5 km resolution in the visible and near-infrared channels. For the Antarctic the OLS provides high-resolution imagery of sea ice conditions under clear skies.

From March 18 to May 6 a total of 250 SSM/I orbits have been archived for post research. The data can only be processed using the NASA algorithms as part of the TeraScan SeaSpace Corporation Software soon to be located at the AWI, University of Bremen and Hanse Institute for Advanced Study, Delmenhorst.

21.3 NOAA Weather Satellites

The NOAA weather satellites are used to map the sea surface temperature for cloud free areas, as well as the traditional cloud motion, and wind-fields in the atmosphere. The High Resolution Picture Transmission (HRPT) is 1.1 km .

21.3.1 Weather

It has been apparent since 1997, and again during this cruise, that the weather office would benefit by using the TeraScan system since there are always new satellites added to the software to be received thus, provides more real-time weather satellite images. Beyond the infrared weather images, there are various satellite products evident in this report that would benefit their interests and requirements. As compared to the present day Met office, the resolution of the images are near an order of magnitude better using the 1.2 m TeraScan antenna,

where the frequency range to capture satellites is large, with a strong signal strength. As an example, there was electrical interference in the receiving of NOAA satellite by the Met office for time periods, which was not the case for the same satellite received by the TeraScan system. As an Appendix 1 to this cruise report, a recommendation has been summarized which involves the BSH and the Seewetteramt, Hamburg in combination with the AWI. The initiation ashore came from Klaus Strübing (Head of Eisdienst, BSH) and Dr. René O. Ramseier (Microwave Group-Ottawa River, Inc.) at an introduction level that was received well by the Seewetteramt (May 1999).

During this cruise, the Meteorologist (Kurt Flechsenhar) had a short demonstration on the type of products the TeraScan system can produce in order to provide more information about weather, sea state and even sea ice conditions. The Met Technician (Hartmut Sonnabend) had a short training session on the steps required to capture and produce an infrared satellite image.

There were a total of 203 NOAA satellite orbits archived on tape from March 18 to May 6.

21.3.2 Sea Surface Temperature

Using the NOAA AVHRR (Advanced Very High Resolution Radiometer) data, sea surface temperature is calculated using different algorithms depending on darkness. However, the algorithms work for cloud-free areas only. These algorithms are provided with the TeraScan software and documentation is available as help window files (SeaSpace Corporation). The sea surface temperature products were an aid in determining the meandering Polar Front, thus guidance for planning oceanographic stations.

21.3.3 Mooring Location

An additional feature of the NOAA satellites is the similar transmitting frequency as from an argos equipped buoy located as an example on a mooring. Thus, if a mooring was lost from sight, and the argos buoy with its transmitter positioned to the surface of the water when the mooring was released, the mooring could be located using the TeraScan system. Since some of the moorings had the transmitter located under the ACP (Automatic Current Profiler), they were not located with the TeraScan system. This did not pose a problem since all five moorings were kept in sight visually, and retrieved successfully.

Using the TeraScan system to locate moorings is free of charge, thus no cost to the AWI for this information, which is not the case at the present time since the AWI uses another method. Peter Roth was trained on the system for locating argos transmitters and he translated the lesson into German. This translation aided the training of the Met technologist, who was trained in a similar manner for making NOAA AVHRR weather images.

21.4 Sea Ice Information

21.4.1 Sea Ice Edge

Using the SSM/I data and the NASA Team algorithm, the sea ice edge defined as the 10 % ice concentration for a 25x25 km grid spacing with an accuracy of +/- 6% is shown in Table 1. The following table shows the sea ice edge at the various longitudes near the ship during the cruise.

Table 1: Sea Ice Edge at Locations of Interest During this Cruise for Bird and Mammal Research

Date	Longitude [deg]	Latitude of Ice Edge South [deg min]
10-Apr-99	12E	66 39.95
11-Apr-99	3E	69 8.51
12-Apr-99	10W	70 9.56
13-Apr-99	8W	Missing data
14-Apr-99	8W	69 0.95
15-Apr-99	8W	69 59.16
16-Apr-99	7W	69 30.00
17-Apr-99	6W	69 31.49
18-Apr-99	3W	69 23.93
19-Apr-99	6W	68 57.47
20-Apr-99	5W	69 11.50
21-Apr-99	0	69 9.68
22-Apr-99	4E	67 35.32
23-Apr-99	8E	67 22.93

21.4.2 Sea Ice Visual Observations

The visual sea ice observation program is not complete due to darkness, and the fact that the ship tended to move during the night, with station stops in the day. This varied however, thus observations were made providing a record of major changes in sea ice conditions as the ship progressed through the ice. Visual observations are difficult due to viewing the sea ice as one would view the cloud cover. The closer to the horizon one looks, one tends to overestimate the sea ice concentrations. Thus, the observations are descriptive more than quantitative. Satellite derived concentrations are quantitative for first year, old ice and total ice, and were provided to the public (Messe II), the Captain and transferred electronically to the senior scientist as a colour image on a regular basis during the time spent in the sea ice. Products were distributed to those requesting a copy. These images would be too expensive to include in the cruise report, thus individuals who require quantitative sea ice information should contact the e-mail address: icedoctors@igs.net. The NASA Team algorithm would be used, thus a 25x25 km averaged sea ice concentration area, however, a 12.5x12.5 km can be obtained, but with more effort due to interpretation requirements.

The sea ice conditions presented below shows typical variability of a sea ice edge from a young ice regime, to first year ice, with old ice (fresh ice) small floes intervening from the ice berg graveyard near Neumayer (AtkaBay). The most appropriate way to present these general sea ice conditions is to be descriptive. Satellite information can augment this description by quantifying the sea ice information as a percent of ice covering the ocean surface. Only the visual observations can estimate the amount of new versus young sea ice, which was the dominant case at this time of ice formation.

Note that general observations such as air temperature, wind speed etc can be obtained from the ship's data (Poldat), thus can augment the sea ice environment if necessary by the user.

April 12 68 49S 5W Dusk to Dark (1600...UTC)

On route to Neumayer, with off shore winds at 8 knots and –30C at the station. A typical sea ice edge was encountered as a pancake ice regime, increasing in concentration southward to 69 10' 6W. Pancake ice concentration varied between 0-100% in bands, thus the SSM/I NASA Team satellite algorithm missed the 10% sea ice edge, due to the 25x25 km resolution at this position. The 12.5x12.5 km resolution could be used to define an ice edge more accurately, under most circumstances, but not all. There was 62 nm (116 km) of sea ice from the ice edge at 8W to the shelf ice at Neumayer.

April 14 70 27S 8 18W Visibility < (less than) 1 km (0800 UTC)

High winds at 21.1 m/s, direction 83 degrees (deg) caused ice pressure to build up. The easterly winds caused little pressure for navigation purposes since the sea ice was only 50 cm thick, 100% concentration, 50% rafting and 50% ridging. This could be a potential situation for krill to hide. The ship waited for the storm to pass.

April 14 70 14S 8 20W Dark (1900-2000 UTC)

Evidence in the sea ice structure showed that it had been under pressure recently. Ice type was grey to grey-white, a maximum thickness of 30cm. Concentration was100% with 10 cm of snow and 0-60% ridging (i.e. variable). Winds remained high, 19 m/s form 92 deg. The tide removed pressure from the ice, counteracting and/or stronger effect than the wind. For the SSM/I satellite foot print (grid spacing of 25x25 km) the ice concentration was 75%.

April 15 70 10S 7 22 W Visibility 2 km (0800-0900 UTC)

Winds increased to 22.5 m/s from 99 deg . The ice concentration and ice types varied considerably as compared to previous observations: open water 10%, white nilas 5%, grey to grey-white ice 15%, and first year 70%.
April 15 70 10S 7 27W Stopped (1000 UTC)

The ship stopped due to high winds and incompatible tides for the day. First year ice was prominent at 100%.

April 16 69 59S 7 48W (0800-0900 UTC)

The floe size became recognizable at 1-3 m (minimum) with a grey-white sea ice concentration of 75% and 5 cm of snow cover. Beginning of the first year ice pack.
April 16 70 9S 6 54W Visibility 4 km with low winds, 3.2 m/s.

The ice floes were <1 m in size being 40% grey ice, 5% dark nilas and 5% open water. The remainder was brash ice.

April 16 70 13S 6 52W (1130-1230 UTC)

There was a station at 1300 UTC, where the sea ice concentration was typically 15% grey ice and 85% brash with none of the floe sizes > (greater than) 1 m. The SSM/I showed 95% ice cover (recall, the concentration if for a larger area than the eye can observe).

April 17 69 58S 6 18W Excellent visibility – Day long ice station

The sea ice was relatively thin for an ice station where the tides tend to put pressure on the ice by the late afternoon, early evening. Grey-white ice (maximum 30 cm, no ridging or rafting included) with a concentration of 95% the remainder being 5% open water. Floe size generally 100-1000 m.

April 18 69 48S 3 47W (0800-0900 UTC)

Floe size near 3 m on average. Dark nilas at 10% with the remaining 90% grey and grey-white ice.

April 18 69 54S 3 36W (0900-1000 UTC)

The pancake ice was well developed and frozen together with a low concentration of 10%. Dark nilas at 25% and grey/grey-white ice at 65% concentration. The grey-white floe size did not change from the above.

April 18 70 3S 3 14W (1000-1100 UTC)

Floe size had increased to 10 m with 90% grey-white ice, 5% white nilas and 5% dark nilas.

April 18 69 51S 3 4W (1100-1130 UTC)

There was a trace of dark nilas, with evidence of past pressured young ice. The floe size of 100% grey/grey-white ice was 25% rafted and floe size averaging 3 m.

April 18 69 51S 3 4W (1130-1200 UTC)

There were many (relative to other areas during this cruise) seals and whales observed at this position with brown ice occupying 5% of the sea ice. The floe size was < 1 m at least 30 cm thick (grey/grey-white) (50%) and pancake ice (50%), well established, thus frozen together into an ice sheet. The first year ice type was rafted 25%, thus providing a thickness > 30 cm. The rafting may provide an area for krill to live in harmony, and predators enjoy the idea of a good feast.

April 18 69 39S 3 8W (1200-1330 UTC)

Typical ice edge with swell overtaking the sea ice. The pancake ice was variable, again typical of an ice edge, with 80-100% ice concentration. Thus, the floe size was < 1 m. The SSM/I showed 80-90% ice cover.

April 19 70 13S 6 13W (0800-0900 UTC)

An ice station with a variable polynya (small) with time covered with 5% grease and slush ice, 5% water and later in the day 5% dark nilas. There was 5% white nilas at the edges of the 30% grey ice and grey-white ice areas.

April 20 69 52S 6 W (0800-1200 UTC)

The floe size was decreasing with time with a trace of old fresh ice. Typical compact ice edge with 25% brash ice and 75% grey/grey-white ice 25% rafted.

April 20 69 7.5S 4 1W (1600 position) (1200-1600 UTC)

There was a sudden decrease in sea ice conditions at 1500 UTC where bands became more apparent. There was 85% pancake ice and 15% open water before the bands were more prominent at the ice edge. The ice floe size decreased considerably at the 1500 UTC change over of ice conditions. The floes were < 1 m. The SSM/I shoed 70% ice cover.

The SSM/I ice cover calculated using the NASA Team algorithm showed different ice concentrations than from visual observations due to: 1) human error in estimated sea ice concentrations from a ship, and 2) the orbit time did not necessarily occur at the time of the visual observation which was averaged over various time periods.

There were a total of 561 good satellite overpasses archived in TeraScan format during this cruise.

APPENDIX 1

MICROWAVE GROUP-OTTAWA RIVER, INC.

3954 Armitage Ave., RR#1
Dunrobin, Ontario K0A 1T0
Canada
e-mail: icedoctors@igs.net

Satellite Receiving Station on RV „Polarstern": ANT XVI-3, March-May 1999

A Recommendation to the AWI, BSH & Seewetteramt, Hamburg

A satellite receiving and processing system located near the Meteorologist Office on the RV „Polarstern" can provide assistance to the Met Office requirements in support of weather and sea ice information. The SeaSpace Corporation TeraScan system belongs to the Alfred Wegener Institute and remains on the ship for all cruises. This system operates on Sun Workstations (Unix based) and offers more NOAA satellites than the present day RV „Polarstern" weather office system. The addition of NOAA 10 and 11 to the NOAA 12,14 plus 15 provides more satellite images on the TeraScan system for weather forecasting. The resolution is 1.1 km, since it is a HRPT receiver as compared to the APT (near an order of magnitude less resolution).

In addition to receiving the NOAA weather satellites, the system is capable of receiving the F-series sensor data from the U.S. Defense Meteorological Satellite Program (DMSP), thus providing additional information based on passive microwave algorithms. The F- satellite data is accessible and free of charge in the Antarctic, south of 60 latitude. The information gained from the passive microwave data is of benefit to ocean going vessels in the Polar Regions where the cloud cover, and sometimes darkness is generally prominent. The microwaves can work with the cloud cover, thus parameters such as: wind-speed at the ocean surface, sea ice coverage, sea ice type/thickness as per WMO definitions only in the winter, rain rate, total liquid water and vapour in the atmosphere are provided as an image similar to the coverage as the NOAA satellites. As with the NOAA satellites, information is in real-time, due to the reception of the raw data directly from the satellite to the ship where it is easily processed.

The software is advanced, thus window oriented for easy viewing and manipulating by the user. The TeraScan system has been on the Polarstern since the early 1990's, and has been continuously updated with the addition of new satellites and products. There are other products that can be generated, for example, chlorophyll_a on the ocean surface, only as an example from another satellite (Orbview-2, SeaWiFS). Scientists use the TeraScan system on some cruises, however there is always the situation where the weather office can connect to the data.

The TeraScan system can be used as a backup system, but more importantly it should be used as the main system due to the versatility and exceptional satellite reception capabilities. The Alfred Wegener Institute (AWI) generally pays for support from SeaSpace Corporation, thus there is an on-going exchange of ideas from the user that can be implemented in the software upgrades received by the AWI.

It is advisable to be trained on the system in order to learn the capabilities of remote sensing, as well as the general theory to assist in the interpretation of the data, to fully take advantage of the facility. Once the knowledge of products is introduced, the TeraScan system can be set-up more automatically with the aims of the knowledgeable user's requirements. The ideal training is in real-time at sea, plus in the sea ice in the Antarctic. The NOAA satellites are not operational for mapping sea ice due to the blinding by cloud and darkness. Only the F-series satellites can provide real-time geophysical parameters under all weather and daylight conditions, to date. The F-series satellites may be received in the Arctic in the future, but there is a need for requests indicating the urgency for this data north of 60S.

There are numerous TeraScan specialists, but few with experience on ships, and in sea ice. One example would be Dr. Caren Garrity from the Microwave Group-Ottawa River, Inc. where she did her Doctorate using the F-series passive microwave data for mapping sea ice conditions. Dr. Garrity has trained others on the use of the TeraScan system and has been successful in providing the basics for exploration by the user.

Experience has shown that training should not be geared to just knowing the commands to provide a product, but rather why the steps are necessary. It is not recommended to expect a system manager of a ship to know the TeraScan system, since it is the user that will need to follow the changes and updates in technology of interest to the „service".

The TeraScan system is as powerful as the user. It is beneficial to the Meteorologists with access to the TeraScan system, to use it for weather AVHRR (NOAA) infrared maps to the other extreme of mapping: winds at different levels in the atmosphere, sea surface temperature, wind speed at the ocean surface, sea ice concentration, ice edge position etc... A ship like the RV „Polarstern", that operates about 90% in Polar Regions, should included sea ice mapping as part of the weather service. It will not be the first time (USCGC Polar Star, USCGC Polar Sea, CCG Louis S. St-Laurent, MV Lance....).

It is strongly recommended that the Meteorological Office on the RV „Polarstern" link-up to the resources of the TeraScan remote sensing system located just around the corner.

Dr. Caren Garrity
President

22. PARTICIPANTS / FAHRTTEILNEHMER ANT XVI/3

Alheit, Ruth	(AWI)
Assmy, Philip	(AWI)
Atkinson, Angus	(BAS)
Bathmann, Ulrich	(AWI)
Bellerby, Richard	(PML)
Boye, Marie	(LIVERPOOL)
Brink, Nico van den	(IBN)
Brocken, Fenneke	(RUG)
Croot, Peter	(NIOZ)
Dauelsberg, Anke	(AWI)
Davey, Margaret	(MBA)
Dieterich, Christian	(AWI)
Flechsenhar, Kurt	(DWD)
Franeker, Jan Andries van	(IBN)
Freier, Ulrich	(AWI)
Garitty, Caren	(AWI)
Gonzalez, Santiago	(NIOZ)
Hanfland, Claudia	(AWI)
Hartmann, Carmen	(AWI)
Jong, Jeroen de	(NIOZ)
Kattner, Gerhard	(AWI)
Kroon, Bernd	(AWI)
Langreder, Jens	(IUPT)
Leach, Harry	(AWI)
Leeuwe, Maria van	(RUG)
Macrander, Andreas	(IfM Kiel)
Meyer-Harms, Bettina	(AWI)
Mock, Thomas	(AWI)
Monsees, Mathias	(AWI)
Oijen, Tim van	(RUG)
Ratje, Andreas	(AWI)
Richter, Klaus-Uwe	(AWI)
Rosenstock, Bernd	(ICBM)
Roth, Peter	(AWI)
Ruttgers v. d. Loeff, Michiel	/AWI)
Schmidt, Katrin	(IOW)
Schoemann, Veronique	(ULB)
Simon, Meinhard	(Oldbg)
Smetacek, Victor	(AWI)
Sonnabend, Hartmut	(DWD)
Strass, Volker	(AWI)
Stübing, Dorothea	(Univ. HB)
Timmermans, Klaas	(NIOZ)
van der Wagt, Bas	(LIVERPOOL)
Veldhuis, Marcel	(NIOZ)
Visser, Ronald	(NIOZ)
Walter, Hans Jürgen	(AWI)
Westernstroeer, Ulrike	(AWI)
Zwisler, Walter	(ICBM)

23. PARTICIPANTING INSTITUTES / BETEILIGTE INSTITUTE

Germany

AWI	Alfred-Wegener-Institut für Polar- und Meeresforschung Columbusstrasse 27515 Bremerhaven
DWD	Deutscher Wetterdienst Geschäftsfeld Seeschiffahrt Bernhard-Nocht-Str. 76 20359 Hamburg
ICBM	Inst. f. Chemie und Biol. des Meeres Universität Oldenburg Carl-v.-Ossietzky-Str. 9-11 26111 Oldenburg
IFM Kiel	Istitut für Meereskunde Düsternborrker Weg 20 23414 Kiel
IOW	Institut für Ostseeforschung Warnemünde Postfach 30 11 61, 18112 Rostock

Belgium

ULB	Groupe de Microbiologie des Milieux Aquatiques Université Libre de Bruxelles ULB Campus de la Plaine, CP 221 B-1050 Brussels

Netherlands

IBN-DLO	Institute for Forestry & Nature Research Postbox 167 NL-1790 AD Den Burg (Texel)
NIOZ	Nederlands Instituut voor Onderzoek der Zee Postbox 59 NL-1790 AB Den Burg/Texel
RuG	University of Groningen Department of Marine Biology P.O. Box 14 9750 AA Haren (Gn)

England

BAS	British Antarctic Survey (BAS) High Cross, Madingley Road Cambridge CB3 OET, UK
DOUL	Dept. of Oceanogr. The University Liverpool, L69 3BX
PML	Plymouth Marine Laboratory Citadel Hill Plymouth PL1 2PB

24. SHIP'S CREW / SCHIFFSBESATZUNG ANT XVI/3

Dienstgrad	Name
Kapitän	Pahl, Uwe
1. Naut. Offizier	Schwarze, Stefan
1. Naut. Offizier	Rodewald, Martin
2. Naut. Offizier	Fallei, Holger
2. Naut. Offizier	Spielke, Steffen
Arzt	NN
Ltd. Ingenieur	Behnes, Stefan
2. Ingenieur	Erreth, Mon. Gyula
2. Ingenieur	Ziemann, Olaf
2. Ingenieur	Fleischer, Martin
Elektriker	Muhle, Heiko
Elektroniker	Dimmler, Werner
Elektroniker	Muhle, Helmut
Elektroniker	Greitemann-Hackl, A.
Elektroniker	Roschinsky, Jörg
Funkoffizier	Koch, Georg
Maschinenwart	Ipsen, Michael
Maschinenwart	Voy, Bernd
Maschinenwart	Grafe, Jens
Maschinenwart	Hartmann, Ernst-Uwe
Maschinenwart	Preußner, Jörg
Zimmermann	Reise, Lutz
Lagerhalter	Müller, Klaus
Bootsmann	Clasen, Burkhard
Matrose	Gil Iglesias, Luis
Matrose	Pousada Martinez, S.
Matrose	Kreis, Reinhard
Matrose	Winkler, Michael
Matrose	Schulz, Ottomar
Matrose	Burzan, G.-Ekkehard
Matrose	Bäcker, Andreas
Matrose	Pulss, Horst
Koch	Haubold, Wolfgang
Kochsmaat	Völske, Thomas
Kochsmaat	Martens, Michael
1. Steward/ess	Jürgens, Monika
Stewardess/Krankenschwester	NN
2. Steward/ess	Czyborra, Bärbel
2. Steward/ess	Deuß, Stefanie
2. Steward/ess	Neves, Alexandre
2. Steward	Tu, Jian Min
2. Steward	Mui, Kee Fung
Wäscher	Yu, Chung Leung

FAHRTABSCHNITT ANT XVI/4 KAPSTADT – BREMERHAVEN (11.5.99 – 4.6.99)

A. Fahrtroute ANT XVI/4

M. Reinke (AWI)

"Polarstern" verließ Kapstadt in Richtung Bremerhaven am 11.Mai 1999 gegen 19 Uhr.
Erstes Ziel war die Verankerung V3/K10 des Instituts für Meereskunde in Kiel auf 30°S und 5°E. Sie wurde vor 2 Jahren von FS Polarstern im Rahmen des KAPEX ("Kap der Guten Hoffnung Experiment") ausgebracht. Sie verfügte eine Schallquelle, die zusammen mit 2 weiteren Verankerungen zur Unterwasser-navigation von freitreibenden Schwebekörpern (RAFOS-Floats) verwandt werden. In KAPEX wird der Zwischenwasser-Austausch im Tiefenhorizont von knapp 1000m vor dem südlichen Afrika untersucht. Dieser interozeanische Austausch zwischen Indik und Atlantik ist Teil der globalen ozeanischen Zirkulation, welche in den Konvektionsgebieten des Nordatlantiks angetrieben wird, und der Auswirkungen bis zum Pazifik hat. Inzwischen hatten alle Floats ihre Missionen beendet und nach ihrem Auftauchen die gesammelten Daten über eine Satellitenfunkverbindung nach Kiel abgesetzt. Die aufgenommene Schallquelle hatte somit ihre Aufgabe erfolgreich erfüllt. Die verbleibenden zwei Schallquellen aus Kiel sollen im kommenden Jahr von FS Meteor bzw. Polarstern geborgen werden.

Die weitere Fahrt der Polarstern führte nach Norden in Richtung der Kapverdischen Inseln. Nach Durchquerung des SE Passats erreichte sie die Zone der innertropischen Konvergenz (ITC). In der Nacht von Donnerstag auf Freitag, den 21.5.1999 überquerte sie gegen 0 Uhr UTC den Äquator bei 18 Grad West. Abgesehen von wenigen nicht sonderlich ergiebigen Schauern und Wetterleuchten am Morgen des 22.05.1999 wurde die ITC ohne weitere nennenswerte Wetterereignisse durchfahren. Am Montag den 24.5.1999 lief Polarstern bei mäßiger Sicht und Wind aus NNE mit 5 Bft durch die Inselgruppe der Kapverden mit neuem Kurs Richtung Kanarische Inseln. Am 28.05.1999 wurden gegen 10 Uhr auf der Reede von Las Palmas zwei weitere Mitreisende an Bord genommen. Ab dem 29.05.1999 führte der Kurs durch den Einflußbereichs eines Tiefs nahe 44N und 15W, das mit einer anfangs nordwestlichen, später südwestlichen Strömung kühlere Luftmassen heranführte. Der Starkwindbereich auf der Rückseite des Tiefs brachte kurzzeitig eine aus Nordwest heranlaufende, bis zu 3 m hohe Dünung. Auf dem letzten Abschnitt der Reise sorgte eine Azorenhoch mit einem nach Schottland gerichteten Keil für überwiegend ruhiges Wetter.

Die drei Arbeitsgruppen, die Experimente der letzten Expedition (ANT XVI/3) fortführten, beschäftigten sich mit Teilaspekten des marinen Kohlenstoffkreislaufs und der Biologie des antarktischen Krills. Der Kohlenstoffkreislauf wurde im Rahmen des internationalen Programms "Joint Global Ocean Flux Study" (JGOFS) und die Krillbiologie im Rahmen von "Global Ocean Ecosystem Dynamics" (GLOBEC) erforscht

Im wissenschaftlich-technischen Bereich wurden auf diesem Fahrtabschnitt die Grundlagen für die Erneuerung und Erweiterung des wissenschaftlichen Bordrechnersystems erarbeitet. Diese Arbeiten wurden im Rahmen der Überholungsmaßnahmen des Schiffes in den Jahren 1998 bis 2000 durchgeführt und sollen die hohe Leistungsfähigkeit von Polarstern als wissenschaftliche Plattform und als schwimmendes Observatorium für die nächsten Jahre sichern.

Am 3. Juni 1999 abends erreichte Polarstern planmäßig ihren Heimathafen Bremerhaven.

B. Itinerary ANT XVI/4

M. Reinke

On Mai 11, 1999 RV "Polarstern" left Capetown as planned at 19:00, with 10 scientists and 41 crew members on board.

Two days later it reached the sound source mooring V3/K10 of the "Institut für Meereskunde", Kiel at 30°S and 5°W, which was deployed two years ago by RV "Polarstern" within the framework of KAPEX. KAPEX (Cape of Good Hope Experiments) is an oceanographic research project, which focuses on the spreading and inter-ocean exchange of subsurface water around Southern Africa. Between April 1997 and June 1998, a total of 6 cruises were carried out to establish a sound source array and to launch the RAFOS floats. These floats performed underwater navigation using acoustics signals, which were transmitted by the moored sound sources. They transmitted their collected data via satellite, which are evaluated and analysed by the laboratories involved. The mooring was quickly detected and brought up.

RV "Polarstern" headed for the Cape Verde Islands and crossed the equator on Mai 21, 1999. On Mai 28, 1999 at the Canary Islands two technicians arrived on board. On June 3, 1999 RV "Polarstern" reached Bremerhaven.

Three biological and geo chemical working groups conducted experiments on material which was collected during the last leg (ANT XVI/3) of RV "Polarstern". This work was focused on the biology of krill Euphausia superba and on the marine carbon cycle in the framework of the programs "Global Ocean Ecosystem Dynamics" (GLOBEC) and "Joint Global Ocean Flux Study" (JGOFS)

A technical working group developed the basic structures of a new scientific information technology network on RV "Polarstern", which will be implemented within the next year.

C. PODEV Nachfolge

M. Reinke, J. Hofmann, P.Gerchow

Während ANT XVI/4 wurden von der Gruppe des AWI-Rechenzentrums drei Themen verfolgt.

- Erstellung einer Spezifikation für das Nachfolgesystem des jetzigen PODEV-Systems, das im Jahr 2000 ersetzt werden soll.
- Dokumentation und Aufnahme der Verkabelung des wissenschaftlichen Datennetzwerkes als vorbereitende Arbeit der Erneuerung des Netzwerkes im Herbst 1999.
- Tests mit dem Echtzeit-Datenbanksystem DAVIS der Fa. WERUM (Lüneburg).

Für die Nachfolge des bestehenden Bordrechnersystems wurde ein Betriebskonzept erarbeitet, welches den Rahmen für die detaillierte Spezifikation der neuen wissenschaftlichen Datenerfassung bildet. Kernpunkte dieses Konzeptes sind:

- Verkabelung aller Funktions- und Wohnräume des Schiffes auf Glasfaserbasis mit einem zentralen Knotenpunkt im Bordrechnerraum.
- Aufteilung des physikalischen Netzwerkes in mehrere logische Teilnetze (Subnets), nach Funktionalität und Sicherheitsrelevanz.
- Einsatz eines UNIX- und eines Windows-NT-Servers für zentrale Dienste.

Darauf aufbauend wurde ein Lastenheft erstellt, welches die Erfahrungen mit dem bisherigen PODEV-System auswertet und die Grundanforderungen an das neue System definiert. Das Lastenheft wurde mit einem Mitarbeiter der Fa. WERUM (Lüneburg), der in Las Palmas an Bord kam, ausführlich diskutiert, wobei dessen Erfahrungen bei der Realisierung und Installation der wissenschaftlichen Datenerfassungssysteme auf den Forschungsschiffen "Meteor" und "Sonne" einflossen.

Die Aufnahme und die Dokumentation aller Übertragungssysteme (Ethernet-Netzwerk und serielle Datenübertragungssysteme) in allen Funktionsräumen des Schiffes wurde in Zusammenarbeit mit den Bordelektronikern. Als Ergebnis steht jetzt eine Datenbank im MS-Access-Format zur Verfügung, die Auskunft über die installierten Systeme gibt. Desweiteren wurden die Hardwareanforderungen für das neue Datennetzwerk formuliert. Dabei wurde besonderer Wert auf Flexibilität und Zukunftssicherheit der Investition gelegt. Die zukünftigen Anschlußorte wurden festgelegt und die Konzepte für die Strukturierung der Verkabelung erarbeitet.

Die Tests mit dem Echtzeit-Datenbanksystem waren eine Fortsetzung der Arbeiten, die auf ANT XV/1 begonnen wurden. Während es damals um grundsätzliche Fragen der Eignung des Systems als Grundlage für Observatoriums-Datenerfasungssysteme ging, wurden diesmal an einem laufenden System mit realen Daten aus der Bordwetterwarte gearbeitet. Ziel war die Optimierung von Systemkonfiguration, -performance und -stabilität.

Auch hier konnten am laufenden System verschiedene Fragen direkt mit dem Mitarbeiter von der Herstellerfirma WERUM geklärt werden. Außerdem wurde eine Datenbasis geschaffen, die Grundlage weiterer Tests im Institut sein wird.

D. The Scientific Computimg Network on RV "Polarstern"

M. Reinke, J. Hofmann, P. Gerchow

The scientic computing network provides the basis for scientific work on board of RV "Polarstem". Besides ist scientific infra-structure function, it is used to collect, archive and distribute ship and environmental parameters. The system PODEV, which was implemented in 1993, has to be replaced due to technical considerations. During this leg new specifications have been developed concerning the new physical fiber network, connecting all rooms and laboratories of the ship, the partitioning of the physical network into logical subnets and the use of a UNIX and Windows NT-Server for central services.
As a prerequisite the existing network, which has evolved over 15 years, was analysed and documented into a database. The new data acquisition and distribution system will be based on a real-time database management system (RTDBMS). It is already used on the German RV "Meteor" and "Sonne". During this leg a test data set was produced in order to evaluate stability and performance of the RTDBMS system. Further testing and development of the system will be carried out in Bremerhaven.

E. Nahrungsökologie und Energetik des antarktischen Krill

D. Stübing

Die Diskussion über die Überwinterungsmechanismen des antarktischen Krill Euphausia superba ist noch immer in vollem Schwunge. Derzeit werden fünf Strategien kontrovers diskutiert: Reduktion der Stoffwechselaktivität, Nutzung von Speicherstoffen (Lipide, Proteine), Reduktion der Körpergröße, Fraß von Eisalgen, Übergang zu einer carnivoren Ernährungsweise.

Kondition und Ernährungssituation der beprobten Krillpopulationen sollen zum kritischen Zeitpunkt des Übergangs zum Winter anhand von lipidbiochemischen und Isotopenanalysen, die in den Institutslaboren durchgeführt werden sollen, charakterisiert werden. Lipidgehalt und Lipidklassenzusammensetzung geben Aufschluß über Menge und Art der Energiereserven und werden getrennt für die jeweiligen ontogenetischen Stadien bestimmt. Die Fettsäurezusammensetzung läßt ebenso wie die Anreicherung der stabilen Isotope des Kohlenstoffs und des Stickstoffs auf die Nahrungsgewohnheiten der Tiere während der vergangenen Wochen rückschließen.

Die Probennahme fand während ANT XVI/3 statt; ein Teil der Tiere wurde direkt eingefroren und bildet die Datengrundlage für das Feldmaterial. Ein weiterer Teil wurde für 4-7 Wochen unter verschiedenen Bedingungen gehältert. Auf diesem Fahrtabschnitt wurden die Langzeitexperimente weitergeführt. Furcilien, Juvenile und Adulte wurden mit Eisalgen, Phytoplankton bzw. Copepoden gefüttert, um mögliche Nahrungspräferenzen festzustellen und zu ermitteln, ob sich Lipidmuster bzw. Isotopensignal der Nahrungsorganismen im Krill abbilden. Somit dienen die Experimente zugleich als Interpretationshilfen für die Felddaten. In Hungerexperimenten soll die vorzugsweise Nutzung bestimmter Energiereserven sowie die Änderung im Isotopensignal verfolgt werden.

F. Trophodynamics and energetics of the Antarctic krill

D. Stübing

Conflicting hypotheses prevail on the overwintering mechanisms of the Antarctic krill Euphausia superba. Currently, five different strategies are being controversially discussed: reduction of metabolic activity, utilisation of storage products (lipids, protein), shrinkage feeding on ice algae, carnivory.

This study aimed at characterising physiological condition and feeding behaviour of krill prior to the critical over-wintering period by means of lipid and stable isotope analyses that will be carried out in the home laboratories. Lipid content and lipid class composition indicate the amount and kind of energy reserves and will be measured separately for each ontogenetic stage. The fatty acid composition as well as the enrichment of stable carbon and nitrogen isotopes reflect the animals' feeding histories integrated over several weeks.

Sampling was carried out during ANT XVI/3, part of the animals were directly frozen to provide information on field krill. The rest was kept alive for 4-7 weeks in aquaria under different conditions. During this leg, long term experiments were continued. Furciliae, juveniles and adults were fed with ice algae, phytoplankton, or copepods, to unravel possible food preferences and to prove whether the lipid patterns and isotopic signals of the food organisms are reflected in the krill specimens. Thus, the experiments also help interpret the field data. Starving experiments were conducted to reveal preferential use of specific energy reserves as well as to document changes in the isotopic signal.

G. Source regions and transport paths of iron in the Antarctic Circumpolar Current

C. Hanfland

During ANT XVI/3, our aim had been to identify the sources and transport mechanisms of the iron into the Atlantic Sector of the Southern Ocean. Principle iron sources are: aeolian inputs from southern South America and the Antarctic Peninsula, advective inputs from their respective continental shelves, and upwelling of deep water. We use ^{228}Ra as a tracer for input from the continental shelves and ^{232}Th, Al and Nd for aeolian input.

The aim of ANT XVI/4 was mainly to continue and finish sample processing and measuring of samples from the previous cruise. Samples taken during ANT XVI/3 for the analysis of dissolved radium were processed by the ^{228}Th ingrowth method. For detailed objectives, sampling strategy and sample processing see chapter 19.

As a completion of the surface water sampling of suspended particles during ANT XVI/3 to estimate today's role of aeolian input into the S-Atlantic Ocean (described in detail in chapter 19), six additional samples of particulate matter from surface waters have been taken off Namibia and off the Sahara. Aeolian material deposited in these regions should carry a strong fingerprint from the old African craton. Its Nd isotopic composition should therefore be much less radiogenic than expected for the aeolian component of particulate material taken in the Southern Ocean, where the influence of a young volcanic component (high $^{143}/^{144}$Nd) should be dominant. Analyses of the suspended particles will show whether it is indeed possible to elucidate the origin of their aeolian component from their Nd isotope signature.

particles will show whether it is indeed possible to elucidate the origin of their aeolian component from their Nd isotope signature.

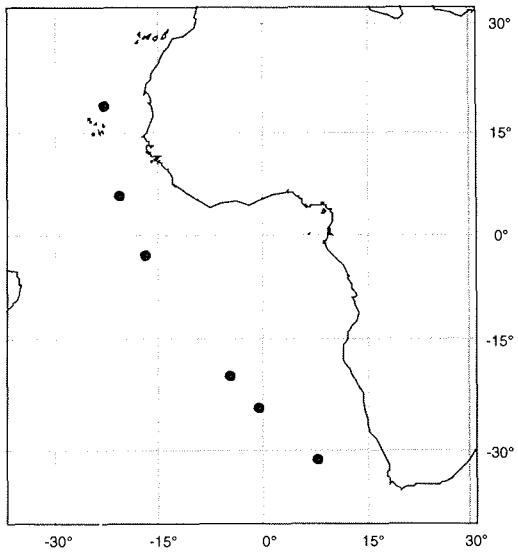

Fig. 1: Surface water sample locations of particulate matter for the analysis of the Nd isotopic composition. Samples have been taken by a continuous flow centrifuge.

H. Bio-optik und Bio-chemie von Eisalgen und Phytoplankton

T. Mock , U. Westernströer

Die während des dritten Fahrtabschnittes der Expedition ANT XVI angefangenen Chemostat- Experimente mit planktonischen Algen (*Chaetoceros* spp., *Thalassiosira* spp.) und Eisalgen (*Fragilariopsis* spp., *Pseudonitzschia* spp.) wurden während des vierten Fahrtabschnittes erfolgreich beendet. Die Bestimmung von biophysikalischen und biochemischen Unterschieden zwischen beiden Algengruppen war Ziel dieser Untersuchung. Durch die Laborexperimente an nährsalzgesättigten und nitratlimitierten Kulturen wurde der Effekt unterschiedlicher Lichtintensitäten (3 µmol Photonen m^{-2} s^{-1} und 20 µmol Photonen m^{-2} s^{-1}) auf die Photosynthese und die biochemische Zusammensetzung untersucht. Zudem wurden für beide Algengruppen Nitrataufnahmekinetiken durchgeführt. Alle Versuche fanden in einem Kühlcontainer bei - 1°C statt.

Erste Ergebnisse aus den Fluoreszenz-Induktionskurven und den P (photosynthesis) / I (irradiance) - Kurven, die mit Hilfe eines puls-amplituden-modulierten Fluorometers durchgeführt wurden, deuten darauf hin, daß die Eisalgen photophysiologisch dynamischer reagieren können, als die planktonischen Algen, obwohl die Eisalgen in einem stabileren Habitat leben. Im Meereis findet eine vertikale Durchmischung so gut wie niemals statt. Z.B. war der Quanten-Yield der Eisalgen unter optimaler Nährstoffversorgung sowohl bei 3 µmol Photonen m^{-2} s^{-1} als auch bei 20 µmol Photonen m^{-2} s^{-1} größer, als der der planktonischen Algen. Während der Wachstumslimitation durch Nitratmangel wurde allerdings sichtbar, daß die planktonischen Algen unter beiden Lichtintensitäten höhere Quanten-Yield´s aufwiesen. Das Reoxidationsverhalten von Q_A scheint bei beiden Algengruppen und unter den verschiedenen experimtellen Bedingungen sehr konstant zu bleiben. Eine weitere Besonderheit der Eisalgen, die ausschließlich unter ausreichender Nährstoffversorgung beobachtet wurde, ist das Auftreten der Chlororespiration nach längerer Zeit (4 Stunden) im Dunkeln. Ein Nachweis hierfür konnte für die pelagischen Algen nicht gefunden werden. Desweiteren deuten die Nitrataufnahmekinetiken der Eisalgen auf einen sehr effizienten und schnellen Aufnahmemechanismus durch die Zellwand hin. Die Aufnahmeraten sind sehr ähnlich zu denen von Algen aus temperierten Regionen. Die Aufnahmeraten der planktonischen Algen liegen etwas unter denen der Eisalgen. Inwieweit sich die biochemische Zusammensetzung der beiden Algengruppen unter den genannten experimentellen Bedingungen unterscheidet, kann erst nach der Analyse der gewonnenen Proben im Institut gesagt werden.

I. Bio-optics and bio-chemistry of ice algae and phytoplankton

T. Mock , U. Westernströer

Chemostat experiments with antarctic phytoplankton (*Chaetoceros* spp., *Thalassiosira* spp.) and ice algae (*Fragilariopsis* spp., *Pseudonitzschia* spp.)which were established during ANT XVI/3 were successfully completed during the fourth leg of the cruise ANT XVI/4. The aim of this study was to determine biophysical and biochemical differences between both groups of algae with regard to the different environmental conditions. The effects of different light intensities on bio-physical processes at photosystem II and the biochemical composition of the algae were investigated during nitrate limited growth. Additional experiments on nitrate uptake kinetics were conducted for both algal groups. All the experiments were carried out in a culture container at – 1°C.

First results from fluorescence induction curves indicated that the ice algae had a higher photophysiologically action spectrum than the planktonic algae despite the fact that they live in a more stable environment were there is no mixing. At 3 µmol photons m^{-2} s^{-1} and 20 µmol photons m^{-2} s^{-1} for instance, the quantum yield under replete nutrient concentrations was higher for ice algae. However, under nitrat limited growth the planktonic algae had a higher quantum yield under both light intensities. The reoxidation of Q_A seems to be very similar and stable for both algal groups and for all applied experimental conditions. Another peculiarity of the ice algae is the onset of chlororespiration after 4 h darkness. The nitrat uptake of the ice algae is very efficient and similar to that in algae living in more temperate regions. Chemical analyses of the biochemical compositions and pigments as well as the activity of the carboxylation enzymes will be conducted in the home laboratory.

K. Participants / Fahrtteilnehmer ANT XVI/4

1.	Buldt, Klaus	(DWD)
2.	Gerchow, Peter	(AWI)
3.	Hofmann, Jörg	(AWI)
4.	Köhler, Herbert	(DWD)
5.	Lanning, Giesela	(AWI)
6.	Reich, Michael	(IFM) Kiel
7.	Reinke, Manfred	(AWI)

L. Participanting Institutes / Beteiligte Institute

Germany

AWI	Alfred-Wegener-Institut für Polar- und Meeresforschung Columbusstrasse 27515 Bremerhaven
DWD	Deutscher Wetterdienst Geschäftsfeld Seeschiffahrt Bernhard-Nocht-Str. 76 20359 Hamburg
IFM Kiel	Istitut für Meereskunde Düsternborrker Weg 20 23414 Kiel

M. Ship's Crew / Schiffsbesatzung ANT XVI

Dienstgrad	Name
Kapitän	Pahl, Uwe
1. Naut. Offizier	Schwarze, Stefan
2. Naut. Offizier	Peine, Lutz
2. Naut. Offizier	Spielke, Steffen
Arzt	Schulz, Rüdiger
Ltd. Ingenieur	Behnes, Stefan
2. Ingenieur	Erreth, Mon. Gyula
2. Ingenieur	Ziemann, Olaf
2. Ingenieur	Fleischer, Martin
Elektriker	Muhle, Heiko
Elektroniker	Bretfeld, Holger
Elektroniker	Muhle, Helmut
Elektroniker	Greitemann-Hackl, A.
Elektroniker	Roschinsky, Jörg
Funkoffizier	Koch, Georg
Maschinenwart	Ipsen, Michael
Maschinenwart	Voy, Bernd
Maschinenwart	Grafe, Jens
Maschinenwart	Hartmann, Ernst-Uwe
Maschinenwart	Elsner, Klaus
Zimmermann	Reise, Lutz
Lagerhalter	Preußner, Jörg
Bootsmann	Clasen, Burkhard
Matrose	Gil Iglesias, Luis
Matrose	Pousada Martinez, S.
Matrose	Kreis, Reinhard
Matrose	Schulz, Ottomar
Matrose	Burzan, G.-Ekkehard
Matrose	Bastigkeit, Kai
Koch	Haubold, Wolfgang
Kochsmaat	Völske, Thomas
Kochsmaat	Martens, Michael
1. Steward/ess	Jürgens, Monika
2. Steward/ess	Czyborra, Bärbel
2. Steward/ess	Deuß, Stefanie
2. Steward/ess	Neves, Alexandre
2. Steward	Tu, Jian Min
2. Steward	Mui, Kee Fung
Wäscher	Yu, Chung Leung

Folgende Hefte der Reihe „Berichte zur Polarforschung" sind bisher erschienen:

* **Sonderheft Nr. 1/1981** – „Die Antarktis und ihr Lebensraum"
Eine Einführung für Besucher – Herausgegeben im Auftrag von SCAR
* **Heft Nr. 1/1982** – „Die Filchner-Schelfeis-Expedition 1980/81"
zusammengestellt von Heinz Kohnen
* **Heft Nr. 2/1982** – „Deutsche Antarktis-Expedition 1980/81 mit FS „Meteor"
First International BIOMASS Experiment (FIBEX) – Liste der Zooplankton- und Mikronektonnetzfänge
zusammengestellt von Norbert Klages
* **Heft Nr. 3/1982** – „Digitale und analoge Krill-Echolot-Rohdatenerfassung an Bord des Forschungsschiffes ‚Meteor'" (im Rahmen von FIBEX 1980/81, Fahrtabschnitt ANT III), von Bodo Morgenstern

Heft Nr. 4/1982 – „Filchner-Schelfeis-Expedition 1980/81"
Liste der Planktonfänge und Lichtstärkemessungen
zusammengestellt von Gerd Hubold und H. Eberhard Drescher

* **Heft Nr. 5/1982** – "Joint Biological Expedition on RRS 'John Biscoe', February 1982"
by G. Hempel and R. B. Heywood
* **Heft Nr. 6/1982** – „Antarktis-Expedition 1981/82 (Unternehmen ‚Eiswarte')"
zusammengestellt von Gode Gravenhorst

Heft Nr. 7/1982 – „Marin-Biologisches Begleitprogramm zur Standorterkundung 1979/80 mit MS ‚Polarsirkel' (Pre-Site Survey)" – Stationslisten der Mikronekton- und Zooplanktonfänge sowie der Bodenfischerei
zusammengestellt von R. Schneppenheim

Heft Nr. 8/1983 – "The Post-Fibex Data Interpretation Workshop"
by D. L. Cram and J.-C. Freytag with the collaboration of J. W. Schmidt, M. Mall, R. Kresse, T. Schwinghammer
* **Heft Nr. 9/1983** – "Distribution of some groups of zooplankton in the inner Weddell Sea in summer 1979/80"
by I. Hempel, G. Hubold, B. Kaczmaruk, R. Keller, R. Weigmann-Haass

Heft Nr. 10/1983 – „Fluor im antarktischen Ökosystem" – DFG-Symposium November 1982
zusammengestellt von Dieter Adelung

Heft Nr. 11/1983 – "Joint Biological Expedition on RRS 'John Biscoe', February 1982 (II)"
Data of micronecton and zooplankton hauls, by Uwe Piatkowski

Heft Nr. 12/1983 – „Das biologische Programm der ANTARKTIS-I-Expedition 1983 mit FS ‚Polarstern'"
Stationslisten der Plankton-, Benthos- und Grundschleppnetzfänge und Liste der Probennahme an Robben und Vögeln, von H. E. Drescher, G. Hubold, U. Piatkowski, J. Plötz und J. Voß

* **Heft Nr. 13/1983** – „Die Antarktis-Expedition von MS ‚Polarbjörn' 1982/83" (Sommerkampagne zur Atka-Bucht und zu den Kraul-Bergen), zusammengestellt von Heinz Kohnen
* **Sonderheft Nr. 2/1983** – „Die erste Antarktis-Expedition von FS ‚Polarstern' (Kapstadt, 20. Januar 1983 – Rio de Janeiro, 25. März 1983)", Bericht des Fahrtleiters Prof. Dr. Gotthilf Hempel

Sonderheft Nr. 3/1983 – „Sicherheit und Überleben bei Polarexpeditionen"
zusammengestellt von Heinz Kohnen

* **Heft Nr. 14/1983** – „Die erste Antarktis-Expedition (ANTARKTIS I) von FS ‚Polarstern' 1982/83"
herausgegeben von Gotthilf Hempel

Sonderheft Nr. 4/1983 – "On the Biology of Krill *Euphausia superba*" – Proceedings of the Seminar and Report of the Krill Ecology Group, Bremerhaven 12. - 16. May 1983, edited by S. B. Schnack

Heft Nr. 15/1983 – "German Antarctic Expedition 1980/81 with FRV 'Walther Herwig' and RV 'Meteor'" – First International BIOMASS Experiment (FIBEX) – Data of micronekton and zooplankton hauls
by Uwe Piatkowski and Norbert Klages

Sonderheft Nr. 5/1984 – "The observatories of the Georg von Neumayer Station", by Ernst Augstein

Heft Nr. 16/1984 – "FIBEX cruise zooplankton data"
by U. Piatkowski, I. Hempel and S. Rakusa-Suszczewski

* **Heft Nr. 17/1984** – Fahrtbericht (cruise report) der ‚Polarstern'-Reise ARKTIS I, 1983"
von E. Augstein, G. Hempel und J. Thiede

Heft Nr. 18/1984 – „Die Expedition ANTARKTIS II mit FS ‚Polarstern' 1983/84",
Bericht von den Fahrtabschnitten 1, 2 und 3, herausgegeben von D. Fütterer

Heft Nr. 19/1984 – „Die Expedition ANTARKTIS II mit FS ‚Polarstern' 1983/84",
Bericht vom Fahrtabschnitt 4, Punta Arenas-Kapstadt (Ant-II/4), herausgegeben von H. Kohnen

Heft Nr. 20/1984 – „Die Expedition ARKTIS II des FS ‚Polarstern' 1984, mit Beiträgen des FS ‚Valdivia' und des Forschungsflugzeuges ‚Falcon 20' zum Marginal Ice Zone Experiment 1984 (MIZEX)"
von E. Augstein, G. Hempel, J. Schwarz, J. Thiede und W. Weigel

Heft Nr. 21/1985 – "Euphausiid larvae in plankton from the vicinity of the Antarctic Penisula, February 1982" by Sigrid Marschall and Elke Mizdalski

Heft Nr. 22/1985 – "Maps of the geographical distribution of macrozooplankton in the Atlantic sector of the Southern Ocean" by Uwe Piatkowski

Heft Nr. 23/1985 – „Untersuchungen zur Funktionsmorphologie und Nahrungsaufnahme der Larven des Antarktischen Krills *Euphausia superba* Dana" von Hans-Peter Marschall

Heft Nr. 24/1985 – „Untersuchungen zum Periglazial auf der König-Georg-Insel Südshetlandinseln/ Antarktika. Deutsche physiogeographische Forschungen in der Antarktis. – Bericht über die Kampagne 1983/84" von Dietrich Barsch, Wolf-Dieter Blümel, Wolfgang Flügel, Roland Mäusbacher, Gerhard Stäblein, Wolfgang Zick

* **Heft Nr. 25/1985** – „Die Expedition ANTARKTIS III mit FS ‚Polarstern' 1984/1985" herausgegeben von Gotthilf Hempel.

* **Heft Nr. 26/1985** – "The Southern Ocean"; A survey of oceanographic and marine meteorological research work by Hellmer et al.

* **Heft Nr. 27/1986** – „Spätpleistozäne Sedimentationsprozesse am antarktischen Kontinentalhang vor Kapp Norvegia, östliche Weddell-See" von Hannes Grobe

Heft Nr. 28/1986 – „Die Expedition ARKTIS III mit ‚Polarstern' 1985 mit Beiträgen der Fahrtteilnehmer, herausgegeben von Rainer Gersonde

* **Heft Nr. 29/1986** – „5 Jahre Schwerpunktprogramm ‚Antarktisforschung' der Deutschen Forschungsgemeisnchaft." Rückblick und Ausblick. Zusammengestellt von Gotthilf Hempel, Sprecher des Schwerpunktprogramms

Heft Nr. 30/1986 – "The Meteorological Data of the Georg-von-Neumayer-Station for 1981 and 1982" by Marianne Gube and Friedrich Obleitner

* **Heft Nr. 31/1986** – „Zur Biologie der Jugendstadien der Notothenioidei (Pisces) an der Antarktischen Halbinsel" von A. Kellermann

* **Heft Nr. 32/1986** – „Die Expedition ANTARKTIS IV mit FS ‚Polarstern' 1985/86" mit Beiträgen der Fahrtteilnehmer, herausgegeben von Dieter Fütterer

Heft Nr. 33/1987 – „Die Expedition ANTARKTIS-IV mit FS ‚Polarstern' 1985/86 – Bericht zu den Fahrtabschnitten ANT-IV/3-4" von Dieter Karl Fütterer

Heft Nr. 34/1987 – „Zoogeographische Untersuchungen und Gemeinschaftsanalysen an antarktischen Makroplankton" von U. Piatkowski

Heft Nr. 35/1987 – „Zur Verbreitung des Meso- und Makrozooplanktons in Oberflächenwasser der Weddell See (Antarktis)" von E. Boysen-Ennen

Heft Nr. 36/1987 – „Zur Nahrungs- und Bewegungsphysiologie von *Salpa thompsoni* und *Salpa fusiformis*" von M. Reinke

Heft Nr. 37/1987 – "The Eastern Weddell Sea Drifting Buoy Data Set of the Winter Weddell Sea Project (WWSP)" 1986 by Heinrich Hoeber und Marianne Gube-Lehnhardt

Heft Nr. 38/1987 – "The Meteorological Data of the Georg von Neumayer Station for 1983 and 1984" by M. Gube-Lenhardt

Heft Nr. 39/1987 – „Die Winter-Expedition mit FS ‚Polarstern' in die Antarktis (ANT V/1-3)" herausgegeben von Sigrid Schnack-Schiel

Heft Nr. 40/1987 – "Weather and Synoptic Situation during Winter Weddell Sea Project 1986 (ANT V/2) July 16 - September 10, 1986" by Werner Rabe

Heft Nr. 41/1988 – „Zur Verbreitung und Ökologie der Seegurken im Weddellmeer (Antarktis)" von Julian Gutt

Heft Nr. 42/1988 – "The zooplankton community in the deep bathyal and abyssal zones of the eastern North Atlantic" by Werner Beckmann

* **Heft Nr. 43/1988** – "Scientific cruise report of Arctic Expedition ARK IV/3" Wissenschaftlicher Fahrtbericht der Arktis-Expedition ARK IV/3, compiled by Jörn Thiede

* **Heft Nr. 44/1988** – "Data Report for FV 'Polarstern' Cruise ARK IV/1, 1987 to the Arctic and Polar Fronts" by Hans-Jürgen Hirche

Heft Nr. 45/1988 – „Zoogeographie und Gemeinschaftsanalyse des Makrozoobenthos des Weddellmeeres (Antarktis)" von Joachim Voß

Heft Nr. 46/1988 – "Meteorological and Oceanographic Data of the Winter-Weddell-Sea Project 1986 (ANT V/3)" by Eberhard Fahrbach

Heft Nr. 47/1988 – „Verteilung und Herkunft glazial-mariner Gerölle am Antarktischen Kontinentalrand des östlichen Weddellmeeres" von Wolfgang Oskierski

Heft Nr. 48/1988 – „Variationen des Erdmagnetfeldes an der GvN-Station" von Arnold Brodscholl

* **Heft Nr. 49/1988** – „Zur Bedeutung der Lipide im antarktischen Zooplankton" von Wilhelm Hagen

* **Heft Nr. 50/1988** – „Die gezeitenbedingte Dynamik des Ekström-Schelfeises, Antarktis" von Wolfgang Kobarg

Heft Nr. 51/1988 – „Ökomorphologie notothenioider Fische aus dem Weddellmeer, Antarktis" von Werner Ekau

Heft Nr. 52/1988 – „Zusammensetzung der Bodenfauna in der westlichen Fram-Straße" von Dieter Piepenburg

* **Heft Nr. 53/1988** – „Untersuchungen zur Ökologie des Phytoplanktons im südöstlichen Weddellmeer (Antarktis) im Jan./Febr. 1985" von Eva-Maria Nöthig

Heft Nr. 54/1988 – „Die Fischfauna des östlichen und südlichen Weddellmeeres: geographische Verbreitung, Nahrung und trophische Stellung der Fischarten" von Wiebke Schwarzbach

Heft Nr. 55/1988 – "Weight and length data of zooplankton in the Weddell Sea in austral spring 1986 (Ant. V/3)" by Elke Mizdalski

Heft Nr. 56/1989 – "Scientific cruise report of Arctic expeditions ARK IV/1, 2 & 3" by G. Krause, J. Meinke und J. Thiede

Heft Nr. 57/1989 – „Die Expedition ANTARKTIS V mit FS ‚Polarstern' 1986/87"
Bericht von den Fahrtabschnitten ANT V/4-5 von H. Miller und H. Oerter

• **Heft Nr. 58/1989** – „Die Expedition ANTARKTIS VI mit FS ‚Polarstern' 1987/88"
von D. K. Fütterer

Heft Nr. 59/1989 – „Die Expedition ARKTIS V/1a, 1b und 2 mit FS ‚Polarstern' 1988"
von M. Spindler

Heft Nr. 60/1989 – „Ein zweidimensionales Modell zur thermohalinen Zirkulation unter dem Schelfeis"
von H. H. Hellmer

Heft Nr. 61/1989 – "Die Vulkanite im westlichen und mittleren Neuschwabenland,
Vestfjella und Ahlmannryggen, Antarktika" von M. Peters

• **Heft Nr. 62/1989** – "The Expedition ANTARKTIS VII/1 and 2 (EPOS I) of RV 'Polarstern'
in 1988/89", by I. Hempel

Heft Nr. 63/1989 – „Die Eisalgenflora des Weddellmeeres (Antarktis): Artenzusammensetzung und Biomasse
sowie Ökophysiologie ausgewählter Arten" von Annette Bartsch

Heft Nr. 64/1989 – "Meteorological Data of the G.-v.-Neumayer-Station (Antarctica)" by L. Helmes

Heft Nr. 65/1989 – "Expedition Antarktis VII/3 in 1988/89" by I. Hempel, P. H. Schalk, V. Smetacek

Heft Nr. 66/1989 – „Geomorphologisch-glaziologische Detailkartierung
des arid-hochpolaren Borgmassivet, Neuschwabenland, Antarktika" von Karsten Brunk

Heft Nr. 67/1990 – "Identification key and catalogue of larval Antarctic fishes",
edited by Adolf Kellermann

Heft Nr. 68/1990 – "The Expedition Antarktis VII/4 (Epos leg 3) and VII/5 of RV 'Polarstern' in 1989",
edited by W. Arntz, W. Ernst, I. Hempel

Heft Nr. 69/1990 – „Abhängigkeiten elastischer und rheologischer Eigenschaften des Meereises vom
Eisgefüge", von Harald Hellmann

• **Heft Nr. 70/1990** – „Die beschalten benthischen Mollusken (Gastropoda und Bivalvia) des
Weddellmeeres, Antarktis", von Stefan Hain

Heft Nr. 71/1990 – „Sedimentologie und Paläomagnetik an Sedimenten der Maudkuppe (Nordöstliches
Weddellmeer)", von Dieter Cordes

Heft Nr. 72/1990 – "Distribution and abundance of planktonic copepods (Crustacea) in the Weddell Sea
in summer 1980/81", by F. Kurbjeweit and S. Ali-Khan

Heft Nr. 73/1990 – „Zur Frühdiagenese von organischem Kohlenstoff und Opal in Sedimenten des südlichen
und östlichen Weddellmeeres", von M. Schlüter

Heft Nr. 74/1990 – „Expeditionen ANTARKTIS-VIII/3 und VIII/4 mit FS ‚Polarstern' 1989"
von Rainer Gersonde und Gotthilf Hempel

Heft Nr. 75/1991 – „Quartäre Sedimentationsprozesse am Kontinentalhang des Süd-Orkey-Plateaus im
nordwestlichen Weddellmeer (Antarktis)", von Sigrun Grünig

Heft Nr. 76/1990 – „Ergebnisse der faunistischen Arbeiten im Benthal von King George Island
(Südshetlandinseln, Antarktis)", von Martin Rauschert

Heft Nr. 77/1990 – „Verteilung von Mikroplankton-Organismen nordwestlich der Antarktischen Halbinsel
unter dem Einfluß sich ändernder Umweltbedingungen im Herbst", von Heinz Klöser

Heft Nr. 78/1991 – „Hochauflösende Magnetostratigraphie spätquartärer Sedimente arktischer
Meeresgebiete", von Norbert R. Nowaczyk

Heft Nr. 79/1991 – „Ökophysiologische Untersuchungen zur Salinitäts- und Temperaturtoleranz
antarktischer Grünalgen unter besonderer Berücksichtigung des b-Dimethylsulfoniumpropionat
(DMSP) - Stoffwechsels", von Ulf Karsten

Heft Nr. 80/1991 – „Die Expedition ARKTIS VII/1 mit FS ‚Polarstern' 1990",
herausgegeben von Jörn Thiede und Gotthilf Hempel

Heft Nr. 81/1991 – „Paläoglaziologie und Paläozeanographie im Spätquartär am Kontinentalrand des
südlichen Weddellmeeres, Antarktis", von Martin Melles

Heft Nr. 82/1991 – „Quantifizierung von Meereseigenschaften: Automatische Bildanalyse von
Dünnschnitten und Parametisierung von Chlorophyll- und Salzgehaltsverteilungen", von Hajo Eicken

Heft Nr. 83/1991 – „Das Fließen von Schelfeisen - numerische Simulationen
mit der Metholde der finiten Differenzen", von Jürgen Determann

Heft Nr. 84/1991 – „Die Expedition ANTARKTIS-VIII/1-2, 1989 mit der Winter Weddell Gyre Study
der Forschungsschiffe ‚Polarstern' und ‚Akademik Fedorov'", von Ernst Augstein,
Nikolai Bagriantsev und Hans Werner Schenke

Heft Nr. 85/1991 – „Zur Entstehung von Unterwassereis und das Wachstum und die Energiebilanz
des Meereises in der Atka Bucht, Antarktis", von Josef Kipfstuhl

• **Heft Nr. 86/1991** – „Die Expedition ANTARKTIS-VIII mit FS ‚Polarstern' 1989/90. Bericht vom
Fahrtabschnitt ANT-VIII/5", von Heinz Miller und Hans Oerter

Heft Nr. 87/1991 – "Scientific cruise reports of Arctic expeditions ARK VI/1-4 of RV 'Polarstern'
in 1989", edited by G. Krause, J. Meincke & H. J. Schwarz

Heft Nr. 88/1991 – „Zur Lebensgeschichte dominanter Copepodenarten (*Calanus finmarchicus,
C. glacialis, C. hyperboreus, Metridia longa*) in der Framstraße", von Sabine Diel

Heft Nr. 89/1991 – „Detaillierte seismische Untersuchungen am östlichen Kontinentalrand des Weddell-Meeres vor Kapp Norvegia, Antarktis", von Norbert E. Kaul

Heft Nr. 90/1991 – „Die Expedition ANTARKTIS-VIII mit FS ‚Polarstern' 1989/90. Bericht von den Fahrtabschnitten ANT-VIII/6-7", herausgegeben von Dieter Karl Fütterer und Otto Schrems

Heft Nr. 91/1991 – "Blood physiology and ecological consequences in Weddell Sea fishes (Antarctica)", by Andreas Kunzmann

Heft Nr. 92/1991 – „Zur sommerlichen Verteilung des Mesozooplanktons im Nansen-Becken, Nordpolarmeer", von Nicolai Mumm

Heft Nr. 93/1991 – „Die Expedition ARKTIS VII mit FS ‚Polarstern', 1990. Bericht vom Fahrtabschnitt ARK VII/2", herausgegeben von Gunther Krause

Heft Nr. 94/1991 – „Die Entwicklung des Phytoplanktons im östlichen Weddellmeer (Antarktis) beim Übergang vom Spätwinter zum Frühjahr", von Renate Scharek

Heft Nr. 95/1991 – „Radioisotopenstratigraphie, Sedimentologie und Geochemie jungquartärer Sedimente des östlichen Arktischen Ozeans", von Horst Bohrmann

Heft Nr. 96/1991 – „Holozäne Sedimentationsentwicklung im Scoresby Sund, Ost-Grönland", von Peter Marienfeld

Heft Nr. 97/1991 – „Strukturelle Entwicklung und Abkühlungsgeschichte von Heimefrontfjella (Westliches Dronning Maud Land/Antarktika)", von Joachim Jacobs

Heft Nr. 98/1991 – „Zur Besiedlungsgeschichte des antarktischen Schelfes am Beispiel der Isopoda (Crustacea, Malacostraca)", von Angelika Brandt

* **Heft Nr. 99/1992** – "The Antarctic ice sheet and environmental change: a three-dimensional modelling study", by Philippe Huybrechts

* **Heft Nr. 100/1992** – „Die Expeditionen ANTARKTIS IX/1-4 des Forschungsschiffes ‚Polarstern' 1990/91" herausgegeben von Ulrich Bathmann, Meinhard Schulz-Baldes, Eberhard Fahrbach, Victor Smetacek und Hans-Wolfgang Hubberten

Heft Nr. 101/1992 – „Wechselbeziehungen zwischen Schwermetallkonzentrationen (Cd, Cu, Pb, Zn) im Meerwasser und in Zooplanktonorganismen (Copepoda) der Arktis und des Atlantiks", von Christa Pohl

Heft Nr. 102/1992 – „Physiologie und Ultrastruktur der antarktischen Grünalge *Prasiola crispa ssp. antarctica* unter osmotischem Streß und Austrocknung", von Andreas Jacob

* **Heft Nr. 103/1992** – „Zur Ökologie der Fische im Weddellmeer", von Gerd Hubold

Heft Nr. 104/1992 – „Mehrkanalige adaptive Filter für die Unterdrückung von multiplen Reflexionen in Verbindung mit der freien Oberfläche in marinen Seismogrammen", von Andreas Rosenberger

Heft Nr. 105/1992 – "Radiation and Eddy Flux Experiment 1991 *(REFLEX I)*", von Jörg Hartmann, Christoph Kottmeier und Christian Wamser

Heft Nr. 106/1992 – „Ostracoden im Epipelagial vor der Antarktischen Halbinsel - ein Beitrag zur Systematik sowie zur Verbreitung und Populationsstruktur unter Berücksichtigung der Saisonalität", von Rüdiger Kock

* **Heft Nr. 107/1992** – „ARCTIC '91: Die Expedition ARK-VIII/3 mit FS ‚Polarstern' 1991", von Dieter K. Fütterer

Heft Nr. 108/1992 – „Dehnungsbeben an einer Störungszone im Ekström-Schelfeis nördlich der Georg-von-Neumayer-Station, Antarktis. – Eine Untersuchung mit seismologischen und geodätischen Methoden", von Uwe Nixdorf.

* **Heft Nr. 109/1992** – „Spätquartäre Sedimentation am Kontinentalrand des südöstlichen Weddellmeeres, Antarktis", von Michael Weber.

* **Heft Nr. 110/1992** – „Sedimentfazies und Bodenwasserstrom am Kontinentalhang des nordwestlichen Weddellmeeres", von Isa Brehme.

Heft Nr. 111/1992 – „Die Lebensbedingungen in den Solekanälchen des antarktischen Meereises", von Jürgen Weissenberger.

Heft Nr. 112/1992 – „Zur Taxonomie von rezenten benthischen Foraminiferen aus dem Nansen Becken, Arktischer Ozean", von Jutta Wollenburg.

Heft Nr. 113/1992 – „Die Expedition ARKTIS VIII/1 mit FS ‚Polarstern' 1991", herausgegeben von Gerhard Kattner.

* **Heft Nr. 114/1992** – „Die Gründungsphase deutscher Polarforschung, 1865 - 1875", von Reinhard A. Krause.

Heft Nr. 115/1992 – "Scientific Cruise Report of the 1991 Arctic Expedition ARK VIII/2 of RV 'Polarstern' (EPOS II)", by Eike Rachor.

Heft Nr. 116/1992 – "The Meteorological Data of the Georg-von-Neumayer-Station (Antarctica) for 1988, 1989, 1990 and 1991", by Gert König-Langlo.

Heft Nr. 117/1992 – „Petrogenese des metamorphen Grundgebirges der zentralen Heimefrontfjella (westliches Dronning Maud Land / Antarktis)", von Peter Schulze.

Heft Nr. 118/1993 – „Die mafischen Gänge der Shackleton Range / Antarktika: Petrographie, Geochemie, Isotopengeochemie und Paläomagnetik", von Rüdiger Hotten.

* **Heft Nr. 119/1993** – „Gefrierschutz bei Fischen der Polarmeere", von Andreas P. A. Wöhrmann.

* **Heft Nr. 120/1993** – "East Siberian Arctic Region Expedition '92: The Laptev Sea - its Significance for Arctic Sea-Ice Formation and Transpolar Sediment Flux", by D. Dethleff, D. Nürnberg, E. Reimnitz, M. Saarso and Y. P. Sacchenko. – "Expedition to Novaja Zemlja and Franz Josef Land with RV 'Dalnie Zelentsy'", by D. Nürnberg and E. Groth.

* **Heft Nr. 121/1993** – „Die Expedition ANTARKTIS X/3 mit FS ‚Polarstern' 1992", herausgegeben von Michael Spindler, Gerhard Dieckmann und David Thomas

Heft Nr. 122/1993 – „Die Beschreibung der Korngestalt mit Hilfe der Fourier-Analyse: Parametrisierung der morphologischen Eigenschaften von Sedimentpartikeln", von Michael Diepenbroek.

* **Heft Nr. 123/1993** – „Zerstörungsfreie hochauflösende Dichteuntersuchungen mariner Sedimente", von Sebastian Gerland.

Heft Nr. 124/1993 – „Umsatz und Verteilung von Lipiden in arktischen marinen Organismen unter besonderer Berücksichtigung unterer trophischer Stufen", von Martin Graeve.

Heft Nr. 125/1993 – „Ökologie und Respiration ausgewählter arktischer Bodenfischarten", von Christian F. von Dorrien.

Heft Nr. 126/1993 – „Quantitative Bestimmung von Paläoumweltparametern des Antarktischen Oberflächenwassers im Spätquartier anhand von Transferfunktionen mit Diatomeen", von Ulrich Zielinski

* **Heft Nr. 127/1993** – „Sedimenttransport durch das arktische Meereis: Die rezente lithogene und biogene Materialfracht", von Ingo Wollenburg.

Heft Nr. 128/1993 – "Cruise ANTARKTIS X/3 of RV 'Polarstern': CTD-Report", von Marek Zwierz.

Heft Nr. 129/1993 – „Reproduktion und Lebenszyklen dominanter Copepodenarten aus dem Weddellmeer, Antarktis", von Frank Kurbjeweit

Heft Nr. 130/1993 – „Untersuchungen zu Temperaturregime und Massenhaushalt des Filchner-Ronne-Schelfeises, Antarktis, unter besonderer Berücksichtigung von Anfrier- und Abschmelzprozessen", von Klaus Grosfeld

Heft Nr. 131/1993 – „Die Expedition ANTARKTIS X/5 mit FS ‚Polarstern' 1992", herausgegeben von Rainer Gersonde

Heft Nr. 132/1993 – „Bildung und Abgabe kurzkettiger halogenierter Kohlenwasserstoffe durch Makroalgen der Polarregionen", von Frank Laturnus

Heft Nr. 133/1994 – "Radiation and Eddy Flux Experiment 1993 *(REFLEX II)*", by Christoph Kottmeier, Jörg Hartmann, Christian Wamser, Axel Bochert, Christof Lüpkes, Dietmar Freese and Wolfgang Cohrs

* **Heft Nr. 134/1994** – "The Expedition ARKTIS-IX/1", edited by Hajo Eicken and Jens Meincke

Heft Nr. 135/1994 – „Die Expeditionen ANTARKTIS X/6-8", herausgegeben von Ulrich Bathmann, Victor Smetacek, Hein de Baar, Eberhard Fahrbach und Gunter Krause

Heft Nr. 136/1994 – „Untersuchungen zur Ernährungsökologie von Kaiserpinguinen *(Aptenodytes forsteri)* und Königspinguinen *(Aptenodytes patagonicus)*", von Klemens Pütz

* **Heft Nr. 137/1994** – „Die känozoische Vereisungsgeschichte der Antarktis", von Werner U. Ehrmann

Heft Nr. 138/1994 – „Untersuchungen stratosphärischer Aerosole vulkanischen Ursprungs und polarer stratosphärischer Wolken mit einem Mehrwellenlängen-Lidar auf Spitzbergen *(79° N, 12° E)*", von Georg Beyerle

Heft Nr. 139/1994 – „Charakterisierung der Isopodenfauna (Crustacea, Malacostraca) des Scotia-Bogens aus biogeographischer Sicht: Ein multivariater Ansatz", von Holger Winkler.

Heft Nr. 140/1994 – „Die Expedition ANTARKTIS X/4 mit FS ‚Polarstern' 1992", herausgegeben von Peter Lemke

Heft Nr. 141/1994 – „Satellitenaltimetrie über Eis – Anwendung des GEOSAT-Altimeters über dem Ekströmisen, Antarktis", von Clemens Heidland

Heft Nr. 142/1994 – "The 1993 Northeast Water Expedition. Scientific cruise report of RV 'Polartstern' Arctic cruises ARK IX/2 and 3, USCG 'Polar Bear' cruise NEWP and the NEWLand expedition", edited by Hans-Jürgen Hirche and Gerhard Kattner

Heft Nr. 143/1994 – „Detaillierte refraktionsseismische Untersuchungen im inneren Scoresby Sund Ost-Grönland", von Notker Fechner

Heft Nr. 144/1994 – "Russian-German Cooperation in the Siberian Shelf Seas: Geo-System Laptev Sea", edited by Heidemarie Kassens, Hans-Wolfgang Hubberten, Sergey M. Pryamikov and Rüdiger Stein

* **Heft Nr. 145/1994** – "The 1993 Northeast Water Expedition. Data Report of RV ‚Polarstern' Arctic Cruises IX/2 and 3", edited by Gerhard Kattner and Hans-Jürgen Hirche.

Heft Nr. 146/1994 – "Radiation Measurements at the German Antarctic Station Neumayer 1982 - 1992", by Torsten Schmidt and Gerd König-Langlo.

Heft Nr. 147/1994 – „Krustenstrukturen und Verlauf des Kontinentalrandes im Weddell-Meer / Antarktis", von Christian Hübscher.

* **Heft Nr. 148/1994** – "The expeditions NORILSK/TAYMYR 1993 and BUNGER OASIS 1993/94 of the AWI Research Unit Potsdam", edited by Martin Melles.

** **Heft Nr. 149/1994** – „Die Expedition ARCTIC '93. Der Fahrtabschnitt ARK-IX/4 mit FS ‚Polarstern' 1993", herausgegeben von Dieter K. Fütterer.

Heft Nr. 150/1994 – „Der Energiebedarf der Pygoscelis-Pinguine: eine Synopse", von Boris M. Culik.

Heft Nr. 151/1994 – "Russian-German Cooperation: The Transdrift I Expedition to the Laptev Sea", edited by Heidemarie Kassens and Valeriy Y. Karpiy.

Heft Nr. 152/1994 – „Die Expedition ANTARKTIS-X mit FS ‚Polarstern' 1992. Bericht von den Fahrtabschnitten / ANT-X / 1a und 2", herausgegeben von Heinz Miller.

Heft Nr. 153/1994 – „Aminosäuren und Huminstoffe im Stickstoffkreislauf polarer Meere", von Ulrike Hubberten.

Heft Nr. 154/1994 – "Regional and seasonal variability in the vertical distribution of mesozooplankton in the Greenland Sea", by Claudio Richter.

Heft Nr. 155/1995 – „Benthos in polaren Gewässern", herausgegeben von Christian Wiencke und Wolf Arntz.

Heft Nr. 156/1995 – "An adjoint model for the determination of the mean oceanic circulation, air-sea fluxes and mixing coefficients", by Reiner Schlitzer.

Heft Nr. 157/1995 – „Biochemische Untersuchungen zum Lipidstoffwechsel antarktischer Copepoden", von Kirsten Fahl.

** **Heft Nr. 158/1995** – „Die Deutsche Polarforschung seit der Jahrhundertwende und der Einfluß Erich von Drygalskis", von Cornelia Lüdecke.

* **Heft Nr. 159/1995** – "The distribution of $\delta^{18}O$ in the Arctic Ocean: Implications for the freshwater balance of the halocline and the sources of deep and bottom waters", by Dorothea Bauch.

* **Heft Nr. 160/1995** – „Rekonstruktion der spätquartären Tiefenwasserzirkulation und Produktivität im östlichen Südatlantik anhand von benthischen Foraminiferenvergesellschaftungen", von Gerhard Schmiedl.

Heft Nr. 161/1995 – „Der Einfluß von Salinität und Lichtintensität auf die Osmolytkonzentrationen, die Zellvolumina und die Wachstumsraten der antarktischen Eisdiatomeen *Chaetoceros sp.* und *Navicula sp.* unter besonderer Berücksichtigung der Aminosäure Prolin", von Jürgen Nothnagel.

Heft Nr. 162/1995 – „Meereistransportiertes lithogenes Feinmaterial in spätquartären Tiefseesedimenten des zentralen östlichen Arktischen Ozeans und der Framstraße", von Thomas Letzig.

Heft Nr. 163/1995 – „Die Expedition ANTARKTIS-XI/2 mit FS ‚Polarstern' 1993/94", herausgegeben von Rainer Gersonde.

Heft Nr. 164/1995 – „Regionale und altersabhängige Variation gesteinsmagnetischer Parameter in marinen Sedimenten der Arktis", von Thomas Frederichs.

Heft Nr. 165/1995 – „Vorkommen, Verteilung und Umsatz biogener organischer Spurenstoffe: Sterole in antarktischen Gewässern", von Georg Hanke.

Heft Nr. 166/1995 – „Vergleichende Untersuchungen eines optimierten dynamisch-thermodynamischen Meereismodells mit Beobachtungen im Weddellmeer", von Holger Fischer.

* **Heft Nr. 167/1995** – „Rekonstruktionen von Paläo-Umweltparametern anhand von stabilen Isotopen und Faunen-Vergesellschaftungen planktischer Foraminiferen im Südatlantik", von Hans-Stefan Niebler

Heft Nr. 168/1995 – „Die Expedition ANTARKTIS XII mit FS ‚Polarstern' 1993/94. Bericht von den Fahrtabschnitten ANT XII/1 und 2", herausgegeben von Gerhard Kattner und Dieter Karl Fütterer

Heft Nr. 169/1995 – „Medizinische Untersuchung zur Circadianrhythmik und zum Verhalten bei Überwinterern auf einer antarktischen Forschungsstation", von Hans Wortmann

Heft-Nr. 170/1995 – DFG-Kolloquium: Terrestrische Geowissenschaften – Geologie und Geophysik der Antarktis.

Heft Nr. 171/1995 – „Strukturentwicklung und Petrogenese des metamorphen Grundgebirges der nördlichen Heimfrontfjella (westliches Dronning Maud Land/Antarktika)", von Wilfried Bauer.

Heft Nr. 172/1995 – „Die Struktur der Erdkruste im Bereich des Scoresby Sund, Ostgrönland: Ergebnisse refraktionsseismischer und gravimetrischer Untersuchungen", von Holger Mandler.

Heft Nr. 173/1995 – „Paläozoische Akkretion am paläopazifischen Kontinentalrand der Antarktis in Nordvictorialand – P-T-D-Geschichte und Deformationsmechanismen im Bowers Terrane", von Stefan Matzer.

Heft Nr. 174/1995 – "The Expedition ARKTIS-X/2 of RV 'Polarstern' in 1994", edited by Hans-W. Hubberten

Heft Nr. 175/1995 – "Russian-German Cooperation: The Expedition TAYMYR 1994", edited by Christine Siegert and Gmitry Bolshiyanov.

* **Heft Nr. 176/1995** – "Russian-German Cooperation: Laptev Sea System", edited by Heidemarie Kassens, Dieter Piepenburg, Jörn Thiede, Leonid Timokhov, Hans-Wolfgang Hubberten and Sergey M. Priamikov.

Heft Nr. 177/1995 – „Organischer Kohlenstoff in spätquartären Sedimenten des Arktischen Ozeans: Terrigener Eintrag und marine Produktivität", von Carsten J. Schubert

Heft Nr. 178/1995 – "Cruise ANTARKTIS XII/4 of RV 'Polarstern' in 1995: CTD-Report", by Jüri Sildam.

Heft Nr. 179/1995 – „Benthische Foraminiferenfaunen als Wassermassen-, Produktions- und Eisdriftanzeiger im Arktischen Ozean", von Jutta Wollenburg.

Heft Nr. 180/1995 – „Biogenopal und biogenes Barium als Indikatoren für spätquartäre Produktivitätsänderungen am antarktischen Kontinentalhang, atlantischer Sektor", von Wolfgang J. Bonn.

Heft Nr. 181/1995 – „Die Expedition ARKTIS X/1 des Forschungsschiffes ‚Polarstern' 1994", herausgegeben von Eberhard Fahrbach.

Heft Nr. 182/1995 – "Laptev Sea System: Expeditions in 1994", edited by Heidemarie Kassens.

Heft Nr. 183/1996 – „Interpretation digitaler Parasound Echolotaufzeichnungen im östlichen Arktischen Ozean auf der Grundlage physikalischer Sedimenteigenschaften", von Uwe Bergmann.

Heft Nr. 184/1996 – "Distribution and dynamics of inorganic nitrogen compounds in the troposphere of continental, coastal, marine and Arctic areas", by Maria Dolores Andrés Hernández.

Heft Nr. 185/1996 – "„Verbreitung und Lebensweise der Aphroditen und Polynoiden (Polychaeta) im östlichen Weddellmeer und im Lazarevmeer (Antarktis)", von Michael Stiller.

Heft Nr. 186/1996 – "Reconstruction of Late Quaternary environmental conditions applying the natural radionuclides ^{230}Th, ^{10}Be, ^{231}Pa and ^{233}U: A study of deep-sea sediments from the eastern sector of the Antarctic Circumpolar Current System", by Martin Frank.

Heft Nr. 187/1996 – "The Meteorological Data of the Neumayer Station (Antarctica) for 1992, 1993 and 1994", by Gert König-Langlo and Andreas Herber.

Heft Nr. 188/1996 – „Die Expedition ANTARKTIS-XI/3 mit FS ‚Polarstern' 1994", herausgegeben von Heinz Miller und Hannes Grobe.

Heft Nr. 189/1996 – „Die Expedition ARKTIS-VII/3 mit FS ‚Polarstern' 1990", herausgegeben von Heinz Miller und Hannes Grobe

Heft Nr. 190/1996 – "Cruise report of the Joint Chilean-German-Italian Magellan ‚Victor Hensen' Campaign in 1994", edited by Wolf Arntz and Matthias Gorny.

Heft Nr. 191/1996 – „Leitfähigkeits- und Dichtemessung an Eisbohrkernen", von Frank Wilhelms.

Heft Nr. 192/1996 – „Photosynthese-Charakteristika und Lebensstrategie antarktischer Makroalgen", von Gabriele Weykam.

Heft Nr. 193/1996 – „Heterogene Reaktionen von N_2O_5 und Hbr und ihr Einfluß auf den Ozonabbau in der polaren Stratosphäre", von Sabine Seisel.

Heft Nr. 194/1996 – „Ökologie und Populationsdynamik antarktischer Ophiuroiden (Echinodermata)", von Corinna Dahm.

Heft Nr. 195/1996 – „Die planktische Foraminifere *Neogloboquadrina pachyderma* (Ehrenberg) im Weddellmeer, Antarktis", von Doris Berberich.

Heft Nr. 196/1996 – „Untersuchungen zum Beitrag chemischer und dynamischer Prozesse zur Variabilität des stratosphärischen Ozons über der Arktis", von Birgit Heese

Heft Nr. 197/1996 – "The Expedition ARKTIS-XI/2 of 'Polarstern' in 1995", edited by Gunther Krause.

Heft Nr. 198/1996 – „Geodynamik des Westantarktischen Riftsystems basierend auf Apatit-Spaltspuranalysen", von Frank Lisker.

Heft Nr. 199/1996 – "The 1993 Northeast Water Expedition. Data Report on CTD Measurements of RV 'Polarstern' Cruises ARKTIS IX/2 and 3", by Gerion Budéus and Wolfgang Schneider.

Heft Nr. 200/1996 – "Stability of the Thermohaline Circulation in analytical and numerical models", by Gerrit Lohmann.

Heft Nr. 201/1996 – „Trophische Beziehungen zwischen Makroalgen und Herbivoren in der Potter Cove (King George-Insel, Antarktis)", von Katrin Iken.

Heft Nr. 202/1996 – „Zur Verbreitung und Respiration ökologisch wichtiger Bodentiere in den Gewässern um Svalbard (Arktis)", von Michael K. Schmid.

Heft Nr. 203/1996 – „Dynamik, Rauhigkeit und Alter des Meereises in der Arktis – Numerische Untersuchungen mit einem großskaligen Modell", von Markus Harder.

Heft Nr. 204/1996 – „Zur Parametrisierung der stabilen atmosphärischen Grenzschicht über einem antarktischen Schelfeis", von Dörthe Handorf.

Heft Nr. 205/1996 – "Textures and fabrics in the GRIP ice core, in relation to climate history and ice deformation", by Thorsteinn Thorsteinsson.

Heft Nr. 206/1996 – „Der Ozean als Teil des gekoppelten Klimasystems: Versuch der Rekonstruktion der glazialen Zirkulation mit verschieden komplexen Atmosphärenkomponenten", von Kerstin Fieg.

Heft Nr. 207/1996 – „Lebensstrategien dominanter antarktischer Oithonidae (Cyclopoida, Copepoda) und Oncaeidae (Poecilostomatoida, Copepoda) im Bellingshausenmeer", von Cornelia Metz.

Heft Nr. 208/1996 – „Atmosphäreneinfluß bei der Fernerkundung von Meereis mit passiven Mikrowellenradiometern", von Christoph Oelke.

Heft Nr. 209/1996 – „Klassifikation von Radarsatellitendaten zur Meereiserkennung mit Hilfe von LIne-Scanner-Messungen", von Axel Bochert.

Heft Nr. 210/1996 – „Die mit ausgewählten Schwämmen (Hexactinellida und Demospongiae) aus dem Weddellmeer, Antarktis, vergesellschaftete Fauna", von Kathrin Kunzmann.

Heft Nr. 211/1996 – "Russian-German Cooperation: The Expedition TAYMYR 1995 and the Expedition KOLYMA 1995", by Dima Yu. Bolshiyanov and Hans-W. Hubberten.

Heft Nr. 212/1996 – "Surface-sediment composition and sedimentary processes in the central Arctic Ocean and along the Eurasian Continental Margin", by Ruediger Stein, Gennadij I. Ivanov, Michael A. Levitan, and Kirsten Fahl.

Heft Nr. 213/1996 – „Gonadenentwicklung und Eiproduktion dreier *Calanus*-Arten (Copepoda): Freilandbeobachtungen, Histologie und Experimente", von Barbara Niehoff

Heft Nr. 214/1996 – „Numerische Modellierung der Übergangszone zwischen Eisschild und Eisschelf", von Christoph Mayer.

Heft Nr. 215/1996 – „Arbeiten der AWI-Forschungsstelle Potsdam in Antarktika, 1994/95", herausgegeben von Ulrich Wand.

Heft Nr. 216/1996 – „Rekonstruktion quartärer Klimaänderungen im atlantischen Sektor des Südpolarmeeres anhand von Radiolarien", von Uta Brathauer.

Heft Nr. 217/1996 – „Adaptive Semi-Lagrange-Finite-Elemente-Methode zur Lösung der Flachwassergleichungen: Implementierung und Parallelisierung", von Jörn Behrens.

Heft Nr. 218/1997 – "Radiation and Eddy Flux Experiment 1995 (REFLEX III)", by Jörg Hartmann, Axel Bochert, Dietmar Freese, Christoph Kottmeier, Dagmar Nagel and Andreas Reuter.

Heft Nr. 219/1997 – „Die Expedition ANTARKTIS-XII mit FS ‚Polarstern' 1995. Bericht vom Fahrtabschnitt ANT-XII/3, herausgegeben von Wilfried Jokat und Hans Oerter.

Heft Nr. 220/1997 – „Ein Beitrag zum Schwerefeld im Bereich des Weddellmeeres, Antarktis. Nutzung von Altimetermessungen des GEOSAT und ERS-1", von Tilo Schöne.

Heft Nr. 221/1997 – „Die Expeditionen ANTARKTIS-XIII/1-2 des Forschungsschiffes ‚Polarstern' 1995/96", herausgegeben von Ulrich Bathmann, Mike Lukas und Victor Smetacek.

Heft Nr. 222/1997 – "Tectonic Structures and Glaciomarine Sedimentation in the South-Eastern Weddell Sea from Seismic Reflection Data", by László Oszkó.

Heft Nr. 223/1997 – „Bestimmung der Meereisdicke mit seismischen und elektromagnetisch-induktiven Verfahren", von Christian Haas.

Heft Nr. 224/1997 – „Troposphärische Ozonvariationen in Polarregionen", von Silke Wessel.

Heft Nr. 225/1997 – „Biologische und ökologische Untersuchungen zur kryopelagischen Amphipodenfauna des arktischen Meereises", von Michael Poltermann.

Heft Nr. 226/1997 – "Scientific Cruise Report of the Arctic Expedition ARK-XI/1 of RV 'Polarstern' in 1995", edited by Eike Rachor.

Heft Nr. 227/1997 – „Der Einfluß kompatibler Substanzen und Kryoprotektoren auf die Enzyme Malatdehydrogenase (MDH) und Glucose-6-phosphat-Dehydrogenase (G6P-DH) aus *Acrosiphonia arcta* (Chlorophyta) der Arktis", von Katharina Kück.

Heft Nr. 228/1997 – „Die Verbreitung epibenthischer Mollusken im chilenischen Beagle-Kanal", von Katrin Linse.

Heft Nr. 229/1997 – „Das Mesozooplankton im Laptevmeer und östlichen Nansen-Becken - Verteilung und Gemeinschaftsstrukturen im Spätsommer", von Hinrich Hanssen.

Heft Nr. 230/1997 – „Modell eines adaptierbaren, rechnergestützten, wissenschaftlichen Arbeitsplatzes am Alfred-Wegener-Institut für Polar- und Meeresforschung", von Lutz-Peter Kurdelski

Heft Nr. 231/1997 – „Zur Ökologie arktischer und antarktischer Fische: Aktivität, Sinnesleistungen und Verhalten", von Christopher Zimmermann

Heft Nr. 232/1997 – „Persistente chlororganische Verbindungen in hochantarktischen Fischen", von Stephan Zimmermann

Heft Nr. 233/1997 – „Zur Ökologie des Dimethylsulfoniumpropionat (DMSP)-Gehaltes temperierter und polarer Phytoplanktongemeinschaften im Vergleich mit Laborkulturen der Coccolithophoride *Emiliania huxleyi* und der antarktischen Diatomee *Nitzschia lecointei*", von Doris Meyerdierks.

Heft Nr. 234/1997 – „Die Expedition ARCTIC '96 des FS ‚Polarstern' (ARK XIII) mit der Arctic Climate System Study (ACSYS)", von Ernst Augstein und den Fahrtteilnehmern.

Heft Nr. 235/1997 – „Polonium-210 und Blei-219 im Südpolarmeer: Natürliche Tracer für biologische und hydrographische Prozesse im Oberflächenwasser des Antarktischen Zirkumpolarstroms und des Weddellmeeres", von Jana Friedrich

Heft Nr. 236/1997 – "Determination of atmospheric trace gas amounts and corresponding natural isotopic ratios by means of ground-based FTIR spectroscopy in the high Arctic", by Arndt Meier.

Heft Nr. 237/1997 – "Russian-German Cooperation: The Expedition TAYMYR/SEVERNAYA ZEMLYA 1996", edited by Martin Melles, Birgit Hagedorn and Dmitri Yu. Bolshiyanov

Heft Nr. 238/1997 – "Life strategy and ecophysiology of Antarctic macroalgae", by Iván M. Gómez.

Heft Nr. 239/1997 – „Die Expedition ANTARKTIS XIII/4-5 des Forschungsschiffes ‚Polarstern' 1996", herausgegeben von Eberhard Fahrbach und Dieter Gerdes.

Heft Nr. 240/1997 – „Untersuchungen zur Chrom-Spezíation in Meerwasser, Meereis und Schnee aus ausgewählten Gebieten der Arktis", von Heide Giese.

Heft Nr. 241/1997 – "Late Quaternary glacial history and paleoceanographic reconstructions along the East Greenland continental margin: Evidence from high-resolution records of stable isotopes and ice-rafted debris", by Seung-Il Nam.

Heft Nr. 242/1997 – "Thermal, hydrological and geochemical dynamics of the active layer at a continuous permafrost site, Taymyr Peninsula, Siberia", by Julia Boike.

Heft Nr. 243/1997 – „Zur Paläoozeanographie hoher Breiten: Stellvertreterdaten aus Foraminiferen", von Andreas Mackensen.

Heft Nr. 244/1997 – "The Geophysical Observatory at Neumayer Station, Antarctica, Geomagnetic and seismological observations in 1995 and 1996", by Alfons Eckstaller, Thomas Schmidt, Viola Graw, Christian Müller and Johannes Rogenhagen.

Heft Nr. 245/1997 – „Temperaturbedarf und Biogeographie mariner Makroalgen - Anpassung mariner Makroalgen an tiefe Temperaturen, von Bettina Bischoff-Bäsmann.

Heft Nr. 246/1997 – „Ökologische Untersuchungen zur Fauna des arktischen Meereises", von Christine Friedrich.

Heft Nr. 247/1997 – „Entstehung und Modifizierung von marinen gelösten organischen Substanzen", von Berit Kirchhoff.

Heft Nr. 248/1997 – "Laptev Sea System: Expeditions in 1995", edited by Heidemarie Kassens.

Heft Nr. 249/1997 – "The Expedition ANTARKTIS XIII/3 (EASIZ I) of RV 'Polarstern' to the eastern Weddell Sea in 1996", edited by Wolf Arntz and Julian Gutt.

Heft Nr. 250/1997 – „Vergleichende Untersuchungen zur Ökologie und Biodiversität des Mega-Epibenthos der Arktis und Antarktis", von Adreas Starmans.

Heft Nr. 251/1997 – „Zeitliche und räumliche Verteilung von Mineralvergesellschaftungen in spätquartären Sedimenten des Arktischen Ozeans und ihre Nützlichkeit als Klimaindikatoren während der Glazial/Interglazial-Wechsel", von Christoph Vogt.

Heft Nr. 252/1997 – „Solitäre Ascidien in der Potter Cove (King George Island, Antarktis). Ihre ökologische Bedeutung und Populationsdynamik", von Stephan Kühne.

Heft Nr. 253/1997 – "Distribution and role of microprotozoa in the Southern Ocean", by Christine Klaas.

Heft Nr. 254/1997 – „Die spätquartäre Klima- und Umweltgeschichte der Bunger-Oase, Ostantarktis", von Thomas Kulbe

Heft Nr. 255/1997 – "Scientific Cruise Report of the Arctic Expedition ARK-XIII/2 of RV 'Polarstern' in 1997", edited by Ruediger Stein and Kirsten Fahl.

Heft Nr. 256/1998 – „Das Radionuklid Tritium im Ozean: Meßverfahren und Verteilung von Tritium im Südatlantik und im Weddellmeer", von Jürgen Sültenfuß.

Heft Nr. 257/1998 – „Untersuchungen der Saisonalität von atmosphärischem Dimethylsulfid in der Arktis und Antarktis", von Christoph Kleefeld.

Heft Nr. 258/1998 – „Bellingshausen- und Amundsenmeer: Entwicklung eines Sedimentationsmodells", von Frank-Oliver Nitsche.

Heft Nr. 259/1998 – "The Expedition ANTARKTIS-XIV/4 of RV 'Polarstern' in 1997", by Dieter K. Fütterer.

Heft Nr. 260/1998 – „Die Diatomeen der Laptevsee (Arktischer Ozean): Taxonomie und biogeographische Verbreitung", von Holger Cremer

Heft Nr. 261/1998 – „Die Krustenstruktur und Sedimentdecke des Eurasischen Beckens, Arktischer Ozean: Resultate aus seismischen und gravimetrischen Untersuchungen", von Estella Weigelt.

Heft Nr. 262/1998 – "The Expedition ARKTIS-XIII/3 of RV 'Polarstern' in 1997", by Gunther Krause.

Heft Nr. 263/1998 – „Thermo-tektonische Entwicklung von Oates Land und der Shackleton Range (Antarktis) basierend auf Spaltspuranalysen", von Thorsten Schäfer.

Heft Nr. 264/1998 – „Messungen der stratosphärischen Spurengase ClO, HCl, O_3, N_2O, H_2O und OH mittels flugzeuggetragener Submillimeterwellen-Radiometrie", von Joachim Urban.

Heft Nr. 265/1998 – „Untersuchungen zu Massenhaushalt und Dynamik des Ronne Ice Shelfs, Antarktis", von Astrid Lambrecht.

Heft Nr. 266/1998 – "Scientific Cruise Report of the Kara Sea Expedition of RV 'Akademic Boris Petrov' in 1997", edited by Jens Matthiessen and Oleg Stepanets.

Heft Nr. 267/1998 – „Die Expedition ANTARKTIS-XIV mit FS ‚Polarstern' 1997. Bericht vom Fahrtabschnitt ANT-XIV/3", herausgegeben von Wilfried Jokat und Hans Oerter.

Heft Nr. 268/1998 – „Numerische Modellierung der Wechselwirkung zwischen Atmosphäre und Meereis in der arktischen Eisrandzone", von Gerit Birnbaum.

Heft Nr. 269/1998 – "Katabatic wind and Boundary Layer Front Experiment around Greenland (KABEG '97)", by Günther Heinemann.

Heft Nr. 270/1998 – "Architecture and evolution of the continental crust of East Greenland from integrated geophysical studies", by Vera Schlindwein.

Heft Nr. 271/1998 – "Winter Expedition to the Southwestern Kara Sea - Investigations on Formation and Transport of Turbid Sea-Ice", by Dirk Dethleff, Per Loewe, Dominik Weiel, Hartmut Nies, Gesa Kuhlmann, Christian Bahe and Gennady Tarasov.

Heft Nr. 272/1998 – „FTIR-Emissionsspektroskopische Untersuchungen der arktischen Atmosphäre", von Edo Becker.

Heft Nr. 273/1998 – „Sedimentation und Tektonik im Gebiet des Agulhas Rückens und des Agulhas Plateaus („SETA-RAP')", von Gabriele Uenzelmann-Neben.

Heft Nr. 274/1998 – "The Expedition ANTARKTIS XIV/2", by Gerhard Kattner.

Heft Nr. 275/1998 – „Die Auswirkung der 'NorthEastWater'-Polynya auf die Sedimentation von NO-Grönland und Untersuchungen zur Paläo-Ozeanographie seit dem Mittelweichsel", von Hanne Notholt.

Heft Nr. 276/1998 – „Interpretation und Analyse von Potentialfelddaten im Weddellmeer, Antarktis: der Zerfall des Superkontinents Gondwana", von Michael Studinger.

Heft Nr. 277/1998 – „Koordiniertes Programm Antarktisforschung". Berichtskolloquium im Rahmen des Koordinierten Programms „Antarktisforschung mit vergleichenden Untersuchungen in arktischen Eisgebieten", herausgegeben von Hubert Miller.

Heft Nr. 278/1998 – „Messung stratosphärischer Spurengase über Ny-Ålesund, Spitzbergen, mit Hilfe eines bodengebundenen Mikrowellen-Radiometers", von Uwe Raffalski.

Heft Nr. 279/1998 – "Arctic Paleo-River Discharge (APARD). A New Research Programme of the Arctic Ocean Science Board (AOSB)", edited by Ruediger Stein.

Heft Nr. 280/1998 – „Fernerkundungs- und GIS-Studien in Nordostgrönland" von Friedrich Jung-Rothenhäusler.

Heft Nr. 281/1998 – „Rekonstruktion der Oberflächenwassermassen der östlichen Laptevsee im Holozän anhand von aquatischen Palynomorphen", von Martina Kunz-Pirrung.

Heft Nr. 282/1998 – "Scavenging of ^{231}Pa and ^{230}Th in the South Atlantic: Implications for the use of the ^{231}Pa/^{230}Th ratio as a paleoproductivity proxy", by Hans-Jürgen Walter.

Heft Nr. 283/1998 – „Sedimente im arktischen Meereis - Eintrag, Charakterisierung und Quantifizierung", von Frank Lindemann.

Heft Nr. 284/1998 – „Langzeitanalyse der antarktischen Meereisbedeckung aus passiven Mikrowellendaten", von Christian H. Thomas.

Heft Nr. 285/1998 – „Mechanismen und Grenzen der Temperaturanpassung beim Pierwurm *Arenicola marina* (L.)", von Angela Sommer.

Heft Nr. 286/1998 – „Energieumsätze benthischer Filtrierer der Potter Cove (King George Island, Antarktis)", von Jens Kowalke.

Heft Nr. 287/1998 – "Scientific Cooperation in the Russian Arctic: Research from the Barents Sea up to the Laptev Sea", edited by Eike Rachor.

Heft Nr. 288/1998 – „Alfred Wegener. Kommentiertes Verzeichnis der schriftlichen Dokumente seines Lebens und Wirkens", von Ulrich Wutzke.

Heft Nr. 289/1998 – "Retrieval of Atmospheric Water Vapor Content in Polar Regions Using Spaceborne Microwave Radiometry", by Jungang Miao.

Heft Nr. 290/1998 – „Strukturelle Entwicklung und Petrogenese des nördlichen Kristallingürtels der Shackleton Range, Antarktis: Proterozoische und Ross-orogene Krustendynamik am Rand des Ostantarktischen Kratons", von Axel Brommer.

Heft Nr. 291/1998 – „Dynamik des arktischen Meereises - Validierung verschiedener Rheologieansätze für die Anwendung in Klimamodellen", von Martin Kreyscher.

Heft Nr. 292/1998 – „Anthropogene organische Spurenstoffe im Arktischen Ozean, Untersuchungen chlorierter Biphenyle und Pestizide in der Laptevsee, technische und methodische Entwicklungen zur Probenahme in der Arktis und zur Spurenstoffanalyse", von Sven Utschakowski.

Heft Nr. 293/1998 – „Rekonstruktion der spätquartären Klima- und Umweltgeschichte der Schirmacher Oase und des Wohlthat Massivs (Ostantarktika)", von Markus Julius Schwab.

Heft Nr. 294/1998 – „Besiedlungsmuster der benthischen Makrofauna auf dem ostgrönländischen Kontinentalhang", von Klaus Schnack.

Heft Nr. 295/1998 – „Gehäuseuntersuchungen an planktischen Foraminiferen hoher Breiten: Hinweise auf Umweltveränderungen während der letzten 140.000 Jahre", von Harald Hommers.

Heft Nr. 296/1998 – "Scientific Cruise Report of the Arctic Expedition ARK-XIII/1 of RV 'Polarstern' in 1997", edited by Michael Spindler, Wilhelm Hagen and Dorothea Stübing.

Heft Nr. 297/1998 – „Radiometrische Messungen im arktischen Ozean - Vergleich von Theorie und Experiment", von Klaus-Peter Johnsen.

Heft Nr. 298//1998 – "Patterns and Controls of CO_2 Fluxes in Wet Tundra Types of the Taimyr Peninsula, Siberia - the Contribution of Soils and Mosses", by Martin Sommerkorn.

Heft Nr. 299/1998 – "The Potter Cove coastal ecosystem, Antarctica. Synopsis of research performed within the frame of the Argentinean-German Cooperation at the Dallmann Laboratory and Jubany Station (Kind George Island, Antarctica, 1991 - 1997)", by Christian Wiencke, Gustavo Ferreyra, Wolf Arntz & Carlos Rinaldi.

Heft Nr. 300/1999 – "The Kara Sea Expedition of RV 'Akademik Boris Petrov' 1997: First Results of a Joint Russian-German Pilot Study", edited by Jens Matthiessen, Oleg V. Stepanets, Ruediger Stein, Dieter K. Fütterer, and Eric M. Galimov.

Heft Nr. 301/1999 – "The Expedition ANTARKTIS XV/3 (EASIZ II)", edited by Wolf E. Arntz and Julian Gutt.

Heft Nr. 302/1999 – „Sterole im herbstlichen Weddellmeer (Antarktis): Großräumige Verteilung, Vorkommen und Umsatz", von Anneke Mühlebach.

Heft Nr. 303/1999 – „Polare stratosphärische Wolken: Lidar-Beobachtungen, Charakterisierung von Entstehung und Entwicklung", von Jens Biele.

Heft Nr. 304/1999 – „Spätquartäre Paläoumweltbedingungen am nördlichen Kontinentalrand der Barents- und Kara-See. Eine Multi-Parameter-Analyse", von Jochen Knies.

Heft Nr. 305/1999 – "Arctic Radiation and Turbulence Interaction Study (ARTIST)", by Jörg Hartmann, Frank Albers, Stefania Argentini, Axel Bochert, Ubaldo Bonafé, Wolfgang Cohrs, Alessandro Conidi, Dietmar Freese, Teodoro Georgiadis, Alessandro Ippoliti, Lars Kaleschke, Christof Lüpkes, Uwe Maixner, Giangiuseppe Mastrantonio, Fabrizio Ravegnani, Andreas Reuter, Giuliano Trivellone and Angelo Viola.

Heft Nr. 306/1999 – "German-Russian Cooperation: Biogeographic and biostratigraphic investigations on selected sediment cores from the Eurasian continental margin and marginal seas to analyze the Late Quaternary climatic variability", edited by Robert R. Spielhagen, Max S. Barash, Gennady I. Ivanov, and Jörn Thiede.

Heft Nr. 307/1999 – „Struktur und Kohlenstoffbedarf des Makrobenthos am Kontinentalhang Ostgrönlands", von Dan Seiler.

Heft Nr. 308/1999 – "ARCTIC '98: The Expedition ARK-XIV/1a of RV 'Polarstern' in 1998", edited by Wilfried Jokat.

Heft Nr. 309/1999 – „Variabilität der arktischen Ozonschicht: Analyse und Interpretation bodengebundener Millimeterwellenmessungen", von Björn-Martin Sinnhuber.

Heft Nr. 310/1999 – „Rekonstruktion von Meereisdrift und terrigenem Sedimenteintrag im Spätquartär: Schwermineralassoziationen in Sedimenten des Laptev-See-Kontinentalrandes und des zentralen Arktischen Ozeans", von Marion Behrends.

Heft Nr. 311/1999 – „Parameterisierung atmosphärischer Grenzschichtprozesse in einem regionalen Klimamodell der Arktis", von Christoph Abegg.

Heft Nr. 312/1999 – „Solare und terrestrische Strahlungswechselwirkung zwischen arktischen Eisflächen und Wolken", von Dietmar Freese.

Heft Nr. 313/1999 – "Snow accumulation on Ekströmisen, Antarctica", by Elisabeth Schlosser, Hans Oerter and Wolfgang Graf.

Heft Nr. 314/1999 – „Die Expedition ANTARKTIS XV/4 des Forschungsschiffes ‚Polarstern' 1998", herausgegeben von Eberhard Fahrbach.

Heft Nr. 315/1999 – "Expeditions in Siberia in 1998", edited by Volker Rachold.

Heft Nr. 316/1999 – „Die postglaziale Sedimentationsgeschichte der Laptewsee: schwermineralogische und sedimentpetrographische Untersuchungen", von Bernhard Peregovich.

Heft-Nr. 317/1999 – „Adaption an niedrige Temperaturen: Lipide in Eisdiatomeen", von Heidi Lehmal.

Heft-Nr. 318/1999 – „Effiziente parallele Lösungsverfahren für elliptische partielle Differentialgleichungen in der numerischen Ozeanmodellierung", von Natalja Rakowsky.

Heft-Nr. 319/1999 – „The Ecology of Arctic Deep-Sea Copepods (Euchaetidae and Aetideidae). Aspects of their Distribution, Trophodynamics and Effect on the Carbon Flux", by Holger Auel.

Heft-Nr. 320/1999 – „Modellstudien zur arktischen stratosphärischen Chemie im Vergleich mit Meßdaten", von Veronika Eyring.

Heft-Nr. 321/1999 – „Analyse der optischen Eigenschaften des arktischen Aerosols", von Dagmar Nagel.

Heft-Nr. 322/1999 – „Messungen des arktischen stratosphärischen Ozons: Vergleich der Ozonmessungen in Ny-Ålesund, Spitzbergen, 1997 und 1998", von Jens Langer

Heft-Nr. 323/1999 – „Untersuchung struktureller Elemente des südöstlichen Weddellmeeres / Antarktis auf der Basis mariner Potentialfelddaten", von Uwe F. Meyer.

Heft-Nr. 324/1999 – „Geochemische Verwitterungstrends eines basaltischen Ausgangsgesteins nach dem spätpleistozänen Gletscherrückzug auf der Taimyrhalbinsel (Zentralsibirien) - Rekonstruktion an einer sedimentären Abfolge des Lama Sees", von Stefanie K. Harwart.

Heft-Nr. 325/1999 – „Untersuchungen zur Hydrologie des arktischen Meereises - Konsequenzen für den kleinskaligen Stofftransport", von Johannes Freitag.

Heft-Nr. 326/1999 – „Die Expedition ANTARKTIS XIV/2 des Forschungsschiffes 'Polarstern' 1998", herausgegeben von Eberhard Fahrbach.

Heft-Nr. 327/1999 – „Gemeinschaftsanalytische Untersuchungen der Harpacticoidenfauna der Magellanregion, sowie erste similaritätsanalytische Vergleiche mit Assoziationen aus der Antarktis", von Kai Horst George.

Heft-Nr. 328/1999 – „Rekonstruktion der Paläo-Umweltbedingungen am Laptev-See-Kontinentalrand während der beiden letzten Glazial/Interglazial-Zyklen anhand sedimentologischer und mineralogischer Untersuchungen", von Claudia Müller.

Heft-Nr. 329/1999 – „Räumliche und zeitliche Variationen atmosphärischer Spurengase aus bodengebundenen Messungen mit Hilfe eines Michelson Interferometers", von Justus Notholt.

Heft-Nr. 330/1999 – „The 1998 Danish-German Excursion to Disko Island, West Greenland", edited by Angelika Brandt, Helge A. Thomsen, Henning Heide-Jørgensen, Reinhardt M. Kristensen and Hilke Ruhberg.

Heft-Nr. 331/1999 – „Poseidon" Cruise No. 243 (Reykjavik - Greenland - Reykjavik, 24 August - 11 September 1998): Climate change and the Viking-age fjord enviroment of the Eastern Settlement, sw Greenland", by Gerd Hoffmann, Antoon Kuijpers, and Jörn Thiede.

Heft-Nr. 332/1999 – „Modeling of marine biogeochemical cycles with an emphasis on vertical particle fluxes", by Regina Usbeck.

Heft-Nr. 333/1999 – „Die Tanaidaceenfauna des Beagle-Kanals und ihre Beziehungen zur Fauna des antarktischen Festlandsockels", von Anja Schmidt.

Heft-Nr. 334/1999 – „D-Aminosäuren als Tracer für biogeochemische Prozesse im Fluß-Schelf-Ozean-System der Arktis", von Hans Peter Fitznar.

Heft-Nr. 335/1999 – „Ökophysiologische Ursachen der limitierten Verbreitung reptanter decapoder Krebse in der Antarktis", von Markus Frederich.

Heft-Nr. 336/1999 – „Ergebnisse der Untersuchung des grönländischen Inlandeises mit dem elektromagnetischen Reflexionsverfahren in der Umgebung von NGRIP", von Fidan Göktas.

Heft-Nr. 337/1999 – „Paleozoic and mesozoic tectono-thermal history of central Dronning Maud Land, East Antarctica, – evidence from fission-track thermochronology", by Stefanie Meier.

Heft-Nr. 338/1999 – „Probleme hoher Stoffwechselraten bei Cephalopoden aus verschiedenen geographischen Breiten", von Susanne Zielinski.

Heft-Nr. 339/1999 – „The Expedition ARKTIS XV/1", edited by Gunther Krause.

Heft-Nr. 340/1999 – „Microbial Properties and Habitats of Permafrost Soils on Taimyr Peninsula, Central Siberia", by Nicolé Schmidt.

Heft-Nr. 341/1999 – „Photoacclimation of phytoplankton in different biogeochemical provinces of the Southern Ocean and its significance for estimating primary production", by Astrid Bracher.

Heft-Nr. 342/1999 – „Modern and Late Quaternary Depositional Environment of the St. Anna Trough Area, Northern Kara Sea", edited by Ruediger Stein, Kirsten Fahl, Gennadij I. Ivanov, Michael A. Levitan, and Gennady Tarasov.

Heft-Nr. 343/1999 – „ESF-IMPACT Workshop/Oceanic impacts: mechanisms and environmental perturbations, 15 - 17 April 1999 in Bremerhaven", edited by Rainer Gersonde and Alexander Deutsch.

Heft-Nr. 344/1999 – „Die Klimageschichte der hohen nördlichen Breiten seit dem mittleren Miozän: Hinweise aus sedimentologischen-tonmineralogischen Analysen (OPD Leg 151, zentrale Framstraße)", von Amelie Winkler.

Heft-Nr. 345/1999 – „Kurzfristige Klimaschwankungen im Scotiameer und Ergebnisse zur Kalbungsgeschichte der Antarktis während der letzten 200 000 Jahre", von Annette Hofmann.

Heft-Nr. 346/2000 – „Glazialmarine Sedimentationsentwicklung am westantarktischen Kontinentalrand im Amundsen- und Bellingshausenmeer - Hinweise auf Paläumweltveränderungen während der quartären Klimazyklen", von Claus-Dieter Hillenbrand

Heft-Nr. 347/2000 – „Zur Ökologie des Phytoplanktons im arktischen Laptevmeer - ein jahreszeitlicher Vergleich", von Kirsten Tuschling.

Heft-Nr. 348/2000 – „Untersuchungen zum Fettstoffwechsel des Südlichen See-Elefanten *(Mirounga leonina* L.) in der Antarktis", von Sven Ramdohr.

Heft-Nr. 349/2000 – „Licht- und Temperatureinfluß auf den enzymatischen Oxidationsschutz der antarktischen Eisdiatomee *Entomoneis kufferathii* Manguin", von Raimund Schriek.

Heft-Nr. 350/2000 – „Die Expedition ARKTIS XV/3 des Forschungsschiffes 'Polarstern' 1999" herausgegeben von Ursula Schauer.

Heft-Nr. 351/2000 – „Dissolution kinetics of biogenic silica in marine environments", by Dirk Rickert.

Heft-Nr. 352/2000 – „Geometrie und Kinematik des tertiären Deckenbaus im West Spitzbergen Falten- und Überschiebungsgürtel, Brøggerhalvøya, Svalbard", von Kerstin Saalmann.

Heft-Nr. 353/2000 – „Zur Ökologie der Benthos-Foraminiferen der Potter Cove (King George Island, Antarktis)", von Michaela Mayer.

Heft-Nr. 354/2000 – „Expeditions in Siberia in 1999", edited by Volker Rachold.

Heft-Nr. 355/2000 – „Temperaturrekonstruktion im Tropischen Atlantik für das Letzte Glaziale Maximum: CLIMAP neu betrachtet.", von Carsten Porthun.

Heft-Nr. 356/2000 – „Niederfrequente Variabilität großräumiger atmosphärischer Zirkulationsstrukturen in spektralen Modellen niederer Ordnung", von Antje Weisheimer.

Heft-Nr. 357/2000 – „Late Quaternary paleoclimatic reconstructions along the Eurasian continental margin", by Hans Peter Kleiber.

Heft-Nr. 358/2000 – „Holocene environmental history of East Greenland - evidence from lake sediments", by Bernd Wagner.

Heft-Nr. 359/2000 – „Scientific Cooperation in the Russian Arctic: Ecology of the White Sea with Emphasis on its Deep Basin", edited by Eike Rachor.

Heft-Nr. 360/2000 – „Scientific Cruise Report of the Joint Russian-German Kara-Sea Expedition of RV 'Akademik Boris Petrov' in 1999", edited by Ruediger Stein and Oleg Stepanets.

Heft-Nr. 361/2000 – „Planktic foraminifer ecology and stable isotope geochemistry in the Arctic Ocean: implications from water column and sediment surface studies for quantitative reconstructions of oceanic parameters" by Renate Volkmann.

Heft-Nr. 362/2000 – „Eisbohrkernuntersuchungen zur räumlichen und zeitlichen Variabilität von Temperatur und Niederschlagsrate im Spätholozän in Nordgrönland", von Matthias Schwager.

Heft-Nr. 363/2000 – „Benthische Peracarida (Crustacea, Malacostraca) des arktischen Mellemfjordes, West-Grönland", von Anne-Nina Lörz.

Heft-Nr. 364/2000 – Die Expeditionen ANTARKTIS XVI / 3-4 des Forschungsschiffes „POLARSTERN" 1999, herausgegeben von Ulrich Bathmann, Victor Smetacek und Manfred Reinke.

* vergriffen/out of print.
** nur noch beim Autor/only from the author.